Investigation of cryomilling as a potential tool for the production of amorphous solid dispersions

Ghaidaa Sulaiman Hameed, MSc

Thesis submitted to The University of Nottingham
for the degree of Doctor of Philosophy

January 2017

I declare that this thesis titled, *Investigation of cryomilling as a potential tool for the production of amorphous solid dispersions*, and the work presented in it are my own. No part of my work has been submitted for any other degree at the university of Nottingham or any other institution. The source is always given when I quoted from the work of others. Help from others is acknowledged as appropriate.

Signed:

Date:

Dedicated

I dedicate this work to my daughter who kicks me inside the belly. You are the reason for this PhD journey.

Abstract

Amorphous solid dispersions over the last decade or so have been widely investigated by the pharmaceutical industry as a formulation method to increase the effective solubility of poorly water soluble drugs and subsequently their bioavailability. Cryomilling is attractive technique to render crystalline materials amorphous without using heat or solvent as are typically used in current processes.

The possibility of amorphous formation via cryomilling was studied for three different types of drugs with different glass forming ability (GFA); Felodipine (class III) an easy glass former, paracetamol (class II) a moderate glass former and aspirin (class I) a poor glass former. These drugs were cryomilled alone, cryomilled then mixed with cryomilled hydroxypropyl methylcellulose (HPMC) physically (i.e. cryomilled separately) or co-cryomilled with HPMC together. The subsequent formulations were characterised by DSC, XRPD and FTIR. It was found that when felodipine is cryomilled alone, it can be transformed into the amorphous form, however no amorphous formation was achieved when cryomilling paracetamol or aspirin alone. It is thought that the relatively higher T_g of felodipine compared to paracetamol,and aspirin enables this transformation, however, this transformation was difficult to achieve for paracetamol or aspirin due to their rapid recrystallisation directly after cryomilling due to their low T_g and their resistance to mechanical disorder. Although felodipine was rendered amorphous when milled alone it then recrystallised within a day. It was thought that the conversion of these three drugs into amorphous form or not depends on the glass forming ability of each drug. The amount of polymer required to stabilise the amorphous form of each drug varied according to their

glass forming ability with more polymer required for poor glass formers.

Felodipine was selected as a model drug for further study with different polymers. This is because felodipine is widely used for the production of amorphous solid dispersion by hot melt extrusion and spray drying. Secondly this drug is practically insoluble but it is an important drug in the emergency treatment of hypertension due its high selectivity and its lack of a negative inotropic effect. Felodipine was co-cryomilled with different polymers and polymer blends that varied in water solubility namely HPMC, HPMCAS, Soluplus®, PMMA, HPMC:HPMCAS, HPMC:PMMA and Soluplus®:HPMCAS at 5, 25, 50 and 75% (w/w) drug loadings. For each mixture the miscibility was predicted using the Gordon-Taylor equation and solubility parameter value. All these mixtures at 50% drug loading were further investigated in dissolution studies for 6 hours under sink condition. All co-cryomilled samples except PMMA showed a high level of drug release ($> 90\%$) after 6 hours dissolution. Only PMMA, which is water insoluble, retarded the release of felodipine from the co-cryomilled mixtures but in ternary mixture felodipine-HPMC/PMMA it showed more than 95% drug release after 6 hours dissolution.

As felodipine with Soluplus® showed a good miscibility and stability at 0% humidity and high drug release this co-cryomilled mixture with 50% drug loading was used in the formulation of an orodispersible tablets (ODTs). Six different formulations were manufactured using different superdisintegrants such as F-melt and Glycolate. All the co-cryomilled formulas showed a higher release of felodipine compared to the physical mixtures.

Obtaining miscible and stable amorphous solid dispersions without heat or solvent through co-cryomilling is promising as a manufacturing method. Use of heat or solvents can lead to instability in the dispersions and degrade certain drugs. Following this work, amorphous solid dispersions formed via co-cryomilling with a high drug loading can be considered for future development for the formulation of fast release dosage form and for drugs liable to thermal or solvent mediated degradation.

Acknowledgements

My deepest gratitude to my supervisor **Dr. Jonathan Burley** for all of his kind support, encouragement and enthusiasm during my PhD study and completion of this project. He always cares about his students and encourages them to make greater achievements in their work. I am deeply indebted to my second supervisor **Professor Clive Roberts** for his active guidance and advice.

To my friends in Boots Science Building for their help (Masar Mohamed, Laudina Safo, Dr.Vincenzo Taresco, Mohamed Elustohy and Mary Kyobula). Special thanks to the former PhD student, Dr. Andrew Megarry for his support at the start of my PhD. Thanks to Miss Laura Mason for her support on the use of the tablets machine and to Mrs. Gudrun Fridgeirsdottir for the HME work support.

To my family; my Mother, my father and my sisters for all their support and encouragement. A big thank you to the sacrificial husband,♡ Bashar ♡, who encouraged and supported me during my study.

Finally I would like to thank my sponsor the Ministry of Higher Education and Scientific Research in Iraq (MOHESER) for funding.

Contents

List of Figures

List of Tables

Abbreviations

ATR-FTIR	Attenuated total reflectance- Fourier Transformed Infrared Spectroscopy
BCS	Biopharmaceutics Classification System
CSD	Cambridge Structural Database
DCS	Developability Classification System
DSC	Differential Scan Calorimetry
EP	Europin Pharmacopia
FDA	Food and Drug Administration
GFA	Glass Forming Ability
HME	Hot Melt Extrusion
HPMC	Hydroxy Propyl Methyl Cellulose
HPMCAS	Hydroxypropyl Methyl Cellulose Acetate Butyrate
ODT	Orodispersible Tablet
PMMA	Poly Methyl Methacrylic Acid
PVP	Poly Vinyl Pyrrolidone
SEM	Scanning Electron Microscopy
USP	United States Pharmacopeia
XRPD	X-ray Powder Diffraction

Symbols

A	surface area
B	basic drug
B	half-value breadth in 2θ
C_s	the saturated solubility
C	instantaneous solubility
CED	cohesive energy per unit volume
h	thickness of the diffusion layer
HA	weak acidic drug
K	constant = 0.93
pKa	negative logarithm of the acid dissociation constant Ka
T_g	glass transition temperature
V_m	molar volume
W_i	weight fraction of each component
ΔE_v	energy of vaporisation
ΔH_f	heat of fusion of crystalline
$\Delta H_f m$	heat of fusion of the milled
ΔH_r	recrystallisation heat
λ	wave length of incident X-ray

θ	Bragg angle.
ρ_i	density

Chapter 1

Introduction

1.1 Dissolution and solubility in oral solid dosage forms

Oral solid dosage forms are the most common method for the administration of drugs. About 65%-70% of the marketed dosage forms are solid forms that include tablets and capsules [7]. In general, oral solid dosage forms are preferred over liquid or semisolid due to the lower cost of manufacturing, better physical and chemical stability, smaller pill burden and greater convenience for combination of drugs [1, 8, 9]. About 55% of current drugs in the market and about 80% in the research and development pipeline are poorly water soluble [10]. There is a challenge in the formulation of these poorly water soluble drugs into oral solid dosage form due to the small surface area of the tablet which results in lowering the bioavailability [1]. Figure 1.1 shows how tablet disintegration affects the surface area and rate of drug dissolution.

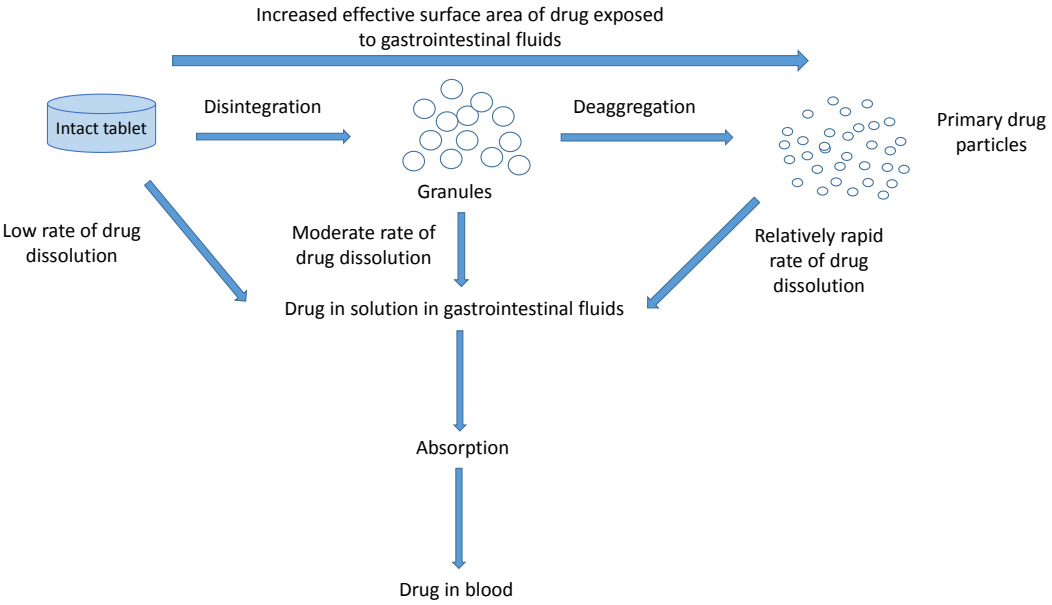

Figure 1.1: Mechanistic representation of the drug release process from a tablet by disintegration and dissolution. Adapted from reference [1], not to scale.

Dissolution can be defined as "transferring the molecules or ions from the solid state into solution" while solubility "is the amount of solute that passes into solution when equilibrium is established between the solute and the excess of undissolved substance" [1]. Dissolution rate is influenced by factors giving in the Noyes-Whitney equation (see Equation 1.1.1) which are outlined in Table 1.1.

$$\frac{dm}{dt} = \frac{DA(C_s - C)}{h} \tag{1.1.1}$$

Where dm/dt is the rate of the drug dissolution, D is the diffusion coefficient, A is the effective surface area of the solid, C_s is the saturated solubility, C is the instantaneous solubility and h is the thickness of the diffusion layer.

Factors that affect the solubility of the drug include, the temperature, pH, solid state (amorphous or crystalline), polymorph type, counter ion (salt formation) and the component of the dissolution media as outlined by Stegemann *et al* [11].

Table 1.1: Factors affecting the *in vitro* dissolution rates of solid in liquid. This table adapted from reference [1].

Term in Noyes-Whitney equation	Affected by
A, Surface area of un dissolved solid	Size of the particles
	Porosity of solid particles
Cs, Solubility of solid in dissolution medium	Temperature
	Nature of the dissolution media
	Molecular structure of solute
	Crystalline form of solid
	Presence of other compounds
C, Concentration of solute in solution at time t	Volume of dissolution medium
	Any process that removes dissolved solute from the dissolution medium
k, Dissolution rate constant	Thickness of boundary layer
	Diffusion coefficient of the solute in the dissolution medium

1.2 Biopharmaceutics Classification System (BCS) and the Developability Classification System (DCS)

In order to understand the physicochemical and biopharmaceutical characteristics of drugs, four categories are commonly used according to the Biopharmaceutical Classification System (BCS). This system depends on the solubility and intestinal permeability of the drugs [12]: class I (good solubility and permeability), class II (poor solubility and good permeability), class III (good solubility and poor permeability) and class IV (poor solubility and permeability). Butler and Dressman in 2010 introduced a modification to BCS by using 500 mL as realistic volume of dissolution in the GI tract instead of 250 mL that was used by Amidon *et al*, called Developability Classification System DCS [2]. This modification results in classification of class II drugs into either dissolution rate limited or solubility limited [2]. The original and modified classification can be seen in Figure 1.2.

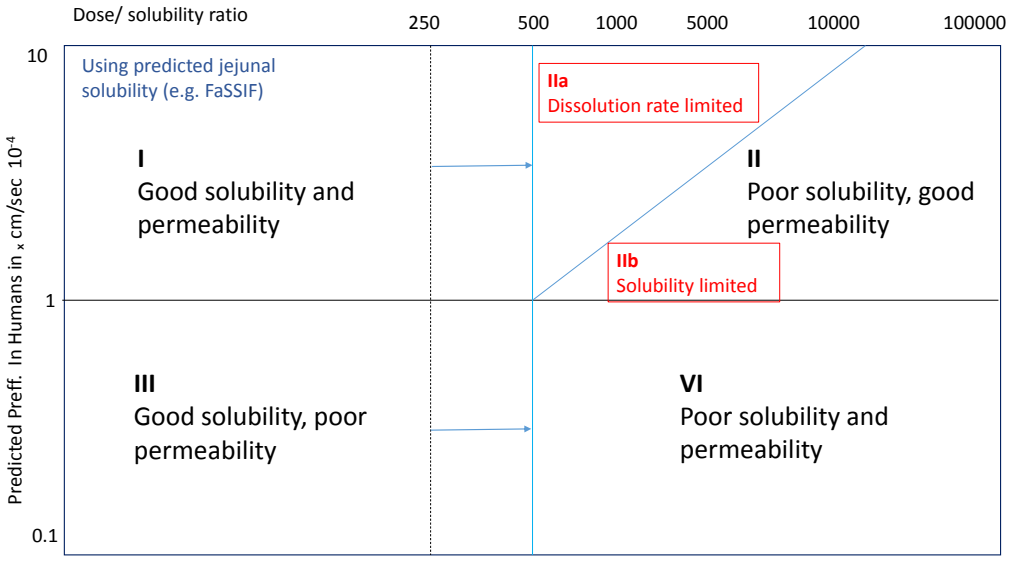

Figure 1.2: Modifying the BCS for more realistic volumes of fluid available in the GI tract and the compensatory nature of permeability on low solubility (modifications from the BCS to DCS are shown in blue). Adapted from reference [2].

1.2.1 Strategies to overcome poorly water soluble drug problems

Current strategies that tend to improve poorly water soluble drug bioavailability are divided into two main categories which are either to improve the dissolution rate or solubility, these include: particle size reduction [13], crystal modification [14], complexion [15], lipid based formulation [16], amorphous solid dispersions [17] and prodrug [18].

Starting with the first strategy of particle size reduction, the reduction in particle size results in increasing surface area of particles and hence dissolution rate according to Noyes-Whitney equation. In addition to increasing the surface area, particle size reduction can result in increased wetting of the particles via reduction of its surface roughness [19]. This reduction can be achieved through milling process [20] as in milling of cilostazol resulted in increasing its dissolution rate and bioavailability [21]. However, particle size reduction can result in polymorphic transformation and/or amorphisation which are considered as unstable forms that might cause stability problems in the final products [22].

The second strategy includes salt and cocrystal formation both of which are examples of crystal modification. Salt formation is a commonly used technique in the pharmaceutical industry to increase the solubility of poorly water soluble acidic or basic drugs [23] in which the difference between the pKa of acid and its base should be 3 and above [24]. An example is the salts of piroxicam monoethanolamine which improves the solubility of piroxicam [25]. The salt form is not suitable for un-ionisable drugs. The major disadvantage of salt formation is the possibility of precipitation after oral administration inside the GI tract [23]. In contrast cocrystal (multi-component molecular crystal) can be obtained form non ionisable molecules in addition to the ionisable one and there is no limitation in the pKa of the molecules that form the cocrystal [14, 26]. In the cocrystal there is no requirement for proton transfer between the molecules but it requires a H-bond to be formed between the molecules that are involved

in the cocrystal structure [27]. An example is danazol and vanillin cocrystal that improved the physiochemical properties of danazol [28].

The use of cyclodextrins is another strategy to improve the dissolution. They are oligosaccharides containing a relatively hydrophobic central cavity and hydrophilic outer surface [29]. There are some toxicological considerations for some cyclodextrins such as nephrotoxicity, GI tract diarrhoea and hemolytic effect, however, this depends on the route of administration of the complex, type of cyclodextrin and dose of the complex [30].

Lipid formulation strategy involves inclusion of the drug in lipid system such as triglycerides, mono and diglycerides, lipophilic surfactants, hydrophilic surfactants and cosolvents [31] that enhances the oral absorption of lipophilic drug [32]. It was proposed that these types of dosage form work through increases the gut permeability and lymphatic transport. Example of drugs that are formulated as lipid based formulation that are commercially available in the market are cyclosporine, ritonavir and saquinavir [32].

Prodrug is another strategy which involves using chemicals with little or no pharmacological activity, undergoing biotransformation to a therapeutically active metabolite [33]. This approach increases the bioavailability of poorly water soluble drugs [34] such as zofenopril which is an ester prodrug [34]. The challenges in the production of prodrug include: the time and cost for synthesis, physicochemical, toxicological and pharmacokinetic assessment [33].

Amorphisation is another strategy to improve drug dissolution. The detail of this method will be described in the next Section 1.3.

1.3 Amorphisation

Crystalline material can be transformed into the amorphous form through four main different routes: supercooling of melt, precipitation from solvents, milling and vapour condensation [35]. The details of the main methods (spray drying and HME) will be discussed in the amorphous solid dispersions parts in

Section 1.4.1.

Non intentional amorphisation via milling

Pharmaceutical companies use milling mainly during pharmaceutical processing such as particle size reduction and mixing [36–38]. Disorder in the solid is sometimes observed by accident during assessing product stability [36]. Milling might result in partial amorphisation which might cause instability of the final product or it might cause polymorphic transformation as that observed on milling of γ indomethacin or milling of α chlorporpamid [39, 40]. Energy formed from the milling process can produce a strain that can cause a fracture then dislocation in the crystal lattice (defect formation) [38, 41]. This results in formation of new surfaces, cracks, defects, nuclei due to the considerable interference of local arrangement of the molecules or it might act as an exothermic reaction [37, 42]. Accumulation of crystalline defects from the milling process can cause amorphisation eventually. Amorphous formation might also result from local melting then quenching of the crystalline materials [43, 44].

Amorphous formation from milling processes depends mainly on the type of milling, milling temperature, humidity, nature of the crystalline material (hydrous or anhydrous) and the type of starting polymorph [36, 41, 45]. It was reported by Willart *et al* that anhydrous crystalline sugars can be transformed by milling into the amorphous form while it was not observed in the milling of hydrous form [45]. Milling can either result in transformation from one polymorph to another such as in case of sulfamerazine I transformation observed into form II after 2 hours room temperature milling [46] or it might result in partial amorphisation such as in the case of indomethacin at room temperature after milling for 10 hours. In contrast, the amorphous form can be obtained from milling of indomethacin for 2-4 hours at 4°C which is below its T_g [47]. Milling of indomethacin at cryogenic temperature results in transformation into amorphous within 20 minutes cryomilling [41]. Descamps *et al* reported that milling of the compound below its T_g results in amorphisation while milling above T_g results in crystal defect. This finding refutes the theory that suggested

amorphisation upon milling results only from local melting of the material being milled followed by quenching [43].

Cryomilling is milling under liquid nitrogen temperature (-196 °C). Milling at cryogenic temperature guarantees milling of the crystalline material below its T_g and reduces the chance of recrystallisation that occurs during milling process [48–50]. Obtaining brittle materials upon cryomilling enhances particles cracking, minimises the energy required for milling, reduces plastic deformation and the chance for particles aggregation [51, 52].

Cryomilling is nowadays under some researchers interest such as Thomas Rades, Anne Marie Healy, Rodolfo Pinal, Peter Wildfong and others. The reported work on cryomilling APIs alone was varied from studying the amorphisation tendency of APIs upon cryomilling such as the work reported by Wildfong *et al* and other cryomilling work on different APIs [38, 49, 53]. Wildfong *et al* reported that some crystalline materials cannot transformed into amorphous form despite long milling time such as aspirin, paracetamol, salicylamide and other materials as seen in Table 1.2 and this was explained in the context of a critical dislocation density model [50]. Some work focuses on differentiation between the amorphous form and crystalline defect such as the study that reported by Rodolfo Pinal *et al* [54]. Others focus on the effect of cryomilling mainly in nanocrystal production and others focus on cocrystal formation upon cryomilling [59, 60].

Milling time was the interest of some researchers due to its role in the transformation of the materials [48]. The effect of cryomilling time on amorphisation tendency was reported on sulfathiazole form I and III in which short milling time results in crystalline defect while longer milling time results in amorphisation [48, 61]. In addition the effect of milling time was reported on griseofulvin in which short milling time results in crystalline defect rather than amorphous transformation [54] while longer milling time for 60 minutes and more results in amorphous formation as reported by Chattoraj *et al* [55]. Milling time affects the recrystallisation behaviour of different sulfamerazine forms I and II [62]. Increasing milling time is also important in improving dissolution rate as in-

Table 1.2: Reported work of the cryomilled APIs.

Materials	Cryomilling time in minutes	Reported T_g in °C	References
D-Trehalose	300	108.7	[38]
D(+)-Trehalose dihydrate	300	26.3	[38]
D-(+)-Trehalose dihydrate	30	21	[49]
β-D-lactose	300	94.6	[38]
α-D-lactose monohydrate	300	45	[38]
Etravirine I and II	180	99	[48]
Sucrose	300	71	[37]
Glibenclamide	180	69	[53]
Griseofulvin	60	60	[37]
Griseofulvin, Felodipine	10	no	[54]
Griseofulvin	4-30	no	[3]
Felodipine	60 and 120	46	[55]
Sulfathiazole III and I	2-180	55.8 and 54.7	[56]
Sulfathiazole III	300	55.3	[38]
Carbamazepine III	300	51.9	[38]
α, β, γ Indomethacin	60	39-45	[41]
γ-Indomethacin	300	37	[38]
Ranitidine hydrochloride I	60	26	[57]
Simvistatin	90	27	[58]
Cimetidine	300	20	[38]
Ketoprofen	300	-4	[38]
Salicylamide, Aspirin, Acetaminophen I, Sulfadiazine, β-D-mannitol, Tolbutamide I, Theophylline, Ibuprofen, Naproxen, β Piroxicam, β Sulfanilamide	300	no	[38]

vestigated by Thomas Rades *et al* on cryomilling of indomethacin for 120, 280 and 240 min [63]. Previously reported work on cryomilling of different APIs can be seen in Table 1.2. Most of the APIs that are either milled or cryomilled are unstable, therefore, there is a need of a carrier for their stabilisation to what are called amorphous solid dispersions.

1.4 Amorphous solid dispersions

An amorphous solid dispersion can be defined as "a mixture comprising an amorphous drug and a carrier dispersed at the molecular level" [64]. Polymers are the most frequent carrier that are used in the stabilisation of the amorphous solid dispersions. The most common polymers that are routinely used in the production of amorphous solid dispersions are poly(vinylpyrrolidone) (PVP), poly(vinylpyrrolidone/vinyl acetate copolymer), hydroxypropylmethyl cellulose (HPMC), hydroxypropylmethyl cellulose acetate/succinate (HPMCAS), hydroxypropylmethyl cellulose phthalate (HPMCP) and the acrylic acid-based enteric Eudragit systems [8]. Using polymers as a carrier system for preparation of amorphous solid dispersions was studied by many researchers such as Lynne Taylor, George Zografi, Ann Newman and many others [8, 35, 65–71]. Another carrier for stabilisation of the amorphous form is co-amorphisation by mixing the drug with small molecular weight carrier such as citric acid in order to stabilise it or mixing two drugs together or mixing with amino acid. These had been studied by some researchers as a tool for stabilisation amorphous solid dispersion [35, 72, 73].

Characterisation of amorphous solid dispersions was reported by different methods including: X-ray powder diffraction (XRPD) which is a gold standard method for investigation of crystalline material even at low concentration [74]. This method also can be used for estimation of the crystalline content and particles size through the Scherrer equation [75] which will be detailed in Section 2.3.3 in Chapter 2. The second method for characterisation of amorphous solid dispersions is thermal analysis by Differential Scanning Calorimetry (DSC). DSC

measures the change in heat capacity associated with solid to liquid transition. Furthermore, the T_g plays an important role in the predication of miscible amorphous solid dispersions or stability study that will be discussed in Section 1.5 and more detailed discussion will be appear in Chapters 2 and 3. Typical range of pharmaceutical material T_g's for APIs and excipients is between -100 to +250 °C [76]. Other methods of characterisation involve spectroscopic methods such as FTIR and Raman. AFM and NMR have been also reported [77–79].

1.4.1 Current techniques in the production of amorphous solid dispersions

Hot melt extrusion (HME)

HME is a process of embedding a drug within thermoplastic polymer and/or binder then heating the mixture above its T_g or above melting point until softening. The dispersion results due to high shear mixing and/or drug polymer interaction [80–83].

HME has been widely applied in food and plastic manufacturing and in the pharmaceutical processing and formulation such as production of pellets, implant, tablet, transdermal formulation [81, 83, 84]. It is preferred over spray drying because it is single process, shorter time, solvent free (more environmentally friendly) and lower cost than spray drying [80–83, 85]. An example of an API that processes by HME is itraconazole with HPMC [86]. The main disadvantage of HME is the thermal degradation for heat sensitive materials [82].

Spray drying

It is a process that involves solubilising of drug and carrier into suitable solvent followed by evaporation of this solvent from the solution or the suspension that formed to transform it into solid product [87–89]. It is used in pharmaceutical processing such as granulation, encapsulation and in pulmonary dosage form [87]. An example of API that formulated as amorphous solid dispersions

by spray drying is ketoconazole with polyvinylpyrrolidone K25 [90]. This technique is suitable for thermosensitive material where HME is contraindicated [89]. Despite this advantage, many limitations for this technique such as the long time required for the production and the usage of solvent that results in additional time, cost and hazard (if organic solvents used). Furthermore, there might be a stability issue that results from the residual solvent that might entrapped in the product [91] and finally some drugs such as aspirin can be unstable in the presence of solvent that can cause hydrolysis [92]. Table 1.3 shows the marketed drug which are formulated as amorphous solid dispersions.

1.4.2 Co-milling and co-cryomilling

Co-milling is milling of two ingredients together either at room temperature or under controlled temperature. If the co-milling was under liquid nitrogen temperature then it is called co-cryomilling. It is important to differentiate between these terms. Co-milling was reported by many researchers such as Marc Descamps and Thomas Rades [93–96]. Co-milling either includes milling the two APIs as investigated by Thomas Rades such as co-milling naproxen with cimetidine (60 minutes at 4°C), indomethacin with ranitidine (60 minutes at 4°C), simvastatin and glipizide (ball milling and cryomilling 60 minutes) [72, 73, 93]. Other work includes co-milling an API with small molecules such as amino acid or other excipients (milling of carbamazepine and indomethacin with amino acid binary and ternary mixtures [94, 94]) or milling ketoprofen, naproxen, and indomethacin with Neusilin (6-24 hour) and budesonide with α-lactose for 12 hours [97, 98]. Examples of co-milling API with polymer includes: milling carbamazepine, dipyridamole, and indomethacin with PVP 120 minutes, indomethacin with PVP K12 at -8°C for 8 hours and Glisentide wih PVP for 120 minutes [95, 96, 99, 100]. Co-milling also involves milling of two excipients such as milling of α anhydrous trehalose with mannitol [101]. All the reported co-milling work demands long milling time to achieve amorphisation. Shorter milling time either results in incomplete amorphisation or causes rapid recrystallisation. Furthermore, PVP seems to be the only polymer used in all reported

Table 1.3: Marketed amorphous drug products. This table adapted from reference [4].

Compound	Trade name	Manufacturer	Carrier	Processing technology	Dosage form
Amorphous solid dispersions (ASDs)					
Etravirine	Intelence®	Janssen	HPMC	Spray drying	Tablet
Everolimus	Certican® /Zortress®	Novartis	HPMC	Spray drying	Tablet
Fenofibrate	Fenoglide®	LifeCycle Pharma	PEG	Spray melt	Tablet
Griseofulvin	Gris-PEG®	Novartis/Pedinol	PEG	Melt extrusion	Tablet
Itraconazole	Sporanox® / Onmel®	GlaxoSmithKline/Stiefel	PVP VA 64	Melt extrusion	Tablet
Ivacaftor	Kalydeco®	Vertex	HPMCAS	Spray drying	Tablet
Lopinavir and Ritonavir	Kaletra®	AbbVie	PVP VA 64	Melt extrusion	Tablet
Nabilone	Cesamet®	Lilly/Valeant	PVP	Melt extrusion	Capsule
Nifedipine	Afeditab® CR	Elan/Watson	Poloxamer or PVP	Melt/absorb on carrier	Tablet
Nilvadipine	Nivadil®	Fujisawa	HPMC	-	Tablet
Nimodipine	Nimotop®	Bayer	PEG	Spray drying/fluid bed	Tablet
Posaconazole	Noxafil®	Merck	HPMCAS	Melt extrusion	Tablet
Ritonavir	Norvir®	AbbVie	PVP VA 64	Melt extrusion	Tablet
Tacrolimus	Prograf® /LCP-Tacro®	LifeCycle Pharma/Veloxis	HPMC	Melt granulation	Tablet
Telaprevir	Incivek® /Incivo®	Vertex/Janssen	HPMCAS	Spray drying	Tablet/Capsule
Troglitazone	Rezulin®	Pfizer (Parke-Davis)	PVP	Melt extrusion	Tablet
Vemurafenib	Zelbora®	Roche		Coprecipitation	Tablet
Verapamil hydrochloride	Isoptin® SR-E 240	AbbVie	HPC/HPMC	Melt extrusion	Tablet
Pure amorphous drugs					
Cefuroxime axetil	Ceftin®	GlaxoSmithKline	-	-	Tablet
Nelfinavir mesylate	Viracept®	Agouron/Pfizer/Roche/ViiV Healthcare	-	-	Tablet
Quinapril hydrochloride	Accupril ®	Pfizer	-	-	Tablet
Rosuvastatin calcium	Crestor®	Shionogi/Astra Zeneca	-	-	Tablet
Zafirlukast	Accolate®	Astra Zeneca	-	-	Tablet

API-polymer works. The previously reported work on co-cryomilling for short time aimed to ensure mixing between components and for reduction of particle size such as milling indomethacin and nifedipine with PVP, PVP/VA, PVAc, d-Mannitol with PVP, doxorubicin with silica-nanoparticle/polycaprolactoneas and phenytoin with some excipients as reported by [102–105]. The only reported work of co-cryomilling was done by Marc Descamps *et al* on co-cryomilling of piroxicam and indomethacin with PVP [106, 107]. Again these two studies used only PVP as polymer for production of amorphous solid dispersion which has a stability problems upon storage in humid conditions. In addition the studies only covered a very limited range of drugs which are piroxicam and indomethacin by milling and co-milling. The current piece of work will investigate co-cryomilling of three different APIs (which was selected according to the variation of T_g with the room temperature) with HPMC (a widely used polymer in production of amorphous solid dispersion by HME and spray drying) for 150 minutes and the second parts of our study will focus on co-cryomilling of felodipine that was widely reported in production as amorphous solid dispersions (by spray drying and HME). Felodipine will be co-cryomilled with different types of biodegradable polymers and polymers mixes that are not reported in any co-milling or co-cryomilling work before but were studied in common methods for production of amorphous solid dispersions such spray drying and HME.

1.5 Stability of amorphous solid dispersions

Single phase amorphous solid dispersion is important for long term stability and prolongation of supersaturation during dissolution [8]. Generally, a single phase amorphous solid dispersion is formed when there is a single T_g achieved between the drug and the carrier [8]. Polymers stabilise the amorphous solid dispersion through: elevation of the T_g which can result in reducing the molecular mobility, reduction of the drug chemical potential, formation a drug-polymer interaction [108], steric effect and hydrophobic interaction [109]. Formation

of H-bond between the drug and the polymer was thought to participate in inhibition of crystallisation even at low polymer concentration and results in prolongation of supersaturation of the drug during dissolution [8]. However, this is not necessarily the case in the presence of moisture [110] where moisture results in recrystallisation of the API in the solid dispersions by water plasticising effect (reduction of the T_g) because water T_g is about -134 °C [111]. Hygroscopic polymers aggravate the effect of moisture on the crystallisation of amorphous solid dispersions [112]. Another factor that worsens the stability of amorphous solid dispersion is the temperature. Storage of the amorphous solid dispersions at higher temperature than their T_gs results in recrystallisation of the APIs [35]. Stability of the amorphous solid dispersions is the interest of many researchers such as Lynne Taylor, Ann Marie Healy, Ann Newman, Guy Van den Mooter and many others [8, 70, 90, 108, 113–116].

Miscibility between the drug and carrier is important in the stability of the amorphous solid dispersions as mentioned earlier in this section. Miscible blending means a single T_g is formed between drug and carrier which can be detected by using the DSC technique. Furthermore miscibility can be predicted from the Gordon Taylor equation and from solubility parameter value (this will be detailed in Section 3.4.5 in Chapter 3). Other prediction model used is the Flory-Huggins interaction parameter. The miscibility of amorphous solid dispersions prepared by spray drying and HME was used as a tool prior to stability study was reported before by many researchers [117–120].

Felodipine stability and miscibility in amorphous solid dispersions prepared by HME and spray drying were also studied before [71, 114, 115, 121–123]. In the present piece of work the miscibility of felodipine prepared by co-cryomilling is done for the first time, in addition, the stability study of amorphous solid dispersions is also investigated here by co-cryomilling to see its effect on maintaining the amorphous within the amorphous solid dispersion as new method for production of amorphous solid dispersion.

Combination of hydrophilic and hydrophobic polymer or surfactant/polymer was previously reported for better inhibition of crystal growth than using sin-

gle polymer and also important in maintaining supersaturation at the same time as reported before by Ilevbare *et al* [124, 125] for protection of ritonavir, celecoxib and efavirenz prepared by spray drying method. The usage of surfactant/polymer or polymer/polymer mixture combination was also reported by Van den Mooter and his group for maintaining the supersaturation of anti-HIV drug UC 781 [126, 127] and on itraconazole [128, 129]. A combination of hydrophilic and hydrophobic polymer for solid dispersions prepared by co-cryomilling is introduced for the first time in our study.

The amorphous solid dispersion produced by co-cryomilling tends to increase both solubility and dissolution rate. Both are important in the formulation of poorly water soluble drugs to fast acting formulation such as ODTs.

1.6 Orodispersible tablet

Orally disintegrating tablets or orodispersible tablets (ODTs) are solid oral dosage forms in which the disintegration and dispersion occur in the mouth cavity where the absorption might occur either partially or completely [130] depending on whether the patient keeps the tablet for short time for complete absorption or swallows it directly. The definition varied slightly between United States Food and Drug Administration (FDA) and European Pharmacopoeia (EP) in which the former defined it as the dosage from that disintegrate within seconds while EP define the disintegration time to be within 3 minutes before swallowing [130, 131].

Fast onset of action and the usage of this dosage form in patients with swallowing difficulties such as paediatric, geriatric medication and patients with dysphagia are the main aims for formulation of the ODTs [132–134]. There is no need for water intake with the medication. The main advantage is the bypassing the hepatic first pass effect because this dosage form enables absorption of the medication to systemic blood circulation before entrance to the main GI tract [135–137]. There are certain requirements in their production which includes: acceptable mouth taste, minimum irritation to the mouth cavity, least

humidity during manufacturing and the tablets should be strong enough to withstand processing, packaging and handling [130].

Poorly water soluble drug is the main stumbling block in the formulation of ODTs as these types of formulations require water soluble drug and/or fast dissolution rate [138]. To solve this problem all of the strategies that were mentioned earlier in Section 1.2.1 can be applied. Felodipine is a calcium channel blocker which is an important drug in the treatment of hypertensive crisis in the emergency due to lack of the negative inotropic effects on the heart [139]. Its poor water solubility is the main hurdle on its formulation as an ODT dosage from. The only rapid onset route of administration of felodipine is the intravenous route [140, 141]. It was reported before that felodipine was formulated into ODTs through HME and spray drying methods [142, 143]. Our work will involve optimisation of felodipine release by co-cryomilling into amorphous solid dispersions which according to DCS will increase both solubility and dissolution rate. Formulation through cryomilling was not reported before for this dosage form or any dosage forms. Processing of ODTs was previously reported including different methods such as lyophilisation (freeze drying), cotton candy process, moulding and compaction such as wet granulation, dry granulation and direct compression [144, 145].

1.7 Aim and objectives

The aim of this Ph.D. is to produce an amorphous solid dispersions via cryomilling technique that can be used by the pharmaceutical industry for poorly water soluble drugs to increase both the solubility and the dissolution rate limited class II drugs.

Objectives:

1. Study the amorphisation tendency of three different APIs, felodipine, paracetamol and aspirin via cryomilling in the presence and absence of HPMC (a widely used polymer for production of amorphous solid disper-

sions by HME and spray drying).

2. Investigate the miscibility and stability of felodipine:polymer dispersion made by cryomilling.

3. Investigate the role of mixing polymers with the API and their impact on the long term stability by co-cryomilling.

4. Assess the potential of cryomilling in making realistic formulations.

5. Study the role of cryomilling on felodipine which is used as model poorly water soluble drug. It has a potential clinical application for fast acting formulation as an ODTs because is only available as prolonged release formulations in the market.

The hypothesis of this work is that the amorphous form of these three drugs can be stabilised by cryo-milling with different types of polymers.

Chapter 2

Cryomilling as an alternative method for the production of amorphous solid dispersions of poorly water-soluble drugs

2.1 Novelty in this chapter

The potential of co-cryomilling drug/polymer blends to produce amorphous solid dispersions, both for APIs that can be processed using conventional methods and for APIs which exhibit chemical instability and therefore cannot be converted to amorphous solid dispersion formulations using conventional methods.

2.2 Introduction

For an orally administered drug to be effective *in-vivo* it needs to dissolve in the gastro-intestinal tract and be absorbed into the circulatory system. However, more than 55% of current drugs on the market and about 80% in the research and development pipeline have poor water solubility that can potentially limit

bioavailability [10]. If no suitably soluble crystalline form of a drug e.g. polymorph, solvate etc. or salt can be found then the use of the amorphous state is the preferred option [146]. The amorphous form of a drug offers increased apparent solubility compared to ordered crystalline forms, but in general has relatively poor physical stability, often converting to an ordered (and hence less soluble) form (recrystallisation). Such conversion cannot be allowed for a commercial product and hence methods of stabilisation are often sought. The amorphous form can, for example, be stabilised by entrapment in a nano or molecular dispersed state within a stable water-soluble matrix to form a so-called amorphous solid dispersion [82, 146, 147].

In pharmaceutical systems the amorphous form (e.g. pure drugs or drug-polymer glass solutions) is prepared by two main methods; hot melt extrusion (HME) and spray drying [67, 108, 116, 125, 148–151]. Water-soluble polymers such as PVP and HPMC are commonly used as the matrix in such amorphous solid dispersion formulations. For example, HPMC is effective in hindering drug crystal growth when miscible blends are prepared with poorly soluble drugs such as felodipine and ritonavir [152]. However, these common methods are not without problems. Thermal degradation of heat sensitive materials that are prepared by HME [147] and solvent usage problems in spray drying [89] are significant hurdles in the preparation of amorphous solid dispersions.

Milling is a pharmaceutical process used in general for particle size reduction and also to encourage proper mixing of multi-component powders [153]. Milling has also been reported to cause the formation of amorphous material in some cases [154]. Milling hence offers a potential alternative method of amorphous material production. Although milling above materials glass transition temperature (T_g) might result in obtaining amorphous material, this amorphous material generally rapidly recrystallises [3] and hence lose the enhanced bioavailability. A potential solution is to mill below the T_g. This can normally be achieved in liquid nitrogen at -196 °C (cryomilling) to minimise recrystallisation [39, 43, 155–161]. Amorphous formation by cryomilling has been reported as a cost effective [51], single step process that avoids solvent usage and minimises thermal degrada-

tion. Milling of drug and polymer together at cryo-temperatures is one method of amorphous stabilisation [162].

Cryo-milling had been applied to some APIs alone without polymer with varying milling time for felodipine, paracetamol, aspirin and many other drugs [56, 116, 154]. It was previously reported that relatively long milling times (such us the 150 minutes used in our work or longer) is important to ensure complete conversion of the crystalline API on its own into amorphous from, to avoid polymorphic transformation and to slow the recrystallisation [62, 63, 163, 163]. For example, Botker *et al* studied the effect cryomilling time of indomethacin on its transformation and stability showing that longer times were beneficial [163]. There is a very limited amount work undertaken on formulating drug/polymer amorphous solid dispersions using cryomilling. Work to date tends to focus on encouraging mixing via short cryomilling time 5 minutes and less after processing by other methods. The only reported drug-polymer amorphous solid dispersion was from the Descamps group [106, 107]. These results were very promising but it is not indicated how it applicable in a pharmaceutical setting. Here we further explore the use of cryomilling as an alternative method to produce amorphous solid dispersions when heat (HME) or solvent (spray-drying) are not applicable. Felodipine is used in our study as an example drug. Felodipine has used to produce a solid dispersions via HME and spray drying [108, 110, 113, 115, 121, 148, 164–166]. Paracetamol is also considered here, for which there are only few papers that consider its processing as an amorphous solid dispersion by conventional methods [82, 167–169]. Finally, aspirin where there is no report of amorphous solid dispersion formation is also studied in this work. Paracetamol and aspirin have been reported as being significantly difficult to convert to the amorphous form due to their critical dislocation density, whereby they are resistant to complete mechanical disordering and remained fully crystalline [50].

Glass-forming ability (GFA) is defined as the easiness to vitrify a liquid on cooling [170]. Non glass-formers are defined as class I compounds. Those which crystallise on heating the melt-quenched material above the T_g, are defined as

class II compounds, and compounds that showed no sign of crystallisation on heating the melt-quenched material were classified as class III compounds [171] (note: in our study we are not making glass by cooling a liquid). We have selected three drugs with different properties as listed in Table 2.1. Previously works has focused on drugs that can easily be made amorphous, however, this does not give a good indication of how generally cryomilling would be applicable in formulation manufacture. The range of compounds selected here mean that this work has the potential to provide a route to amorphous solid dispersion even for drugs which cannot be processed by other methods such as aspirin. The manufactured cryomilled mixture formulations will be subject to stability testing to help assess whether this represents a sensible potential route for formulating drug-polymer amorphous solid dispersions.

Table 2.1: Properties of the selected APIs

API	T_g in °C	pKa	GFA	M.wt in Dalton	Solubility in water
Felodipine	46.4 [114]	2 [172]	III [171]	384.3 [171]	less than 0.5 μg/ml [172]
Paracetamol	24 [50]	9.5 [173]	II [171]	151.2 [171]	14.7 μg/ml [174])
Aspirin	-29 [50]	3.5 [175]	I [171]	180.2 [171]	3.3 mg/ml [176, 177]

In this chapter the selected drugs were mixed with HPMC either by co-cryomilling, or by separately cryomilling the API and the polymer then blending. Potential dispersions produced in these formulations were evaluated using differential scanning calorimetry (DSC) and powder X-ray diffraction (XRPD). Dissolution performance was measured using a standard USP II method. We compare and contrast the resultant formulations produced for the three drugs and discuss the potential of cryomilling as a practical method for the manufacture of solid dispersions.

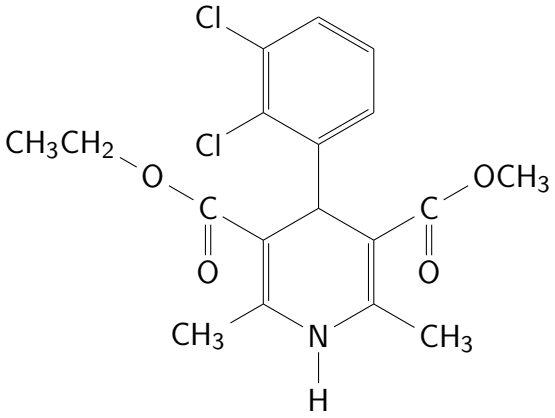

Felodipine

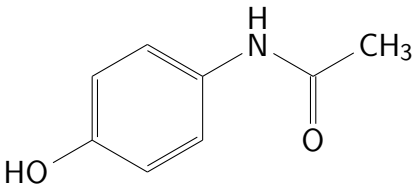

Paracetamol

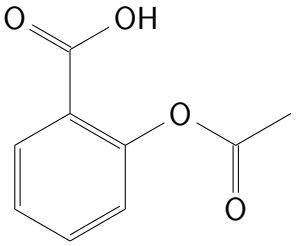

Aspirin

Figure 2.1: Chemical structure of the selected APIs

Cambridge Structure Data Base CSD to predict the possibility of H-bond formation:

The Cambridge Structural Database (CSD) is a repository for reported crystal structures of small molecules (ca. 850,000 entries as of 2016). It is widely used in fields such as crystal engineering, crystal structure prediction, structure solution from powder diffraction, and protein-ligand binding [178]. Specific examples include the confirmation of the existence of the "halogen bond", typically between C-F and electrophiles or nucleophiles [179]. In studying inter-molecular interactions using the CSD, the basic premise is that if a given bonding motif is energetically favourable, it will occur frequently in the database, and a plot of database reports of key inter-molecular distances for that bonding motif will produce a histogram with a tight distribution of distances around the "ideal" bonding distance for that motif. For a strong interaction this "ideal" distance will

be less than the sum of the Van der Waals radii of the relevant atoms [180]. It is therefore possible to use a CSD search predictively, to see whether a particular inter-molecular interaction is expected to be strong (many reports, tight distance histogram) and therefore likely to be of importance in systems having similar chemical functionality, or weak and therefore relatively unimportant. This approach is very well established and forms the basis of much of the field of crystal engineering for example [181].

The vast majority of crystal structures reported in the CSD are determined from single-crystal X-ray diffraction. As X-rays interact with electrons, the outcome is that the positions of hydrogen atoms are not determined well using this method. When discussing hydrogen bond lengths X-H...Y reported in the CSD it is therefore appropriate and conventional to report Y...Y distances rather than H...Y [182].

In this thesis the CSD was used to evaluate the probability of strong H-bonding interactions occurring between selected functional groups on the API and polymer, in order to evaluate whether or not ASD formation was likely to be governed by specific API-polymer interactions. This was achieved by searching in the CSD for the posited interactions and using both the frequency of the relevant motif being reported, and relevant distance histograms measuring the proximity of the two functional groups forming the motif. Note that this approach is not a direct measurement of H-bonding between the selected APIs and polymers used in this thesis, and that this CSD approach is best used for the purposes of predicting likely H-bonding motifs, and/or for rationalising or contextualising data on H-bonding such as shifts in IR peaks, etc.

The CSD was used to investigate the hydrogen-bond length between the donor and acceptor group as reported in [183]. If the donor group is termed X-H and the acceptor group represented by Y, then the H-bond length represents the distance between X....Y since in the CSD it is not possible to measure the distance between H and Y. When describing the strengths of hydrogen bonds a moderate hydrogen bond has a distance of 2.5-3.2 Å, and weak hydrogen bonds have value of 3.2-4.0 Å [184].

When considering possible H-bonding interactions between felodipine and HPMC, three interactions are considered likely based upon Etters rules [185]. These are:Felodipine:felodipine amine...ester, HPMC:HPMC ether...ether; ether...OH; OH...OH, Felodipine:HPMC amine N-H...ether or amine N-H...OH.

Starting with felodipine itself, the crystal structure of the as-received material (polymorph I, reference code DONTIJ) is available in the CSD, as are crystal structures of the other polymorphs reported to date, and therefore the relevant interactions can be directly considered from reported crystallographic data. The primary H-bonding interaction in form I felodipine is 3.155 Å . This can be compared with [interactions and distances in the other polymorphs]. The H-bonding interaction in form I felodipine is therefore significantly longer, and therefore expected to be significantly weaker, than in the other polymorphs. This observation correlates with the infra-red result of a 34 cm^{-1} shift of that peak to lower wave-number (i.e. stronger H-bonding interaction) upon cryomilling, in the sense that the crystalline form I maximises lattice energy at the expense of local H-bonding, whereas in the amorphous (cryo-milled and ASD with HPMC) state lattice energy is not a consideration and therefore much more importance is given to maximising local hydrogen bond strengths. Stronger H-bonding in the amorphous form relative to the crystalline therefore results in the strong red-shift of the NH peak.

Moving next to HPMC:HPMC potential interactions, from basic chemical intuition the only chemically significant ones are expected to be OH...OH. However given the low levels of OH substitution in the grade of HPMC used these are not expected to be a major factor in governing the behaviour of HPMC, either on its own or as a formulated product, and a CSD analysis is therefore not likely to add new knowledge.

Considering finally the potential interactions between felodipine and HPMC, direct crystallographic data are not available (HPMC is amorphous) and therefore an indirect approach is required as outlined above. A set of motifs describing the likely interactions were constructed and used a search terms in the CSD, these are shown in Table 2.2 along with frequency plots of H-bond lengths. From

visual inspection of the plots, the histogram of N...O distance for fragments that form motif "a" show a most common value around 2.65 Å which is shorter than our starting felodipine polymorph I so that it can be interpreted that the crystalline form is more weakly hydrogen bonded than the bond expected to link the felodipine-felodipine functional group. Upon co-cryomilling with HPMC the expected motif for the interaction with HPMC is seen Table 2.2. For the felodipine-HPMC system there is no clear distribution of this possible interaction which can be interpreted easily as there is a low probability of interaction between N-H group of felodipine with O-H of HPMC. It was reported that the probability for the formation of a H-bond between N-H (as in our case felodipine) and O-H (as here for HPMC) is weak [186]. It is supposed that the compounds containing donating group (acidic N-H group) have low performance with the compound that contains the medium acceptor group O-H in HPMC [186].

From CSD Table 2.3 it is confirmed that paracetamol form I (CSD reference code HXACAN01) shows that the distance between N-H and the oxygen of the phenolic O-H with which it is hydrogen bonded is 2.934 Å while the distance of the hydrogen bond between the O-H and the carbonyl oxygen is 2.663 Å which is hence stronger than that connecting the phenolic one. The expected motifs for the interaction can be seen in Table 2.3. A histogram of O...O distances for the fragments which could form motif "a1" show the most common value at around 2.8 Å which is longer than our starting polymorph I. After co-cryomilling with HPMC, the expected motifs for the interaction are seen in Table 2.3. The (O...O) distance histogram for the fragments show a most common value around 2.8 Å for a proposed part RO-H which is higher than the proposed one that connected paracetamol molecules with each other, which is 2.663 Å . This likely indicates that the cryomilling would not likely result in any interaction after cryomilling of paracetamol itself nor after co-cryomilling with the polymer.

From CSD (refcode: ACSALA02) (aspirin polymorph I) we found that the H-bond distance between carboxylic O-H group which is the strong donating group with the carbonyl ester of other aspirin molecule is 2.649 Å . A histogram of (O...O) distances for fragments which could form a motif "a2" in Table 2.4 has the

Table 2.2: Felodipine CSD results.

Felodipine part expected	Motifs	H-bond length in Å	Histogram	Interaction
polymorph	I	3.155	-	-
Felodipine	a 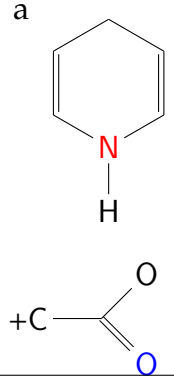	2.65	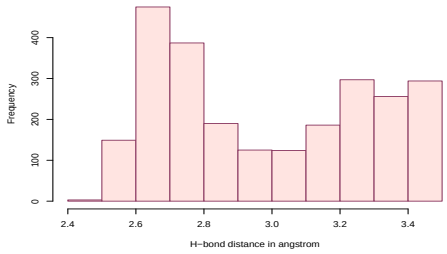	yes
Felodipine HPMC	b 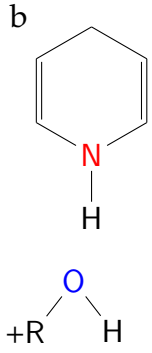	3.5	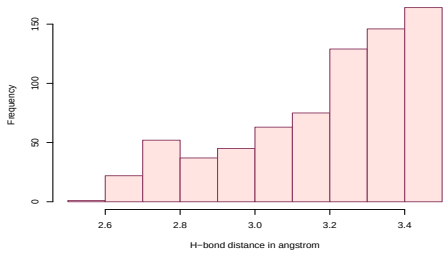	no

Table 2.3: Paracetamol CSD results.

Paracetamol part expected	Motifs	H-bond length in Å	Histogram	Interaction
Polymorph	I	2.663	-	-
Paracetamol	a1 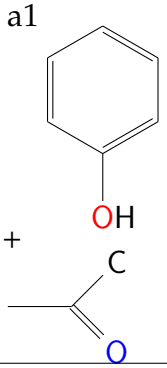	2.8	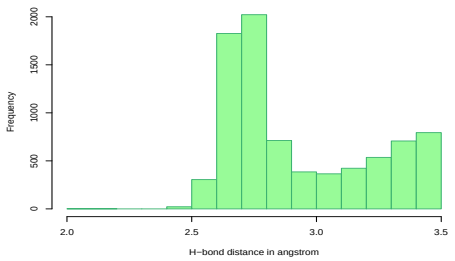	no
Paracetamol-HPMC	b1 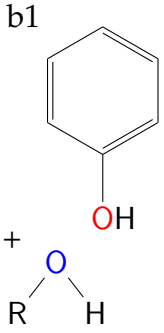	2.8	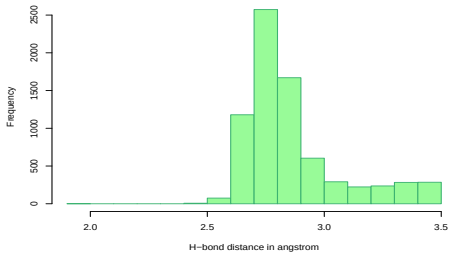	no

Table 2.4: Aspirin CSD results.

Part expected	Motif	H-bond length in Å	Histogram	Interaction
Polymorph	I	2.649		
Aspirin	a2 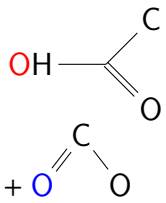	2.7	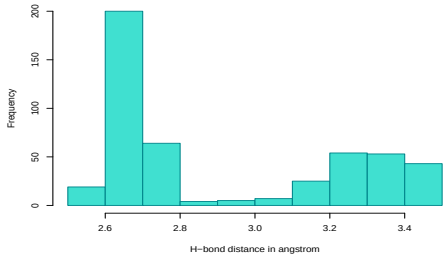	no
Aspirin-HPMC	b2 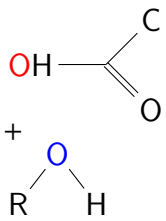	3.6	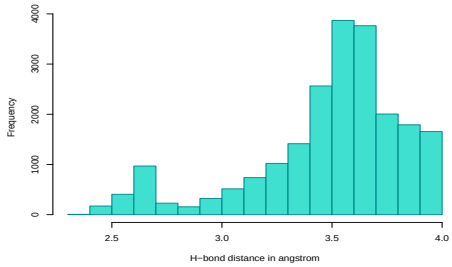	no

most common value around 2.7 Å however, it is a broad histogram. With HPMC, the expected motifs for the interaction are seen in Table 2.4. The histogram (O...O) distance for the fragments shows a most common value around 3.6 Å for a proposed part RO-H which is higher than the proposed one that connected the aspirin molecules with each other (2.649 Å).

All of these analysis suggests that all the selected drugs have a low possibility of interaction with HPMC.

2.3 Materials and Methods

Felodipine was kindly donated by AstraZeneca. Aspirin, paracetamol sodium phosphate dibasic, sodium phosphate monobasic and sodium dodecyl sulphate (SDS) were purchased from Acros. The purity for the selected APIs was confirmed by DSC and XRPD which indicated no unexpected peaks or thermal events compared to literature (see Figure 2.4 and 2.11). Hydroxypropyl methyl cellulose manufactured by Shin Etsu was supplied by AstraZeneca. Potassium carbonate was purchased from Minerals-Water Ltd (Essex, UK) in order to achieve 43% relative humidity for the stability study.

2.3.1 Preparation of physical mixture

The selected drugs were mixed individually with HPMC in different proportion 5%, 25%, 50% and 75% (w/w) in 1 gram total. The mixtures were triturated by hand using a mortar and pestle for 5 minutes at room temperature to encourage proper mixing.

2.3.2 Cryomilling

Cryomilling was done using a 6870 Freezer/Mill (SPEX, Metuchen, NJ). An electromagnetic coil shuttles an impactor bar back and forward inside the vial in order to pulverise the sample. Liquid nitrogen submerges the coil and vial to keep sample temperature at -196 °C. 1 gram as total weight of each API either alone or mixed with polymer in four different concentrations was subjected to cryomilling for 150 minutes. This is done by pre-cooling the materials for 3 minutes then milling for 2 minutes at frequency 10 cycles per second. Throughout, there is a pause of 1 minute between cycles to minimise heat build-up in both sample and coils. After cryomilling all samples are vacuum sealed to reduce the moisture uptake inside a dry glove box. This dry-box is supplied with argon to achieve a humidity about of 7% RH which is the lowest possible in that system. The cryomilling set can be seen in Figure 2.2.

Figure 2.2: The cryomilling set.

2.3.3 Powder X-ray diffraction (XRPD)

XRPD was performed by using flat-plate diffractometer an X'Pert PRO (PANalytical, Almelo, Netherlands). The instrument utilises Cu Kα_1 (λ = 1.54 Å) radiation and operates in Bragg-Brentano geometry. The step size used was 0.02602 θ per degree with total collection time of 5 minutes. The voltage of the generator is set to 40 kV and the current to 40 mA. Brass was used as the plate for the samples. The crystallite size was estimated by using the Scherrer equation [187] (Equation 2.3.1). Fityk software was used to estimate the peak width by using a pseudo-Voigt curve fitting function. A silicon standard peak was used to represent the instrumentation boarding effects.

$$L = \frac{K\lambda}{B(2\theta)\cos\theta} \tag{2.3.1}$$

L is the crystallite size in nm, B is half-value breadth in 2θ , K is constant = 0.93, λ is the wave length of incident X-ray, θ is the Bragg angle.

2.3.4 Differential Scanning Calorimetry (DSC)

DSC was achieved using a Q2000 system (TA, New Castle, DE, United States) supplied with an auto-sampler. Temperature and enthalpy were calibrated using the melting endotherm of indium as performed in the manufacturer's guidelines. The samples of (2-8 mg) were weighed into Tzero pans (TA, New Castle, DE, United States) and hermetically sealed under argon using the dry box. A heating rate of 10 °C/minute was employed, along with a nitrogen flow rate of 50 ml/minute. Analysis of thermograms was done by using TA universal analysis 2000 (version 4.5A). The plotting of thermograms is with the endothermic points down and exothermic point up. Melting points are reported as onset temperature, the T_g value was determined as the mid point as per-recommended practice [188, 189]. The experiments were performed in triplicate (n=3).

2.3.5 Attenuated total reflectance- Fourier Transformed Infrared Spectroscopy (ATR-FTIR)

The IR spectra of the samples were collected using an Agilent-Cary630-FTIR, (United States). All samples approximately (5-10 mg) were applied to the plate of diamond ATR type II crystal. The signal-reflection diamond has a 1 mm diameter sampling surface with 200 μm active area and provides approximately 2 μm depth of penetration for infrared energy at 1700 cm^{-1}. The samples were analysed by Agilent MicroLab PC software. The spectral range was 4000-500 cm^{-1}.

2.3.6 Gordon-Taylor equation

This equation is used to predict the T_g between a miscible drug with a polymer (ideal case):

For two component [190]:

$$T_{g(}mix) = \frac{w_1 T_{g1} + K_1 w_2 T_{g2}}{w_1 + K_1 w_2} \tag{2.3.2}$$

$$K \approx \frac{p_1 T_{g1}}{p_2 T_{g2}} \tag{2.3.3}$$

T_{gi} is the glass transition temperature of each component, W_i is the weight fraction of each component, K is calculated from the p_i density and T_{gi} of each component.

2.3.7 Dissolution study by UV and HPLC

The dissolution was done using a United States Pharmacopeia (USP) type II apparatus at 50 rpm (Erweka Dissolution Tester) in phosphate buffer pH 6.8 containing 1% SDS. The volume of the dissolution media was 600 mL. Dissolution media was maintained at 37°C and a paddle speed of 50 rpm was employed. At designated time intervals, 5 mL samples were withdrawn, filtered (0.45 μm) and analysed by HPLC for felodipine. The dissolution experiments were performed in triplicate. HPLC analysis was carried out using an Agilent 1100 with UV detection at 238 nm, equipped with an Supelco LC-18, 15 cm, 5μm, 4.6 mm column. Setting of the flow rate to 1.0 mL/min and keeping the temperature of the column at 40 °C. Injection volume was 20μml. Acetonitrile (HPLC grade) and water is the consistent of the mobile phase. Calibration curves were performed in triplicate with R^2=0.999. UV method was done by using UV spectrophotometer (Varian, Cary 50) for detection the absorbency for aspirin at 265 nm and paracetamol at 245 nm. Calibration curves for aspirin and paracetamol were performed in triplicate with R^2=0.999. The amount of felodipine is 10 mg in each mixtures.

2.3.8 Scanning electron microscopy(SEM)

The samples were coated with a thin gold layer by sputter coater unit (SPI, USA) to mitigate against surface charging effects. SEM images were taken using a

Joel JSM 6060LV SEM (Japan) operated at an acceleration voltage of 10 kV. The particle size was determined using ImageJ software.

2.3.9 Quantification of crystallinity

The degree of crystallinity was quantified by a DSC method according to the following equation:

$$F = \frac{\Delta H_f m - \Delta H_r}{\Delta H_f} \times 100 \tag{2.3.4}$$

F is the degree of crystallinity percent, $\Delta H_f m$, ΔH_f, is the heat of fusion of the milled and crystalline material respectively, ΔH_r is the recrystallisation heat measured from the exothermic peak [3].

2.3.10 Stability study

A saturated solution of potassium carbonate was prepared and then this solution was placed in a gas-tight environment to achieve the required humidity which is 43% at room temperature. The samples were analysed by XRPD, FTIR and DSC after 1, 2, 5, 20, 40 and 60 days of storage.

2.3.11 Calculation of the % ionisation

The % of ionisation was calculated according to Henderson-Hasselbalch Equation 2.3.5 and 2.3.7.

weak acid

$$pKa = pH + log\frac{HA}{A^-} \tag{2.3.5}$$

The % ionisation will be:

$$log\frac{HA}{A^-} = pKa - pH \tag{2.3.6}$$

weak base

$$pKa = pH + log\frac{BH^+}{B} \tag{2.3.7}$$

The % ionisation will be:

$$log\frac{BH^+}{B} = pKa - pH \tag{2.3.8}$$

HA is the weak acidic drug, B is the basic drug, pKa is the negative logarithm of the acid dissociation constant Ka.

2.3.12 Evaluation of H-Bond length using the Cambridge Structure Data Base (CSD)

The prediction of a hydrogen bond that might formed between two functional groups relies on crystal structures of (version 3.8 CCDC, Cambridge, UK). Queries were built in ConQuest (version 1.18 CCDC) by using fragment structures containing two functional groups of interest which involved the donor and acceptor group between felodipine-felodipine or between felodipine-HPMC. These are combined with a formula query to avoid structures with additional heteroatoms. Intermolecular H-bonds were excluded. In order to identify the suitable donor and acceptor group there is a general rule outlined by Etter:

> "All good proton donors and acceptors are used in hydrogen bonding. Six-membered-ring intramolecular hydrogen bonds in preference to intermolecular hydrogen bonds. The best proton donors and acceptors remaining after intramolecular hydrogen bonds formation from intermolecular hydrogen bonds to one another [185]."

For example, the strongest donor group for felodipine is N-H group which has the ability to form a hydrogen bond with acceptor group C=O of another felodipine molecule. There is also a possibility of formation of hydrogen bond between N-H group of felodipine other functional group of polymers as an acceptor groups. Bonding propensity was investigated by plotting the reported inter-molecular distance as a function of occurrence in the database, with a strong propensity toward bonding interaction qualitatively indicated by frequent occurrence of that bonding motif and a tight histogram of the inter-atomic distance.

2.4 Results and discussion

2.4.1 Particle size reduction

Figure 2.3 and Table 2.5 show the SEM results for the selected APIs before and after cryomilling. All the selected drugs show a reduction in particle size after cryomilling. Felodipine, paracetamol and aspirin particle size are reduced approximately 40, 5 and 11 times, respectively, after cryomilling (Table 2.5). Such a reduction in the particle size was seen also upon cryomilling of microcrystalline cellulose and indomethacin [191].

Table 2.5: Crystallite size and particle size of the selected APIs.

API	Crystallite size estimated by Scherrer equation in nm		Particle size by SEM in μm	
	as received	cryomilled	as received	cryomilled
Felodipine	42	no Bragg peaks	711±44	19±4.5
Paracetamol	97	41	117±15	23±1
Aspirin	2675	58	883±10	81±2.5

The Scherrer equation [192] as detailed in Section 2.3.3 can be used to estimate the crystallite size before and upon cryomilling based on the XRPD data in Figure 2.4. In the Scherrer analysis, sharp Bragg peaks correspond to the large crystallites whereas broad Bragg peaks correspond to small crystallites. This figure presents the XRPD traces of the as-received materials before and after cryomilling. It is important to note that all XRPD traces were collected within an hour or two of cryomilling in order to minimise as far as possible any effects due to recrystallisation or similar. For the as-received materials, the APIs exhibit sharp Bragg peaks whereas the HPMC as seen in Figure 2.5 does not, but rather shows a broad diffuse hump. This indicates that the APIs are crystalline whereas the HPMC is not. This is expected as small-molecule drugs are generally readily crystallised whereas polymers typically are not, and is in full accord with

literature [35, 193].

Upon cryomilling of HPMC, as seen in Figure 2.5 which lacks Bragg peaks before cryomilling, the changes upon cryomilling are minor, with no Bragg peaks appearing. HPMC is therefore amorphous both before and after cryomilling.

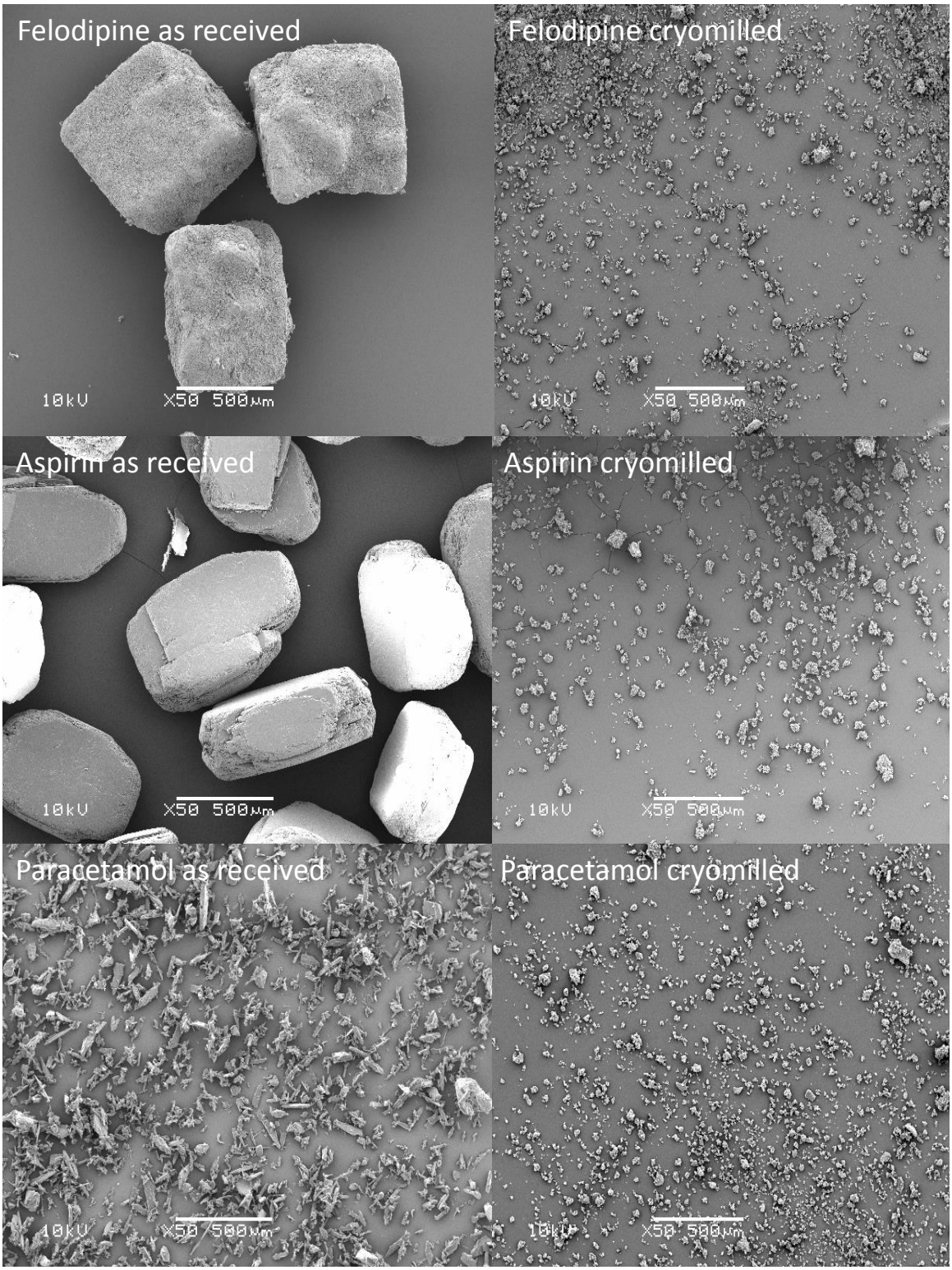

Figure 2.3: The SEM images of felodipine aspirin and paracetamol as received, cryomilled for 150 mins.

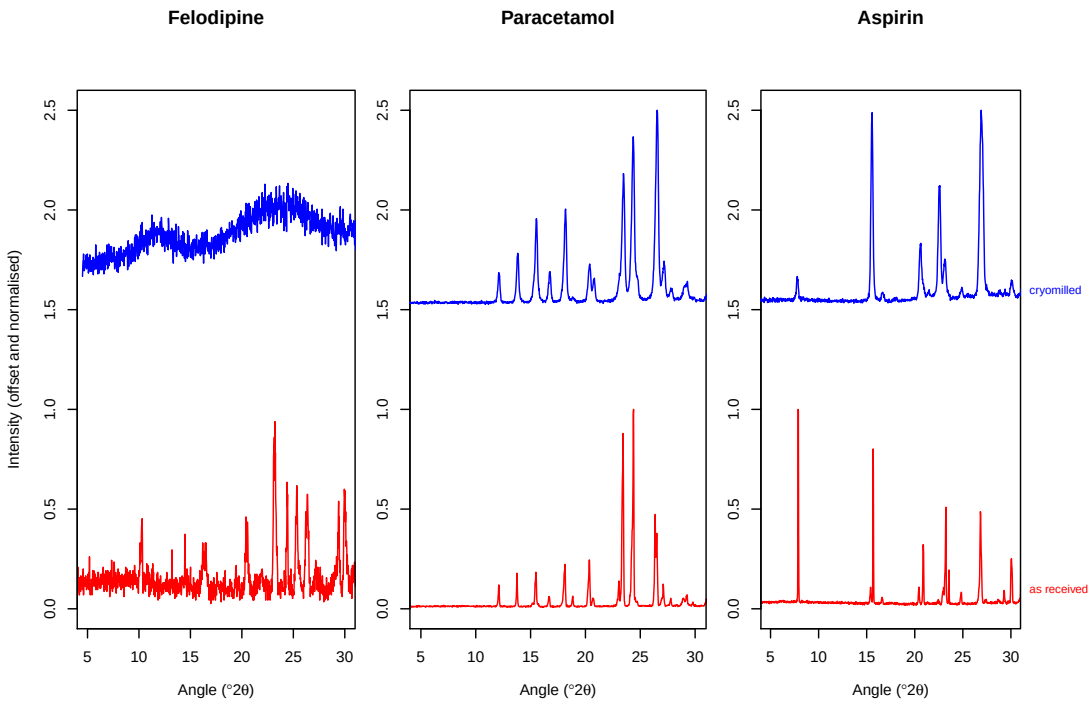

Figure 2.4: The XRPD patterns of felodipine, paracetamol and aspirin before and after cryomilling. Offsets and scales applied for presentational purposes.

Upon cryomilling (Figure 2.4), the Bragg peaks for felodipine largely disappear into the noise, whereas for paracetamol and aspirin the Bragg peaks remain evident, albeit with some minor changes in peak intensity and some peak broadening. For felodipine the disappearance of Bragg peaks indicates that the sample has, upon cryomilling, been transformed from largely crystalline to largely amorphous. This is in full accord with previous work in which a similar phenomenon was reported, both for felodipine [54, 194] and more widely for other drugs [53, 95, 153, 158, 195]. For paracetamol and aspirin the preservation of Bragg peaks upon cryomilling shows that these samples have preserved their crystallinity and have not become amorphous to any detectable degree. The slight changes in peak intensities for these samples are ascribed to the effects of changes in particle size/shape and therefore preferred orientation upon cryomilling [50]. The increase in peak widths upon cryomilling is indicative of

reductions in crystallite size. It can be seen from Table 2.5 and 2.6 that there is a reduction in crystallite size of the as-received in comparison to the cryomilled one. They are estimated at 97 nm to 41 nm (paracetamol) and 2675 nm to 58 nm (aspirin). For felodipine the crystallite size before cryomilling is 42 nm while after cryomilling it is difficult to estimate crystallite size by Scherrer due to lack of Bragg peaks because of the conversion of felodipine to amorphous material (Scherrer equation applies only for crystalline material). The XRPD and SEM data agree in the expected reduction in size for all selected drugs upon cryomilling. It is difficult to compare the size obtained from SEM results with the size obtained from Scherrer equation due to the fact that the Scherrer equation measures crystallite size whereas SEM measures particle size. These particles may include agglomerated material which is expected to be significantly larger than the crystallite size [196].

Table 2.6: Peak width and crystallite size estimated by Scherrer equation from XRPD data.

API	Status	Peak width	Size by Scherrer in nm
Felodipine	as received	0.2	40
	cryomilled	no Bragg peaks	-
	75% cryomilled separately	0.3	30
	75% cryomilled together	no Bragg peaks	-
Paracetamol	as received	0.1	100
	cryomilled	0.2	40
	75% cryomilled separately	0.2	40
	75% cryomilled together	0.3	30
Aspirin	as received	0.03	2675
	cryomilled	0.2	60
	75% cryomilled separately	0.2	60
	75% cryomilled together	0.3	30

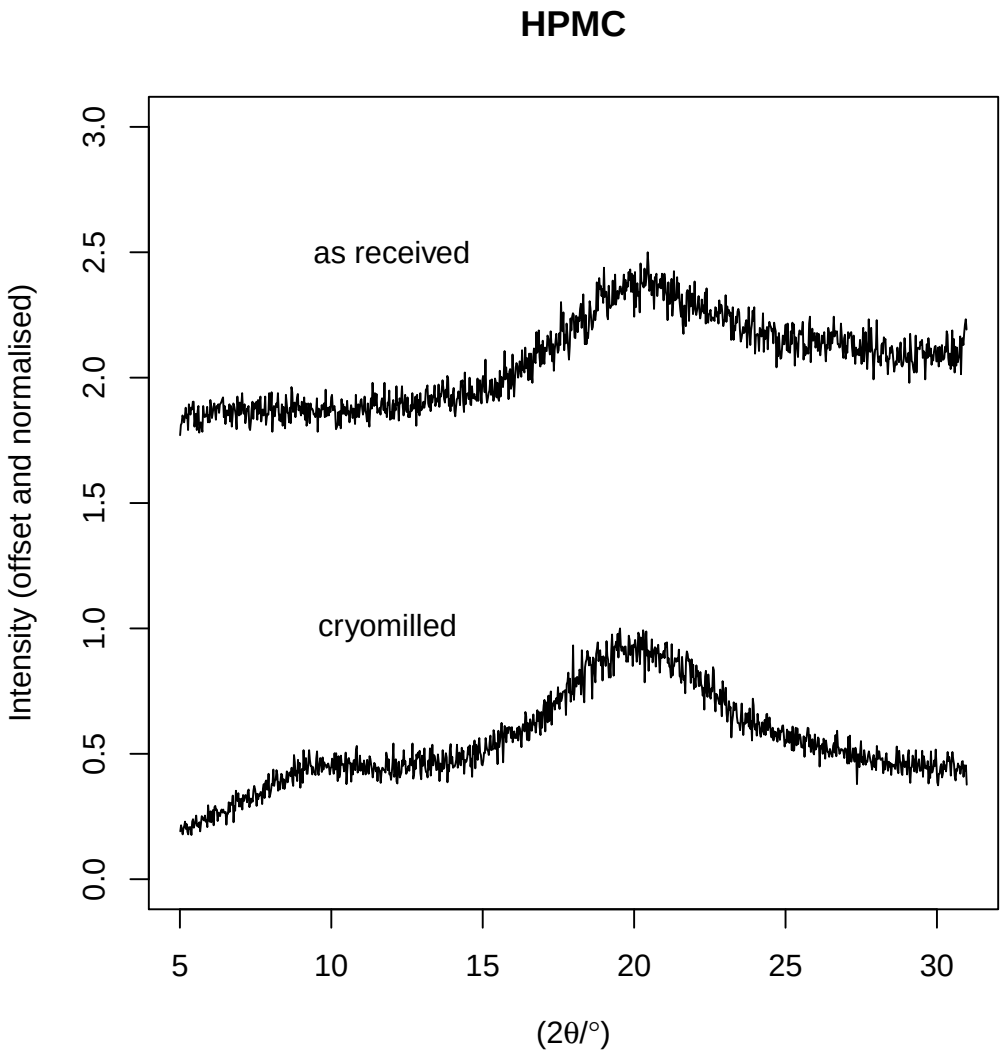

Figure 2.5: The XRPD patterns of HPMC before and after cryomilling. Offsets and scales applied for presentational purposes.

2.4.2 Solid state transformation

From the previous Section 2.4.1, the XRPD results show the impact of cryomilling on particle and crystallite size reduction. In order to investigate another mechanical effect of cryomilling which is solid state transformation, DSC thermograms along with XRPD were undertaken for all as-received APIs both before and after cryomilling for 150 minutes and also after cryomilling with HPMC in four different concentrations. All DSC traces were collected within 15 minutes of

cryomilling. Here we need two assays to assess the solid state transformation; DSC is used because it is more sensitive to low level of amorphous material while XRPD is used because it is very sensitive to crystalline material (1% [197]) and it is furthermore does not involve heating of the sample. In particular the DSC assay was done to investigate at crystalline versus amorphous behaviour, T_g and stability.

After cryomilling of each material, we will focus on three thermal events for each selected drug: the T_g; enthalpy of fusion; melting point onset (Table 2.7) for the materials as-received, cryomilled and upon co-cryomilling with HPMC. Additionally, we will note any re-crystallisation event. Furthermore, the percentage of crystallinity was calculated according to Equation 2.3.4 as illustrated in the material and method Section 2.3.9. HPMC was co-cryomilled with the APIs in weight ratios to the drug of 5%, 25%, 50% and 75%.

Felodipine

As seen in Figure 2.6 and Table 2.7 felodipine polymorph I "as-received" exhibits a single endothermic event which is interpreted as a melting point onset at 142.4 $\pm$0.1 °C (n=3) which is in similar to that one reported by Chamarthy and Rodolfo (141.7 °C) [54]. This melting point with lack of T_g in the thermogram taken in conjunction with our XRPD results where there is no amorphous halo (Section 2.4.1) indicates that the as received felodipine is fully crystalline.

Table 2.7: The thermograms results for felodipine, aspirin and paracetamol as received, cryomilled and co-cryomilled with HPMC in four different concentrations.

API	State	T_g (mid point)°C	Melting point(onset)°C	Heat of fusion J/g	% Crystallinity
Felodipine	as received	-	142.4±0.1	73.1±0.12	100
	cryomilled	46.7±0.5	139.7±0.2	65.1±2.3	27.5±3.2
	75%	46.7±0.2	135.4±0.6	1.2±0.7	2.1±1.3
	50%	51.1±1.4	131.3±0.5	0.2±0.01	0.6±0.03
	25%	53.7±1.7	-	-	0
	5%	59.4±2.2	-	-	0
Paracetamol	as received	-	169.1±0.1	165.8±0.1	100
	cryomilled	-	167.1±0.4	160.5±0.9	96.8±0.5
	75%	42.1±1.5	157.4±2	98.9±1.5	78pm1.2
	50%	43.4±0.5	147±0.3	55.7±2.6	65.9±3
	25%	46.7±2.3	123.6±7.3	4±0.8	9.5±2
	5%	47.7±4.1	104.2±2.2	0.8±0.4	9.9±0.6
Aspirin	as received	-	142.4±0.1	173.1±0.12	100
	cryomilled	-	141.7±0.4	169±2.1	97.5±1.2
	75%	43.1±0.4	120.5±1.5	77.8±2.6	59.6±1.5
	50%	43.1±0.4	107.9±1.4	36.9±1.5	42.6±1.7
	25%	42.8±0.5	86.1±1.2	5.6±0.4	13±1
	5%	42.4±0.2	-	-	0

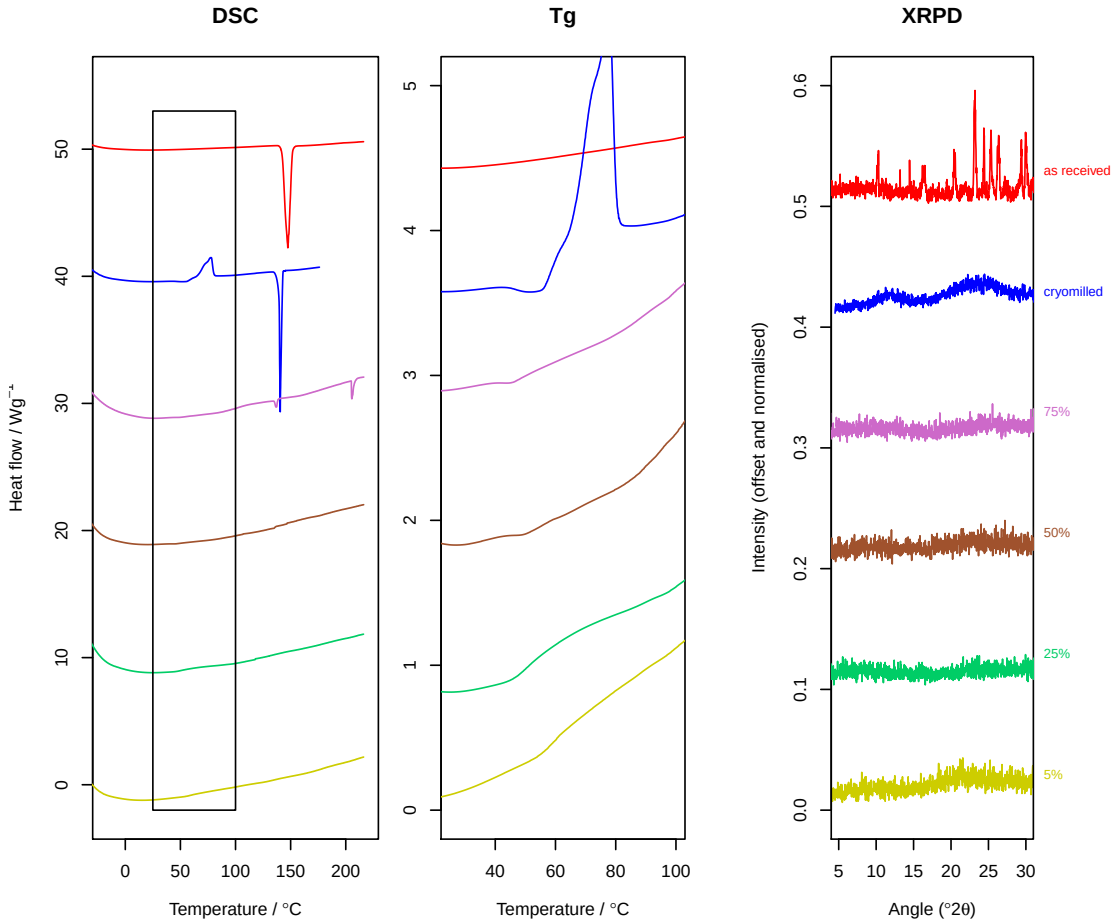

Figure 2.6: The DSC thermogram and XRPD patterns of felodipine as received, cryomilled for 150 mins and cryomilled together with HPMC in different concentrations. Red colour indicates as received materials, blue colour indicates cryomilled materials, purple colour indicates 75% drug loading, brown colour indicates 50% drug loading, green colour indicates 25% drug loading and yellow colour indicates 5% drug loading. Offsets applied for presentational purposes.

Upon cryomilling (Figure 2.6 and Table 2.7) the first thermal event is the appearance of a T_g at 46.7 $\pm$0.5 °C which is comparable to that reported by Marsac *et al* (46.4 °C) obtained from felodipine prepared by spray drying [114]. The second thermal is the exothermic peak at 74 $\pm$2.5 °C. A final endothermic event occurs at 139.7 $\pm$0.2 °C. The T_g appearance is a sign of amorphous material formation along with the exothermic peak which is explained as a recrystallisation peak that reveals the cryomilled felodipine experienced a reduction in

crystallinity (amorphousness or crystal defects have been produced) that re-crystallises on heating. The endothermic peak at 139.7 ±0.2°C is considered as melting peak which is less than the as received felodipine (142.4 ±0.1 °C). There is consequently a reduction in the enthalpy of melting from 73.1 ±0.1 J/g to 65.1 ±2.3 J/g of the "as received" and cryomilled felodipine. The reduction in the enthalpy of fusion is interpreted as a reduction in crystallinity even after the clear re-crystallisation event. The estimated crystalline content after cryomilling changed from ≃ 100% to 27.5 ±3.2% which is comparable to that previously reported one of 29.7 ±1.8% for cryomilling of felodipine for 120 minutes [55]. The DSC results are in good accord with the XRPD results in that felodipine upon cryomilling undergoes a phase transformation in which it became at least partially amorphous.

As amorphous felodipine recrystallises after 24 hour (Section 2.4.4), felodipine was co-cryomilled with HPMC to potentially stabilise the amorphous state. The drug loading is shown in Figure 2.6. The "as-received" felodipine showed a melting peak while the HPMC did not (Figure 2.8). In the Felodipine/HPMC system at 75% drug loading there is a T_g which was not changed (in term of the temperature) in comparison to the cryomilled pure felodipine (Table 2.7). Another important event upon co-cryomilling with HPMC is the disappearance of the re-crystallisation peak that was observed in the cryomilled pure felodipine as discussed early in this section. In addition, there was a melting peak onset at 135.4 ±0.6 °C which is lower than the cryomilled felodipine. The expected melting enthalpy for this dilution (physical mixture of felodipine with HPMC at 75% w/w) would be 54.75 J/g crystalline felodipine, however, the observed (cryomilled) is only 1.2 ±0.7 J/g felodipine (Figure 2.9). The estimated crystalline content reduced from 27 ±3.2% to 2.1 ±1.3% for the cryomilled and 75% respectively. Further reduction in the drug loading shows additional changes in the thermogram data (Figure 2.6 and Table 2.7). The first important change is an increase in T_g's upon co-cryomilling with HPMC. The T_g increased with HPMC concentration. The second change is a reduction in percentage crystalline content that is concomitant with an additional reduction in the melting point and enthalpy of fusion. Felodipine/HPMC system becomes essentially zero per-

cent crystalline within the limit of detection with the disappearance of melting peak at 25% drug loading and lower. These DSC data likely indicate that co-cryomilling with HPMC render cryomilled felodipine from partial amorphous into a fully amorphous solid dispersion. From Figure 2.7 it can be seen that the experimental T_g negatively deviates from the calculated ideal T_g from the Gordon-Taylor equation. In addition the T_g plateaus at certain concentrations. This observation has been reviewed by Konno and Taylor [110] for felodipine with HPMC prepared by spray drying. This indicated poor mixing of felodipine with HPMC or the hygroscopicity of HPMC that results in the observed reduction of the T_g.

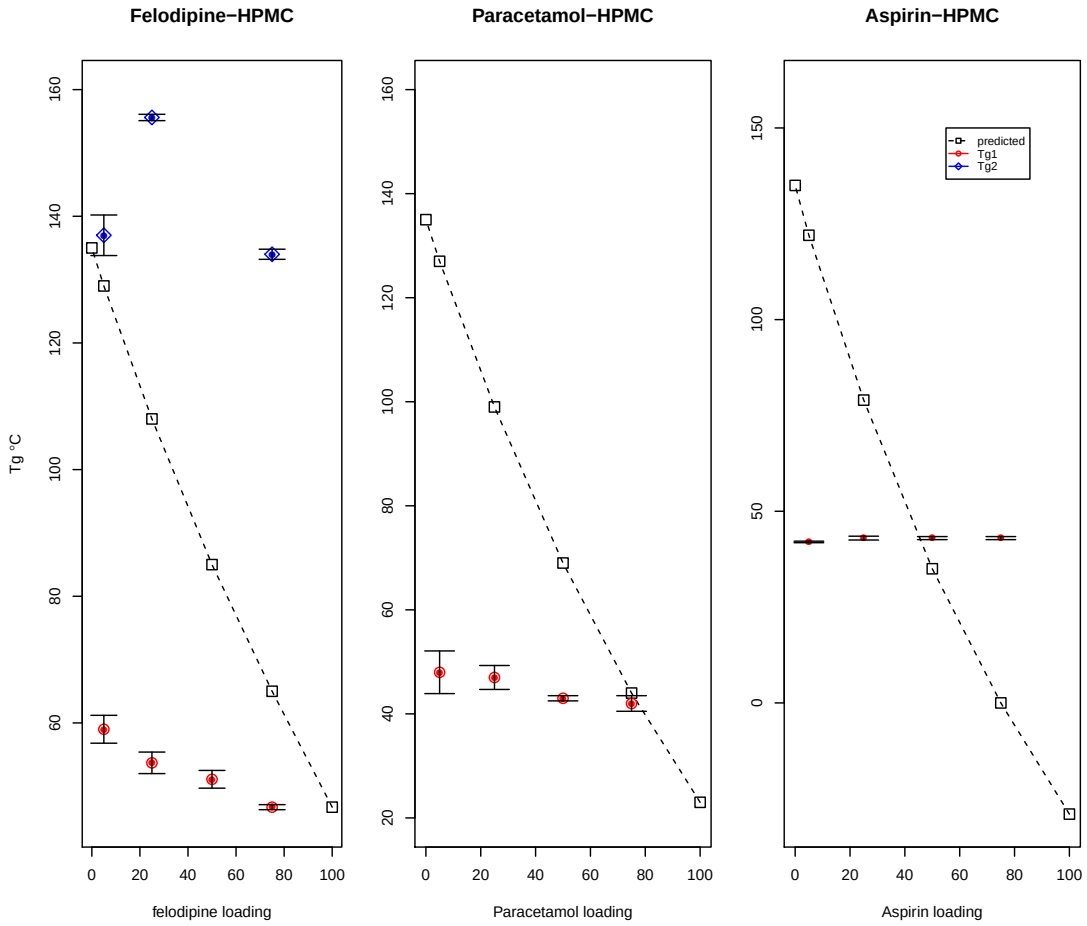

Figure 2.7: Values of T_g for binary mixture felodipine-HPMC, paracetamol-HPMC and aspirin-HPMC at 5%, 25%, 50% and 75% drug loadings. The lines show the predicted from the Gordon-Taylor equation. Dots indicates the experimental T_g performed in triplicate (n=3).

The XRPD results in Figure 2.6 show that all the felodipine-HPMC systems mixtures exhibit a reduction in peak signal to noise ratio with the concomitant appearance of an amorphous halo in comparison to the as received felodipine. This likely indicates amorphous material formation for all co-cryomilled felodipine/HPMC systems. This is similar to the reported behaviour observed for felodipine dispersions prepared by spray drying method with PVP at different drug loadings [198] and of cryomilled indomethacin with PVP in which amorphisation at high drug loading [107]. Our XRPD and DSC data are in agreement of formation of (highly non crystalline content) amorphous solid dispersion for

felodipine by co-cryomilling with HPMC.

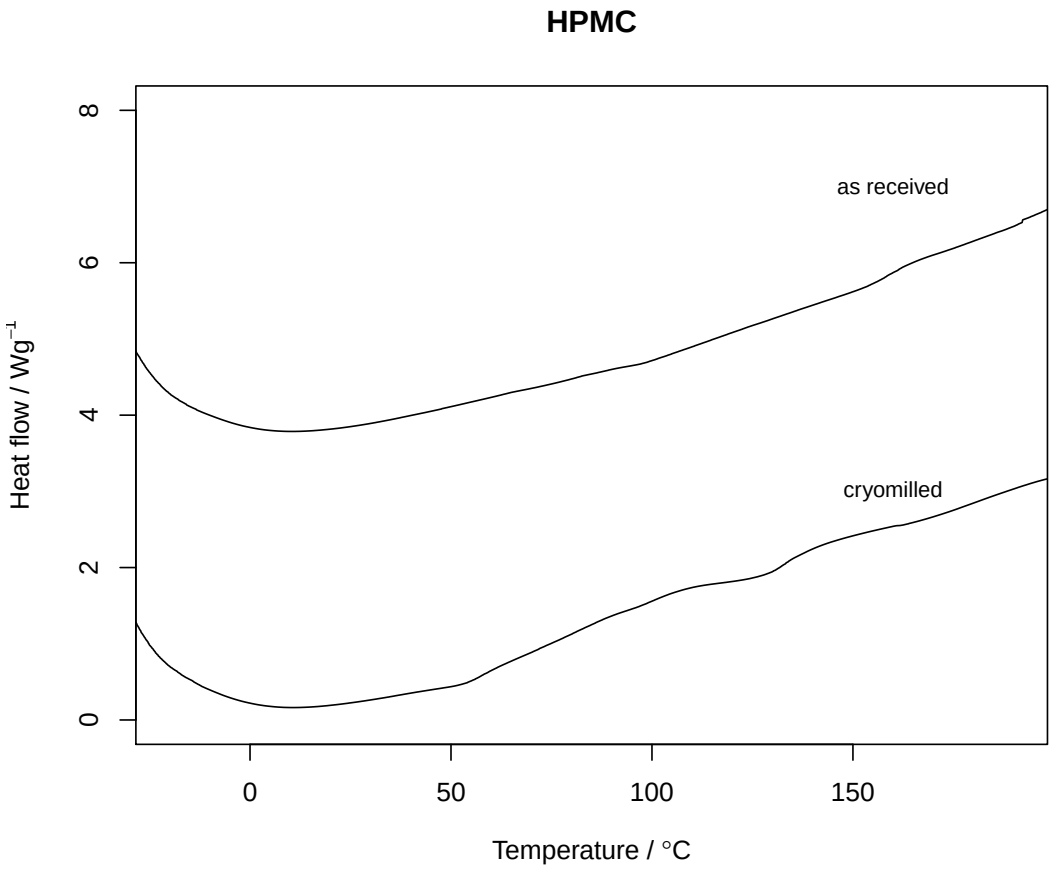

Figure 2.8: DSC thermogram of HPMC as received and cryomilled offsets applied for presentational purposes.

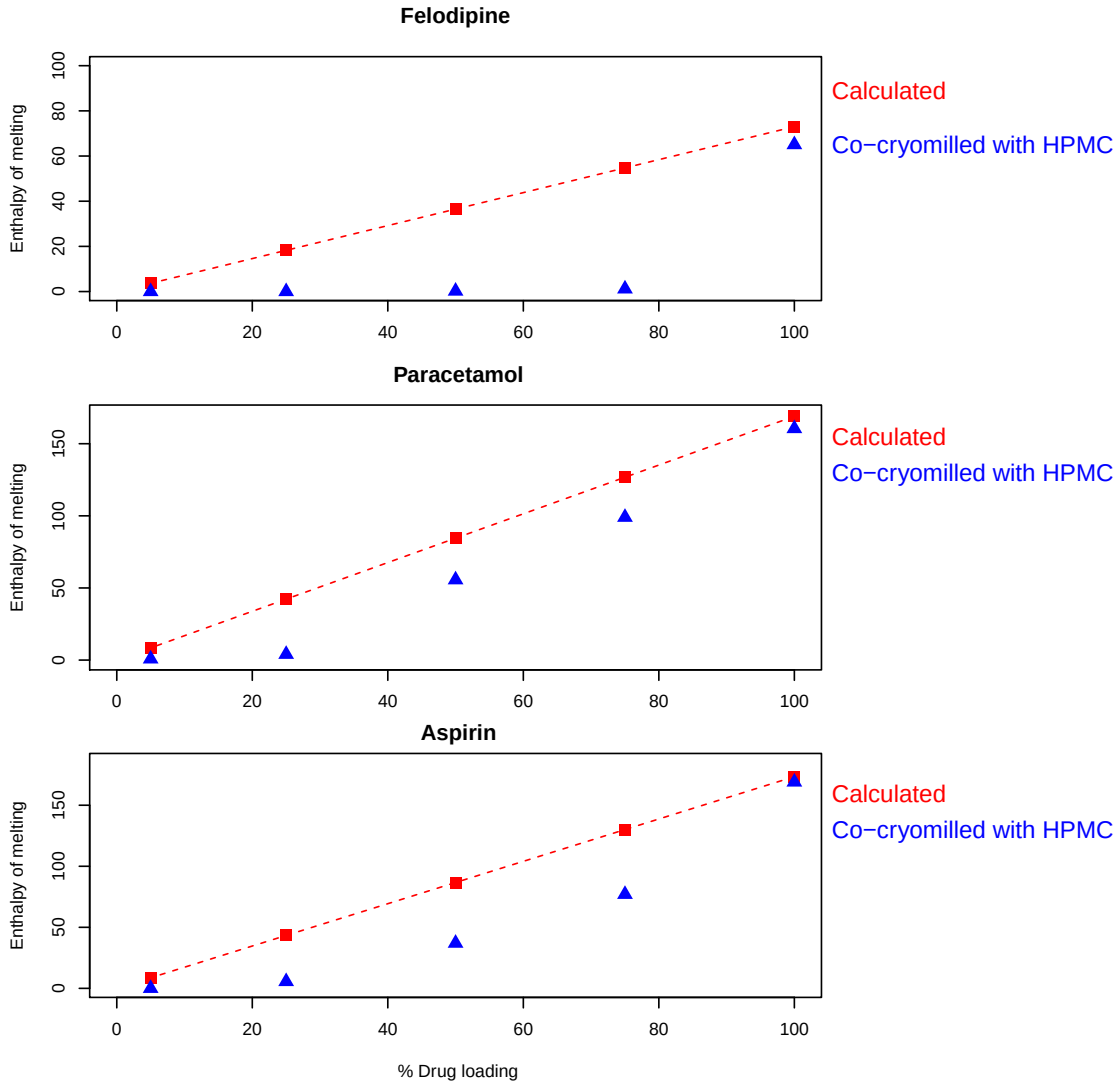

Figure 2.9: The enthalpy of melting for calculated physical mixture, cryomilled together for felodipine, paracetamol and aspirin with HPMC.

Paracetamol

As seen Figure 2.10 and Table 2.7 the paracetamol polymorph I as received displayed only one endothermic event which is a melting peak onset of 169 $\pm$0.1 °C as similarly reported previously [199]. This event along with the clear Bragg peaks observed in our XRPD data in Figure 2.10 indicates that the as received paracetamol is crystalline without a detectable amorphous component.

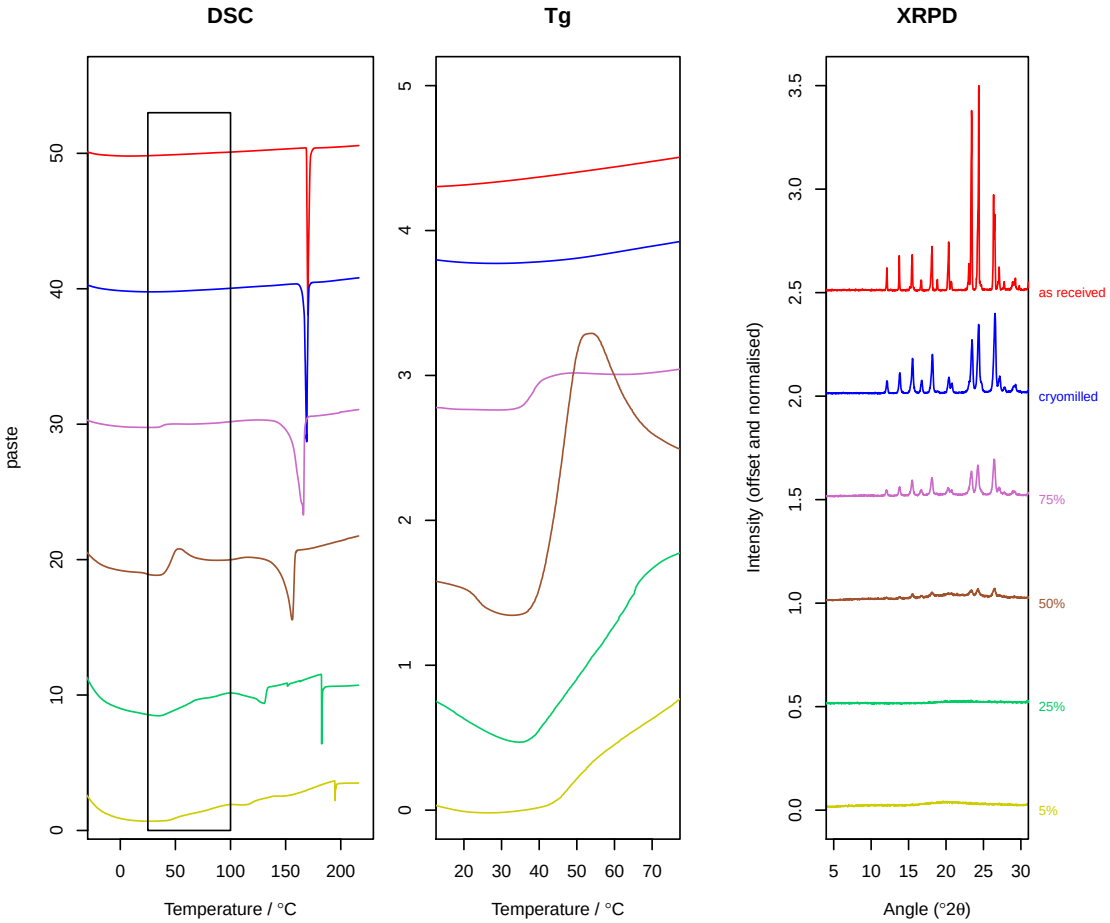

Figure 2.10: The DSC thermogram and XRPD patterns of paracetamol as received, cryomilled for 150 mins and cryomilled together with HPMC in different concentrations. Red colour indicates as received materials, blue colour indicates cryomilled materials, purple colour indicates 75% drug loading, brown colour indicates 50% drug loading, green colour indicates 25% drug loading and yellow colour indicates 5% drug loading. Offsets applied for presentational purposes.

Upon cryomilling, paracetamol did not exhibit a detectable T_g nor an exothermic event (Figure 2.10) as was seen upon felodipine cryomilling. The only thermal event is a minor depression in melting point to 167.1 $\pm$0.4 °C along with a small reduction in the enthalpy of fusion from 165.8 $\pm$0.1 J/g to 160.5 $\pm$0.9 J/g. This is comparable to that reported by Wildfong [50]. As with XRPD data in Section 2.4.1 paracetamol on its own did not significantly convert to the amorphous form upon cryomilling. The only change is the particle size reduction as discussed in

Section 2.4.1.

Paracetamol/HPMC co-cryomilled system at 75% (Figure 2.10) and Table 2.7) showed the appearance of a single T_g at 42.1 ±1.5 °C which was not observed after cryomilling of paracetamol on its own. The second thermal event is the melting peak onset at 157.4 ±2 °C which is lower than the cryomilled paracetamol (167 ±0.4 °C). This is due to simple phase diagram dilution effect rather than polymorphic transformation because the XRPD peaks does not change after co-cryomilling.

The enthalpy of melting is expected to be 126.75 J/g paracetamol for this dilution (75%) (physical mixture) as clearly seen in Figure 2.9, however, the experimental value (co-cryomilled) of 98.9 ±1.5 J/g paracetamol is lower than the expected value. This reflects a reduction in the crystallinity form 96.8 ±0.5% to 78 ±1.2% for cryomilled paracetamol and co-cryomilled at 75% drug loading respectively. Moving to a lower paracetamol/HPMC loading of 50% results in further increase in the T_g with increasing HPMC concentration from 42.1 ±1.5 °C to 43.4 ±0.5 °C (Figure 2.10). The enthalpy of melting is expected to be 84.5 J/g for paracetamol, however, the experimental value of 55.7 ±2.6 J/g paracetamol is lower (Figure 2.9). With increasing HPMC at 25% paracetamol loading there is a further increase in the T_g to 46.7±2.3 °C and a significant reduction in the enthalpy of melting to 4 ±0.8 J/g paracetamol in comparison to the expected value (42.25 J/g paracetamol) which in turn reflects a significant reduction in the crystallinity to 9.5 ±2%. At 5% loading the T_g of the system is not changed in comparison to the 25% loading, the melting peak is further reduce with a reduction in the enthalpy of melting in comparison to the expected value 0.8 ±2.6 J/g paracetamol versus 24.25 J/g paracetamol respectively.

To summarise the most significant change in the thermogram for paracetamol is the elevation of T_g until 5% loading, reduction melting point onset and crystallinity (until 5% loading) with increasing HPMC concentration. The co-cryomilling of paracetamol with HPMC probably leads to amorphous solid dispersion at 25% paracetamol loading and lower based upon the appearance of T_g and the enthalpy of melting (crystalline content). Formation of a single

T_g is interpreted as formation of a single phase amorphous solid dispersion although the experimental T_g is negatively deviated and plateaus, compared to the Gordon-Taylor equation as seen in Figure 2.7. This in turn indicate either poor mixing or a reduction of the T_g as the result of a water plasticising effect.

The XRPD results in Figure 2.10 show that there is a clear reduction in signal to noise ratio with increasing the peak width after co-cryomilling with HPMC at 75% paracetamol/HPMC. This is associated with increasing in the background amorphous halo with increasing polymer concentration at 50% paracetamol/HPMC. At 25% there is an appearance of amorphous halo to indicate amorphous formation. Our XRPD data are in agreement with our DSC results in that the highly amorphous content appears at 25% paracetamol loading and lower as a sign of amorphous solid dispersion formation.

Aspirin

As seen in Figure 2.11 and Table 2.7 aspirin polymorph I as received has one endothermic event which represents the melting point onset of 140.4$\pm$0.8 °C with an enthalpy of fusion of 173.4 $\pm$3.5 J/g which is very close to the reported value [50]. From our XRPD data in Figure 2.4, as received aspirin is crystalline.

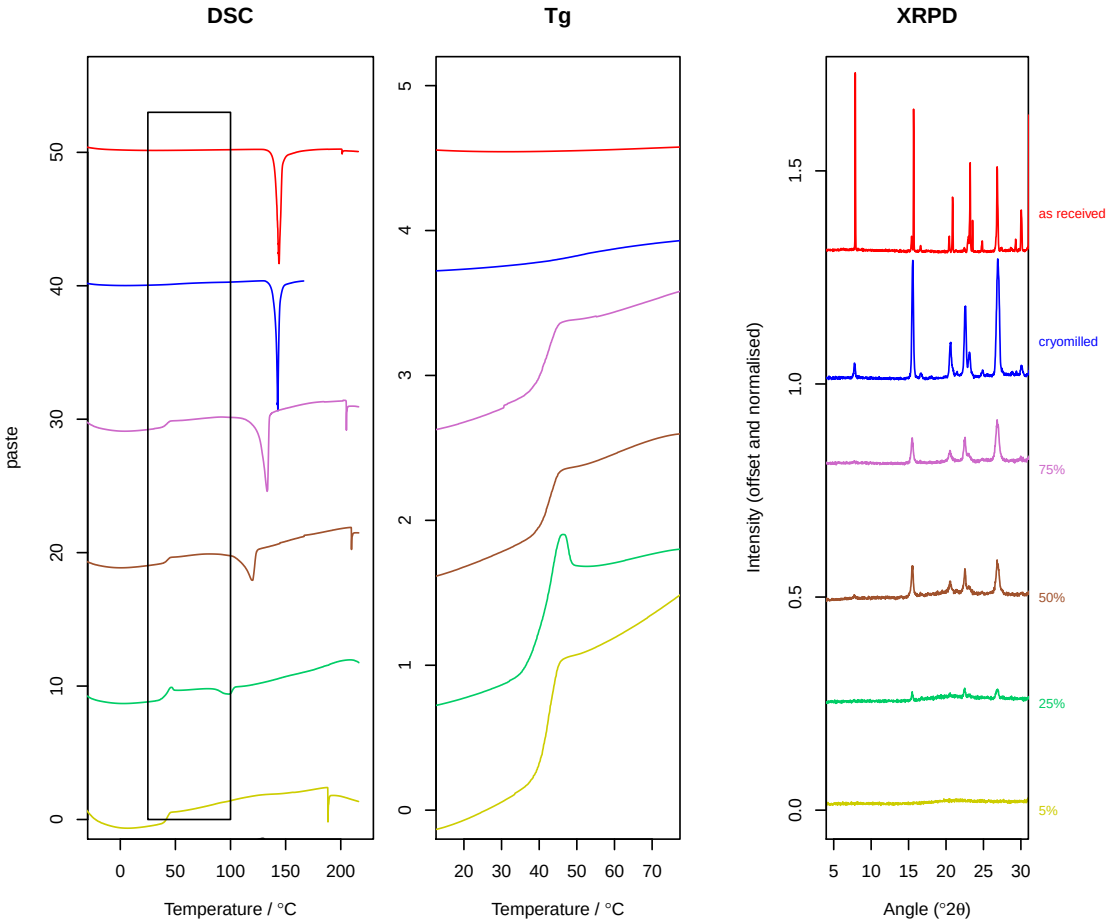

Figure 2.11: The DSC thermogram and XRPD patterns of aspirin as received, cryomilled for 150 mins and cryomilled together with HPMC in different concentrations. Red colour indicates as received materials, blue colour indicates cryomilled materials, purple colour indicates 75% drug loading, brown colour indicates 50% drug loading, green colour indicates 25% drug loading and yellow colour indicates at 5% drug loading. Offsets applied for presentational purposes.

Aspirin does not exhibit a detectable change in melting point and enthalpy of fusion upon cryomilling (Figure 2.11 and Table 2.7) which agreed with our XRPD data in Section 2.4.1 in confirming the highly crystalline content of aspirin after cryomilling. This is agreed with that reported by Wildfong after cryomilling of aspirin although the duration time was longer than in our work (300 minutes) [50].

For aspirin/HPMC system at 75% loading as seen in Figure 2.11 and Table 2.7 the first thermal event is the appearance of a single T_g at 43.1 ±0.4 °C which was not observed after cryomilling of aspirin alone. This T_g is quite distant for the reported aspirin T_g is -29 °C [50] or that reported for HPMC 139 °C [200] being intermediate between that of aspirin and HPMC. Additionally, at this loading the melting point onset becomes 120.5 ±1.5 °C which is lower than the melting point of the cryomilled aspirin 141.7 ±0.4 °C. The expected enthalpy of melting for this diluted mixture as seen in Figure 2.9 is 130.05 J/g aspirin, however, our co-cryomilled mixture exhibited lower enthalpy of 77.8 ±2.6 J/g aspirin. The reduction in the enthalpy of melting reflects the reduction in the crystallinity which is 59.6 % ±1.5 at this drug loading. Moving to lower a aspirin loading, the T_g for 50% aspirin loading was unchanged from that at 75% loading. At 50% aspirin loading there is more of a reduction in the melting point onset. The enthalpy of melting for this dilution is lower than the expected value (36.9 ±2.6 versus 86.5 J/g aspirin) as seen in Figure 2.9. With lowering aspirin concentration there is no change in the T_g but there is a further reduction in the melting point. The enthalpy of melting in comparison to the expected value as seen in Figure 2.9. At 5% drug loading, aspirin/HPMC system the T_g is unchanged from other concentrations. The melting peak disappears and the system becomes effectively 0% crystalline within our limit of detection. The formation of a single T_g at an intermediate point between aspirin and HPMC and the obtaining 0% crystallinity at 5% aspirin loading likely indicates the formation of an amorphous solid dispersion. Although there is a single T_g formed at all drug loadings, there is a deviation from Gordon-Taylor equation as seen in Figure 2.7 which might indicate poor mixing of aspirin with HPMC.

The XRPD results in Figure 2.11 show that there is a clear reduction in signal to noise ratio which coincides with increases in the peak width. At 5% there is an appearance of amorphous halo to indicate amorphous formation. These are in agreement with our DSC results in lacking of the crystallinity 5% aspirin loading.

Table 2.8: Summary for DSC and XRPD results from felodipine, paracetamol and aspirin.

API	Status	DSC	XRPD
Felodipine	as received	crystalline	crystalline
	cryomilled	partial amorphous	amorphous
	cryomilled with HPMC	highly amorphous from 75%	amorphous from 75%
Paracetamol	as received	crystalline	crystalline
	cryomilled	crystalline	crystalline
	cryomilled with HPMC	highly amorphous from 25%	amorphous from 25%
Aspirin	as received	crystalline	crystalline
	cryomilled	crystalline	crystalline
	cryomilled with HPMC	amorphous from 5%	amorphous from 5%

From both XRPD and DSC data it can be concluded that cryomilling felodipine alone can produce a partial crystalline form, while by co-cryomilling with HPMC can produce a highly non crystalline mixture for felodipine at high drug loading (75%). Both paracetamol and aspirin they keep their highly crystalline content when cryomilled alone. Co-cryomilling with HPMC results in a single T_g appearance for these drugs with the highly amorphous form obtained at 25%, 5% drug loading for paracetamol and aspirin respectively. From our data it is clear that the ability of HPMC to protect the re-crystallisation of a drug during cryomilling varied from one APIs to another.

A summary of the solid state transformations discussed as shown in Table 2.8. The predicted and experimental T_g was seen in Figure 2.7. It was previously reported by Konno and Taylor that HPMC is poorly mixed with felodipine as the T_g does not appreciably increase with increasing HPMC concentrations [110] earlier in this section. Furthermore it was reported that there is poor mixing of itraconazol with HPMC in which the researchers correlate this with the hygroscopic nature of HPMC that results in the deviation from Gordon-Taylor equation and poor mixing [201]. This can interpreted as poor mixing of our API with HPMC as their T_gs not clearly changed with increasing HPMC concentration which might attributed to the lack on interaction between these drug with HPMC as reported in our analysis of CSD earlier in the introduction of this chapter.

2.4.3 Synergistic effect of cryomilling

XRPD

As noted above in the XRPD data Figure 2.5, HPMC itself (pre and post cryomilling) exhibits no Bragg peaks, and the reduction in Bragg scattering for the joint cryomilled API-HPMC systems could in principle be ascribed simply to a dilution of crystalline drug with amorphous HPMC, which is undoubtedly a factor in explaining these data. However the difference in behaviour of felodipine compared to paracetamol and aspirin in terms of Bragg peaks is

notable, and raises a question as to whether dilution effects alone are enough to explain the data. Bragg peaks disappear after co-cryomilling with HPMC at 75, 25 and 5% felodipine, paracetamol and aspirin respectively. To answer this, two approaches were taken for each API-HPMC system in which: 1) as-received drug and polymer were cryomilled separately and then mixed "cryomilled separately"; 2) as-received drug and polymer were mixed then cryomilled "cryomilled together" as shown in Figure 2.12 and Figure 2.13. For the case where only dilution is occurring we would expect samples "cryomilled separately" and "cryomilled together" to be identical. If there is any synergy we would expect "cryomilled separately" and "cryomilled together" will be different from each other. The differentiation between the physical mixture and amorphous solid dispersion has been used by many researchers as a tool to confirm formation of amorphous solid dispersion [71, 110, 116].

Figure 2.12 shows the XRPD data for all selected drugs both "cryomilled together" and "cryomilled separately" with different drug loadings. At 75% drug loading; starting with Felodipine-HPMC system the "cryomilled separately" and "cryomilled together" samples do not exhibit obvious Bragg peaks, although we note the presence of what is possibly a very weak Bragg peak from felodipine around 23° in the "cryomilled separately" sample. This overall behaviour mirrors that seen for pure felodipine which also became markedly amorphous upon cryomilling. For the paracetamol-HPMC system at 75% drug loading the Bragg peaks is appeared in both "cryomilled separately" and "cryomilled together" however the peak width around 24° for the "cryomilled separately" are notably sharper than "cryomilled together" (0.114 $\Delta 2\theta$ versus 0.23 $\Delta 2\theta$) respectively (Table 2.6). Aspirin-HPMC at 75% drug loading similar to paracetamol-HPMC system at this loading no difference between cryomilled together and cryomilled separately however peak width are 0.033 $\Delta 2\theta$ versus 0.167 $\Delta 2\theta$ for cryomilled separately and for cryomilled together respectively around 15.6° peak position (Table 2.6). The peak width change for both paracetamol and aspirin at 75% loading is interpreted as previously on the basis of crystallite size reduction for the broader peaks in Section 2.4.1 and from Table 2.6.

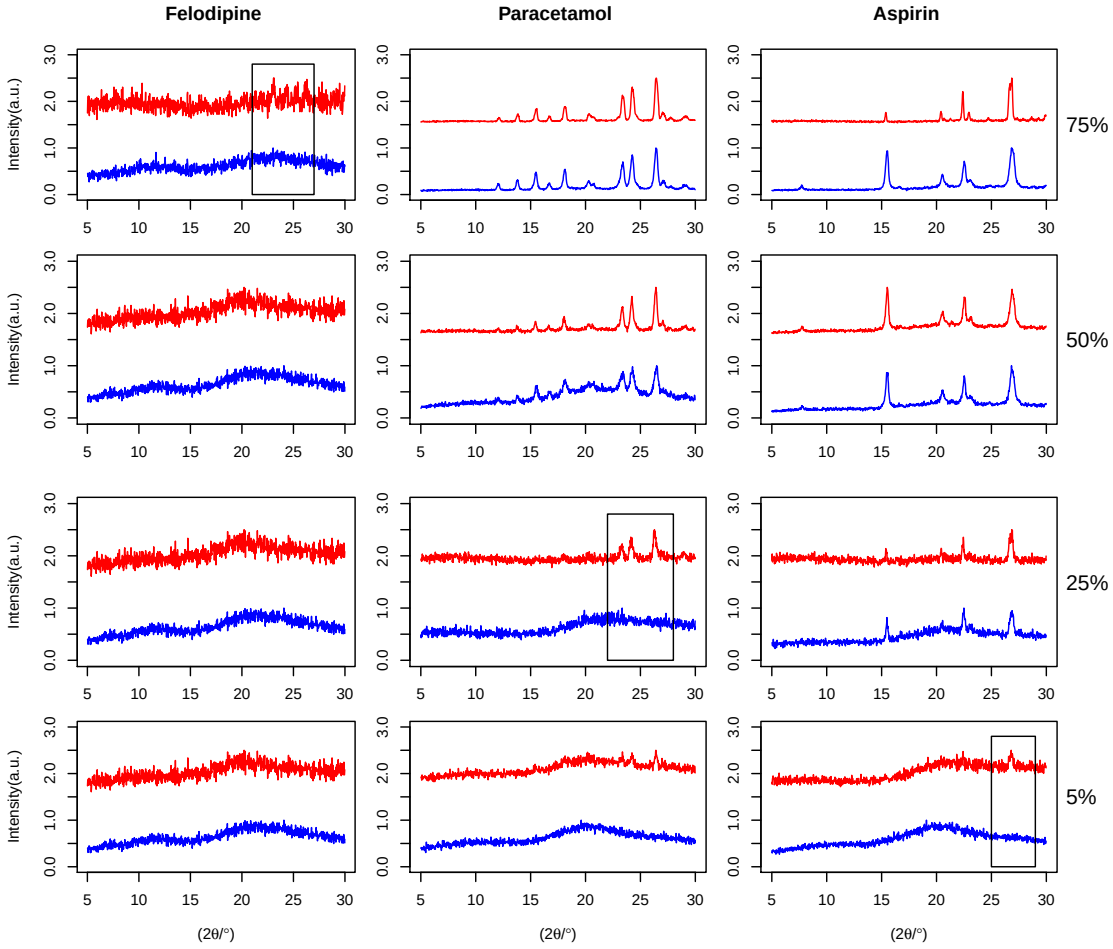

Figure 2.12: The XRPD patterns of 75%, 50%, 25% and 5% drug loading cryomilled separately (red color), cryomilled together (blue color) of felodipine, paracetamol and aspirin. Offsets applied for presentational purpose. Rectangles indicate the loading when the amorphous material appear.

Turning now to the 50% drug loadings (Figure 2.12) for felodipine/HPMC system the Bragg peaks disappeared in the cryomilled separately in addition to amorphous halo which was already seen from felodipine 75% loading cryomilled together system. For paracetamol/HPMC system at 50% loading the cryomilled separately and cryomilled together samples show a reduction in the peak intensity in comparison to 75% loading. There is more reduction in peak intensity and increasing peak width in cryomilled together over the cryomilled separately one for paracetamol/HPMC system at 50% loading. In the aspirin/HPMC system at

50% loading there is no clear difference in the intensity and width of the Bragg peaks in both cryomilled together and separately samples.

At 25% loading for the felodipine-HPMC system (Figure 2.12) the behaviour of the cryomilled separately and cryomilled together samples are identical to the 50% loading. For the paracetamol-HPMC system at 25% the Bragg peaks vanish into the noise in the "cryomilled together" mixture with appearance of amorphous halo. There is a clear reduction in the sharpness and intensity of Bragg peaks for the "cryomilled separately" mixture at 25% paracetamol loading. The aspirin-HPMC system at 25% loading still shows Bragg peaks in both the "cryomilled separately" and the "cryomilled together" however this loading exhibits a lower peak sharpness and intensity in the both cryomilled together and separately mixtures compared to the 50% aspirin-HPMC system.

The 5% system (Figure 2.12) for felodipine-HPMC does not exhibit different behaviour from both the 25 and the 50% felodipine loading for those "cryomilled together" and "separately". For the paracetamol-HPMC system at 5% loading there is a further reduction in the intensity in the Bragg peaks in the "cryomilled separately" mixtures and obviously the amorphous halo in the "cryomilled together" which appeared from 25% loading. For the aspirin-HPMC system at 5% loading the amorphous halo only appeared for the "cryomilled together" rather than the "cryomilled separately" samples.

From the XRPD data the appearance of Bragg peaks at 75% loading and lack of amorphous halo for both paracetamol and aspirin indicates that they are predominantly crystalline. At 50% loading of paracetamol the signal to noise indicated a mixture of amorphous and crystalline material. At 25% loading we no longer detect a Bragg peaks for the "cryomilled together" paracetamol-HPMC system indicating that the mixture is predominately amorphous. At 5% loading there is no Bragg peaks for aspirin-HPMC system and the amorphous halo appears in the cryomilled together mixture. The cryomilled separately samples at 5% loading aspirin do not exhibit obvious Bragg peaks, although we note the presence of what is possibly a weak Bragg peak from aspirin around 27 °.

To summarise the XRPD data, on the basis of the wider Bragg peaks, coupled

with the reduction in the Bragg peak signal to noise and the associated appearance of an amorphous halo noted in the XRPD results for the "cryomilled together" compared to the "cryomilled separately" samples, there is clear evidence that an amorphous solid dispersion is formed for at least the lower API loading when co-cryomilled with HPMC for all three drugs. The disappearance of Bragg peaks (within our limit of detection) occurs at 75, 25 and 5% loading for felodipine, paracetamol and aspirin respectively, and this suggests that the ease of forming an ASD with HPMC is in the order felodipine > paracetamol > aspirin.

DSC

As the DSC is more sensitive to amorphous content than XRPD then DSC was performed to all drugs "cryomilled together" and "separately". Thermogram data in Figure 2.13 and Table 2.9 show the "cryomilled separately" and "cryomilled together" at 75% drug loading for each APIs/HPMC system. For all systems at the 75% drug loading the "cryomilled separately" system exhibits only one thermal events which is the endothermic peak that considered to be a melting peak. The "cryomilled together" system exhibited two thermal events. The first one is the T_g appearance for all cryomilled together systems at 75% drug loading. The second endothermic event is considered to be the melting peak that show lower enthalpy of melting than the cryomilled separately one as seen in Figure 2.13 and Table 2.9 for all selected drugs. Other loadings thermogram results (Figure 1 in appendix) also show the appearance of a T_g only in the cryomilled together but not the cryomilled separately samples which is interesting because it indicates that there is an amorphous material formed.

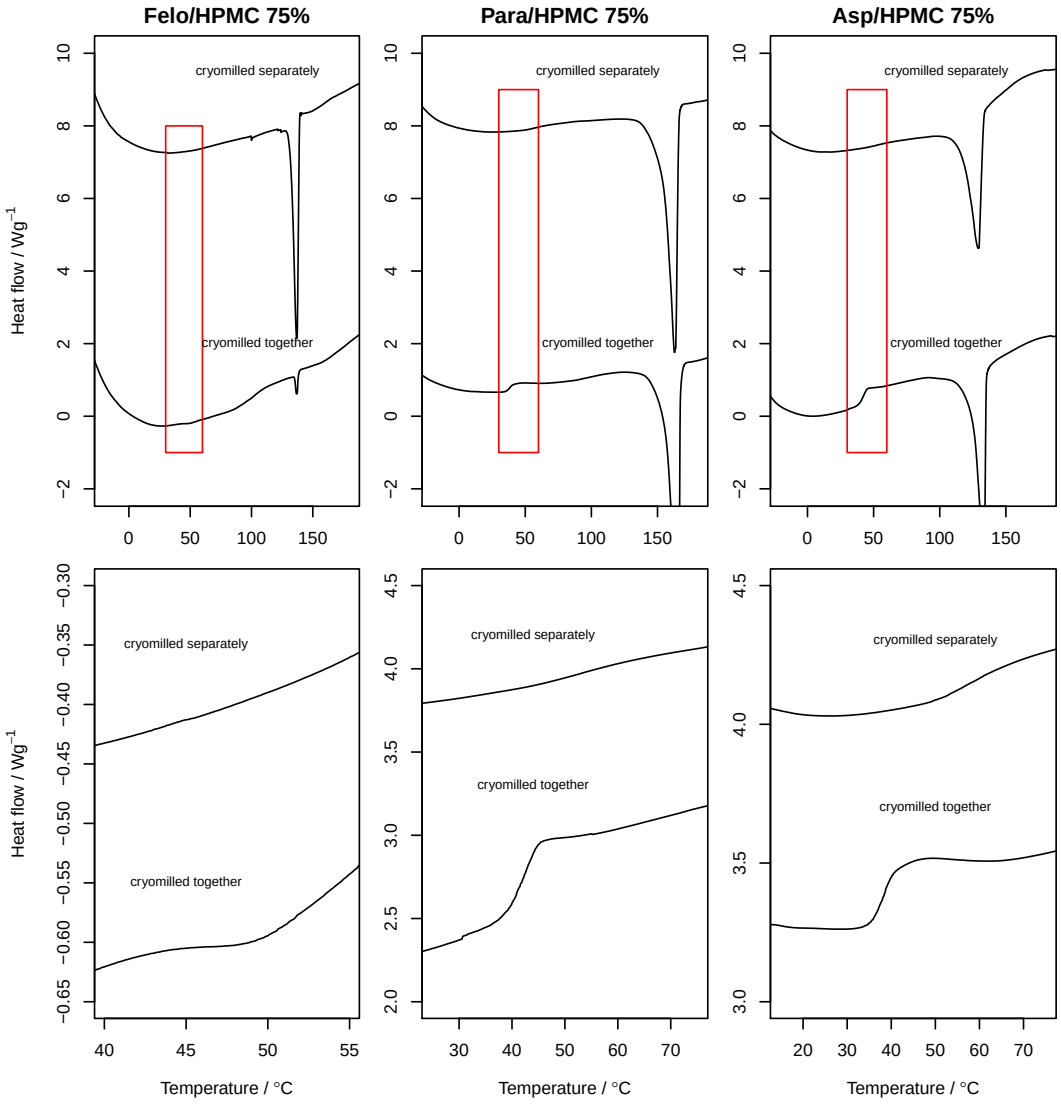

Figure 2.13: The DSC patterns of 75 % loading for physical mixture, cryomilled together and cryomilled separately of felodipine, paracetamol and aspirin. Offsets applied for presentational purpose.

In summary from the XRPD data (Figure 2.12) there is no a clear indication of disappearance of Bragg peaks until 75%, 25% and 5% for felodipine, paracetamol and aspirin respectively. By moving to DSC technique Figure 2.13 which is more sensitive to formation of amorphous materials we can see the appearance of T_g which is an indication of the formation of amorphous material, for felodipine at 75% loading and other loadings (Figure 1 in appendix). Although paracetamol and aspirin-HPMC systems at high drug loading (75%) are crystalline by XRPD but both of them exhibit a T_g which is likely indicate the presence of crystalline

Table 2.9: The thermograms results for 75% drug loading felodipine, aspirin and paracetamol.

API	T_g (mid point)°C	Melting point (onset)°C	Heat of fusion J/g	% Crystallinity
Felodipine cryomilled separately		132.3±0.3	49.1±1.5	89.7±2.7
Felodipine cryomilled together	46.7±0.2	135.4±0.6	1.2±0.7	2.1±1.3
Paracetamol cryomilled separately	-	154.2±0.1	102±2.6	80.4±2
Paracetamol cryomilled together	42.1±1.5	157.4±2	98.9±1.5	78±1.2
Aspirin cryomilled separately	-	122±0.4	88.2±4.2	76.9±3.3
Aspirin cryomilled together	43.1 ±0.4	120.5±0.5	77.8±2.6	59.6±1.5

and amorphous phase together.

2.4.4 Molecular interaction

Cryomilling causes a change in the physical state for all selected drugs as detailed in the Section 2.4.2. We will see whether poor mixing is correlated with the infrared data so that when we have a solubility limit then we will not have an interaction. The likelihood of interaction from CSD Table 2.2, 2.3 and 2.4 was used as a tool to support the FTIR data. Hydrogen bond is a strong intermolecular interactions and consequently leads to the most discernible change in FTIR spectra band. The strength of the hydrogen bond is proportional to the red shift [184]. It was reported that the red shift correlates with a shorter hydrogen bond distance [184]. Peak width, shape, intensity and position was reported previously to differentiate between the amorphous and crystalline form by FTIR [202, 203]. The uncertainty of our FTIR results is about 1 cm^{-1}.

Felodipine

Figure 2.14 shows a selected FTIR spectrum of felodipine as received, cryomilled and co-cryomilled with HPMC in different concentrations shown. This figure shows a part of IR spectrum between 3800-3000 cm^{-1} and 1750-1550 cm^{-1}. We will focus on the N-H more than C=O group as N-H group that characterises felodipine has less overlap than C=O group as suggested by Yang *et al* [204]. N-H group in felodipine has the potential to act as a hydrogen bond donor from the estimated rule suggested by Etter [114, 185]. Figure 2.14 show that the as received felodipine has N-H stretching vibration at 3365 cm^{-1} which is similar to that one reported by reference [204] which is similar to our starting polymorph I. After cryomilling, N-H band of crystalline felodipine shifted from 3365 cm^{-1} to 3330.8 cm^{-1} (shift around 34 cm^{-1}) to lower wave-number (red shift). In addition, the cryomilled felodipine N-H stretching band peak which has a width of 153.2cm^{-1} becomes more broad than the as received felodipine (width of 143.2cm^{-1}). The shift in the N-H stretching peak of cryomilled felodipine is slightly higher than the shift in peak of N-H stretching group for felodipine as reported in reference [110, 204]. The mentioned references suggest that felodipine N-H band shifted by 30 cm^{-1} and 32 cm^{-1} by HME and spray drying respectively over the crystalline felodipine. The as received felodipine has C=O stretching band at 1688 cm^{-1}. Upon cryomilling it splits in to a shoulder peak to 1698 cm^{-1} and 1676 cm^{-1}. Similar changes in the peak width, shape and position were reported after milling of crystalline linaprazan [205] and observed after amorphisation of crystalline bicalutamide [202]. For our cryomilled felodipine this can be interpreted as the N-H functional group which act as H-bond donor has the ability to form a hydrogen bond with carbonyl group of other felodipine molecules which act as an acceptor [71, 110, 206]. The reduction in wave-number of one of the carbonyl groups was interpreted as it is acceptor group as reported by [110]. It was investigated before [184] that in the amorphous phase only one of the carbonyls is hydrogen bonded, whereas the other is non associated or extremely weakly hydrogen bonded [184]. A partial amorphous form was obtained upon cryomilling of felodipine as outlined in

Section 2.4.2. This interaction is expected to be stronger in the amorphous over crystalline form in felodipine due to loss of the crystal packing upon amorphisation that lead to optimisation of H-bond strength of the amorphous form over the crystalline one.

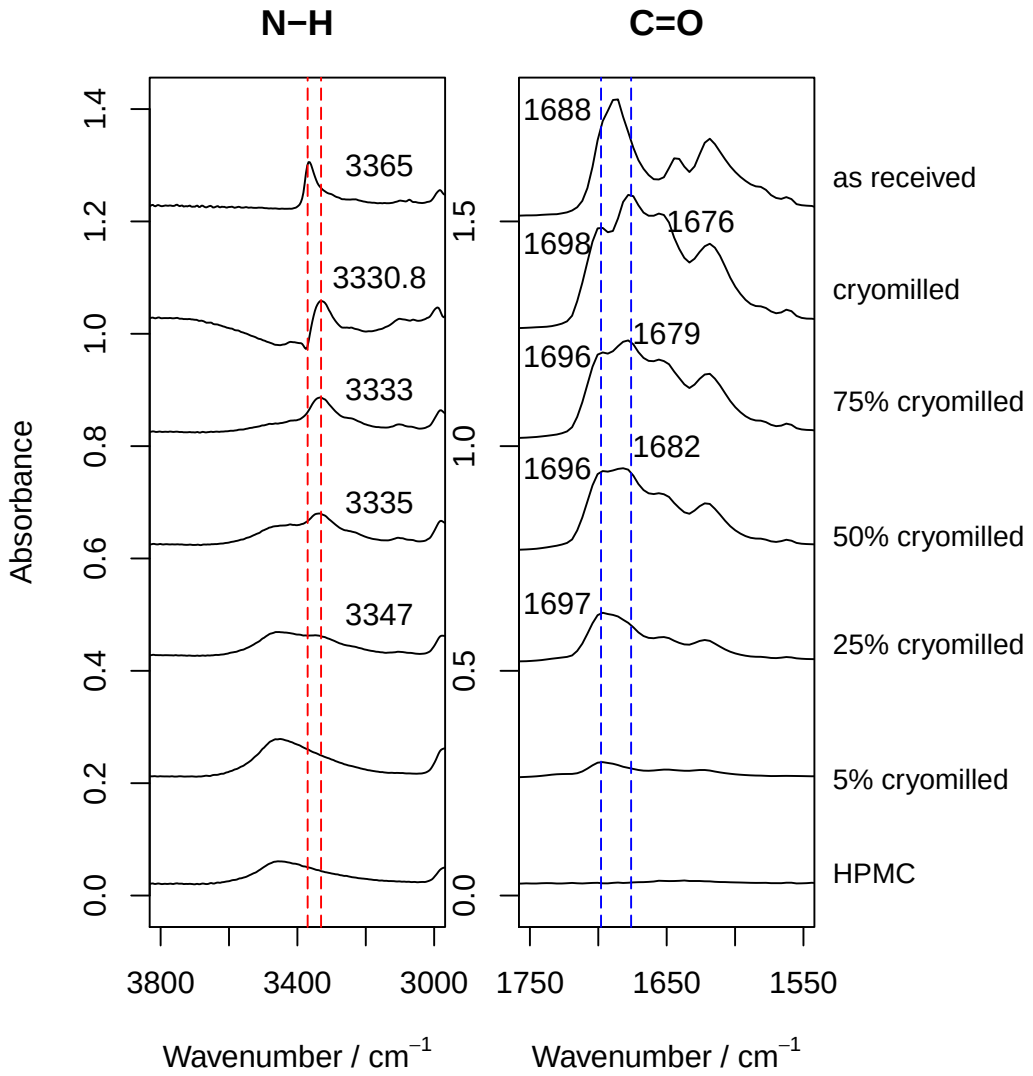

Figure 2.14: The ATR-FTIR of HPMC and felodipine as received, cryomilled for 150 mins and cryomilled together with HPMC in different concentrations. Red dotted line represent NH group position and blue line indicated C=O group position. Offsets applied for presentational purpose.

Upon co-cryomilling with HPMC (Figure 2.14) the N-H stretching band is shifted

to a higher wave number (blue shift) in comparison to the cryomilled felodipine. The N-H stretching peak of the cryomilled felodipine at 3330.8 position becomes 3333 cm^{-1} after co-cryomilling with HPMC at 75% drug loading, 3335 cm^{-1} at 50% drug loading and 3347 cm^{-1} at 25% drug loading. The peak shifted to the higher wave-number with increasing HPMC concentration in comparison to the cryomilled felodipine. This blue shift with increasing polymer concentration can be explained by the dilution effect of HPMC to the cryomilled felodipine rather than formation of the H-bond between the felodipine and HPMC. This finding with the CSD analysis in the Table 2.2 might indicate low probability of hydrogen bond formation between felodipine and HPMC. This finding of the lacking in hydrogen bond between felodipine and HPMC was reported by [110] for spray dried felodipine with HPMC. The simplest explanation from our data is that specific H-bonding interactions between HPMC and felodipine are weak at best. The amorphous dispersion formation likely happened without any hydrogen bond formation.

Paracetamol

Figure 2.15 shows a selected FTIR spectrum of paracetamol as received, cryomilled and co-cryomilled with HPMC in different concentrations shown. This figure shows a part of IR spectrum between 3500-3000 cm^{-1} and 1800-1550 cm^{-1}. The as received paracetamol has an N-H stretching band which is sharp band that appear in the FTIR spectrum at 3321.4 cm^{-1} as seen in Figure 2.15. In addition there is a broad O-H stretching band which is appeared at lower wave-number in comparison to N-H band at 3156 cm^{-1} and 3109 cm^{-1}. The C=O stretching peak was seen at 1650.7 cm^{-1} which is similar to the result obtained from crystalline paracetamol as reported by Martinez et al [207]. The strongest donor group predicted according to Etter [185] is (O-H). The broad shape of the O-H band is indicates involvement of O-H group in a stronger H-bond with other paracetamol molecules than N-H group in the crystal structure.

After cryomilling of paracetamol, there is no change in the main peaks in position and relative intensity from the as received paracetamol as seen in Figure 2.15

as uncertainties in our ATR-FTIR that used in this experiment is about 1 cm^{-1}. Upon co-cryomilling with HPMC if there is an interaction between paracetamol and HPMC, then a red shift (moving to lower wave number) should be expected in the strongest donor group which is O-H group in paracetamol. The polymer should have the ability to break the H-bond between paracetamol-paracetamol molecule and form a new bond [208]. At 75% drug loading there is no different in the position of the O-H stretching N-H stretching band nor in C=O stretching band after co-cryomilling at 75% drug loading as seen Figure 2.15. As we mentioned earlier the uncertainty in the ATR-FTIR instrument about 1 cm^{-1} so this change after cryomilling the as received paracetamol is consider to be not significant. Increasing the concentration of HPMC to 50% results in further increasing blue shift to 3117 cm^{-1} for the suggested donor O-H group. Further increase in the HPMC concentration at 25% loading and lower results in unclear or flat peak position in the (O-H) band. From our CSD data Table 2.3 the possibility of H-bond interaction between paracetamol and HPMC is weak. It was previously reported by researchers in references [149, 186, 209] that there is a weak interaction between phenolic O-H (as in our paracetamol donor group) with moderate acceptor group such as that found in (HPMC). As increasing HPMC concentration in 75 and 50% results in more blue shift comparing to the cryomilled O-H stretching band position this can be interpreted as dilution effect only. To sum up both FTIR and prediction results from CSD are agreed in there is no clear evidence for H-bond interaction between paracetamol and HPMC.

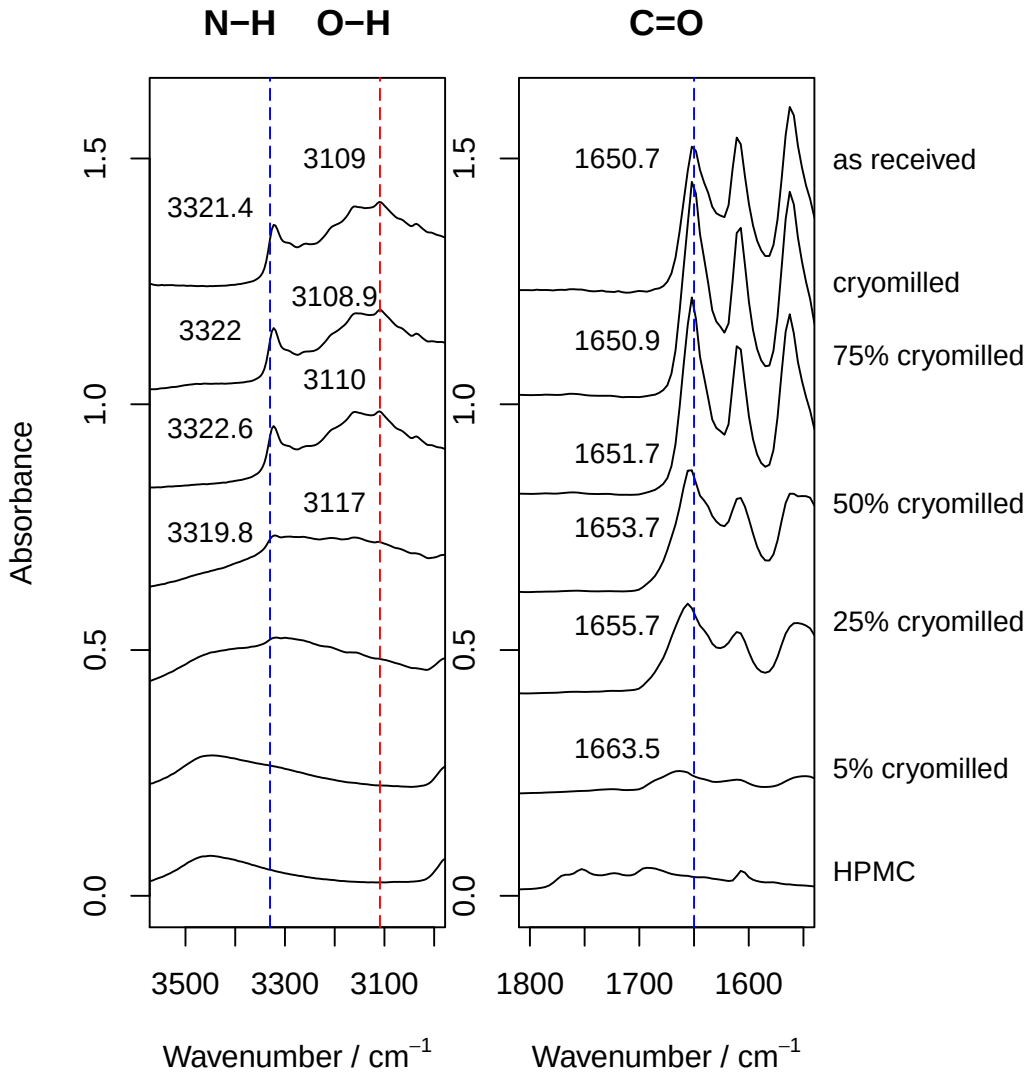

Figure 2.15: The ATR-FTIR of paracetamol as received, cryomilled for 150 mins and cryomilled together with HPMC in different concentrations. Numbers indicates amide and carbonyl stretching peak. Red dotted line represent NH group position and blue line indicated C=O group position. Offsets applied for presentational purpose.

Aspirin

Figure 2.16 shows the a part of FTIR spectra between 4000-3100 cm^{-1} and 1750-1620 cm^{-1} of aspirin as received and aspirin upon cryomilling and upon co-cryomilling with HPMC in different concentrations shown. The strongest

donor according to Etter prediction [185] is O-H. This group has a stretching band at 3491.6 cm^{-1}. In addition the C=O stretching band is sharp at around 1680 cm^{-1}. After cryomilling, no change in the peak position of the main group in the band O-H or in C=O is seen (Figure 2.16). After co-cryomilling with HPMC, it is difficult to follow the O-H stretching band position due to the overlap with O-H stretching of HPMC at 3449.8 cm^{-1}. The C=O stretching band upon co-cryomilling with HPMC shifted to a higher wave number (blue shift) by 2, 4, 5 and 9 cm^{-1} for 75, 50, 25 and 5% loading respectively. There is no clear interpretation for these shifts since it happened in the acceptor not the donor part of the spectra. From the CSD in the Table 2.4 there is a weak probability for H-bond interaction between aspirin and HPMC.

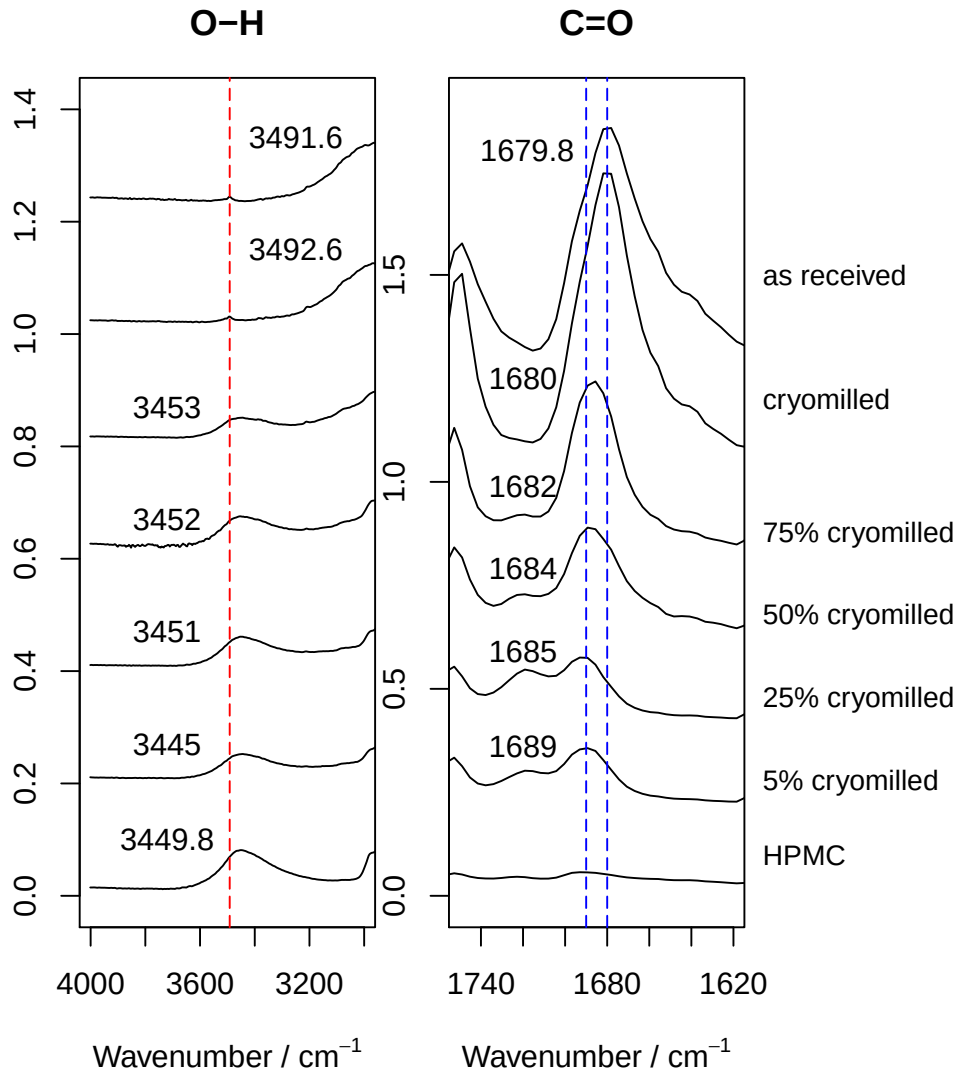

Figure 2.16: The ATR-FTIR of aspirin as received, cryomilled for 150 mins and cryomilled together with HPMC in different concentrations. Offsets applied for presentational purpose.

It can be concluded that although a amorphous solid dispersion is formed for all selected drugs that there is weak probability of H-bond formation between felodipine, paracetamol and aspirin with HPMC. This weak or absence of interaction is possibly consistent with the poor mixing of the selected drugs with HPMC.

2.4.5 Stability study

Stability against chemical decomposition

As received felodipine was yellow in colour (Figure 2.17). After cryomilling of felodipine for 150 minutes a colour change from yellow to white occurred while both paracetamol and aspirin (white colour) colour remain unchanged after cryomilling. This color change for felodipine was reversible upon storage (Figure 2.17). Other cases of colour change upon milling has been reported, for example after room temperature milling of linaprazan and piroxicam [205, 210]. This is typically where the amorphous and crystalline materials have different colours. If the colour change is reversible then the amorphous transformation to the crystalline one might be happened without chemical decomposition [205, 210]. Chemical decomposition upon cryomilling was excluded to have occurred as reported by Decamps et al for the cryomilling of lactose [43] but has happened after room temperature milling of lactose [211]. This is due to the local melting of lactose during milling that results in mutarotation (sign of decomposition) [211] and indicates the ability of cryomilling to better stabilise the amorphous form.

In order to exclude chemical decomposition for felodipine, an FTIR based stability test was done for the as received, cryomilled and stored cryomilled samples after 2 months (Figure 2.17). It is clearly seen in our study that the broad amide peak of felodipine cryomilled spectrum starts to sharpen after storage and returns to the same position of the "as received" sample, again indicating that the amorphous form recrystallises and that no chemical degradation results from cryomilling. In contrast after co-cryomilling of felodipine with HPMC, the mixture turned white and after 2 months storage period no colour change for co-cryomilled felodipine with HPMC was observed (data not shown). This irreversible colour change was also reported by Descamps *et al* for piroxicam cryomilled with PVP [107]. A none reversible colour change is likely due to the inhibitory effect of the polymer against recrystallisation for the experimental time scale.

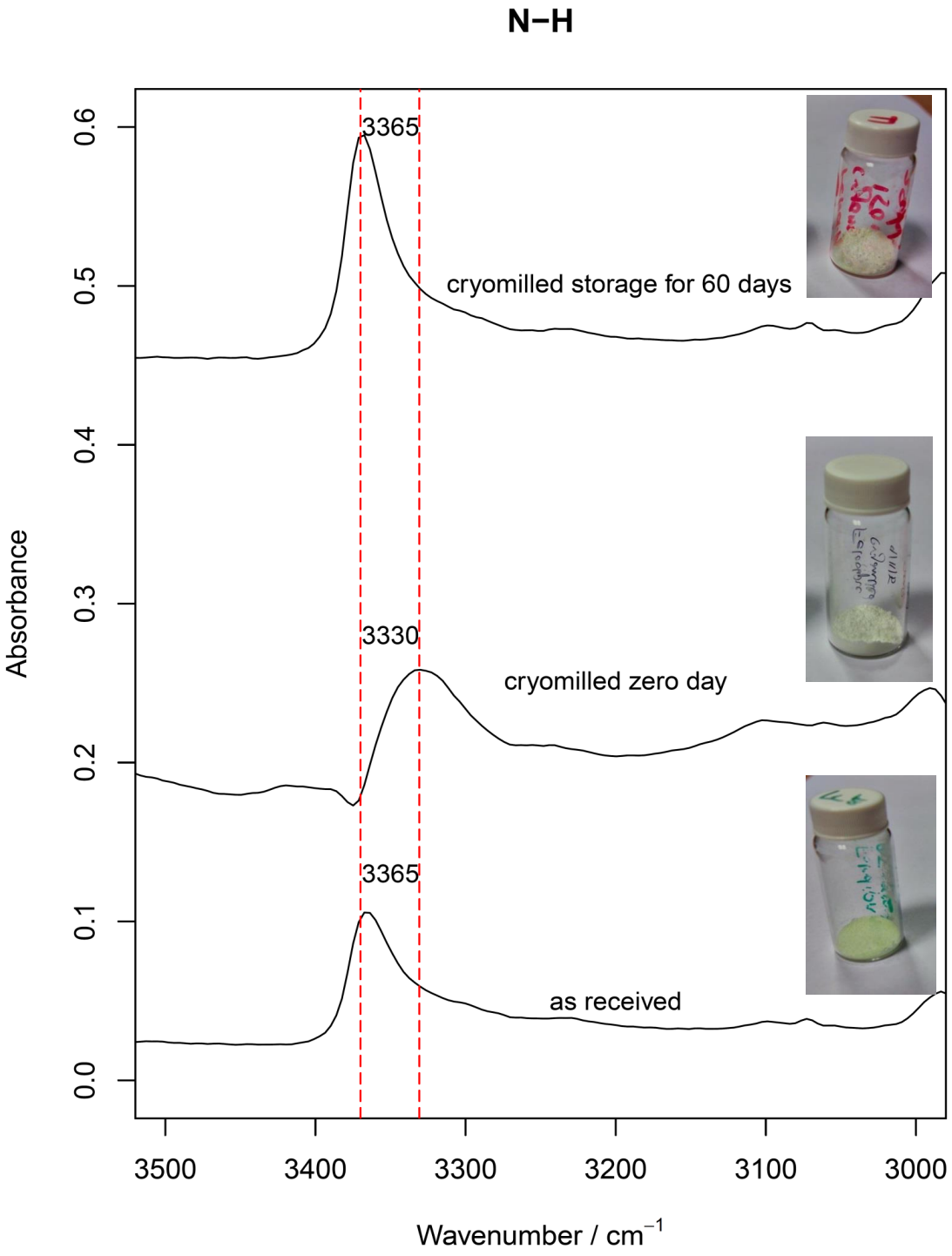

Figure 2.17: The ATR-FTIR of felodipine as received, cryomilled for 150 mins and cryomilled for 150 mins after 60 days. Offsets applied for presentational purpose.

Stability against recrystallisation

Felodipine: Figure 2.18 shows the stability study data for cryomilled and co-cryomilled with HPMC in concentration of 75, 50 and 25% at 25 °C/43% RH for felodipine by DSC and XRPD. "Zero time" means the data collected directly after cryomilling. The XRPD data in Figure 2.18 show that the amorphous halo of the cryomilled felodipine was greatly reduced and sharp Bragg peaks start to appear after storage for 24 hours at 25 °C/43% RH. These conditions of storage were used as a stress test to induce crystallisation. Upon co-cryomilling with HPMC at 75% drug loading (Figure 2.18), the XRPD amorphous halo that appeared upon co-cryomilling was noticeably reduced after the 5th day of storage and this coincided with appearance of Bragg peaks. The Bragg peaks became sharper and/or more intense after 40 days storage than the 5th day. At 50% drug loading, the amorphous halo stayed until the 10th day then greatly reduced as Bragg peaks appeared. The sharpness of the Bragg peaks increased further more after 60 days. At 25% loading the XRPD data did not exhibit any detectable change during the storage period. The 25% felodipine loading does not exhibit detectable recrystallisation within the duration of our study. XRPD results indicate that cryomilling of felodipine on its own results in an unstable partially amorphous form that recrystallises within 24 hr while the addition of HPMC results in a delay of the recrystallisation. The XRPD data also indicate that co-cryomilling with HPMC delays the recrystallisation event for both 75% and 50 % felodipine loading for 5 and 10 days respectively and inhibits crystallisation at 25% drug loading.

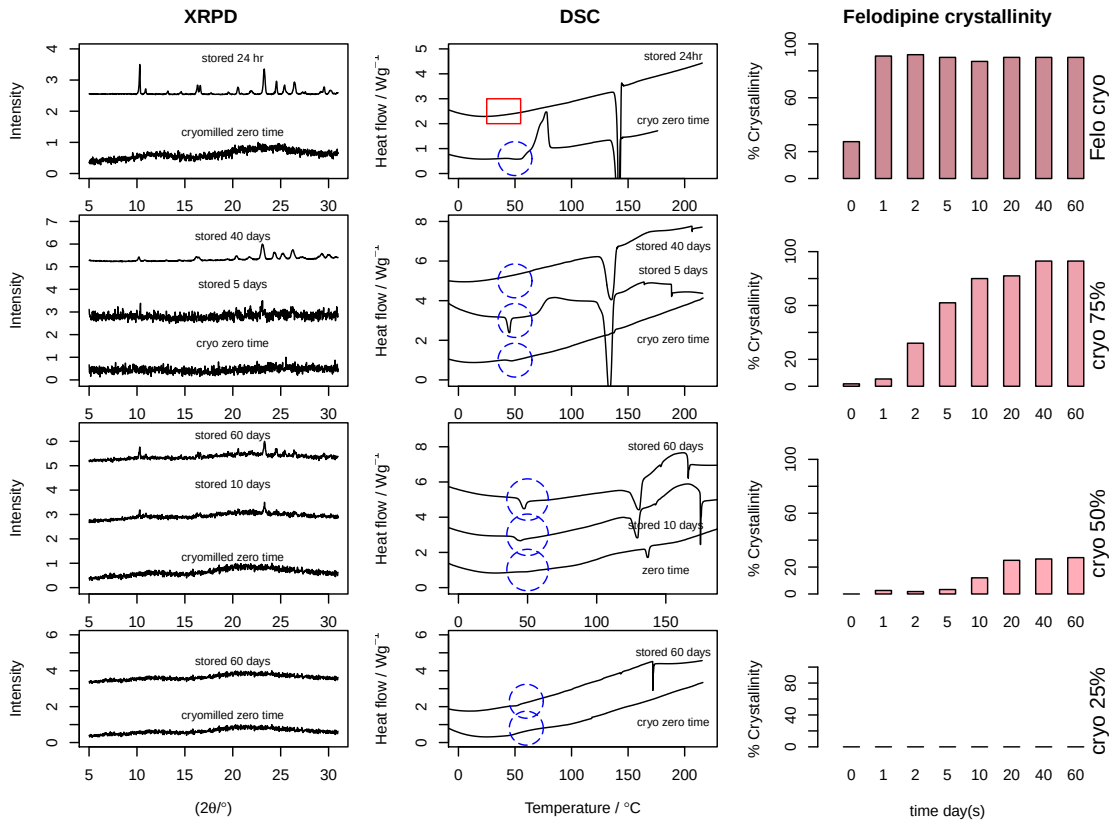

Figure 2.18: DSC thermograms and XRPD results for cryomilled felodipine and co-cryomilled felodipine 75%, 50% and 25% directly after cryomilling "zero time" and within 2 months at 25 °C/ 43% RH. The red box and the blue circle indicates the T_g. Offsets and scales applied for presentational purpose. The crystallinity was quantified by DSC not XRPD.

It is clearly seen from the DSC data in Figure 2.18 that two thermal events appeared upon cryomilling felodipine which are a T_g (46.7 ±0.5 °C) and a recrystallisation peak (74 ±2.5 °C) which are greatly reduced on storage for 24 hour at 25 °C/43% RH. In addition, the enthalpy of melting increased after lengthy storage which is interpreted as due to increase of the crystalline content of felodipine from 27.5% of the cryomilled felodipine to about 92% after 24 hour storage. This is similar to the behaviour of cryomilled sulfathiazole (after 150 minutes) stored under 22 °C/35% RH reported by Hu *et al* [56]. At 75% felodipine loading the sample exhibits a T_g at "zero time" (45.9 ±1.2 °C Table 2.7). This T_g is typically of sigma shape on day zero after and become distinct dip after

storage for 5 days as widely reported in the literature being due to a relaxation phenomenon and often described as an overshoot [161]. This T_g is not observed after 40 days storage in our study. The enthalpy of melting increased gradually which is interpreted as an elevation in the crystalline content of felodipine to become around 90% after 2 months storage. Lowering felodipine loading to 50% shows that upon storage there are two changes in the thermal event by the 10th day of storage. The first one is the T_g was overshot and the second is an increase in the enthalpy of melting. At the 60th day storage the T_g was deeper overshot compared to that one at 10th day storage. In addition, the enthalpy of melting increases which reflects increasing crystallinity within storage period to become 25% crystallinity. Reducing to 25% felodipine loading the Tg of the co-cryomilled mixtures remains unchanged even after 2 months storage. The crystallinity was also unchanged and the mixture stays non crystalline after lengthy storage. DSC data is in agreement with the XRPD results and indicates that cryomilling of felodipine on its own results in an unstable partial amorphous form that recrystallises within 24 hours. Co-cryomilling with HPMC results in either delay the re-crystallisation at high drug loading or inhibits recrystallisation at 25% or less during the storage.

Paracetamol: Figure 2.19 shows the solid state stability data for co-cryomilled paracetamol with HPMC at 25 and 5% at 25 °C/43% RH by DSC and XRPD. These drug loadings were selected because this mixture gave a high amorphous content (Section 2.4.2).

The XRPD data in Figure 2.19 show that the amorphous halo that appeared at zero time starts to disappear into Bragg peaks after 24 hour storage within our limit of detection. After 60 days storage, the Bragg peaks increased in their sharpness. Lowering paracetamol loading to 5%, the amorphous halo was seen even after 60 days storage in the mentioned condition. These XRPD data indicate that although cryomilled paracetamol/HPMC at 25% loading is highly none crystalline, it recrystallises upon storage in the mentioned condition. Increasing HPMC concentration seems to inhibit the recrystallisation with the duration of storage.

The DSC data in Figure 2.19 show that co-cryomilled paracetamol/HPMC at 25% loading exhibits a T_g at 46.7 ±2.3 °C for freshly prepared sample (Table 2.7). The crystallinity of the mixture is around 90%. After storage for 24 hour, there is no change neither in T_g nor in the crystallinity. This T_g was overshot after 60 days storage and the crystalline content is doubled after the lengthy storage period. By lowering paracetamol loading to 5%, the freshly prepared sample exhibits a T_g of 47.7 ±4.1 °C (Table 2.7) which is seen also after 2 months storage in 25 °C/43% RH and the calculated crystalline content was also unchanged after lengthy storage. These DSC data agreed with XRPD data in indicating that a 25% mixture is unstable but increasing polymer concentration likely results in protection of paracetamol from the recrystallisation.

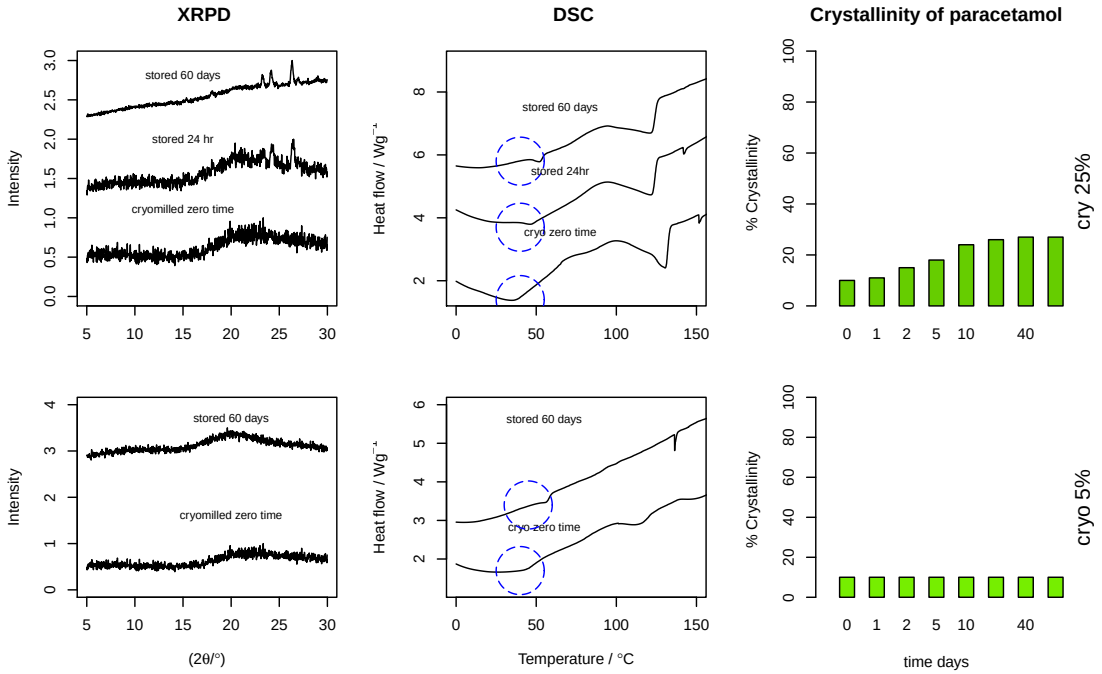

Figure 2.19: DSC thermograms and XRPD results for 25% co-cryomilled paracetamol at "zero time", 24hr and after 60th day storage at 25°C/ 43%RH. The blue circle indicates the T_g of the mixture. Offsets and scales applied for presentational purpose. The crystallinity was quantified by DSC not XRPD.

Aspirin: Figure 2.20 shows a solid state stability data for co-cryomilled aspirin

with HPMC at 5% at 25 °C/43% RH by DSC and XRPD. Paralleled to paracetamol, the stability study was done only on co-cryomilled aspirin with HPMC at 5% drug loading because this is the only concentration that gave a high amorphous content.

The XRPD results in Figure 2.20 show that amorphous halo that was observed after freshly co-cryomilled sample at 5% aspirin loading remained even after 2 months storage. The DSC data show that the T_g that was observed after co-cryomilling with HPMC was also seen after the lengthy storage. In addition the crystalline content that remained at 0% after 2 months. Both XRPD and DSC indicate that the co-cryomilled aspirin with HPMC at 5% drug loading is stable under the storage condition for at least 60 days with no evidence of recrystallisation detected.

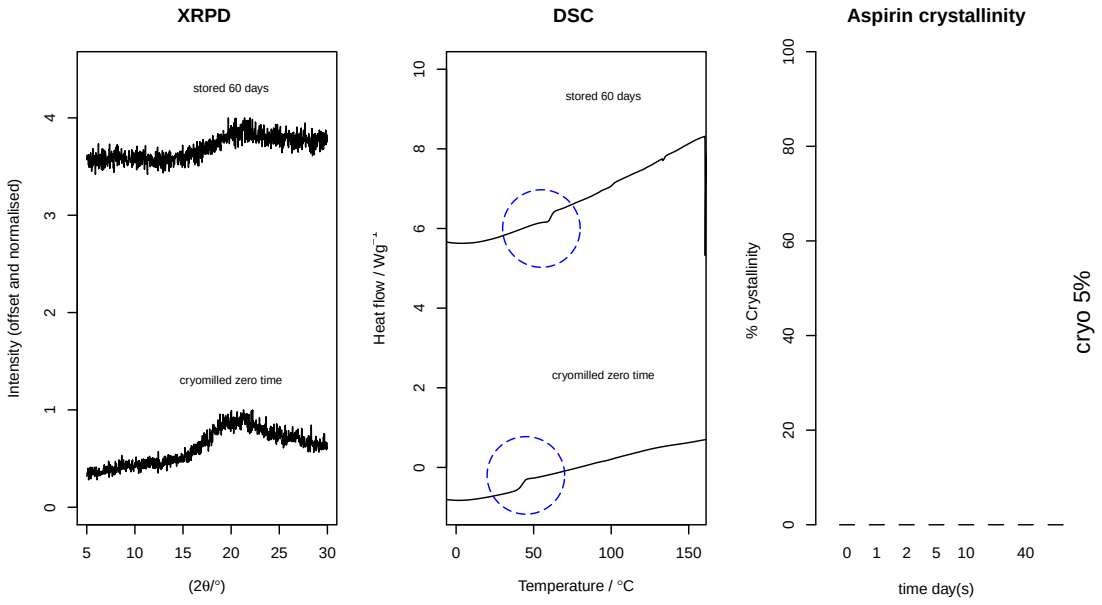

Figure 2.20: DSC thermograms and XRPD results of aspirin cryomilled for 150 mins, cryomilled together with HPMC 5% drug loading for 60 days at 25 °C/43 %RH. Offsets and scales applied for presentational purpose. The crystallinity was quantified by DSC not XRPD.

Overall, this study shows that obtaining highly amorphous content for our

selected drug, felodipine does not mean it is stable against recrystallisation because it readily crystallises upon storage for 24 hr. Although co-cryomilling with HPMC results in highly amorphous content for felodipine, paracetamol and aspirin at 75, 25 and 5% respectively it is not a guarantee of their stability against recrystallisation upon storage. There is a need to increase HPMC concentration for co-cryomilled selected drugs to delay their recrystallisation under storage conditions. Because HPMC is a hygroscopic polymer all the mixtures might absorb water during storage [121]. This water might result in increasing molecular mobility and then recrystallisation as reported by Rumondor and Taylor [121].

In this stability study we can see from Figure 2.18 for felodipine that the T_g becomes lower than the initial value before storage while for both paracetamol and aspirin it becomes higher than before storage as seen in Figure 2.19 and 2.20. Baird and Taylor suggested that the correlation between the T_g and stability is especially necessarily straightforward for multicomponent systems [66] as it can either increase or decrease. In the presence of moisture it makes the detection of T_g difficult due to the desorption of the moisture during heating of the sample that results in a broad endotherm [121]. The increase in the T_g after storage was also reported by Vasanthavada *et al* for griseofulvin-PVP and Indoprofen-PVP mixtures prepared by spray drying method and stored for 90 days at 40 °C/69% RH. The researchers correlate this phenomenon with a phase separation that might have happened prior to crystallisation due to the saturation of drug-rich phase [212].

2.4.6 Dissolution study

Figure 2.21 shows the dissolution results for felodipine, paracetamol and aspirin as received, 50% physical mixture with HPMC before and after cryomilling. After cryomilling, samples were stored for up to 24 hour in a minimum environment humidity at room temperature. For felodipine, it is clearly seen in Figure 2.21 that the release of the as received felodipine is less than 40% after 6 hours of dissolution. Cryomilled felodipine release is more than double that

of the as received. It was previously reported by Karmwar *et al* that percentage of indomethacin release increased after cryomilling. They found that the cryomilled indomethacin for 120 and 180 minutes increased the total amount of the release after 60 minutes dissolution time by 5 and 8 fold respectively. Here, the cryomilled (150 minutes) felodipine amount released after 60 minutes was increased from 11%-72% (Figure 2.21). This elevation in felodipine release after cryomilling is likely due to the effect of cryomilling reducing particle size as observed in Section 2.4.1 and/or to amorphisation [1, 63, 213, 214]. The as received felodipine is a neutral drug with pKa less than 2. The release is independent on the pH of the media unless it is less than 1 [172]. The % ionisation in pH 6.8 is low, 0.000016% calculated by Henderson-Hasselbalch equation (Equation 2.3.8).

After addition of 50% HPMC, the release of felodipine from the physical mixture as seen in Figure 2.21 becomes about 60% after 6 hours which is higher than the as received felodipine (40%) but still lower than the cryomilled one. After co-cryomilling with HPMC, the percentage drug release increases to $\simeq$ 100% after 6 hour dissolution. These results are difficult to compare with other work due to difficulty in achieving the same condition for comparison such as pH, time, polymer, sink conditions *etc.* to minimise the difference in these condition to compare the release of our amorphous solid dispersed felodipine with HPMC with other work for felodipine with PVP prepared by solvent evaporation under sink conditions. The release of felodipine from 50:50 mixture felodipine:PVP after 20 minutes has been reported as less than 10% [215], however, for our co-cryomilled felodipine with HPMC within 15 minutes we achieve a 76% drug release. The elevation of felodipine release from the physical mixture (felodipine with HPMC physically mixed by mortar and pestle) before cryomilling could attributed to the surfactant effect of HPMC. HPMC can act as surfactant that increases the release of an API [216]. The elevation in felodipine release upon co-cryomilling with HPMC in comparison to the cryomilled felodipine might be related to the solubilising effect of HPMC which was observed after co-cryomilling and/or its reported to have a protection against recrystallisation during dissolution in aqueous media [35, 217].

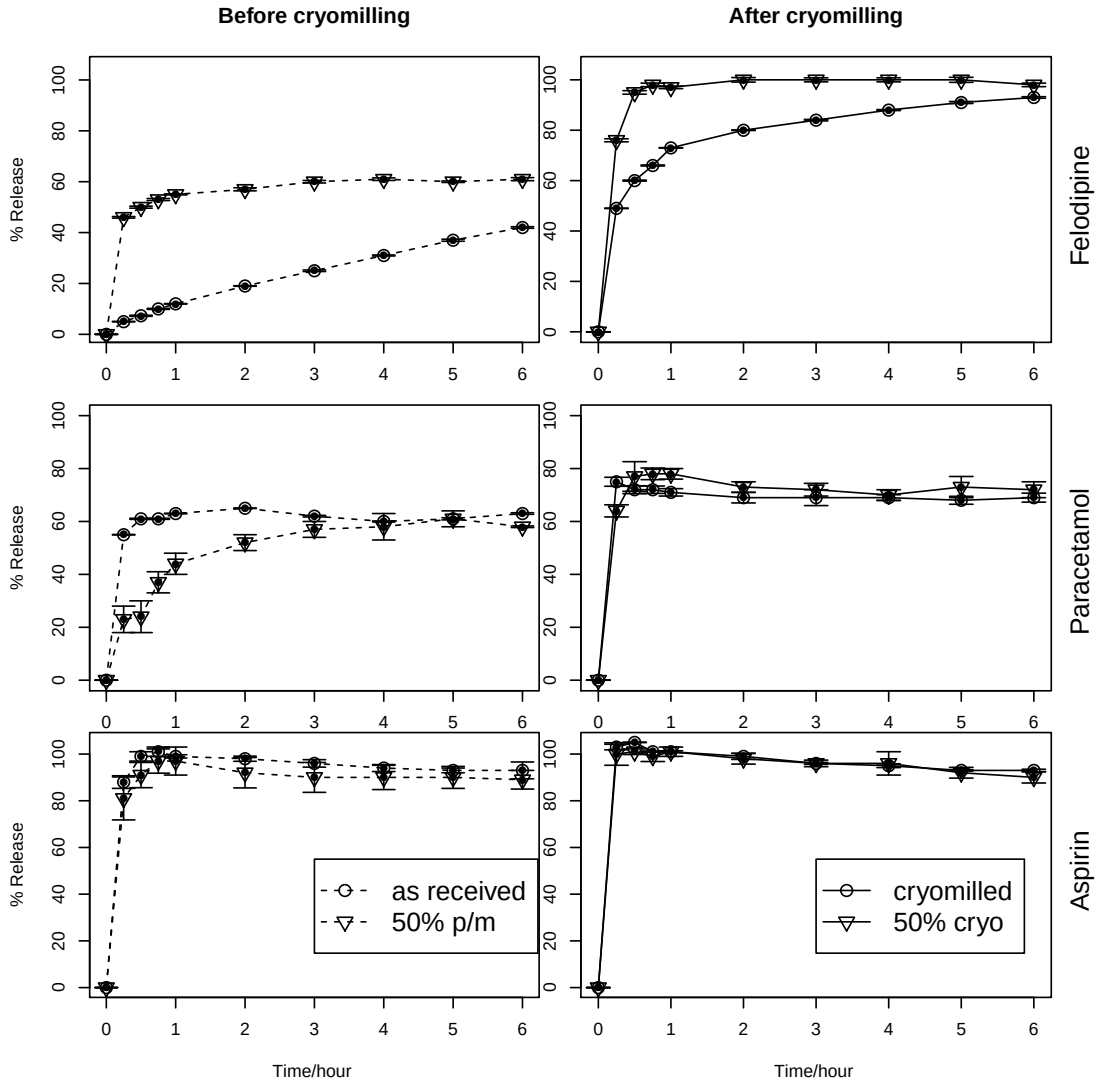

Figure 2.21: The release profile of felodipine aspirin and paracetamol as received, physically mixed (p/m) with HPMC, cryomilled (cryo) for 150 mins and cryomilled together with HPMC in 50% drug loading (n=3).

Paracetamol release is seen in Figure 2.21. The release of the as received paracetamol is approximately 62% after 6 hours dissolution. The cryomilled paracetamol showed a higher release 69% over the as received one after 6 hours dissolution. This is likely indicate that the cryomilling of paracetamol increases the release rate of paracetamol in comparison to the as received one which is probably due to the particles size reduction as investigated in Section 2.4.1. This results in increasing the surface area and hence the dissolution rate. Paracetamol is unionized (degree of ionization is 0.2%) calculated by Henderson-Hasselbalch

(Equation 2.3.6) in pH 6.8 (with pKa of 9.5 [174]).

The release of paracetamol for the physical mixture is slightly lower than the as received paracetamol before 6 hour, however, after 6 hour the release of paracetamol from the 50% physical mixture with HPMC did not show any different in comparison to the as received paracetamol. The co-cryomilled paracetamol with HPMC did not show any difference from the cryomilled paracetamol after 6 hours dissolution from the cryomilled paracetamol. This likely indicates that there is no role of HPMC in increasing paracetamol release neither before nor after cryomilling. The slight retardation of drug release from the physical mixture could be attributed to the increasing the concentration of HPMC in the dissolution media (due to different in the potency of each drug in our experiment in the dissolution media to achieve 1:1 drug:polymer concentration) that results in increasing the viscosity of the media in case of paracetamol/HPMC system and hence a retardation of the drug release according to Stoke-Einstein's equation, where the diffusion coefficient is inversely proportional to the viscosity of the system [218]. This is different from behaviour of HPMC with felodipine, likely due to the different in the concentration of HPMC in felodipine-HPMC system in comparison to the paracetamol-HPMC system or due to failure of HPMC in protection of paracetamol against recrystallisation during dissolution. Furthermore, it was reported that there is a complex relationship between HPMC and the SDS that used in the experiment here. There is a certain ratio of HPMC and SDS that can affect the critical micelles concentration and hence affecting the water solubilising effect of this complex on the drug release [219–221]. This ratio was not investigated in this study since we focused only on the effect of cryomilling on the release of the selected drugs upon cryomilling and co-cryomilling with polymer.

For aspirin as seen Figure 2.21 the release is high at essentially 100% for the as received, physical mixture, cryomilled and co-cryomilled with HPMC. There is no remarkable difference between the cryomilled and non cryomilled samples or addition of HPMC. A slight reduction in the aspirin release rate was observed after physically mixed with HPMC. This high release rate of aspirin is

probably due to its high percent of ionization at pH 6.8 of 99.98% (calculated by Henderson-Hasselbalch Equation 2.3.6) as aspirin is an acidic drug with pKa of 3.5 [176, 177]. This high percentage of the aspirin release is possibly independent on other factors such that affect the dissolution like particle size reduction. The slight reduction in the release of aspirin from the physical mixture is interpreted similar to HPMC effect on paracetamol release.

For all selected drugs due to the differences in their dissolution under pH 6.8, the effect of cryomilling on release is varied. Cryomilling significantly increases the release rate of felodipine, relatively moderately increase the release rate for paracetamol and does not significantly affect aspirin release rate. Physical mixing with HPMC can enhance felodipine release but slightly retards paracetamol and aspirin release. Co-cryomilling with HPMC, only increased the release of felodipine in comparison to the to being cryomilled alone while, it is not effective for both of cryomilled paracetamol or aspirin.

2.5 Conclusion

For the first time we have demonstrated the effect of co-cryomilling as a generic route to produce amorphous solid dispersions for both drugs which either have been processed by other methods or hardly been studied at all before due to their stability issues. The observation of clear evidence of a T_g and a clear difference in behaviour between the physical mixture and cryomilled one indicate that true dispersions have been formed. The three drugs we have considered in this study possess different physicochemical properties and consequently different co-cryomilling behaviour with HPMC, exhibiting a clear T_g only at certain drug loadings. This suggests that producing amorphous solid dispersion by co-cryomilling with a polymer of could be viable for wide range of drugs albeit with the limitation of absolute drug loading. When we examined drug release from these formulations we found that there is either an enhancement or no clear change (for materials which is already rapid drug release) in drug release. The implications are quite exciting for applying this methodology to a wider

Table 2.10: Conclusion of Chapter 2.

Change	Status	API		
		Felodipine	Paracetamol	Aspirin
Size reduction	Cryomilled	✓	✓	✓
	Co-cryomilled with HPMC	✓	✓	✓
Solid state transformation	Cryomilled	✓	✗	✗
	Co-cryomilled with HPMC	✓	✓	✓
H-Bond	Cryomilled	✓	✗	✗
	Co-cryomilled with HPMC	✗	✗	✗
Enhanced stability with respect recrystallisation	Cryomilled	✗	✗	✗
	Co-cryomilled with HPMC	✓	✓	✓
Increase drug release	Cryomilled	✓	✓	✗
	Co-cryomilled with HPMC	✓	✗	✗

range of drugs, particularly those with poor solubility such as felodipine.

Although there is amorphous formation for the selected mixtures there is a solubility limit with HPMC, therefore in the next Chapter 3 we will focus on selection of other polymers that might have a better solubility and stability and form a single phase via co-cryomilling route.

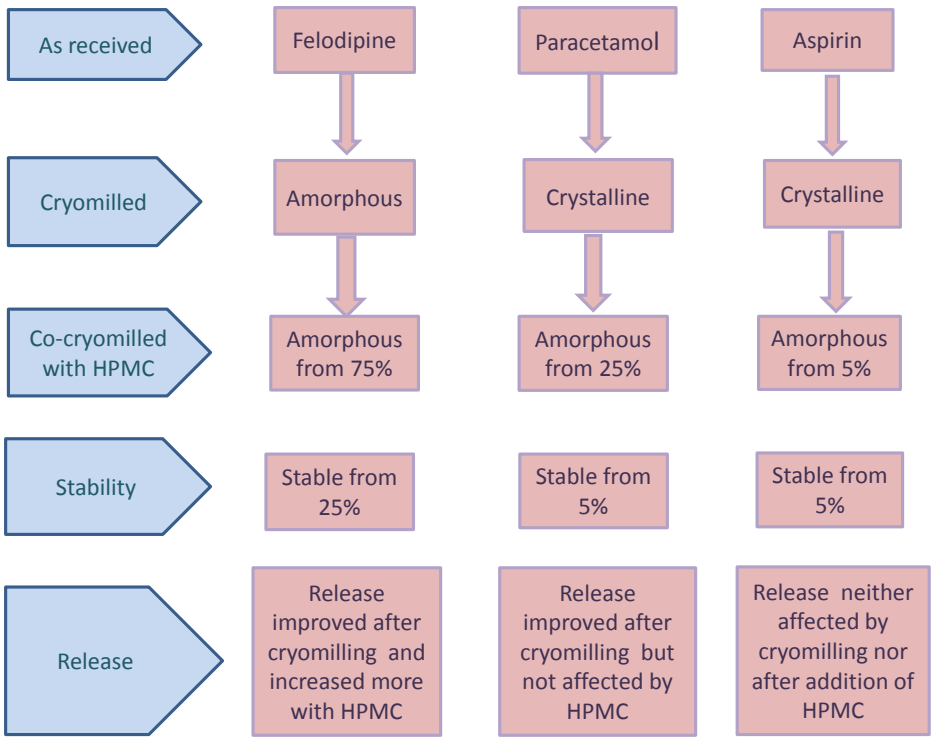

Figure 2.22: Summary of Chapter 2 main results.

Chapter 3

Can cryomilled amorphous solid dispersion be miscible at high drug loading?

3.1 Novelty in this chapter

A pre-formulation study looking at the stability of cryomilled drug-polymer amorphous solid dispersions in which multiple polymer mix has not been done before using cryomilling technique. In addition, this is the first study for the miscibility of amorphous solid dispersion via co-cryomilling.

3.2 Introduction

Amorphous solid dispersion can be produced by different methods such as spray drying and HME. The main principle is mixing drug (low molecular weight) with polymer (high molecular weight), however, there is no guarantee for full miscibility between the drug and the polymer. Similarity in the hydrophilic or lipophilic properties between the drug and the polymer or possessing a functional group for interaction results in good miscibility between them [222] although this is difficult to be achieved in the reality due to the difference in the

nature of the drug and the polymer so the the selection of the best polymer will be challenge.

The purpose of the amorphous solid dispersion is to increase the bioavailability of the drug. It was reported in Chapter 2 that amorphous solid dispersion can be produced via cryomilling. Under mechanical activation, crystalline material can be converted to amorphous form under this "Green Chemistry" [162, 223]. A single supersaturated metastable phase of the API and the polymer is achieved from a miscible blend. This blend can affect the properties of the components such as the molecular mobility, crystallisation and chemical degradation when stored for a period of time [224]. Phase separation and structural relaxation might result after obtaining a miscible blend. Miscibility can be either predicted by modelling or experimentally by long-term stability studies [225, 226].

The aim of the formulator is to achieve the highest drug loading as possible with the excipient. Amorphous solid dispersions are miscible up to 30-40% without any phase separation [227]. T_g is frequently used as a tool to indicate the miscibility of the amorphous solid dispersions [66]. The possibility of the blend mixtures are: 1) completely miscible system exhibits only one T_g that should be intermediate to the T_g's of each components. 2) phase separated has two T_gs that represents the T_gs of the components. 3) partially miscible has either one or two T_gs depending on the concentration of the components [66, 212]. The Gordon-Taylor equation [228] is used as an empirical method for prediction the T_g of binary and ternary mixtures. Various solubility parameters are additional tools to estimate the solubility of the drug in the polymer. Furthermore, the Flory-Huggins model can be used as a guide to predict the miscibility of the amorphous solid dispersion. These tools were reported by many researchers [117, 124, 222, 226, 229–240].

Water can adversely affect the miscibility of amorphous solid dispersions either by interfering with the H-bond between the drug and the polymer or by plasticising the mixtures (T_g = -134 °C) [241, 242]. Hygroscopicity of the drug and/or polymer increases the moisture uptake [241, 243] and hence worsen the miscibility. The hydrophobic polymer enhances the interaction with hydrophobic drugs

while water soluble polymers such as HPMC or PVP are used to enhance the dissolution of the drug [152]. The more hydrophobic the polymer, the better the inhibition from crystallisation of the amorphous drug in solid dispersion such as ritonavir and felodipine [67, 244]. The combination of water soluble and water insoluble polymer can give the dual properties for the mixture [152]. Using a polymer blend of Eudragit E PO and PVP AV stabilises felodipine prepared by hot melt extrusion method better than using a single polymer [243].

In the amorphous solid dispersion, selection of the best polymer with the maximum drug loading is a double-edged sword because it is important for desired dissolution [103, 245], however, this is a hurdle in the amorphous solid dispersion as high drug loading in the final formulation might result in stability issues [246]. Usually 50%-80% drug loading is required for the best dissolution [245]. Miscibility has been reported to be an important sign of stability of the amorphous solid dispersion. Miscibility and stability studies were reported by many researchers on the the amorphous solid dispersions produced by HME and spray drying and on co-milled samples by room temperature milling as reported by Anne Marie Healy, Thomas Rades, Lynne Taylor and many others [71, 72, 94, 113, 116, 118, 190, 247–253]. There was a study by Anne Marie Healy and her group to study the miscibility and stability of the ball milled sulphonamides with Soluplus and with PVP [254] for 2 weeks only 25 °C/60% RH. This study used Flory-Huggins to predicate the miscibility. Work that was reported by Mahieu *et al* involved the miscibility study of the room temperature milling of indomethacin with PVP (room temperature milling for 15 hours) [95]. No miscibility study was conducted before for amorphous solid dispersions produced by co-cryomilling method. Co-cryomilled felodipine from Chapter 2 showed a good stability with HPMC at 25% drug loading at 25 °C/43% RH for 2 months duration. However at 50% loading in the mentioned condition felodipine was unstable. Therefore our study was developed to shed the light on the production an amorphous solid dispersion via co-cryomilling felodipine with water soluble, water insoluble polymers (binary mixture) and mixture of both (ternary mixture). The pre-formulation study will be performed by using a high drug loading to examine the mixtures miscibility and long term

stability (six months). Finally, we will investigate how mixing of two polymers will affect the stability of felodipine against recrystallisation.

Potential dispersions of our mixture were evaluated by XRPD and DSC for miscibility and stability determination. Four different conditions were used to assess the stability of all mixtures under these conditions (25 °C/0% RH, 25 °C/43% RH, 25 °C/75% We applied in our study harsh conditions although the stability of the drug could be compromised under non harsh condition. This will evaluate felodipine stability in the formulation which is the concern of many pharmaceutical companies during pharmaceutical processing and packaging.

CSD: The likelihood of formation of each potential H-bond in its crystal structure is predicted from CSD analysis [255]. This probability will give us an idea about how our mixture might behave regarding to H-bond.

The chemical structure of the selected polymers are seen in Figure 3.1. From CSD we found that there is no evidence of drug polymer interaction between HPMC and felodipine. For this reason we will focus on felodipine with different polymers that processes different functional groups and different water solubility which is HPMC, HPMCAS, Soluplus, PMMA as seen in Table 3.1. Both HPMCAS and PMMA have C=O groups while Soluplus has alcohol group in a addition to C=O functional group.

From Chapter 2 as received felodipine (CSD reference code is DONTIJ) was reported as exhibiting the weakest felodipine...felodipine H-bonding with bond length of 3.155 Å between N...O. From Chapter 2 CSD analysis and from the big shift in the FTIR data as discussed previously in Section 2.4.4, the amorphous felodipine has a stronger H-bond than the crystalline form. Upon co-cryomilling with HPMC, HPMCAS, PMMA and Soluplus the potential motifs for the interaction are seen Table 3.1. The N-H group in felodipine is supposed to be the donor group while (C=O) group in HPMCAS, PMMA and Soluplus is considered as strong acceptor [186]. The most common value in the histogram of N..O distance for fragments which form motif "a" is around 2.65 Å. The probability of H-bond formation between felodipine N-H group and C=O group that found in Soluplus, PMMA and HPMCAS is high. In addition felodipine-Soluplus mixture

Table 3.1: The Cambridge Structure Database results proposed for felodipine, felodipine-polymer and polymer-polymer.

Felodipine part expected	Motifs	H-bond length in Å	Histogram	Interaction
polymorph	I	3.155	-	-
Felodipine, Felodipine-HPMCAS, Felodipine-PMMA, Felodipine-Soluplus	a 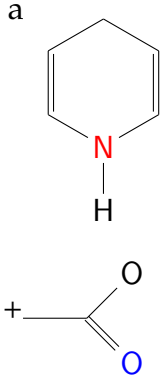	2.65	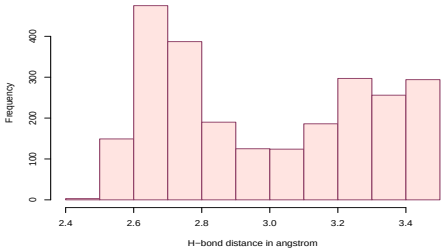	yes
Felodipine HPMC	b 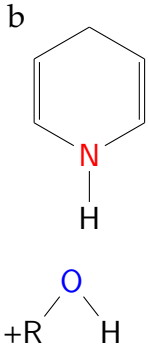	no clear distribution	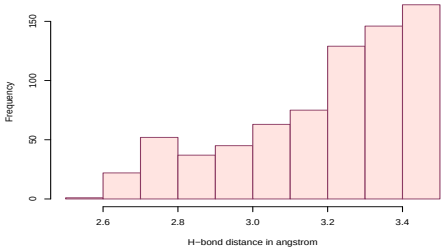	no
Felodipine-Soluplus, HPMC-HPMCAS, HPMC-PMMA, Soluplus-HPMCAS	c 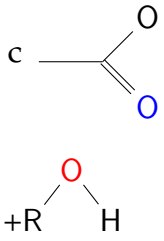	2.6	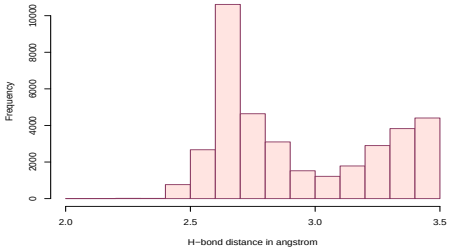	yes

has another possibility of H-bond formation between O-H group of Soluplus as a donor group and the C=O group of felodipine as an acceptor group. The distance between these two motif is 2.6 Å which is shorter than other interactions. While for felodipine-HPMC system as reported in Chapter 2 there is no clear distribution of the histogram and thus low probability of interaction between N-H group of felodipine with O-H of HPMC. From this analysis we can then conclude that there is a strong possibility of hydrogen bond formation between felodipine with HPMCSAS, PMMA and Soluplus. Felodipine-Soluplus has two site of interactions which could have the strongest interaction than other polymers, while felodipine with HPMC the possibility of interaction is weak at the best.

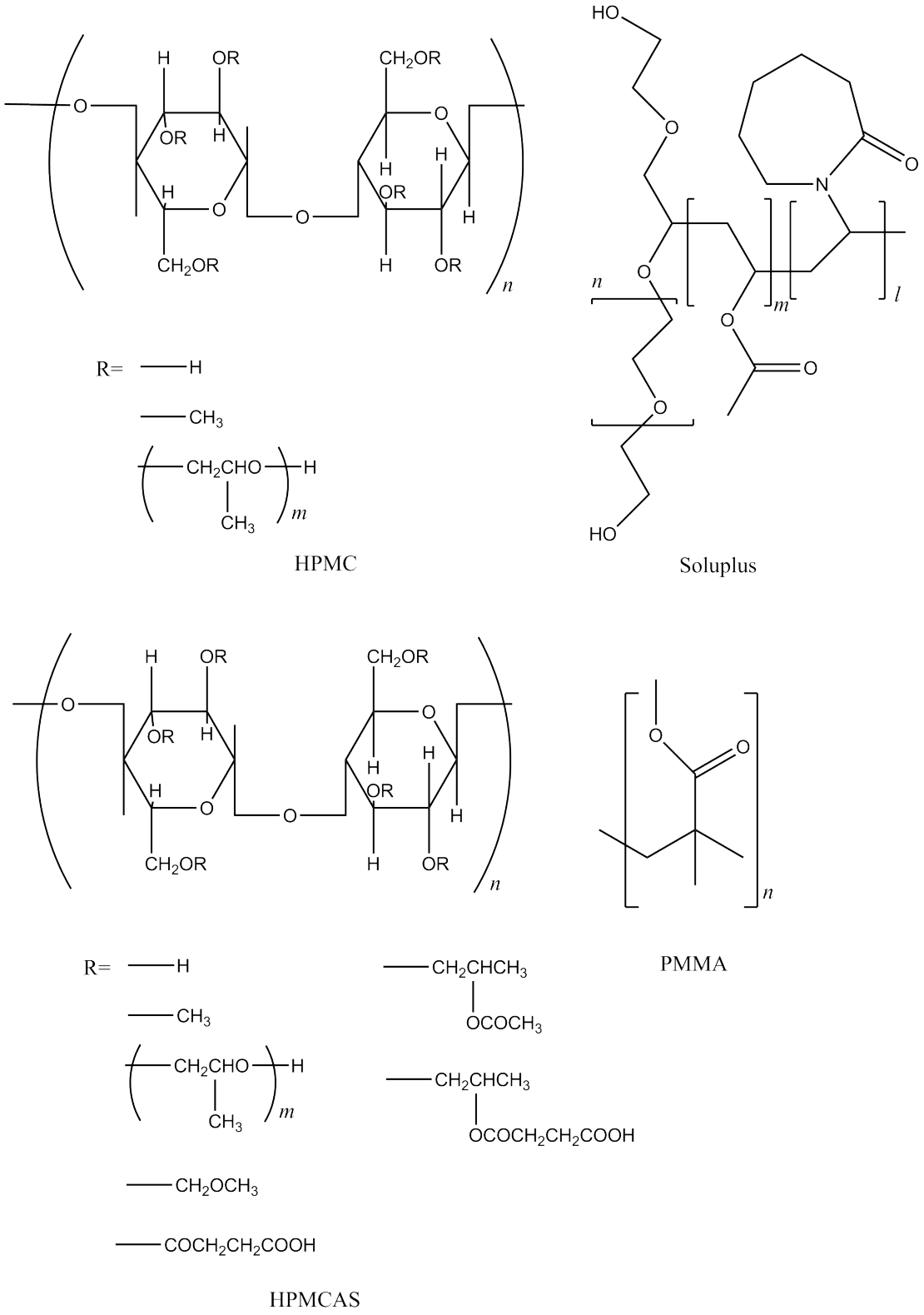

Figure 3.1: The chemical structures of the selected polymers.

From Table 3.1, the expected interaction between polymers themselves can

Table 3.2: The possibility of hydrogen bond formation between felodipine and selected polymers in our study.

Co-cryomilled mixture	Possibility of interaction from CSD analysis	From FTIR results in literatures
Felodipine-HPMC	no	weak [110]
Felodipine-HPMCAS	yes	weak [71, 110]
Felodipine-Soluplus	yes	yes strong [71]
Felodipine-PMMA	yes	-
HPMC-HPMCAS	yes	yes [152]
HPMC-PMMA	yes	-
Soluplus-HPMCAS	yes	-

be predicted from CSD for HPMC-HPMCAS, HPMC-PMMA and Soluplus-HPMCAS. The histogram of O..O distance for fragments which form motif "c" has a most common value around 2.6 Å. This distance is shorter than the expected interaction between felodipine and the mentioned polymers except with Soluplus. This might suggest that the probability of H-bond formation between polymer-polymer mix in ternary mixture is higher than felodipine-polymer itself.

3.3 Materials and Methods

3.4 Materials

Soluplus® was kindly donated from BASF company. PMMA (polymethylmethacrylate) was purchased from Sigma Aldrich. Sodium dodecyl sulfate was purchased from Acros Organics. Potassium carbonate was purchased from Minerals-Water Ltd (Essex, UK) in order to achieve 43% relative humidity for the stability study. NaCl was purchased from Breckland Science Supplies (Norfolk,

UK) in order to achieve relative humidity 75%. Molecular sieves were purchased from Sigma to achieve the minimum humidity 0%.

3.4.1 Cryomilling

As per Section 2.3.2 in Chapter 2.

3.4.2 Powder X-ray diffraction (PXRD)

As per Section 2.3.3 in Chapter 2.

3.4.3 Differential Scanning Calorimetry (DSC)

As per Section 2.3.4 in Chapter 2. The experiments were performed in triplicate (n=3) because there is a key test while the stability study was performed using a single sample because the limited amount of samples that were used for stability study.

3.4.4 Quantification of crystallinity

As per Section 2.3.9 in Chapter 2.

3.4.5 Mathematical prediction

Gordon-Taylor equation:

For two component [190]:

$$T_{g(mix)} = \frac{w_1 T_{g1} + K_1 w_2 T_{g2}}{w_1 + K_1 w_2} \tag{3.4.1}$$

$$K \approx \frac{p_1 T_{g1}}{p_2 T_{g2}} \tag{3.4.2}$$

For three component [190]:

$$T_{g(mix)} = \frac{w_1 T_{g1} + K_1 w_2 T_{g2} + K_2 w_3 T_{g3}}{w_1 + K_1 w_2 + K_2 w_3} \tag{3.4.3}$$

T_{gi} is the glass transition temperature of each component, W_i is the weight fraction of each component, K is calculated from the p_i density and T_{gi} of each component.

Solubility Parameter [256]: It is defined the square root of a molecule's cohesive energy density (CED).

$$\delta = (CED)^{0.5} = \left(\frac{\Delta E_v}{V_m}\right)^{0.5} \tag{3.4.4}$$

ΔE_v is the energy of vaporisation and V_m is the molar volume of the compound. CED, the cohesive energy per unit volume.

According to Hanson's approach [256]:

$$\delta = (\delta_d^2 + \delta_p^2 + \delta_h^2)^{1/2} \tag{3.4.5}$$

Where δ_d^2, δ_p^2, and δ_h^2 are the partial solubility parameters indicating contributions from Van der waals dispersion forces, dipole-dipole interactions, and hydrogen bonding, respectively.

In this chapter we are not going to apply these equations to our work because we will use the reported values from the published literatures.

3.4.6 Hydrophilicity/hydrophobicity predication

The hydrophilicity/hydrophobicity of the selected polymer and felodipine was predicated by two methods the first one is from log P values that was predicted using MarvinSketch 2016 from ChemAxon. The highest number is the the more hydrophobic value [257]. The second method is the prediction from solubility parameter. It was reported by Ilevbare *et al* that the more hydrophobic polymer possesses the lower solubility parameter [67].

3.4.7 Stability study

A saturated solution of potassium carbonate or NaCl was prepared and then this solution was placed in a gas-tight environment to achieve the required humidity which is 43% and 75% respectively at room temperature. Molecular sieve were used to achieve the minimum humidity 0%. The samples was stored at 25 °C/0% RH, 25 °C/43% RH, 25 °C/75% RH and 50 °C/0% RH. They were analysed by XRPD and DSC at zero time of collection and after 2, 5, 10, 20, 40 and 60, 90, 120, 150 and 180 days of storage. The humidity measured by using hygrometer .

3.4.8 Evaluation of H-Bond length using Cambridge Structure Data Base CSD

As described in Chapter 2 Section 2.3.12

3.5 Results and discussion

3.5.1 Prediction of the hydrophilicity and hydrophobicity

Polymers that were used in this study are shown in Table 3.3. The hydrophilicity and hydrophobicity predicted from ChemAxon are outlined in Table 3.3. The polymers are ranked by logP from more hydrophobic to more hydrophilic PMMA > HPMCAS > Soluplus > HPMC. However the rank according to the solubility parameter value as seen in Table 3.4 will be PMMA > HPMCAS > HPMC > Soluplus.

3.5.2 Miscibility in cryomilled mixtures

In order to assess the miscibility of each polymer or polymer blend in the amorphous solid dispersions XRPD and DSC are mainly applied in this study. If there is any peak in the XRPD then there is an indication of phase separation and

Table 3.3: Polymers properties and classification [5, 6].

Polymer	Name	Classification	Water solubility	Log P value predicted from ChemAxon
HPMC	Hydroxypropyl methycellulose	non ionic cellulose ether	Water soluble	-1.75
Soluplus	Polyvinylcaprolactam-polyvinylAcetate-Polyetheylene Glycol Graft copolymer	non ionic polyvinyllactam	Water soluble	-0.6
HPMCAS	Hydroxypropyl methycellulose acetate Succinate MF	ionic cellulose ether ester	pH dependendent anionic soluble > 5.5	0.23
PMMA	polymethylmethacrylate	synthetic acrylic	Water insoluble	2.17

subsequent recrystallisation of the API. The miscibility also will be evaluated by DSC in which there are three possibilities which are: single phase by having only one T_g, phase separation and no recrystallisation there is two T_gs and finally if we have phase separation and recrystallisation with appearance of melting peak of drug and one T_g which might related to the polymer and or/drug. Further methods used in this study which are the predicted methods such as the solubility parameter value and Gordon-Taylor equation. Raman was used for further characterisation of amorphous material formation.

Prediction

The solubility parameter:

The solubility parameter was used to predict the miscibility between felodipine with each polymer and between polymer-polymer for the polymer mixes. It was previously reported that if the difference in solubility parameter less than 7 $MPa^{\frac{1}{2}}$ then the mixture is miscible while higher than 10 $MPa^{\frac{1}{2}}$ is likely to be immiscible [81]. The calculated solubility parameter for felodipine is 24.39 $MPa^{\frac{1}{2}}$. The difference in the solubility parameter between felodipine and HPMC is 0.24 $MPa^{\frac{1}{2}}$. For HPMCAS, Soluplus and PMMA the differences are 1.99, 6.83 and 5.1 $MPa^{\frac{1}{2}}$ respectively. For the polymer blend HPMC/HPMCAS the difference

Table 3.4: Physicochemical properties of materials that are used in this study.

Materials	M.wt in dalton	Solubility in water	SP value in MPa $^{\frac{1}{2}}$	$\Delta SP\ in\ MPa^{\frac{1}{2}}$ $(SP_{drug} - SP_{polymer})$	Tg in °C	Density g/ml
Felodipine	384.26 [247]	insoluble	24.39 [117]		47 [258]	1.28 [247]
HPMC	35600 [110]	soluble [259]	22.68 [125]	0.42	139 [200]	1.3 [260]
HPMCAS	18000 [110]	soluble at pH≥5.5[261]	22.4 [152]	1.99	120 [152]	1.3 [262]
Soluplus	118000 [263]	soluble	31.22 [117]	6.83	71 [254]	1.16 [254]
PMMA	15000	insoluble [264]	18 [222]	5.1	107[265]	1.118 [266]

is 1.57 MPa$^{\frac{1}{2}}$. The difference in the solubility parameters between Soluplus and HPMCAS is 4.48 MPa$^{\frac{1}{2}}$ and finally between HPMC and PMMA 4.68 MPa$^{\frac{1}{2}}$. According to this rule all felodipine-polymer and polymer-polymer mixtures that are used in the experiment are expected to be fully miscible. The results for solubility parameters are summarized in Table 3.4.

Gordon-Taylor equation:

All the T_gs of felodipine-polymer in binary and ternary mixture were predicted by using Gordon-Taylor equation as detailed in the experimental part in Section 3.4.5. The predicted results then will be compared with the experimental T_g. This will be explained in detail in the DSC part in this Section 3.5.2.

XRPD

From Chapter 2 the XRPD data showed that the as received felodipine is crystalline. Upon cryomilling (Figure 2.4 in Chapter 2), the Bragg peaks of the as received felodipine are largely disappeared into noise to indicate transfor-

mation of felodipine into amorphous form. Figure 3.2 shows the XRPD pattern of the co-cryomilled mixtures at 50% loading for felodipine co-cryomilled with, HPMC, HPMCAS, Soluplus, HPMC/HPMCAS, HPMC/PMMA and Soluplus/HPMCAS. It clearly notice that all mixtures show amorphous halo upon cryomilling which indicates that they transformed to the amorphous form.

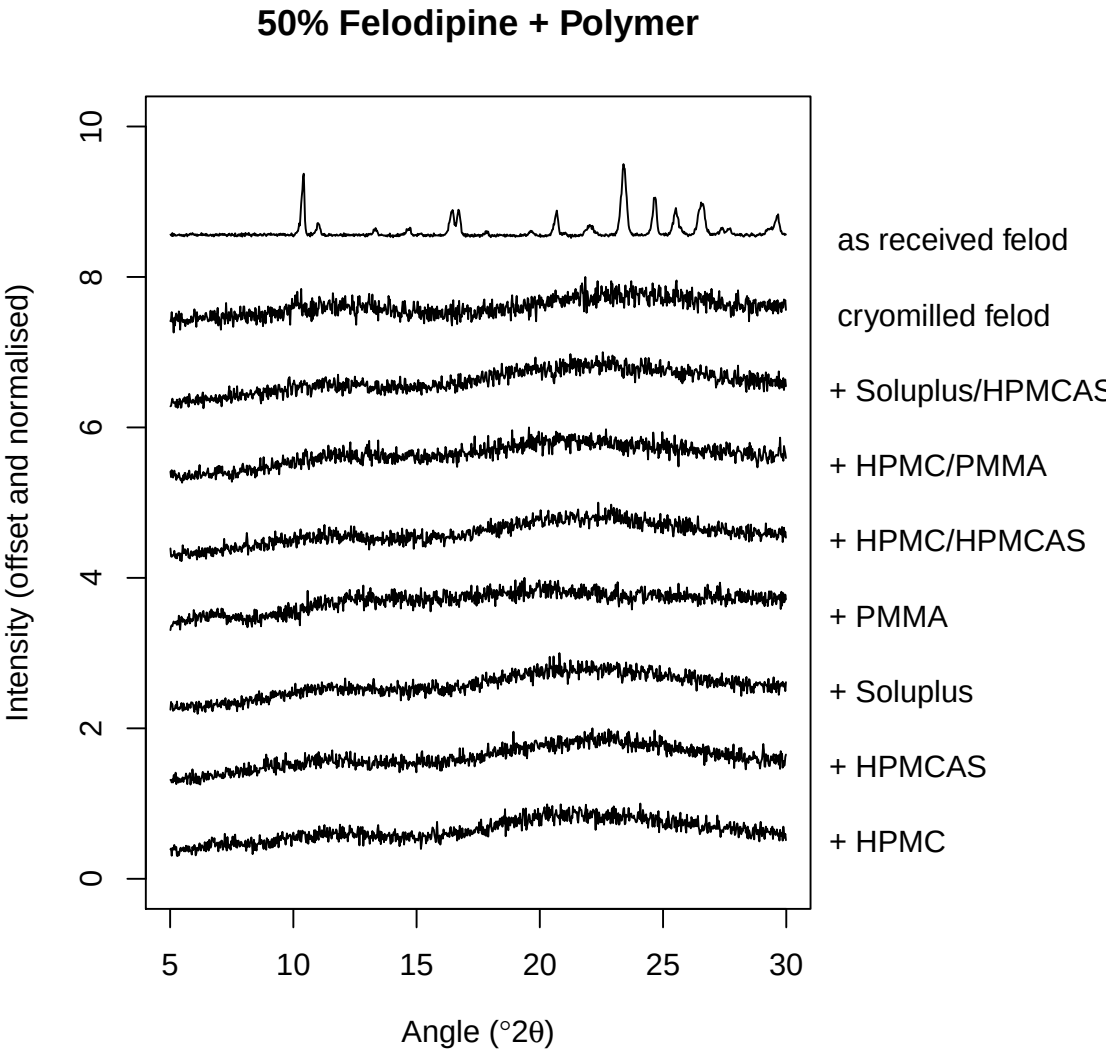

Figure 3.2: The XRPD of felodipine as received, cryomilled and co-cryomilled at 50% drug loading with HPMC, HPMCAS, Soluplus, PMMA, HPMCHPMCAS, HPMC/PMMA, Soluplus/HPMCAS. Offsets and scales applied for presentational purposes.

Raman

Figure 3.3 shows the Raman spectroscopy of felodipine as received, co-cryomilled with HPMC, HPMCAS, Soluplus, PMMA, HPMC/HPMCAS, HPMC/PMMA and Soluplus/HPMCAS at 50% drug loading. It can be seen that the as received felodipine in the phonon region has a peak at 93.4 cm^{-1} with a shoulder peak at 61.4 cm^{-1} while all co-cryomilled mixtures show one broad peak all near about 60 cm^{-1} which is called as a boson peak [267, 268]. The boson peak is an indication of amorphous material. The carbonyl region has a sharp peak at 1643 cm^{-1} which is comparable to the reported one in reference [194] for as received felodipine at carbonyl region at 1642 cm^{-1} while all co-cryomilled mixtures have a broad peak at 1645 cm^{-1}. Both Raman with XRPD results indicate that all co-cryomilled felodipine-polymer mixtures are amorphous. It seems from the solubility parameter prediction and from XRPD and Raman results that all mixtures are miscible, however, DSC is more sensitive technique to indicate the miscibility that will be detailed in the next Section 3.5.2.

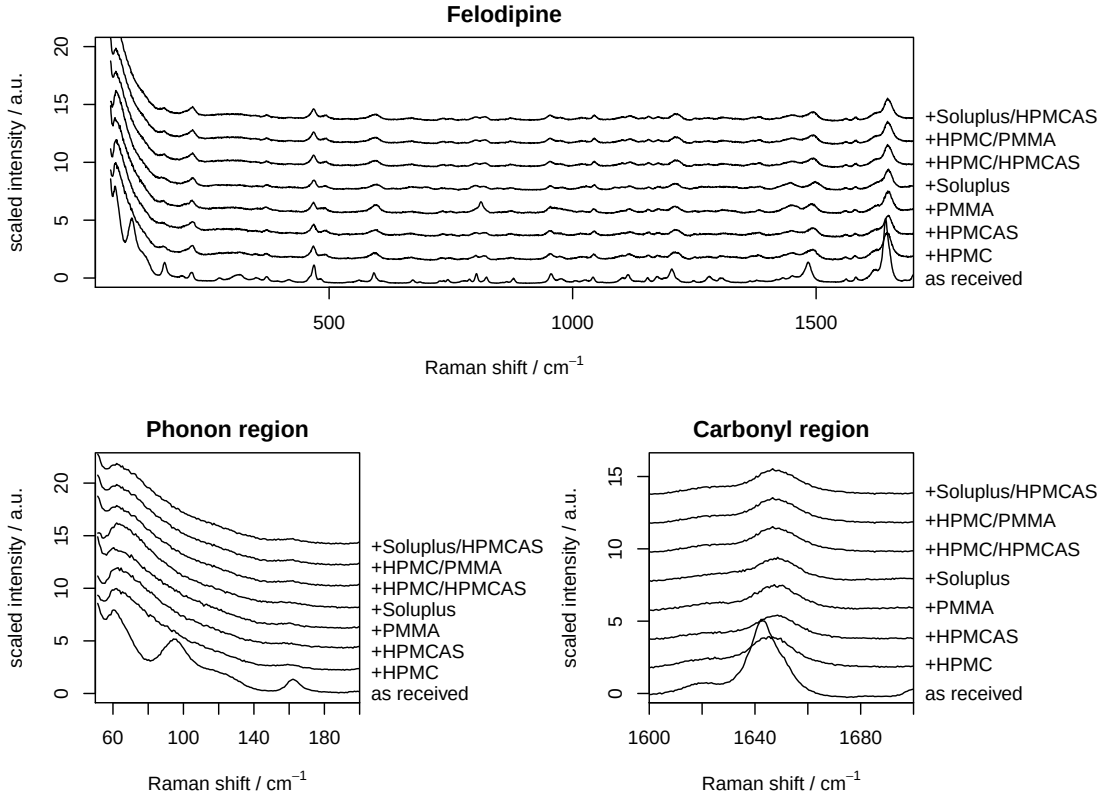

Figure 3.3: Raman of felodipine cryomilled and felodipine cryomilled with HPMC, Soluplus, HPMCAS, PMMA, HPMC:HPMCAS (1:1), HPMC:PMMA (1:1) and Soluplus:HPMCAS (1:1) at 50% drug loading immediately after cryomilling.

DSC

Both XRPD and Raman are sensitive to small amounts of crystalline material, whereas DSC is sensitive to small amounts of amorphous material. In order to assess the miscibility of the amorphous solid dispersions of the selected co-cryomilled mixture by DSC, four different concentrations were used in order to investigate the effect of drug loading on the miscibility. Figure 3.4 and 3.5 and Table 3.5 show a thermogram results for all binary and ternary co-cryomilled mixtures at 5, 25, 50 and 75% drug loading with HPMC, HPMCAS, Soluplus, HPMCAS, PMMA, HPMC/HPMCAS, HPMC/PMMA and Soluplus/HPMCAS. It was reported early in this study in Chapter 2 that cryomilled felodipine

exhibits a T_g of 46.7 ±0.5 °C.

Binary polymer mixes without felodipine:

The thermogram results of binary polymer mixtures can be seen in Figures 3.4, 3.5 and Table 3.5. The binary mixture of HPMC/HPMCAS displays one T_g at 121.7 ±1 °C. This is slightly lower than the predicted value 125 °C. It was previously reported that HPMC-HPMCAS form a miscible blend by spray drying method [152]. In the HPMC/PMMA system, the mixture exhibits 2 T_gs at 84.3 ±7.5 °C and 142.6 ±4.1 °C. In addition, Soluplus/HPMCAS mixture also displays 2 T_gs one of them is 57.5 ±0 °C and the other is 136 ±5 °C. The presence of a single T_g indicates the formation of a miscible phase between two the polymers such as in the case of HPMC/HPMCAS. Furthermore the predicted value is near the experimental value for this reason this mixture is considered to be miscible [66]. While for Soluplus/HPMCAS and HPMC/PMMA the presence of 2 T_gs is an indication of immiscible phase system for these polymer mixes. This is unexpected to get two T_gs as the solubility parameter prediction earlier in this section suggested that these mixtures are expected to be miscible and from CSD analysis they are predicted to be able to form a H-bond.

Thermogram results of 75% binary and ternary mixes:

Table 3.6 shows all co-cryomilled binary and ternary mixtures at 75% drug loading. Mixtures such as felodipine-HPMCAS, felodipine-Soluplus, felodipine-PMMA and felodipine-HPMC/HPMCAS display a single T_g that is an indication of the single phase formation (Figures 3.4 and 3.5). However, (felodipine-HPMC, felodipine-HPMC/PMMA and felodipine-Soluplus/HPMCAS) exhibit 2 T_gs which is an indication of phase separation and hence immiscibility. Furthermore, all mixtures that exhibit a single T_g showed lower value than the predicted one from Gordon-Taylor equation as seen in Figure 3.6 and 3.7 (lower by 8-18 °C) which might related to the moisture uptake that results in lowering T_g of the mixtures [226]. T_g appearance at lower value than the predicted one for felodipine-HPMCAS mixture was also reported by Konno and Taylor for felodipine-HPMCAS and felodipine-HPMC mixtures prepared by spray drying and single T_g was observed [148]. It was reported by Tian *et al.* nearly at this

Table 3.5: T_g value of the all mixtures in °C. The red text indicts a single T_g. The experimental one was performed in triplicate n=3.

W/W	T_g status	HPMC	HPMCAS	Soluplus	PMMA	H/HAS	H/PM	S/HAS
0%	predicted	-	-	-	-	125	118	86
	experimental	134.7±2.3	116±4.2	61.5±0.4	101±11	121.7±1	84.3±7.5 – 142.6 ± 4.1	57.5±0.5 – 136 ± 5
5%	predicted	129	111	60	99	120	112	82
	experimental	59±2.2 – 137.5 ± 3.2	55.3±1.7 – 129.3 ± 3.7	57.3±3.3	55.6±1.2 – 109 ± 4.3	52.4±1 – 121 ± 9	55±1.1 – 106 ± 2.8	59.5±3.5 – 150 ± 0.05
25%	predicted	108	96	57	87	97	99	74
	experimental	53.7±1.7 – 155.6 ± 0.5	51.7±1.2 – 142 ± 4.8	54±6	53.2±0.6	50±1.4 – 127 ± 7	48.5±3.9	49±3 – 148 ± 2
50%	predicted	85	78	54	73	79	80	65
	experimental	51.1±1.4	50.7 ±0.6	47.1±3	43.1±0.6	47.21±1.95 – 122 ± 2.1	48.9±3	46.3±1 – 125 ± 5
75%	predicted	65	61	51	60	62	63	56
	experimental	46.7±0.4 – 134 ± 0.8	44.7±0.4	43.3±0.3	42.9±0.5	43.7±0.6	42.3±1 – 92 ± 0.1	44.9±0.6 – 94 ± 2

loading that felodipine-HPMCAS displays 2 T_gs after HME [71]. The exhibition of 2 T_gs at 75% loading for felodipine-HPMC, felodipine-HPMC/PMMA and felodipine-Soluplus/HPMCAS indicates that these mixtures are immiscible at 75% loading while mixtures such as felodipine-HPMCAS, felodipine-Soluplus, felodipine-PMMA and felodipine-HPMC/HPMCAS are considered to be miscible.

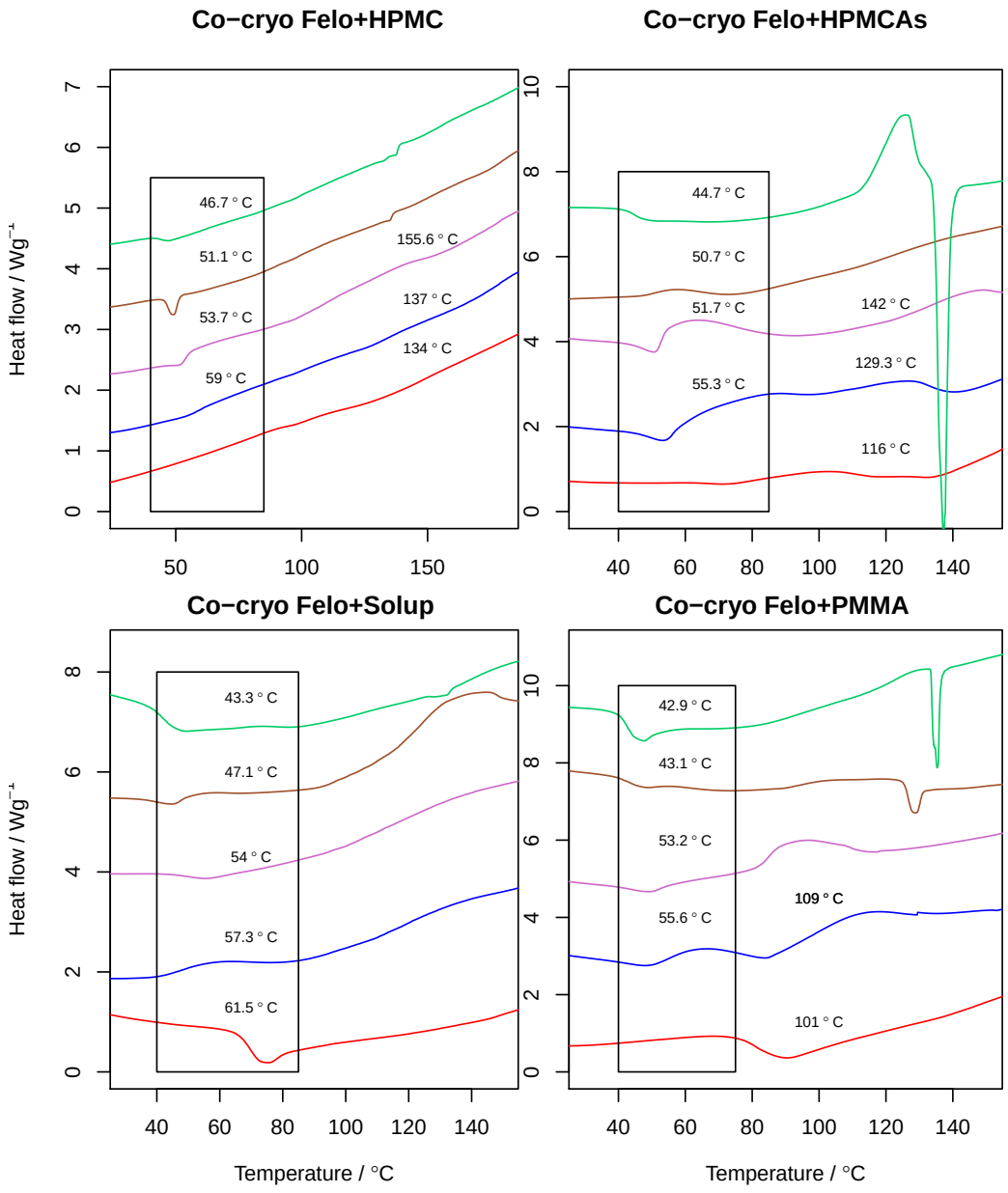

Figure 3.4: The DSC patterns of the cryomilled felodipine with the single polymer 0% drug loading, felodipine co-cryomilled at 5%, 25%, 50% and 75% drug loading with HPMC, HPMCAS, Soluplus and PMMA. The numbers inside the figure represent the T_gs of the polymer or the co-cryomilled mixture. Red, blue, purple, brown and green colour indicate felodipine co-cryomilled with polymer at 0%, 5%, 25%, 50% and 75% drug loading respectively. Data offset and scale for presentational purpose.

Table 3.6: The thermogram results of 75% co-cryomilled felodipine loading with various polymer and polymer mixes.

Solid dispersions 75% loadings	T_{g1} in °C	T_{g2} in °C	T_g Expected by Gordon Taylor in °C	Recrystallisation peaks in °C	Enthalpy of recrystallisation in J/g	Melting point in °C	Enthalpy of melting in J/g
Felodipine-HPMC	46.7±0.4	134±0.8	65	-	-	136±0.9	1.3±0.4
Felodipine-HPMCAS	44.7±0.4	-	61	126±1	7±1	135±0.8	12±1
Felodipine-Soluplus	43.3±0.3	-	51	-	-	-	-
Felodipine-PMMA	42.9±0.5	-	60	-	-	133±0.3	2±0.3
Felodipine-HPMC/HPMCAS	43.7±0.6	-	62	120±0.4	3±0.9	134±0.3	4±0.4
Felodipine-HPMC/PMMA	42.3±1	92±0.1	63	-	-	132±3	6±0.9
Felodipine-Soluplus/HPMCAS	44.9±0.6	94±2	56	124±0.5	0.4±0.3	133±0.3	6±0.2

The second thermal event (Table 3.6, Figures 3.4 and 3.5) that appears on some mixtures at 75% loading is the recrystallisation peaks for felodipine-HPMCAS, felodipine HPMC/HPMCAS and felodipine-Soluplus/HPMCAS (all HPMCAS containing mixtures) which is an indication of amorphous formation then recrystallisation during the DSC characterisation. The final thermal event (Table 3.6) at this drug loading is the presence of melting peak in all mixtures except felodipine-Soluplus. The enthalpy of melting of all mixtures is lower than the expected value for felodipine physical mixtures at 75% drug loading which is 54.75 J/g felodipine. This is an indication of presence of high amorphous content in all mixtures. The absence of melting peak between felodipine and Soluplus might be related to the strong interaction between felodipine and Soluplus from our CSD analysis.

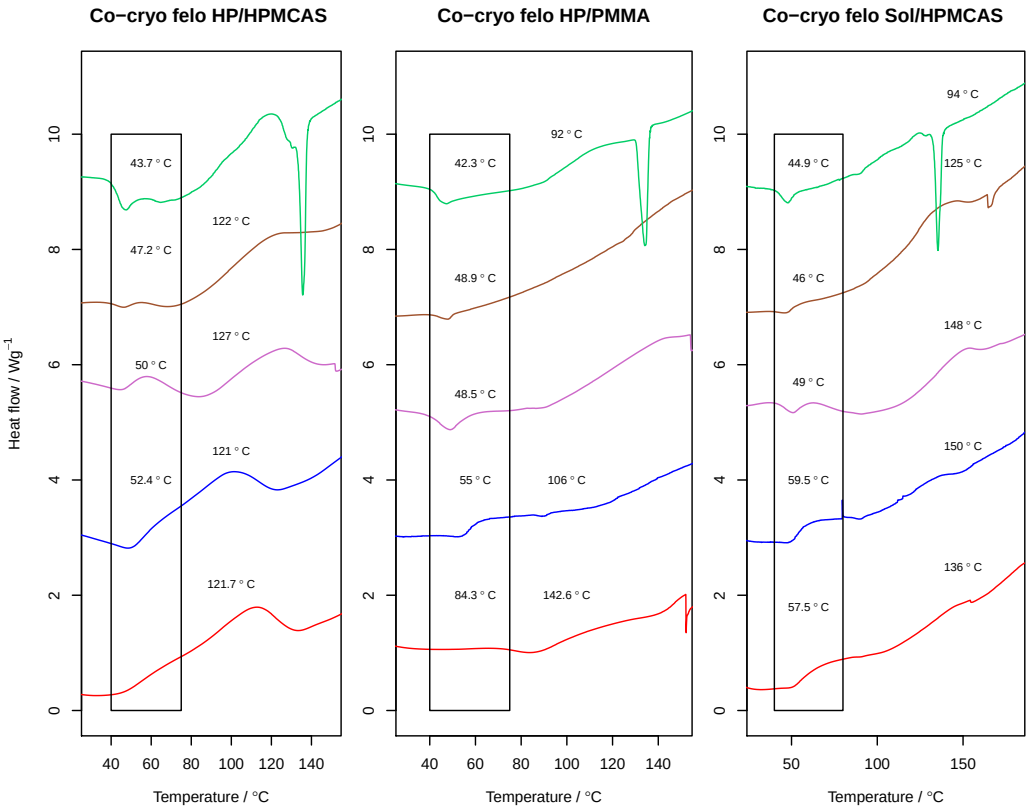

Figure 3.5: The DSC patterns of the cryomilled felodipine with the polymer mixes at 0% drug loadings, felodipine co-cryomilled at 5%, 25%, 50% and 75% drug loading with HPMC-HPMCAS, HPMC-PMMA and Soluplus-HPMCAS. The numbers inside the figure represent the T_g(s) of the polymer or the co-cryomilled mixture. Red, blue, purple, brown and green colour indicate felodipine co-cryomilled with polymer at 0%, 5%, 25%, 50% and 75% drug loading respectively. Data offset and scale for presentational purpose.

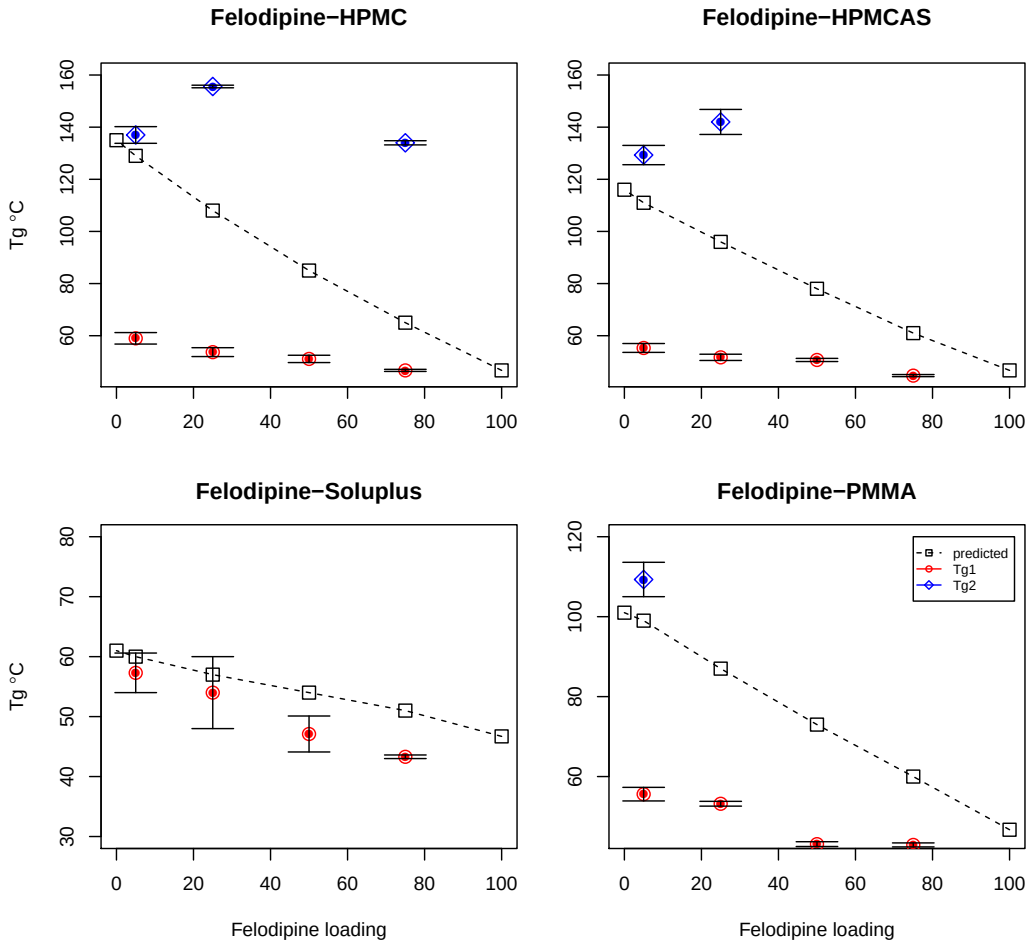

Figure 3.6: Values of T_g for binary mixture felodipine-HPMC, felodipine-HPMCAS, felodipine-Soluplus and felodipine-PMMA at 5, 25, 50 and 75% felodipine loadings. The lines show the predicted from the Gordon-Taylor equation and dots indicate the experimental T_g(s) performed in triplicate (n=3).

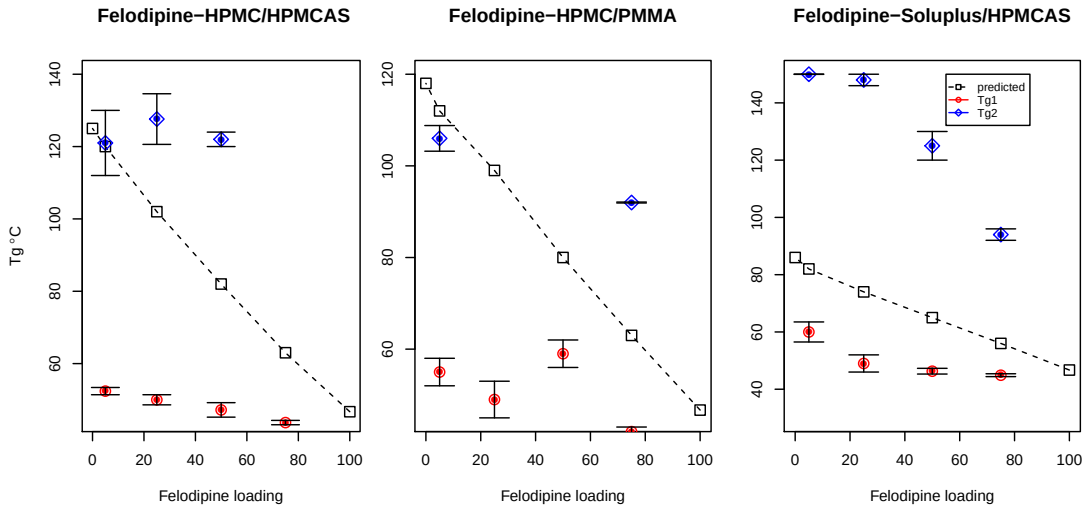

Figure 3.7: Values of T_g for ternary mixture felodipine-HPMC/HPMCAS, felodipine-HPMC/PMMA and felodipine-Soluplus/HPMCAS at 5, 25, 50 and 75% felodipine loadings. The lines show the predicted from the Gordon-Taylor equation and dots indicate the experimental T_g(s) performed in triplicate (n=3).

Thermogram results of 50% binary and ternary mixes:

Table 3.7, Figures 3.4 and 3.5 shows the thermogram results at 50% drug loading. All binary mixtures display a single T_g while in the ternary mixtures only felodipine-HPMC/PMMA exhibits a single T_g. All mixtures that exhibited a single T_g are lower than the predicted value from Gordon-Taylor equation (lowering varied from 7-35 °C) as seen in Figure 3.6 and 3.7. Our experimental T_g for for felodipine-HPMCAS system is higher than that reported one prepared by spray drying method 53.9 °C [148] and lower than that one prepared by HME method 58.6 °C [71]. A single T_g of the felodipine-HPMC mixture is lower than that previously reported for that mixture prepared by spray drying [148]. The second thermal event is melting peak that seen in felodipine-HPMC and felodipine-PMMA with lower enthalpy of melting than the calculated value at this loading 36.5 J/g that reflects the high amorphous contents for both mixtures.

Thermogram results of 25% binary and ternary mixes:

Table 3.8 and Figure 3.4 show the thermogram results for 25% drug. All mixtures

Table 3.7: The thermogram results of 50% co-cryomilled felodipine loading with various polymer and polymer mixes.

Solid dispersions 50% loadings	T_{g1} in °C	T_{g1} °C	Predicted T_g from Godron Taylor in °C	Melting point in °C	Enthalpy of melting in J/g
Felodipine-HPMC	51.1±1.4	-	85	133±1.4	0.3±0.2
Felodipine-HPMCAS	50.7 ±0.6	-	78	-	-
Felodipine-Soluplus	47.1±0.3	-	54	-	-
Felodipine-PMMA	43.1±0.6	-	73	125±0.5	1.2±0.1
Felodipine-HPMC/HPMCAS	47.21±1.95	122±2.1	79	-	-
Felodipine-HPMC/PMMA	48.9±3	-	80	-	-
Felodipine-Soluplus/HPMCAS	46.3±1	125±5	65	-	-

display two T_gs with the exception of felodipine-Soluplus, felodipine-PMMA and felodipine-HPMC/PMMA mixtures which exhibit a single T_g. The mixtures that exhibit a single T_g have lower experimental value than the predicted value from Gordon-Taylor equation as seen in Figures 3.6 and 3.7. The difference is varied from 3 °C in felodipine-Soluplus to 50 °C in felodipine HPMC/PMMA. It was reported previously that around this loading felodipine-HPMC exhibits a single T_g around 50 °C [148] for felodipine-HPMC prepared by spray drying method. It was reported by Konno and Taylor that felodipine-HPMCAS prepared by spray drying exhibits a single T_g around 50 °C. At 25% drug loadings felodipine-Soluplus, felodipine-PMMA and felodipine-HPMC/PMMA form a single phase while other mixtures at this drug loading were phase separated. All mixtures at 25% drug loading do not show a melting peaks which indicates that the mixtures at 25% drug loading are completely amorphous.

Thermogram results of 5% binary and ternary mixes:

Table 3.8, Figures 3.4 and 3.5 show the thermogram results of felodipine co-cryomilled with polymer and polymer mixes at 5% drug loading. All mixtures display two T_gs except felodipine-Soluplus exhibits a single T_g that is almost

Table 3.8: The thermogram results of 25% co-cryomilled felodipine loading with various polymer and polymer mixes.

Solid dispersions 25% loadings	T_{g1} in °C	T_{g2} in °C	T_g predicted from Gordon Taylor in °C	Melting point in °C	Enthalpy of melting in J/g
Felodipine-HPMC	53.7±1.7	155.6±0.5	108	-	-
Felodipine-HPMCAS	51.7±1.2	142±4.8	96	-	-
Felodipine-Soluplus	54±6	-	57	-	-
Felodipine-PMMA	53.2±0.6	-	87	-	-
Felodipine-HPMC/HPMCAS	50±1.4	127±7	97	-	-
Felodipine-HPMC/PMMA	48.5±3.9	-	99	-	-
Felodipine-Soluplus/HPMCAS	49±3	148±2	74	-	-

identical to the predicted value from Gordon-Taylor equation as seen in Figures 3.6 and 3.7. The presence of two T_gs indicates phase separation and immiscibility which is the case in most mixtures at 5% drug loading except co-cryomilled felodipine-Soluplus. All mixtures at 5% drug loading do not show a melting peak which indicates that these mixtures are amorphous.

The XRPD, Raman and DSC are in agreement in formation of amorphous phase for all co-cryomilled mixtures (binary or ternary). All mixtures are predicted to be miscible from the solubility parameter value. In addition from CSD analysis all binary mixtures (except felodipine-HPMC) have a possibility to form H-bond. The DSC data indicate that the mixtures are miscible only at certain concentrations then they become saturated at other concentrations. This might indicate the partial miscibility of these components [66]. From our DSC data almost all mixtures at low drug loading are immiscible but they become miscible at higher felodipine loading.

It was clear from the DSC results that the mixtures that form a single phase, with increasing polymer concentration there is no elevation in the T_g which is not much different from the amorphous felodipine (except for felodipine-

Table 3.9: The thermogram results of 5% co-cryomilled felodipine loading with various polymer and polymer mixes.

Solid dispersions 5% loadings	T_{g1} in °C	T_{g2} in °C	T_g predicted by Gordon Taylor in °C	Melting point in °C	Enthalpy of melting in J/g
Felodipine-HPMC	59±2.2	137.5±3.2	129	-	-
Felodipine-HPMCAS	55.3±1.7	129.3±3.7	111	-	-
Felodipine-Soluplus	57.3±3.3	-	60	-	-
Felodipine-PMMA	55.6±1.2	109±4.3	99	-	-
Felodipine-HPMC/HPMCAS	52.4±1	121±9	120	-	-
Felodipine-HPMC/PMMA	55±1.1	106±2.8	112	-	-
Felodipine-Soluplus/HPMCAS	59.5±3.5	150±0.05	82	-	-

soluplus mixture). The T_g are negatively deviated from the Gordon-Taylor equation (Figure 3.6 and 3.7) that indicate poor mixing ability of felodipine with the selected polymers (except for felodipine-soluplus mixture) or might related to the presence of water that results in lowering the T_g of the mixtures. The non ideal mixing of felodipine was also reported by Konno and Taylor for solid dispersion that prepared by solvent evaporation for felodipine with HPMC and with HPMCAS [110]. Konno and Taylor reported that the T_gs of their mixtures did not significantly increase with increasing polymer concentration. They also suggested that the solid dispersions formed from these mixtures are negativity deviated from Gordon-Taylor equation, however, they have inhibitory effect against nucleation [110]. The only exception in our study is co-cryomilled felodipine-Soluplus mixture which from our DSC data (Figure 3.6 and 3.7) exhibits an ideal mixing with felodipine and forms a single phase at all concentrations.

The presence of T_g for all co-cryomilled mixtures around 43-59 °C might lead to think about presence of defective crystalline felodipine rather than forming an amorphous phase. In order to answer this question we can exclude this suggestion by these three supports: the first one is the mixtures at least for 50% drug

loading (where XRPD done) forming an amorphous halo rather than reduction in the crystallinity of the Bragg peaks. The reduction in the Bragg peaks intensity after cryomilling indicates crystalline defect rather than amorphous formation as reported previously by Rodolfo Pinal group in differentiation between amorphous and defective crystalline of griseofulvin [3] as seen Figure 3.8. Secondly at 50% drug loading in our Raman data there is a clear indication of formation an amorphous material as early in Raman part in this Section. The third important consideration is reported by Rodolfo on cryomilled griseofulvin. He suggested that the recrystallisation peak appears below the glass transition temperature in case of crystalline defect of griseofulvin which occurs around 58 °C while the T_g of amorphous griseofulvin is 90 °C as seen in Figure 3.9. In our study for all co-cryomilled mixtures exhibit a T_g around the T_g of the amorphous form which is 46.7 °C or around it. By these three findings there is an indication of amorphous formation rather than crystalline defect.

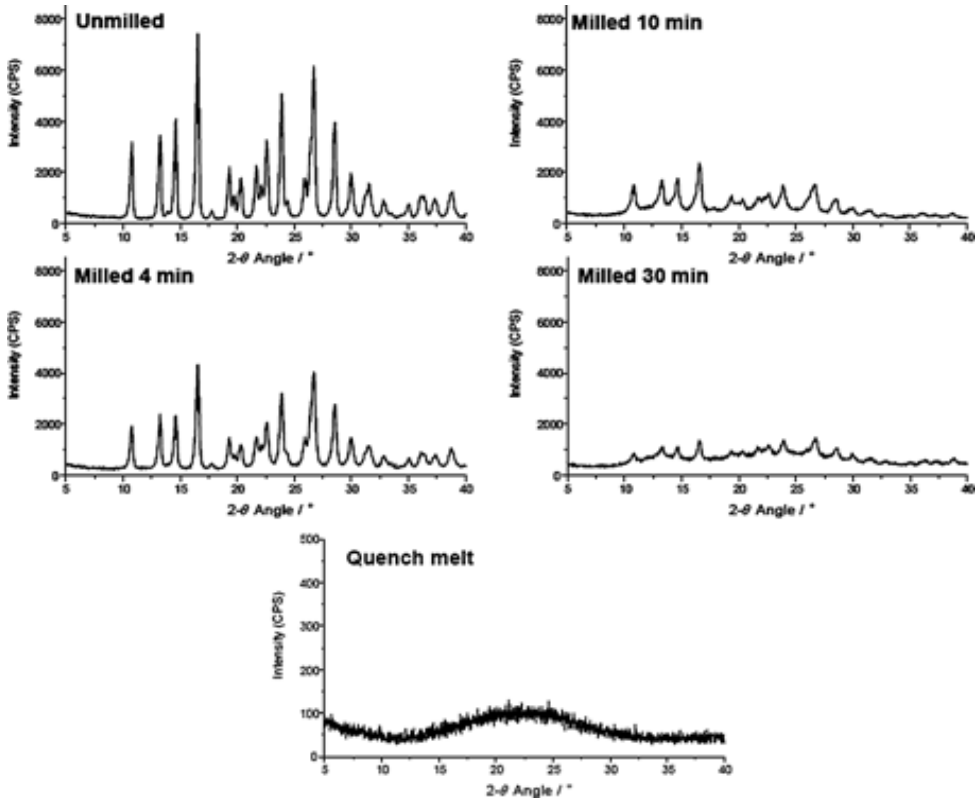

Figure 3.8: PXRD patterns from griseofulvin samples subjected to different cryogenic milling times. The PXRD pattern of the amorphous (quench melt) material is shown for comparison. This figure adapted from reference [3].

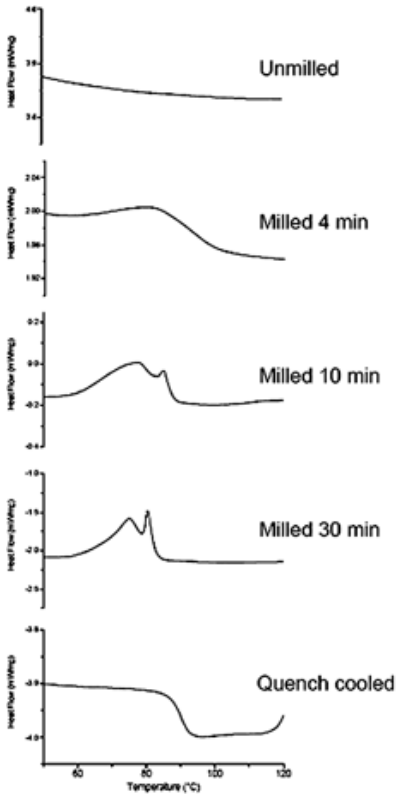

Figure 3.9: Zoom in view of the DSC thermograms of griseofulvin samples subjected to different cryogenic milling time in the temperature range 50-120 °C. This figure adapted from reference [3].

3.5.3 Stability study of the cryomilled dispersion under challenge conditions

The aim of our study is to examine the miscibility and hence stability of the co-cryomilled mixtures at high drug loadings. For this reason the 50% drug loadings for all mixtures were stored for six months to assess their stability at stress conditions which are either humidity or temperature (storage above felodipine T_g) or both. Both DSC and XRPD are using in the assessment of the stability. The crystalline content was quantified by DSC not XRPD. In the following section we will use different challenge conditions to determine which polymer is the most effective in stabilisation of the amorphous state of felodipine upon cryomilling. Appearance of the Bragg peaks by XRPD instead

of amorphous halo indicates recrystallisation of the mixtures and/or by the DSC either by disappearance of the T_g from the mixture or appearance of melting peak.

Humidity effect

25 °C/0% RH:

Figure 3.10 shows the stability study for the co-cryomilled felodipine with HPMC, HPMCAS, Soluplus, PMMA, HPMC/HPMCAS, HPMC/PMMA and Soluplus/HPMCAS by DSC and XRPD at 50% drug loading before and after storage of the samples for 6 months at 25 °C/0% RH. The XRPD data (Figure 3.10) show that the amorphous halo of the co-cryomilled felodipine with all polymers and polymers mixes was unchanged from the "zero time" samples after storage. From these XRPD results, co-cryomilling with the selected polymers and polymers mixes results in protection of felodipine from recrystallisation within the lengthy storage.

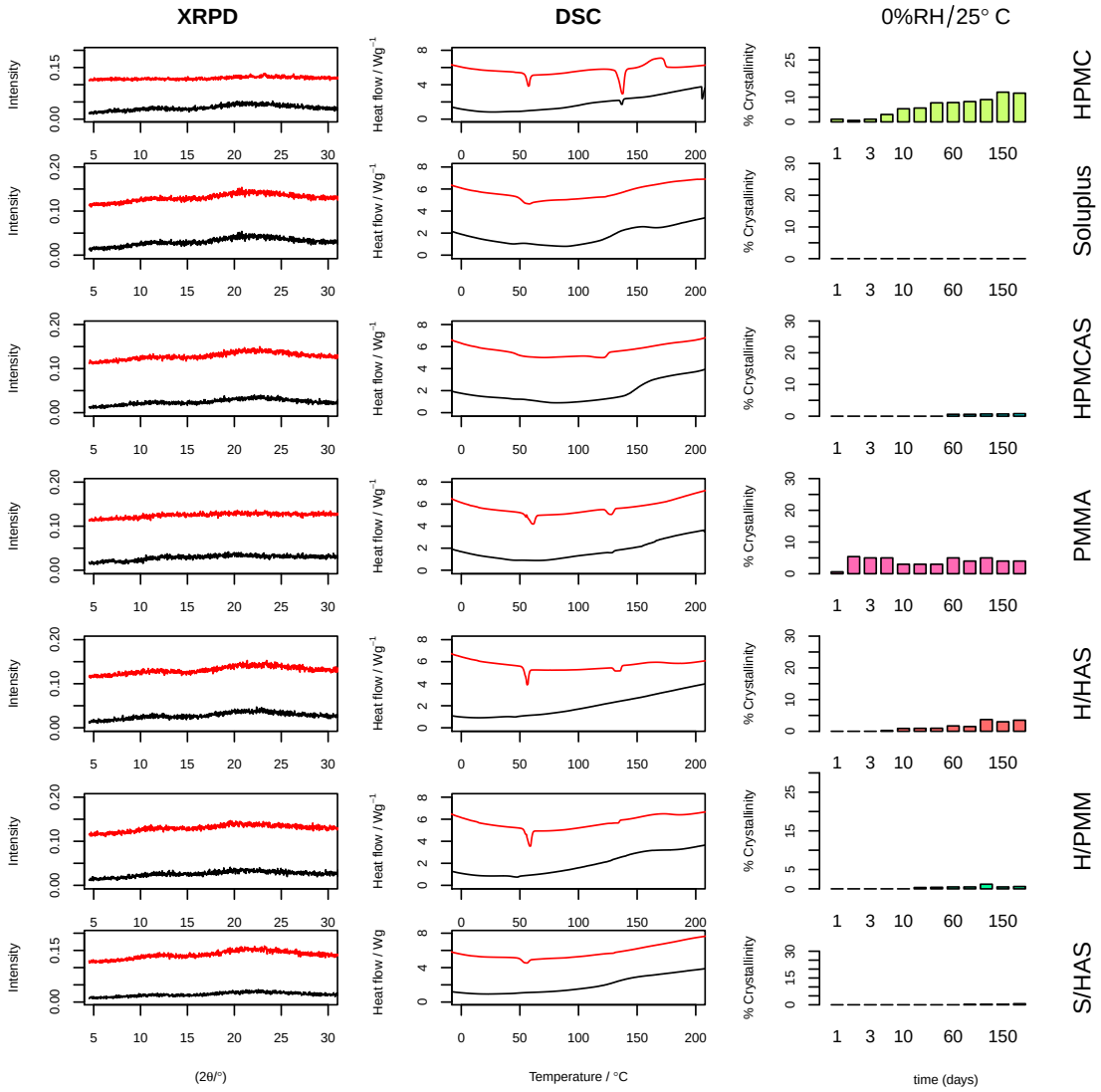

Figure 3.10: DSC thermograms and XRPD results for co-cryomilled felodipine at 50 % drug loading with HPMC, HPMCAS, Soluplus, HPMCAS, HPMC/HPMCAS, HPMC/PMMA and Soluplus/HPMCAS directly after cryomilling. Zero time indicated by black colour. Red colour indicated 6 months storage at 25 °C/0% RH. Offsets and scales applied for presentational purpose. The crystallinity was quantified by DSC not XRPD.

The DSC data show that all co-cryomilled mixtures that exhibit a T_g at "zero time" keep these T_g after storage period. All mixtures exhibit a relaxation in the T_g except the co-cryomilled felodipine-HPMCAS mixture in which there is no sign of relaxation in the T_g. All mixtures crystalline content stayed below 5% after

6 months storage in the mentioned conditions except co-cryomilled felodipine-HPMC which shows a crystalline content $\simeq$ 12% after storage period. In this mixture there was an increase in the enthalpy of melting that reflects an increase in the crystallinity of felodipine-HPMC which indicating its recrystallisation. The XRPD and DSC data are in agreement that all the mixtures keep their highly amorphous content except felodipine-HPMC mixture (see summary Table 3.10). Adding the pH dependent polymer (HPMCAS) or water insoluble polymer (PMMA) to the co-cryomilled felodipine-HPMC (ternary mixture) results in minimising the crystallisation as it leads to reduction of the crystalline content of co-cryomilled felodipine-HPMC from 12% to 4% and 1% of co-cryomilled felodipine-HPMC/HPMCAS and felodipine-HPMC/PMMA respectively after storage period.

25 °C/43% RH:

Figure 3.11 shows the stability study for co-cryomilled felodipine with HPMC, HPMCAS, Soluplus, PMMA, HPMC/HPMCAS, HPMC/PMMA and Soluplus/HPMCAS before and after storage at 25 °C/43% RH by DSC and XRPD at 50% drug loading for 6 months. The XRPD data show that the amorphous halo of the felodipine-HPMC, felodipine-Soluplus and Felodipine-Soluplus/HPMCAS systems was greatly reduced and sharp Bragg peaks started to appear after storage (more clear at Figure 3.18). Other co-cryomilled mixtures keep their amorphous halo after 6 months storage. The presence of the Bragg peaks for felodipine-HPMC, felodipine-Soluplus and felodipine-Soluplus/HPMCAS indicted the recrystallisation of these mixtures as sign of instability.

DSC data (Figure 3.11) show that all mixtures except felodipine-Soluplus exhibit a relaxation in the T_g. There is appearance of a melting peak for all mixtures except felodipine-Soluplus as seen clearly in Figures 3.12, 3.13, 3.14, 3.15, 3.16, 3.17 and 3.18. The enthalpy of melting reflects increasing in the crystalline content to about 22% for felodipine-HPMC mixture, 8% for HPMC/HPMCAS mixture. Other mixtures' crystalline content stays below 5% (high amorphous content). It was reported that amorphous form of trehalose is stable if stored at low humidity however upon exposure to moisture, the mixtures are plasticized, and the molec-

ular mobility increases as a sign of recrystallisation [241]. It was reported before that systems with strong drug-polymer interactions and a less hygroscopic polymer will be less susceptible to moisture-induced phase separation [258]. The addition of pH dependent polymer (HPMCAS) to the felodipine-HPMC and felodipine-Soluplus systems can minimise felodipine recrystallisation. Also addition of PMMA to the felodipine-HPMC system can protect this system from recrystallisation (see summary Table 3.10). Our DSC data with XRPD data indicate that felodipine-Soluplus were not any more stable against recrystallisation with increasing the humidity (43%) in comparison to that stored one at 25 °C/0% RH. Co-cryomilling of felodipine with PMMA or HPMCAS (both have ability to H-bond with felodipine from CSD analysis) results in more protection against recrystallization. At this point co-cryomilling felodipine with relatively hydrophobic polymer (HPMCAS and PMMA) that form a H-bond with felodipine results in protection of felodipine from recrystallisation. The addition of PMMA to the co-cryomilled felodipine-HPMC (ternary system) can protect the system from recrystallisation. Meanwhile, the presence of H-bond between felodipine and water soluble polymer (as in case of felodipine-Soluplus) under this stress condition seems to be not effective in protection of felodipine from recrystallisation.

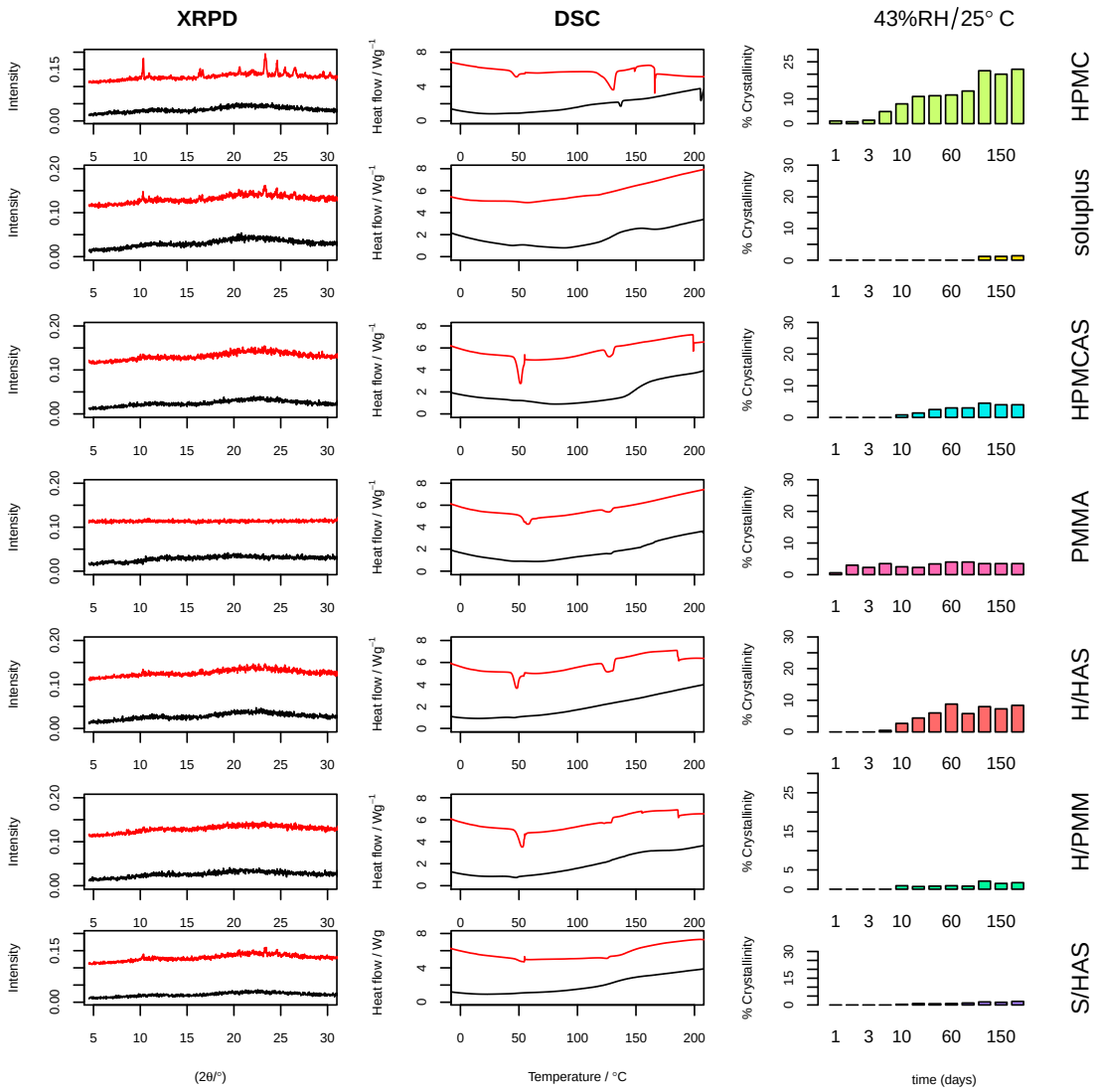

Figure 3.11: DSC thermograms and XRPD results for co-cryomilled felodipine at 50 % drug loading with HPMC, HPMCAS, Soluplus, HPMCAS, HPMC/HPMCAS, HPMC/PMMA and Soluplus/HPMCAS directly after cryomilling. Zero time indicated by black colour. Red colour indicated the samples that stored after 6 months at 25 °C/43% RH. Offsets and scales applied for presentational purpose. The crystallinity was quantified by DSC not XRPD.

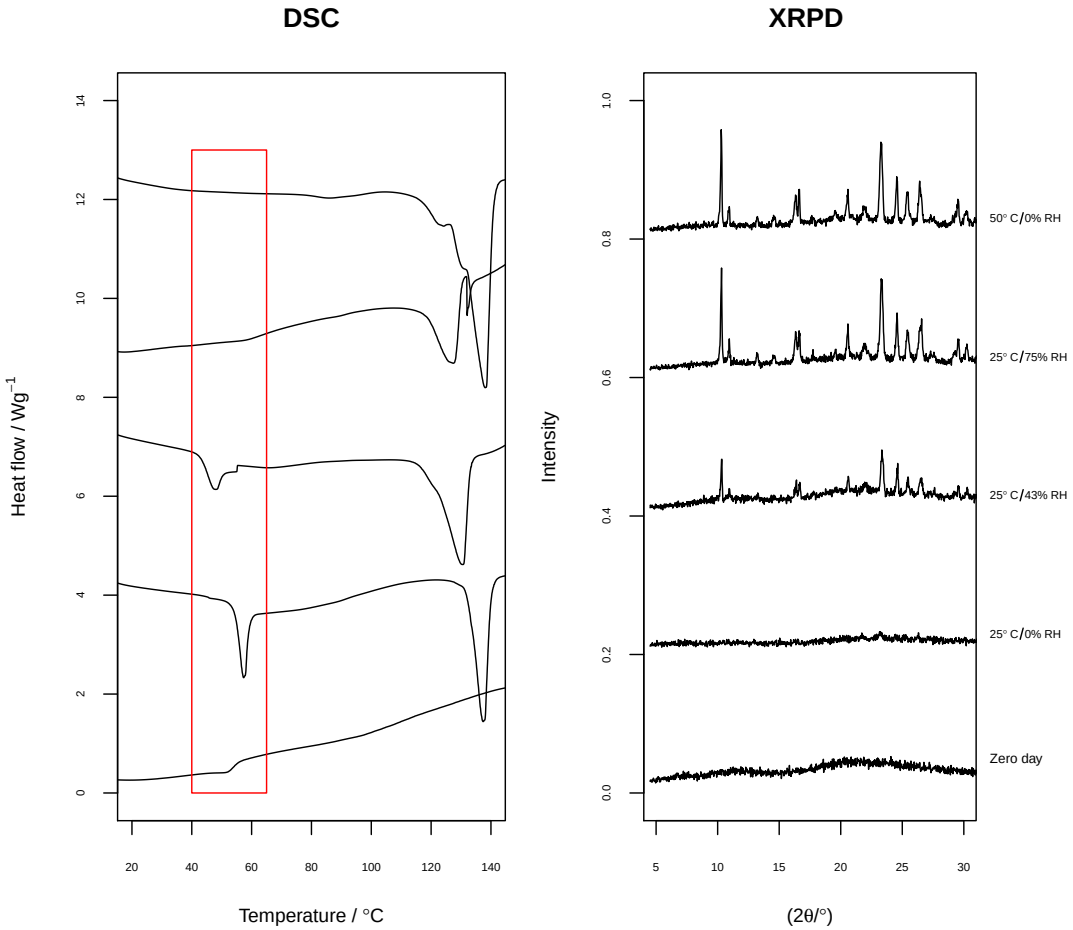

Figure 3.12: The DSC thermogram and XRPD patterns of co-cryomilled felodipine with HPMC at 50% drug loading at zero time of detection and under diffrent storage conditions stored for 6 months (25 °C/0% RH, 25 °C/43% RH, 25 °C/75% RH, 50 °C/0% RH). Offsets applied for presentational purposes.

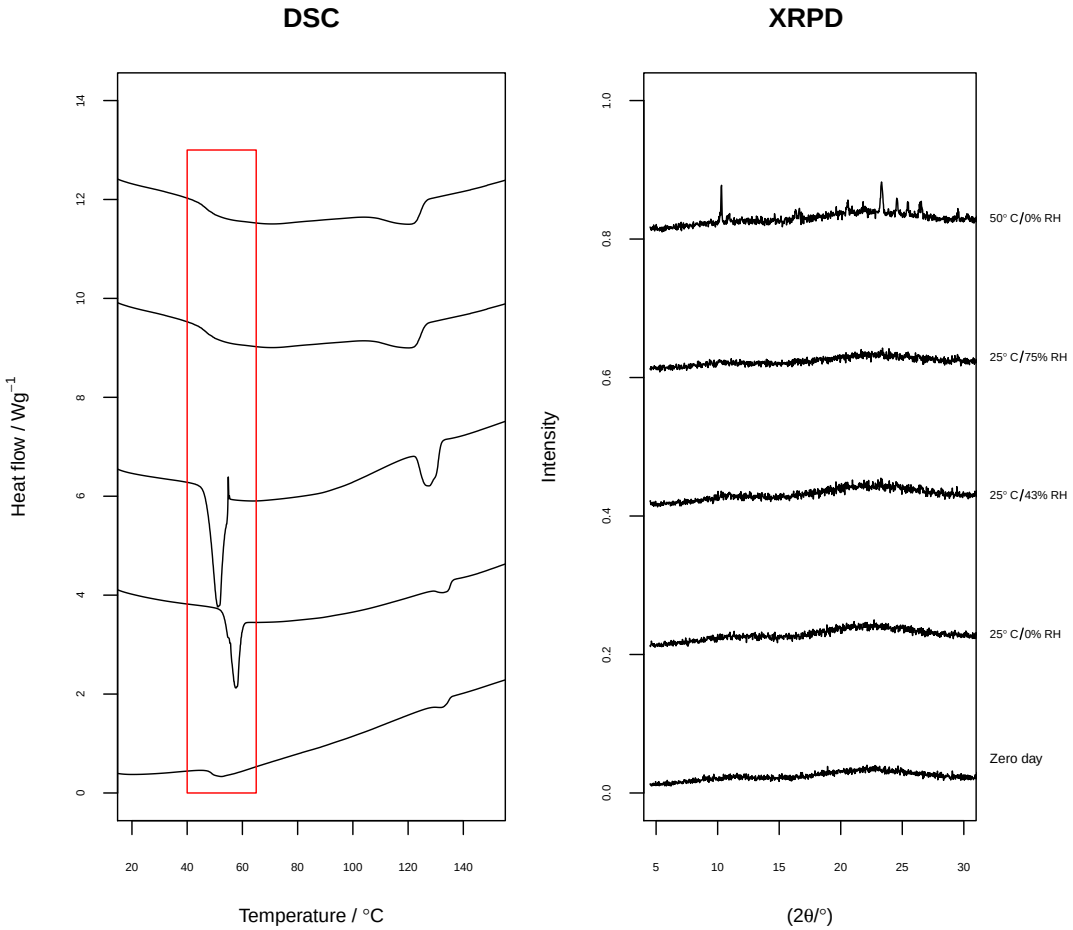

Figure 3.13: The DSC thermogram and XRPD patterns of co-cryomilled felodipine with HPMCAS at 50% drug loading at zero time of detection and under diffrent storage conditions stored for 6 months (25 °C/0% RH, 25 °C/43% RH, 25 °C/75% RH, 50 °C/0% RH). Offsets applied for presentational purposes.

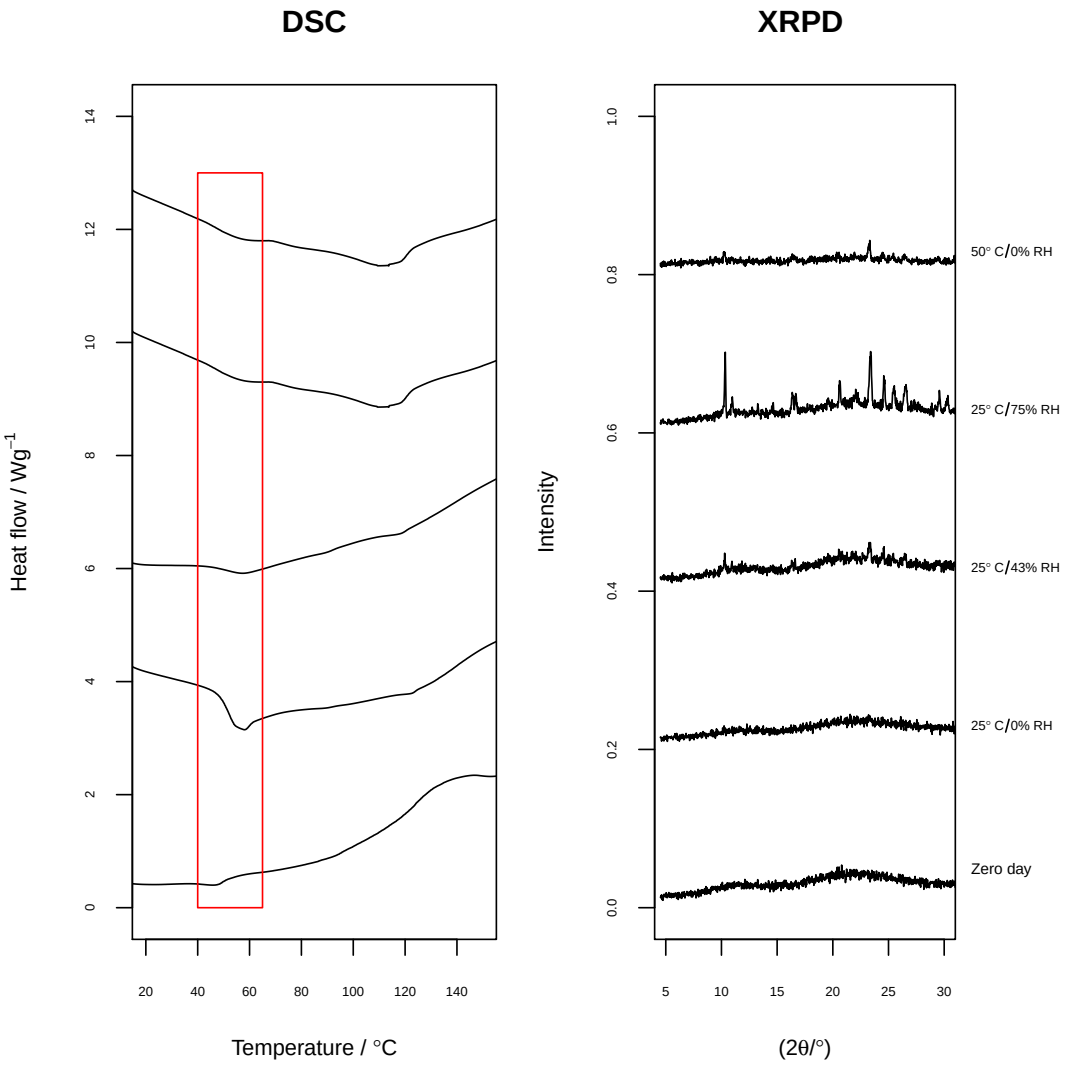

Figure 3.14: The DSC thermogram and XRPD patterns of co-cryomilled felodipine with Soluplus at 50% drug loading at zero time of detection and under diffrent storage conditions stored for 6 months (25 °C/0% RH, 25 °C/43% RH, 25 °C/75% RH, 50 °C/0% RH). Offsets applied for presentational purposes.

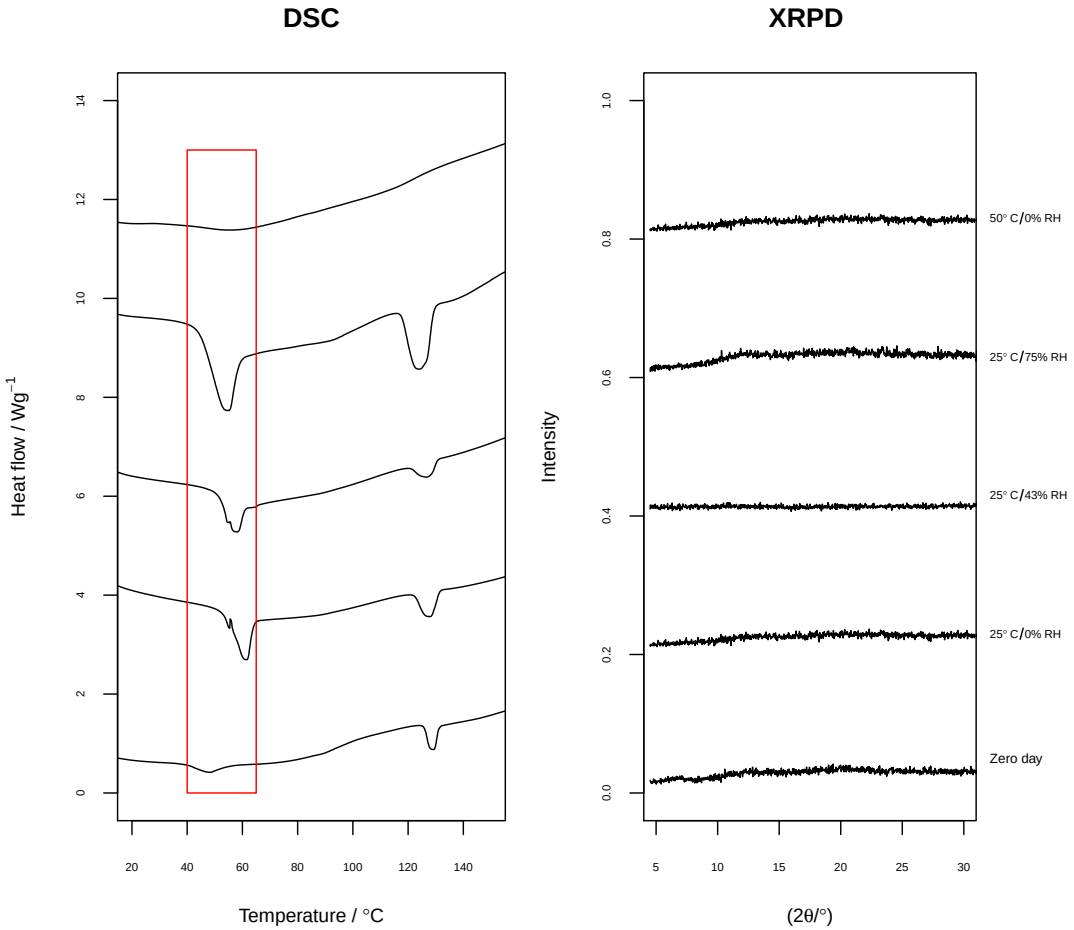

Figure 3.15: The DSC thermogram and XRPD patterns of co-cryomilled felodipine with PMMA at 50% drug loading at zero time of detection and under diffrent storage conditions stored for 6 months (25 °C/0% RH, 25 °C/43% RH, 25 °C/75% RH, 50 °C/0% RH). Offsets applied for presentational purposes.

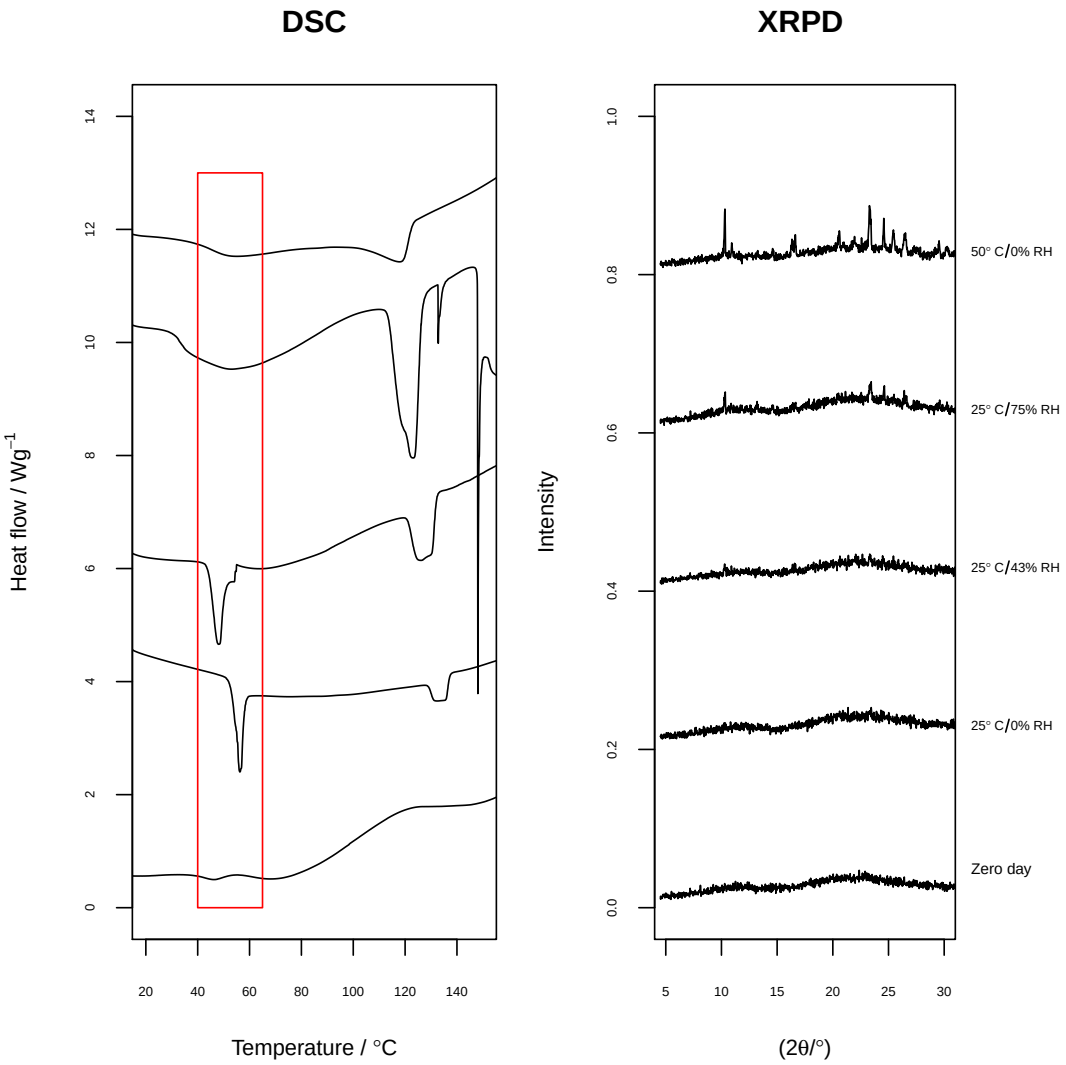

Figure 3.16: The DSC thermogram and XRPD patterns of co-cryomilled felodipine with HPMC/HPMCAS at 50% drug loading at zero time of detection and under diffrent storage conditions stored for 6 months (25 °C/0% RH, 25 °C/43% RH, 25 °C/75% RH, 50 °C/0% RH). Offsets applied for presentational purposes.

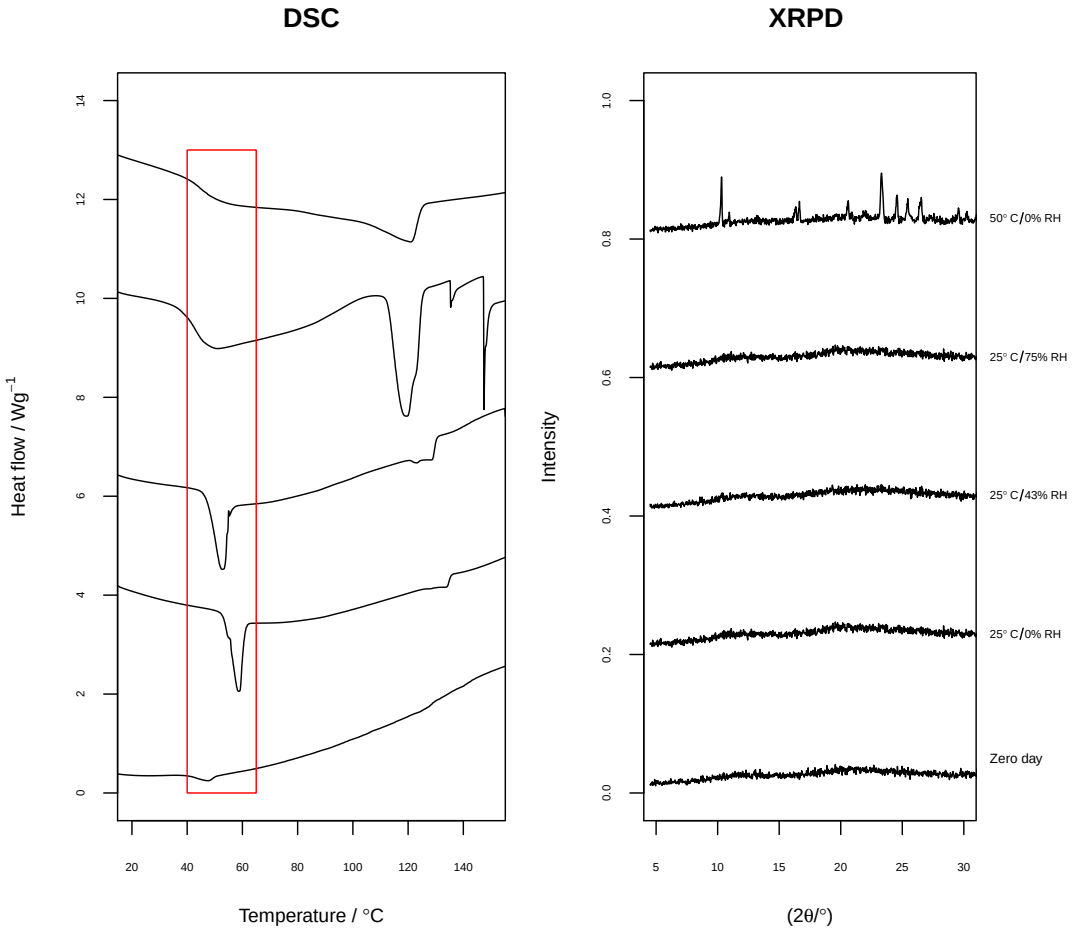

Figure 3.17: The DSC thermogram and XRPD patterns of co-cryomilled felodipine with HPMC/PMMA at 50% drug loading at zero time of detection and under diffrent storage conditions stored for 6 months (25 °C/0% RH, 25 °C/43% RH, 25 °C/75% RH, 50 °C/0% RH). Offsets applied for presentational purposes.

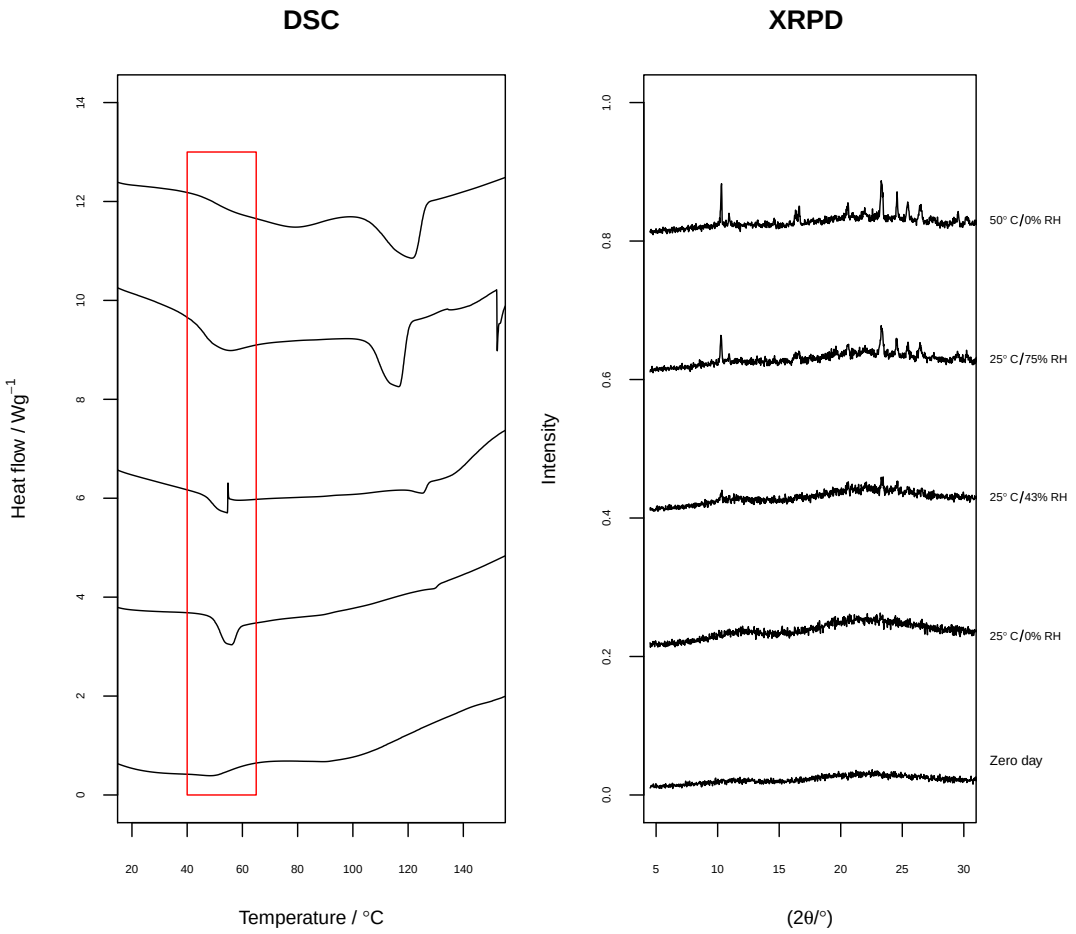

Figure 3.18: The DSC thermogram and XRPD patterns of co-cryomilled felodipine with Soluplus/HPMCAS at 50% drug loading at zero time of detection and under diffrent storage conditions stored for 6 months (25 °C/0% RH, 25 °C/43% RH, 25 °C/75% RH, 50 °C/0% RH). Offsets applied for presentational purposes.

25 °C/75% RH:

Figure 3.19 shows the stability study for co-cryomilled felodipine with HPMC, HPMCAS, Soluplus, PMMA, HPMC/HPMCAS, HPMC/PMMA and Soluplus/HPMCAS before and after storage at 25 °C/75% RH by DSC and XRPD at 50% drug loading. The XRPD data in Figure 3.19 show that the amorphous halo of all co-cryomilled are disappeared into Bragg peaks except for felodipine-HPMCAS, felodipine-PMMA and felodipine-HPMC/PMMA as they retain their amorphous halo after lengthy storage. This indicates that increasing the hu-

midity induces recrystallisation for water soluble polymer felodipine-HPMC, felodipine-Soluplus in the binary mixture and felodipine-HPMC/HPMCAS and felodipine-soluplus/HPMCAS for the ternary mixes. In contrast, the binary mixture that contain water insoluble and pH dependent polymer and the ternary felodipine-HPMC with PMMA mixture did not show any sign of recrystallisation by XRPD.

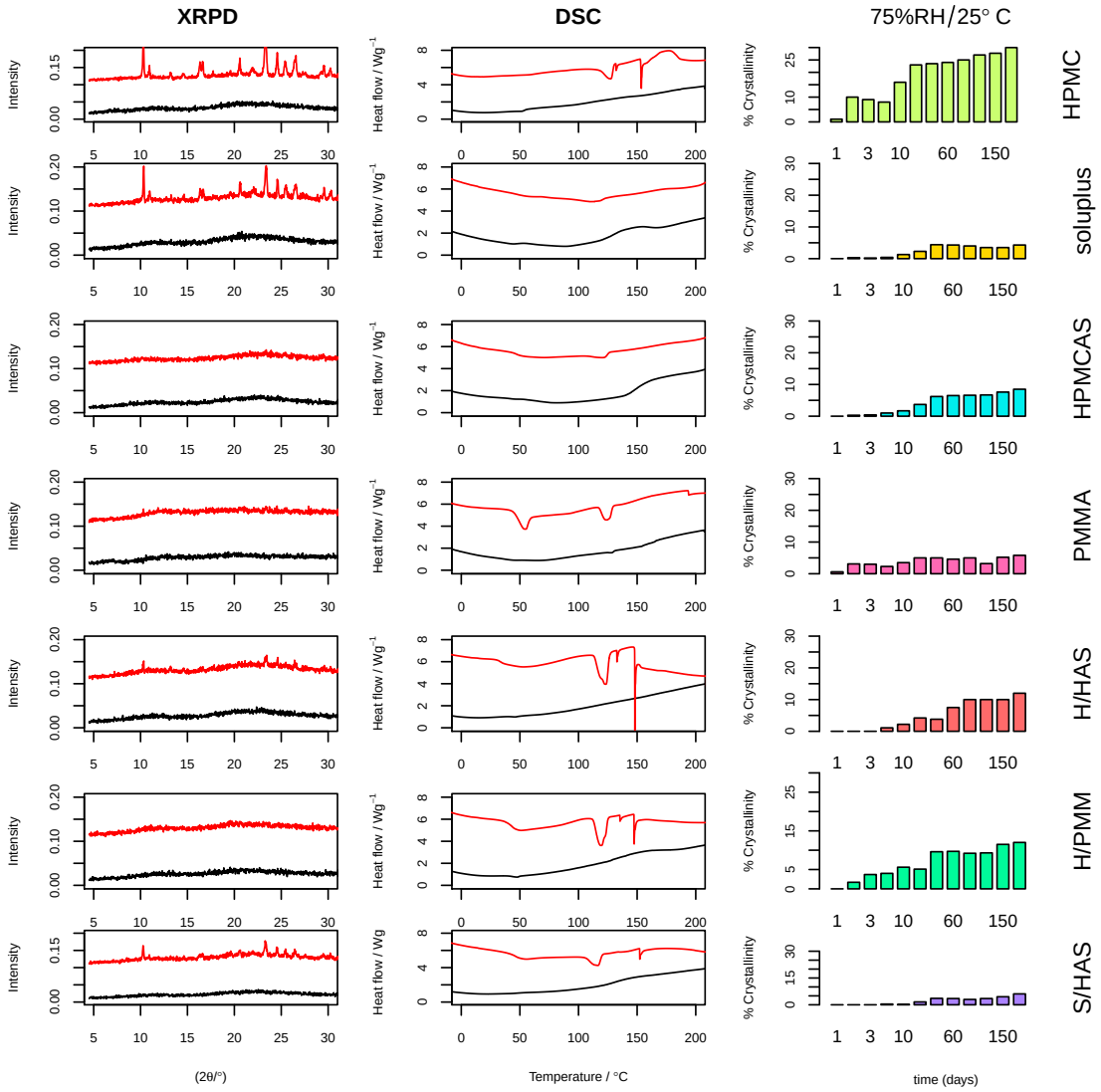

Figure 3.19: DSC thermograms and XRPD results for co-cryomilled felodipine at 50 % drug loading with HPMC, HPMCAS, Soluplus, HPMCAS, HPMC/HPMCAS, HPMC/PMMA and Soluplus/HPMCAS directly after cryomilling. Zero time indicated by black colour. Red colour indicated stability after 6 months storage 25 °C/75% RH. Offsets and scales applied for presentational purpose. The crystallinity was quantified by DSC not XRPD.

It is clearly seen from the DSC data in Figure 3.19 that the T_g of felodipine-HPMC disappeared after 6 months storage at 25 °C/75% RH. Felodipine-HPMCAS shows a reduction in T_g by 9 °C. Felodipine-Soluplus T_g was reduced by 3 °C and about 6 °C for felodipine-HPMC/PMMA. Only co-cryomilled felodipine-

PMMA show no change in the T_g after storage. The only change in the T_g is the relaxation after storage (Figures 3.12, 3.13, 3.14, 3.15, 3.16, 3.17and 3.18). It was previously reported that felodipine-PVP (50% drug loading) prepared by spray drying method underwent crystallisation by exposing to high humidity at room temperature 25 °C/84% RH despite the high drug polymer interaction between felodipine and PVP [258]. However, it has been reported that felodipine-HPMCAS (50% loading) prepared by spray drying system exhibits resistance from crystallisation at that harsh condition as it less hygroscopic polymer than PVP according to the opinion of researchers in [258]. Our DSC and XRPD data indicate that under harsh conditions of 25 °C/75% RH only felodipine containing water insoluble polymer (PMMA) is stable after storage. However all co-cryomilled mixtures that contain water soluble polymer recrystallise either from the appearance of Bragg peaks, changing the T_g or appearance of melting peaks. The addition of water insoluble polymer to a co-cryomilled mixture of felodipine-HPMC can greatly minimise its recrystallisation. The effect of humidity can summarised in Figure 3.20.

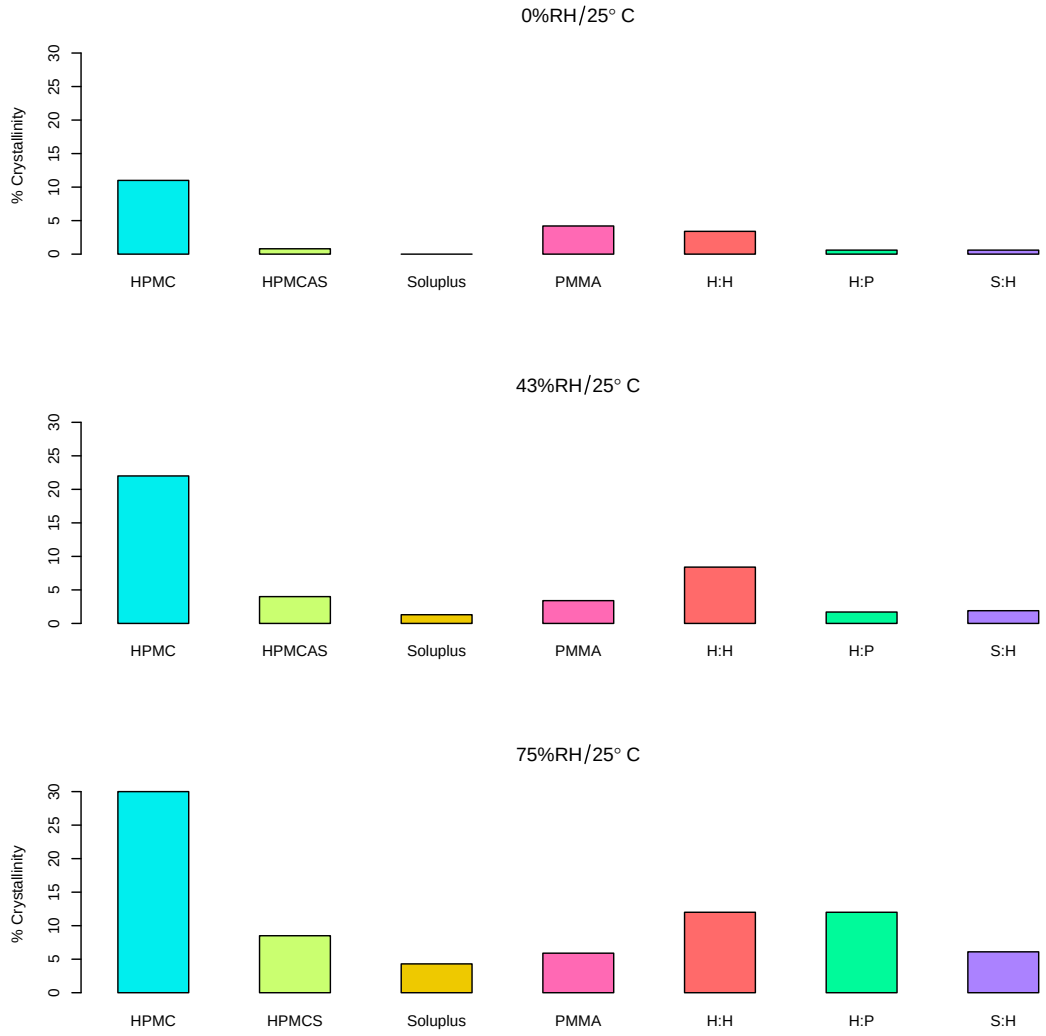

Figure 3.20: The crystallinity of the co-cryomilled felodipine with HPMC, HPMCAS, Soluplus, PMMA, HPMC/HPMCAS, HPMC/PMMA, Soluplus/HPMCAS after 6 months storage at 25 °C/0%, 43% and 75% RH respectively.

Temperature effect

Figure 3.21 shows the stability study for co-cryomilled felodipine with HPMC, HPMCAS, Soluplus, PMMA, HPMC/HPMCAS, HPMC/PMMA and Soluplus/HPMCAS before and after storage at 50 °C/0% RH for 6 months by DSC and XRPD at 50% drug loading. The XRPD data in Figure 3.21 show that the

amorphous halo of the co-cryomilled felodipine with all selected polymers was greatly reduced and sharp Bragg peaks started to appear after 6 months storage at 50 °C/0% RH except felodipine-PMMA keep the amorphous halo. The appearance of the Bragg peaks in the mixtures indicates recrystallisation of the mixtures at 50 °C/0% RH except felodipine-PMMA. This temperature was selected as a stress test to see the effect of the storage temperature (above felodipine T_g) on amorphous solid dispersion stability.

Its clearly seen from the DSC data in Figure 3.21 that all mixtures exhibit a T_g after 6 months storage at 50 °C/0% RH except felodipine-HPMC mixture. The T_g of the co-cryomilled mixtures felodipine-HPMCAS, felodipine-HPMC/HPMCAS and felodipine-HPMC/PMMA were reduced $\simeq$3 °C. There is an appearance of melting peaks of some mixtures. It was reported that storage above the T_g temperature results in recrystallisation [241] so that to ensure the stability of amorphous solid dispersion it is important to store them below its glass transition temperature [269]. From the DSC and XRPD data all mixtures recrystallises upon storage above the T_g of the mixture except felodipine-PMMA (the most hydrophobic polymer). Figure 3.22 summarises the effect of storing the co-cryomilled mixture above its T_g at 50 °C/0% RH.

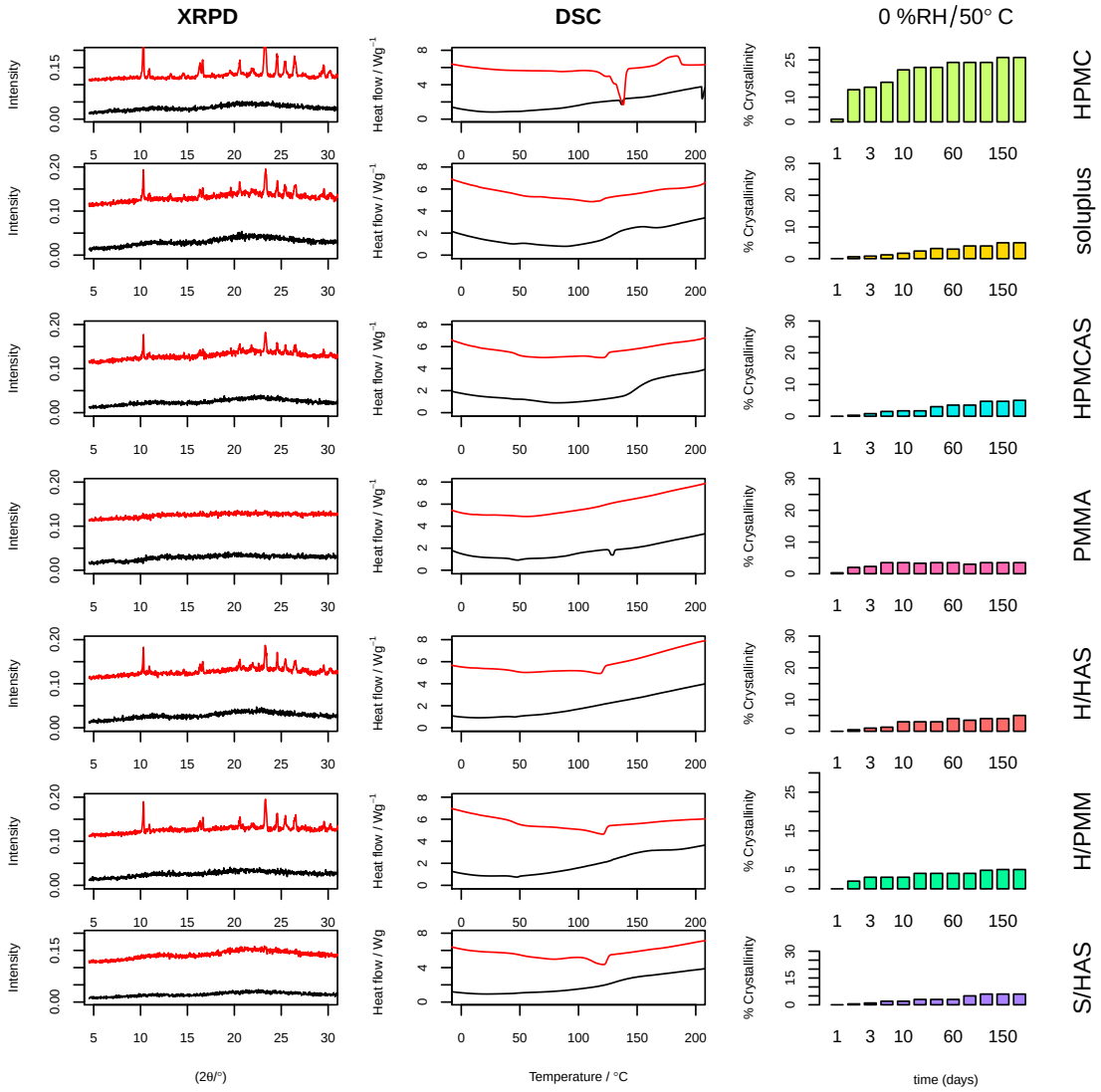

Figure 3.21: DSC thermograms and XRPD results for co-cryomilled felodipine at 50 % drug loading with HPMC, HPMCAS, Soluplus, HPMCAS, HPMC/HPMCAS, HPMC/PMMA and Soluplus/HPMCAS directly after cryomilling. Zero time indicated by black colour. Red colour indicated samples that stored 6 months at 50 °C/0% RH. Offsets and scales applied for presentational purpose. The crystallinity was quantified by DSC not XRPD.

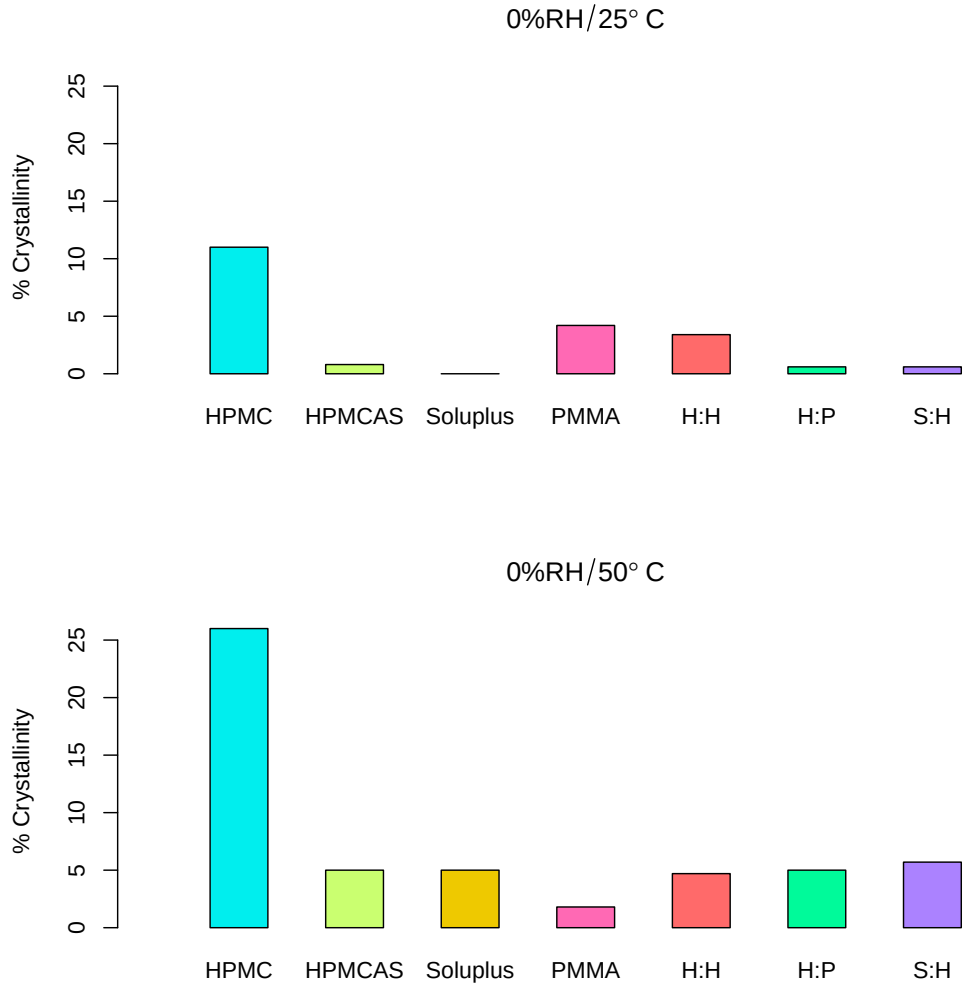

Figure 3.22: The crystallinity of the co-cryomilled felodipine with HPMC, HPMCAS, Soluplus, PMMA, HPMC/HPMCAS, HPMC/PMMA, Soluplus/HPMCAS after 6 months storage at different temperatures which are 25 °C/0% and 50 °C/0%.

To summarise the stability of the co-cryomilled mixtures see table Table 3.10.

According to the storage results in the all mentioned conditions from both DSC and XRPD results the mixtures can be ranked according to their stability in the mentioned conditions as seen in Figure 3.23. It can be concluded that the most stable mixture is felodipine-PMMA (the most hydrophobic polymer and from CSD analysis PMMA has a potential to form a H-bond with felodipine)

Table 3.10: Stability of all selected mixtures under different conditions.

Mixture	25°C/0% RH	25°C/43% RH	25°C/75% RH	50°C/0% RH	Ranking
Felodipine-HPMC	recrystallise (DSC)	recrystallise (DSC,XRPD)	recrystallise (DSC, XRPD)	recrystallise (DSC, XRPD)	4
Felodipine-Soluplus	No recrystallisation	recrystallise (XRPD)	recrystallise (XRPD)	recrystallise (XRPD)	3
Felodipine-HPMCAS	No clear recrystallisation	No clear recrystallisation	recrystallise (DSC)	recrystallise(XRPD)	2
Felodipine-PMMA	No clear recrystallisation	No clear recrystallisation	No clear recrystallisation	No clear recrystallisation	1
Felodipine-HPMC/HPMCAS	No clear recrystallisation	recrystallise (DSC)	recrystallise (DSC, XRPD)	recrystallise (XRPD)	3
Felodipine-HPMC/PMMA	No clear recrystallisation	No clear recrystallisation	recrystallise (DSC)	recrystallise (XRPD)	2
Felodipne-Soluplus/HPMCAS	No clear recrystallisation	recrystallise (XRPD)	recrystallise (XRPD,DSC)	recrystallise (XRPD,DSC)	3

which is stable against the harshest conditions investigated in our work. The most hydrophobic polymer was reported to inhibit the crystallisation of amorphous drug in solid dispersion such as ritonavir [67, 244]. Felodipine/HPMCAS and felodipine/HPMC-PMMA mixtures are on the second ranking as they are stable only under the zero and moderate humidity conditions which are 25 °C/0% RH and 25 °C/43% RH. These 2 mixtures contain either HPMCAS which is the pH dependent polymer or the mixture of hydrophilic and hydrophobic polymer HPMC/PMMA (HPMCAS from CSD analysis HPMCAS has ability to form H-bond with felodipine). The third ranking are stable only at 25 °C/0% RH) but can not withstand any increasing in humidity or storage above T_g. These groups involve the binary mixture felodipine-Soluplus and the ternary mixes (felodipine-Soluplus/HPMCAS and felodipine-HPMC/HPMCAS which contain hydrophilic polymers with HPMCAS). Soluplus is the third rank of hydrophobicity and has show a H-bond interaction with felodipine and it shows miscibility with felodipine in all proportions by DSC. Finally the worst mixture is felodipine-HPMC which is hydrophilic polymer that is unstable even at 25 °C/0% RH which is mild stress condition of storage (HPMC is the last

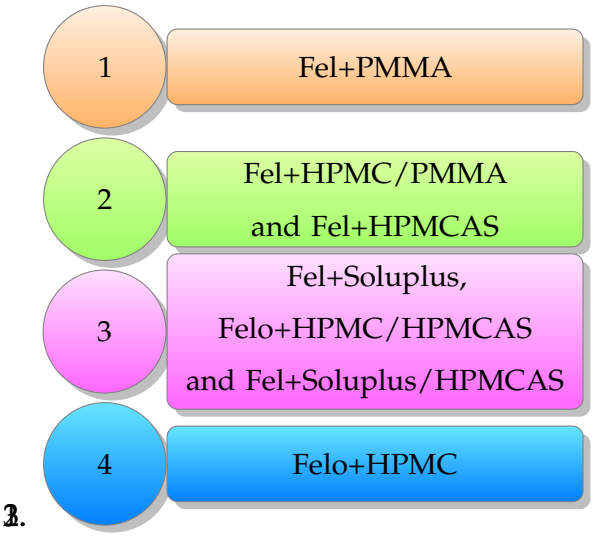

Figure 3.23: Ranking of the co-cryomilled mixtures according to their stability at different temperatures and humidities.

ranking from hydrophobicity and show no H-bond interaction with felodipine). Konno and Taylor correlate the relationship between the hydrophobicity and stability of amorphous solid dispersion in which the more hydrophobic the mixture, the more its stability against recrystallisation [148]. The ranking of the stability depending mainly on the hydrophobicity of the polymer and secondly on the drug-polymer interaction. Mixing of hydrophilic and hydrophobic polymer is important to improve the stability of the least stable mixture (felodipine-HPMC). The degree of protection also affected by the hydrophobicity of the polymer that is mixed with such as PMMA gave better protection when mixed in the ternary mixtures than HPMCAS.

3.6 Conclusion

This pre-formulation study of the co-cryomilled mixtures is a promising study for production of an amorphous solid dispersion via this approach. The top formulation in which no recrystallisation was observed at any challenge condition is the co-cryomilled felodipine-PMMA while the worst drug is the co-cryomilled

felodipine-HPMC that crystallises even on mild challenge conditions. The more hydrophobic polymer the more resistant to the recrystallisation. If we consider the output of CSD analysis in terms of expected interaction we will see that the the best formulation for stabilising felodipine is also predicted to have a strong interaction from our CSD research where the weak interaction is the worst stable. In between of this rank the co-cryomilled mixtures are ranked according to their hydrophobic nature. For this reason hydrophobicity is the most influential factor for the stability of the amorphous solid dispersion then the drug-polymer interaction. Within our finding, the miscibility of the amorphous solid dispersion is important but it is not the main factor affecting the stability at least in this study. Mixing the hydrophilic and hydrophobic polymers together is efficient in minimising the recrystallisation of most mixture in this study. This mixing at the same time might ensure acceptable drug release. Future work in the next Chapter 4 will focus on the dissolution of all selected drug co-cryomilled with the selected polymer and co-cryomilled with polymer mixes in order to be selected as the best mixture for the formulation of the ODT in Chapter 5.

Table 3.11: Summary table of chapter 3 results.

Co-cryomilled	Solid state	Miscibility	Interaction predicted from CSD	Hydrophobicity predicted from LogP	Ranking of stability according to the DSC and XRPD
Felodipine-HPMC	amorphous	miscible	no	4	4
Felodipine-Soluplus	amorphous	miscible	yes	3	3
Felodipine-HPMCAS	amorphous	miscible	yes	2	2
Felodipine-PMMA	amorphous	miscible	yes	1	1
Felodipine-HPMC/HPMCAS	amorphous	miscible	-	-	3
Felodipine-HPMC/PMMA	amorphous	miscible	-	-	2
Felodipine-Soluplus/HPMCAS	amorphous	immiscible	-	-	3

Chapter 4

Release of felodipine from the co-cryomilled mixtures

4.1 Novelty in this Chapter

1. This is the first study that focuses on the dissolution of amorphous solid dispersion by formulating/cryomilling with wide range of polymers.
2. First comparative study between hot melt extrusion as a common method to obtain amorphous solid dispersion and cryomilling as a developing approach.
3. Relatively high drug loading (50%) was used in this study which is unusual due to the stability issue and expectation of low % drug release.

4.2 Introduction

The target of formulating an API as amorphous solid dispersion is to deliver the drug into the systemic circulation from the GI tract. The bioavailability then depends on the drug release from the dosage form. In order to evaluate the rate of the drug dissolution an *in vitro* dissolution test was used which mimics the in vivo condition where absorption is dissolution-rate limited in class II

drugs [270, 271].

The most commonly used media to assess the amorphous solid dispersions formulations are water and pH 6.8 with either simulated gastric fluid or surfactant for non-ionised drugs [8]. Sink conditions occurs if the volume of dissolution media is 3-10 times greater than the volume required for a drug to be saturated [8, 12, 271]. To ensure sink conditions, different approaches were used including organic solvent addition, pH modification, using large volume of dissolution and addition of surfactant [8, 272, 273]. The dissolution test is important in amorphous solid dispersion because it can be a useful guide for the selection of suitable polymer that enhances the API dissolution [274]. The dissolution test is not only important to evaluate the dissolution rate of the drug only but also important to evaluate the prolongation of supersaturation to select the best polymer in the formulation [274]. Amorphous drugs are highly energetic and this can result in in achieving a higher kinetic solubility (supersaturation) than the expected crystalline solubility [275]. Meanwhile, particle size reduction results in increasing the surface area and hence the dissolution rate. Particle size reduction occurs due to milling and cryogrinding [21, 276–278]. Cryomilling from Chapter 2 can achieve an increasing in both solubility and dissolution rate.

The role of the polymer in enhancement of the drug dissolution is not fully clear. It might be related to changing the physical state or drug-polymer interaction [274]. Craig made a simple model to understand the mechanism of the drug release form solid dispersion which is either carrier-controlled or drug-controlled dissolution, depending on drug solubility in the concentrated polymer layer [279]. This model is important in the formulation step [280]. For the carrier controlled mechanism, the release of the drug is controlled by diffusion according to Stokes-Einstein equation and the rate limiting step is the release of the drug from polymer itself which affected by the viscosity of the carrier layer. Some polymers sorb water and swell so the release will be due to other mechanisms. The second case which is drug-controlled release in which the dissolution will be affected by the drug property itself such as the particle size and the physical form. The reduction in particle size will result in increasing the

surface area, increasing wetting and reduce the agglomeration between particles. For this reason a high drug loading is preferred to make the dissolution of the drug the rate limiting step rather than diffusion which might cause a retardation of the drug release [279]. The dissolution rate limiting step is the target for fast releasing formulations.

The dissolution rate of poorly water soluble drug increases mainly by particle size reduction [96, 278, 281]. Particles size reduction results in changing the surface property and surface free energy [213] for micronised felodipine. Vogt *et al* develop a method to increase the dissolution of fenofibrate by micronsiation then spray drying of the micronised particles [278]. Co-grinding of compound KCA-098 with hydroxypropyl cellulose enhances the dissolution of this compound [282]. Cryomilling ensure increasing in both dissolution rate and solubility of poorly water soluble drug such as cryomlling of indomethacin [63].

As felodipine as discussed in the introduction is a practically insoluble drug and as reported previously it has a vital role in the treatment of hypertensive crisis [283]. In addition, there is no immediate release formulation in the market for felodipine due to its solubility issue, therefore there is a clear need for a formulation strategy that achieved an immediate release formulation which is difficult to achieve by traditional processing technique. The previous release study was done on the cryomilled drug itself such as the study that done by Karmwar *et al* [63] which focuses on the effect of milling time of indomethacin on its own release and the study on the release of the co-amorphised indomethacin, carbimazipine with amino acid [94]. We are therefore at this stage undertaking a performulation strategy looking at the effect of polymers on stabilising the amorphous solid to boost the drug release compare to the crystalline form. In this chapter we explore the effect of co-cryomilling to improve the dissolution of felodipine as it results in both particle size reduction and amorphisation at the same time.

Felodipine was co-cryomilled with HPMC, HPMCAS, Soluplus, HPMCAS, HPMC-HPMCAS, HPMC-PMMA and Soluplus-HPMCAS at 50% drug loading. The dissolution was measured according to the United States Pharmacopeia

(USP) by using dissolution apparatus type II by using water with SDS as surfactant to ensure sink conditions. Felodipine-Soluplus co-cryomilled mixtures was selected for comparative study with HME method. Finally the release from felodipine-Soluplus mixture was studied at different drug loadings.

4.3 Materials and Methods

4.3.1 Materials

See Chapter 2 and 3 materials

4.3.2 Cryomilling

As in chapter 2 Section 2.3.2

4.3.3 Release study

All co-cryomilled powder of the felodipine with HPMC, HPMCAS, Soluplus, PMMA, HPMC/HPMCAS, HPMC/PMMA and HPMCAS/Soluplus release were evaluated through the dissolution test. The dissolution was done by using the United States Pharmacopeia (USP) Type II apparatus at 50 rpm (Erweka Dissolution Tester) in water containing 1% SDS to ensure sink conditions (this is according to the USP method for felodipine modified release tablets except the media is water here in this study not pH 6.5 that mentioned in the USP for felodipine tablet). The dissolution test and HPLC are identical to Chapter 2 method Section 2.3.7.

4.3.4 HME

The polymers were blended with the API as a powder. Each sample was subsequently melt extruded using a twin-screw extruder (HAAKE Minilab, Thermo

Fisher Scientific, Loughborough, UK) at 50 rpm/160 C for 15 minutes. After extrusion, the melt extrudates were cooled to ambient temperature and stored in glass vials with a rubber-lined cap for further studies. The mixture was cryomilled for 10 minutes to ensure a small particle size for the dissolution study. This work was kindly done with aid of Mrs.Gudrun Fridgeirsdottir.

4.4 Results and discussion

4.4.1 Release for polymer and polymer mix

Figure 4.1 shows the dissolution results under sink conditions for felodipine as received, cryomilled and co-cryomilled with HPMC, HPMCAS, Soluplus, PMMA, HPMC/HPMCAS, HPMC/PMMA and Soluplus/HPMCAS. After cryomilling, samples were stored for 24 hours in minimum humidity at room temperature. It is clearly seen in Figure 4.1 that the release of the as received felodipine is less than 40% after 6 hours of dissolution which was reported previously in Chapter 2. It was also reported early in Chapter 2 in our study that the cryomilled felodipine release is more than double that of the as received one over this time. This elevation in felodipine release after cryomilling is likely due to the effect of cryomilling on particle size reduction and/or to amorphisation as observed in our study in Section 2.4.1 which is also suggested by the researchers in references [63, 213].

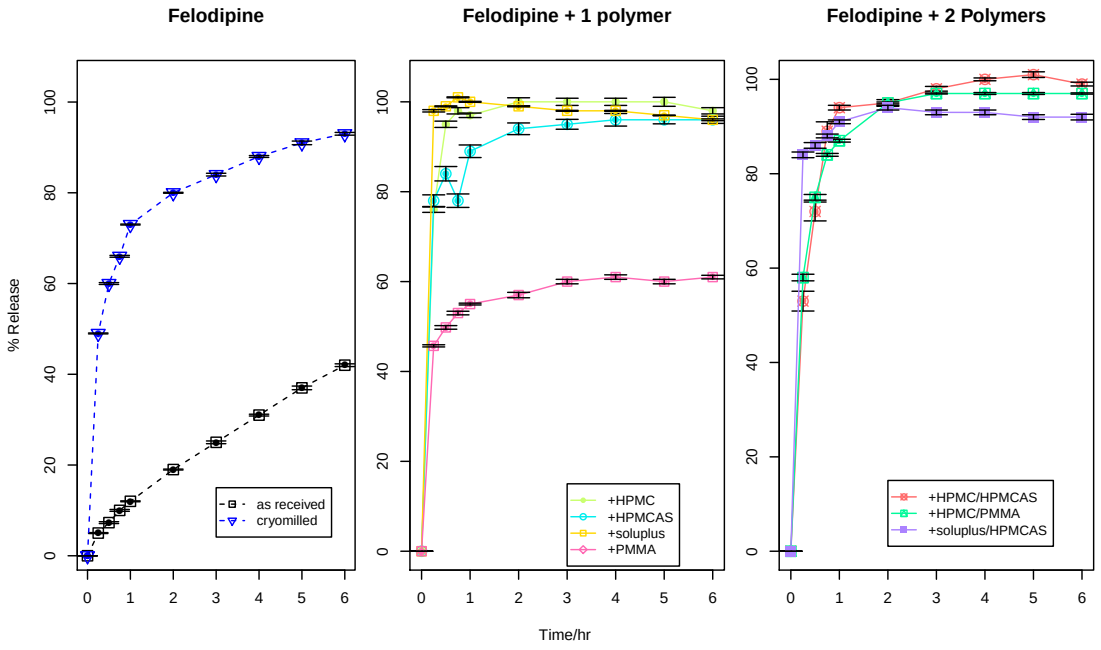

Figure 4.1: The release profile of felodipine as received, cryomilled for 150 minutes and cryomilled together with HPMC, HPMCAS, Soluplus, PMMA, HPMC/HPMCAS , HPMC/PMMA and Soluplus/HPMCAS (1:1) at 50% drug loading (n=3).

In felodipine-HPMC mixture (Figure 4.1), the percentage of the drug release increases to about 100% after 6 hour dissolution which is higher than the cryomilled felodipine itself. At the same time felodipine-Soluplus gave almost identical release to the felodipine-HPMC (both polymers are water soluble). The dissolution rate is high from the first 15 minutes. The elevation in felodipine dissolution rate upon co-cryomilling with HPMC or with Soluplus in comparison to the cryomilled felodipine might be related to the solubilising effect of HPMC and Soluplus and/or its protection against recrystallisation during dissolution in aqueous media [35, 217].

Co-cryomilled felodipine-HPMCAS (Figure 4.1) started with slower dissolution rate in comparison to co-cryomilled felodipine with HPMC or Soluplus but it is faster dissolution rate than felodipine and cryomilled felodipine. Co-cryomilled felodipine-HPMCAS percentage release is $\simeq$ 80% in the first 15

minutes in comparison to more than 95% for co-cryomilled felodipine-HPMC and felodipine-Soluplus in the first 15 minutes. The dissolution rate for co-cryomilled felodipine-HPMCAS starts to increase slowly until the percentage of drug release become 96% after 6 hours dissolution. The dissolution rate from co-cryomilled felodipine-PMMA (water insoluble polymer) is much lower than the other polymers or even the cryomilled felodipine. The percentage release starts from 46% and after 6 hours it becomes only 61%. It was reported previously that the release of indomethacin under sink conditions from water insoluble polymer such as ethylcellulose was retarded [284]. It is clear from the data in our study that the dissolution rate from water soluble polymer is much quicker than the pH-dependent polymer HPMCAS and is much slower if the polymer is water insoluble polymer such as PMMA.

Co-cryomilling with polymer mixes can be seen in Figure 4.1 which shows that the percentage release from the polymer mixes is high for all three polymer mixes that are used in this study. The dissolution rate of both felodipine-HPMC/HPMCAS and felodipine-HPMC/PMMA started slow (the percentage release not more than 58%) in the first 15 minutes. Then the percentage release became $\simeq$ 100% after 6 hours dissolution. Whereas, the co-cryomilled felodipine-Soluplus/HPMCAS system dissolution rate was higher than the two mentioned mixtures (the percentage release is 83%) in the first 15 minutes of the dissolution then the % release became 91% after 6 hours dissolution. Karavas *et al* studied the percentage release of felodipine from water soluble polymer (PVP) prepared by solvent evaporation under sink conditions by using different drug loadings. They found that the percentage release of felodipine from 50:50 mixture felodipine:PVP and felodipine:PEG after 20 minutes is less than 10% [280] and it became around 80% and 70% for PVP and PEG respectively after 100 minutes. However, in all our mixtures the percentage release of felodipine is higher except from the water insoluble polymer PMMA. Karavas *et al* found that the dissolution rate of felodipine becomes higher with decreasing drug loading. They get the highest percentage release only (for 10-20% felodipine loading) after 100 minutes dissolution. They correlate the low percentage release of felodipine from their study at high drug loading with the dominant mechanism of the

drug release which is dissolution (drug-dependent) which might be affected by factors related to felodipine itself such as particle size. Furthermore they thought that high drug loading (high amount of hydrophobic drug felodipine) results in poor wettability of the solid dispersion [280]. However our experiments showed that the dissolution rate of felodipine is high even at relatively high drug loading. Mixing of water insoluble polymer and pH-dependent polymer retards the dissolution rate at the beginning in comparison to the dissolution from the water soluble polymers (HPMC and Soluplus). Then dissolution rate increased gradually and the percentage of the drug release became 92% after 6 hours dissolution.

4.4.2 Effect of Soluplus concentration on the release from co-cryomilled mixture

As the percentage release of felodipine from water soluble polymer (HPMC and Soluplus) is high from the first 15 minutes dissolution, then these polymers should be the most favourite for further study. Felodipine-Soluplus mixture showed a very good stability at low humid conditions 25 °C/0 % RH from Chapter 3 while Felodipine-HPMC was unstable. In addition, Soluplus is a nonionic polymer thus its solubility does not change along the GI tract. It is slightly surface active and hence it is useful to maintain supersaturation of poorly soluble drugs in the gastrointestinal tract [285]. For all these reasons felodipine-Soluplus will be the selected mixture for further investigations before formulation. Felodipine-Soluplus mixture were selected with two additional drug loadings which are 10% and 75% to study the release of felodipine from co-cryomilled mixture as seen in Figure 4.2. Starting with 75% drug loading, it can be seen the % release started $\simeq$ 65% within first 15 minutes then there was a gradual increase in the % release until it reaches 98% after 6 hours dissolution. This release profile is similar but slightly higher than the release of cryomilled felodipine alone. At 50%, the % release became 98% after 15 minutes drug release which is faster than the % release from 75% felodipine loading and remains high after 6 hours dissolution. Further increases in Soluplus concentration (10%

drug loading) resulted in slowing the drug dissolution rate in comparison to 50% and 75% loading. The percentage release became about 82% after 6 hours dissolution. It was previously reported that increasing the concentration of Soluplus results in retardation of celecoxib-Soluplus freeze dried mixture [286]. The authors correlate that with formation of a viscous layer with increasing Soluplus concentration around drug particles that results in retarding the drug release according to the opinion of the researchers in references [286, 287]. For this reason 50% drug loading is preferred for immediate release formulation as it gave the highest dissolution rate within short period of time while higher Soluplus concentration is preferred in the modified release formulation that gave both protection from recrystallisation and retardation of the drug release.

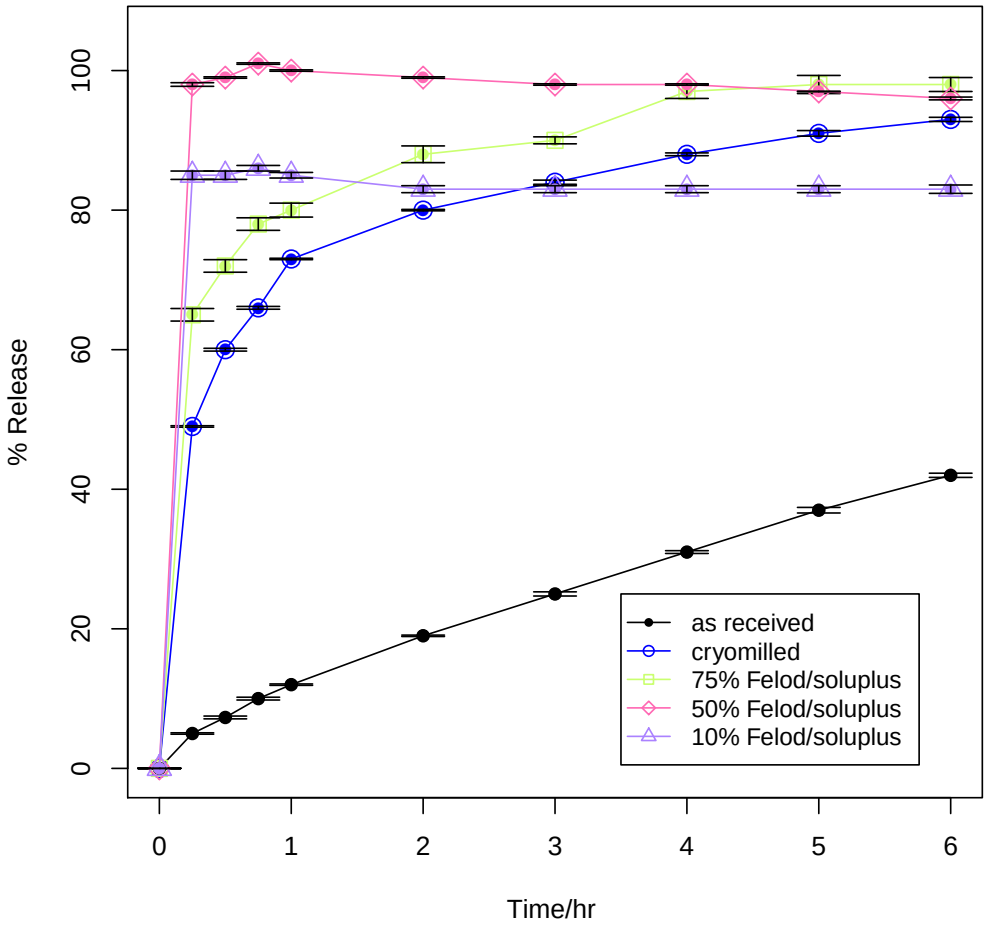

Figure 4.2: The release profile of felodipine as received, cryomilled for 150 minutes and cryomilled together with Soluplus at 50% drug loading (n=3).

4.4.3 Comparison of felodipine release from co-cryomilled mixture by different method of preparation

Co-cryomilling with polymer is a new approaches for production of solid dispersions method. For this reason it is useful to make a comparative study with other methods that are currently used in production of amorphous solid dispersions

such as HME. The release profile from both methods was compared using the same polymer; Soluplus. Figure 4.3 shows a comparative study between the percentage release of felodipine from Soluplus via both cryomilling and HME. It can be seen that the dissolution rate of felodipine from HME starts slightly slower than the dissolution rate from the co-cryomilled felodipine-Soluplus then both release becomes identical around 3 hours dissolution. After 3 hours, the dissolution rate from HME slightly increases and the co-cryomilled one was slightly lower than the initial release. At the end there is not so much difference between the percentage release form both methods as they are showing 97-104% drug release after 6 hours dissolution. It can be concluded that the co-cryomilling method produces a similar drug release profile to HME in at least in our study here with Soluplus at 50% drug loading.

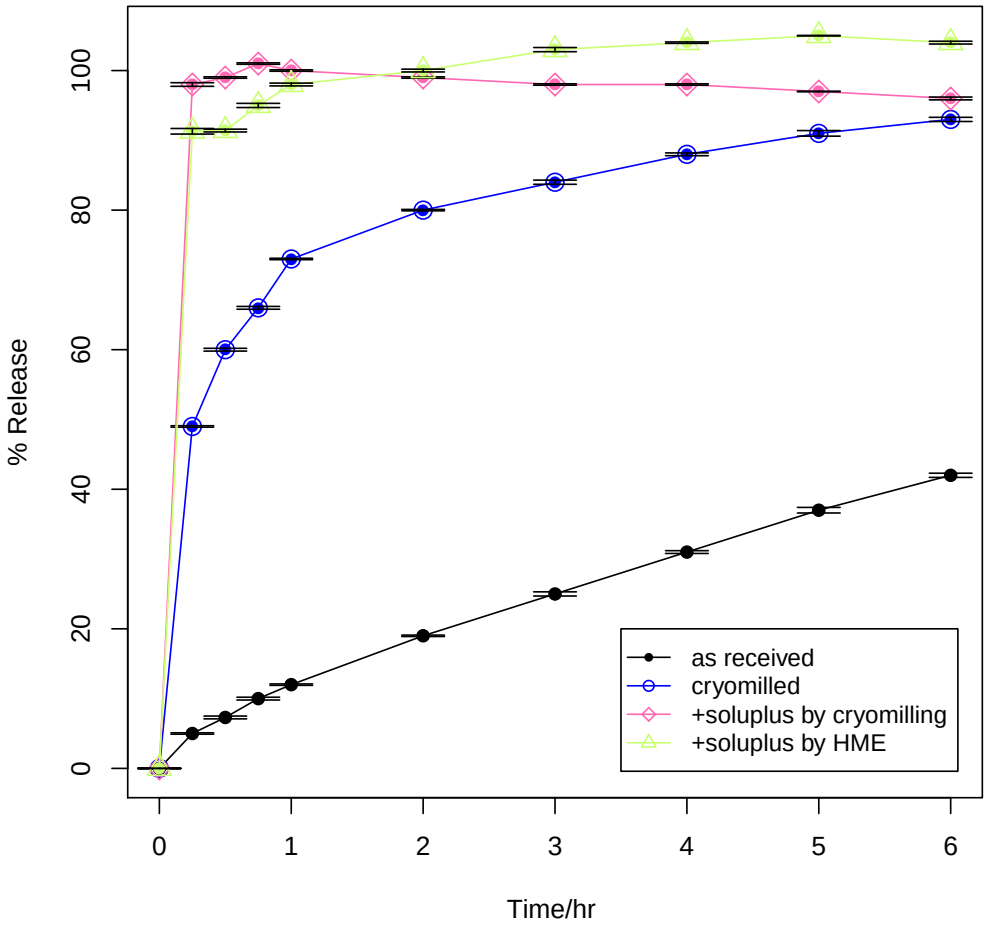

Figure 4.3: The release profile of felodipine as received and felodipine+Soluplus at 50% drug loading cryomilled and HME (n=3).

4.5 Conclusion

It can be concluded that with co-cryomilling it was possible to get the optimum release with high felodipine loading (50%) when it was reported to be difficult as felodipine will be the controller of the release. The release of felodipine from Soluplus is not much different from that one that applied widely by the manufactures which is HME in addition to its stability in low humid conditions.

For this reason this mixture will be selected to be formulated into a rapid release dosage form in the next Chapter 5 as ODTs dosage form.

Chapter 5

Can a practically water insoluble drug be formulated as fast acting medicine via co-cryomilling?

5.1 Novelty in this Chapter

First formulation of ODTs from the co-cryomilled dispersion.

5.2 Introduction

Felodipine is in the dihydropyridines class of the selective calcium channel blocker. Other drugs of calcium channel blockers include amlodipine, diltiazem, nicardipine, nifedipine, nisoldipine, verapamil etc. It is used for its vasodilation effect mainly for arterial hypertension. It is an important drug among other hypertensive drugs during emergency due to lack of negative inotropic effect (not affecting heart rate or contraction) [288, 289]. It was reported that more than 90% of the patient responded appropriately to felodipine infusion [140, 142, 143, 290].

Although felodipine has a vital role in the emergency treatment via infusion,

this drug is practically insoluble orally and classified under class II Biopharmaceutical Classification System (BCS). The only oral dosage form in the market is the prolonged-release one (Plendil®) [291]. To achieve fast action for class II there are different methods to enhance the solubility and/or dissolution rate as discussed in the introduction chapter in the thesis. Among these methods is the amorphous solid dispersions.

An ODTs is a solid oral dosage form that disintegrate in the mouth cavity rapidly to allow the drug releasing directly from the site of absorption [290]. ODTs disintegrate in the mouth cavity with not more than 3 minutes which ensures rapid onset of action and avoidance of hepatic first pass effects. All these advantages make this dosage form comfortable and convenient delivery route in comparison to the intravenous route [130, 131, 135–137, 143, 292, 293]. There is no requirement for chewing or drinking water with this dosage form which is important for patients whom suffer from swallowing difficulties such as paediatric and geriatric patients or patients with dysphagia and unconcious patients [131–134, 294]. The active ingredient should be soluble in this type of dosage form therefore it should be palatable in order to increase patient compliance [132, 292].

Many processing methods are used in manufacturing of ODTs such as lyophilization, moulding, cotton candy processes and direct compression [145, 295]. Direct compression is most favourable over other methods because of its low cost, time saving and simple technologies machines [131, 296]. The main hurdle in the direct compression technique is the selection of suitable excipients that can fit the disintegration time requirement [133].

One of the methods mentioned in the introduction chapter must be applied to increase solubility and/or dissolution of poorly water soluble drug must applied prior to formulation as ODTs. The most commonly used method as reported in the literature is the amorphous solid dispersion via HME and spray drying such as iboprofen by HME [132], compound X by HME with PVP, Soluplus and HPMCAS at 33% drug loading [297], HME nimodipine in PVP and Eudragit [298], mefenamic acid by hot melt extrusion with Eudragit [299], nisoldipine by spray

drying with different polymers such as PVP, HPMC, Pluronic and PEG [300] and risperidone with cyclodextrin by solvent evaporation method [292]. There is currently no fast acting formulation of felodipine despite there being a clinical need. To ensure rapid release of felodipine from the formulation, then orally disintegrating tablets or (ODTs) can potentially be utilised to get rapid onset of action.

This is the first study that involves formulation of felodipine via co-cryomilling with Soluplus into ODTs with relatively high drug loading (50%) as an amorphous solid dispersions. There are only two reported works for formulations of felodipine as ODTs by spray drying and liquid-solid formulation. One of them involves formulation of felodipine with HPMC through spray drying method [143] which composed of felodipine:HPMC ratio of 1:3. The other reported work is the formulation of felodipine into ODTs via liquid-solid medication formulation with PEG and PG [142]. The methods reported before tend to increase the solubility of felodipine in the GI tract. These studies focus on the formulation using limited superdisintegrants types and there is no preformulation stability test which is essential for drugs like felodipine in the amorphous solid dispersions. Therefore, felodipine:Soluplus (1:1) co-cryomilled mixture (from Chapter 3 and 4 this mixture is stable at 25 °C/0% RH and it gives 100% felodipine release) will be used in the formulation of ODTs in the present piece of work. This not only increases solubility but also increases the dissolution rate of felodipine via co-cryomilling. Furthermore, our study was involved from Chapter 3 and 4 a full preformulation study before starting formulation into ODTs. Six types of superdisintegrants were used to ensure a rapid disintegration time in this study. Superdisintegrants act either by absorbing water and the subsequent swelling leads to separation of the tablet particles [132] or disintegrants acts due to their high porosity thorough wicking via capillary action. Subsequently, water is rapidly absorbed and disrupts tablets matrix bonds which results in the tablets falling apart [132].

In our study all the official and non official test for tablets will be performed. The disintegration time and the dissolution of felodipine from these formations

were evaluated according to the USP requirements for ODTs. The release from the physical mixture of felodipine:Soluplus for all formulations were compared to the co-cryomilled one by using the standard USP II dissolution method. It was reported that release from the ODTs in the pregastric route occurs but it was varied from on patients to another depends on how long time the tablet stays in the patient mouth before its swallowing . Therefore to guarantee that almost all the drug was released within short period of time, the release study was performed with 0.1 N HCl [301].

5.3 Materials and Methods

5.3.1 Materials

Sodium dodecyl sulfate was purchased from Acros Organics (Spain). Glycolate (Na starch glycolate) is kindly donated from Roquette (UK) company, F-melt (D-mannitol 66.7%, xylitol 4.6%, micro crystallinecellulose 14%, crospovidone 7.9%, magnesium aluminometasilicate 6.2%) was kindly donated form Fuji Chemical Industry (Japan), Kollidon CL (polyvinylpyrrolidone, crosslinked) was kindly donated from BASF company (Germany), Polyplasdone XL (crospovidone) was kindly donated from Ashland company (Netherlands), Prosolv (microcrystalline cellulose 21.6%, colloidal silicon dioxide 2%, mannitol 67.3%, fructose 4.9%, crospovidone 4.3%) was kindly donated from JRS (Germany), Vivasol (corscarmellose Na) was purchased from JRS (Germany), spray dried lactose was kindly donated donated from Foremost Frams (USA), colloidal silicon dioxide was purchased from Sigma (Germany) and magnesium stearate was purchased from Sigma Aldrich (USA).

5.3.2 Cryomilling

Cryomilling same as in Chapter 2

5.3.3 Release study

The dissolution study followed the ODTs dissolution test according to the the United States Pharmacopeia (USP) by using type II apparatus at 50 rpm (Erweka Dissolution Tester) in 0.1 N HCl containing 1% SDS to ensure sink conditions. The volume of the dissolution media was 500 mL. Dissolution media was maintained at 37 °C and a paddle speed of 50 rpm [302] was employed for 10 minutes. The HPLC method was performed the same as in Section 2.3.7. There is no special official requirement that applied to all drugs dissolution but the the method and time of dissolution was taken for some drugs such as risperidone and ondansetron in which not less than 80% of the drug should be released within 10 minutes. Some drugs disintegration time in USP is within 6 minutes such as loratidine and others longer to 30 minutes such as ibuprofen.

5.3.4 Tablet compression

Blends containing cryomilled 1:1 felodipine:Soluplus was mixed with other excipients at 0.8% drug loading (2.5 mg felodipine in 300 mg tablet). The therapeutic dose of felodipine is between 2.5-10 mg once daily. A different formulations containing felodipine:Soluplus, spray dried lactose, silicon dioxide and 6 different types of superdisintegrants were used to prepare 6 different formulations (sieved through a 425 μm screen to facilitate the content uniformity). The formulations all listed in Tablet 5.1. 60 g batches were prepared in the turbo blender (blended for 10 minutes), then lubricant (1% magnesium stearate) was added and mixed for 2 minutes. The tablets were compressed by using standard concave punches on an instrumented Piccola multi-station press (Riva S.A., Argentina) using 8 mm flat, round tooling (I. Holland, Nottingham, UK) to a target mass of 300 mg, to prepare tablets between 4 and 12 kN compression force.

Table 5.1: The composition of each formulation in mg

Formulas	felodipine:soluplus (1:1)	superdisintegrants	spray dried lactose	colloidal silicon dioxide	magnesium stearate	total weight in mg
F1/Kollidon CL	5	15	271	6	3	300
F2/Vivasol	5	60	226	6	3	300
F3/Polyplasdone XL	5	30	256	6	3	300
F4/Glycolate	5	15	271	6	3	300
F5/F-melt	5	292	-	-	3	300
F6/Prosolv	5	240	52	-	3	300

5.3.5 Disintegrations time

Six tablets were immersed in the distilled water to determine the disintegration time by using the USP disintegration apparatus (Erweka, ZT43, Heusenstamm, Germany) at 37$\pm$0.5°C. The time required for complete disintegration of the six tablets (no or rare solid residue on the screen) is then considered as the disintegration time.

5.3.6 Weight variation

According to the European pharmacopoeia twenty tablets were selected from each formulation. The weight of each tablet was taken and the mean of all tablets were calculated.

5.3.7 Content uniformity

The content uniformity test was performed according to the USP procedure for felodipine tablets. Ten tablets were selected from each formulation. Each tablet was added into to a 100-mL volumetric flask, then 40 mL of acetonitrile added to it. The mixture was sonicated for 20 minutes. 20 mL of methanol was then added to the mixture, and shaken by mechanical means for 30 minutes. The mixture was then diluted with water to the required volume, and mixed. The

mixture was then centrifuged at high speed for 15 minutes. The supernatant was then diluted with water to obtain a solution containing 20 μL of felodipine per mL which was then analysed by HPLC. The HPLC method used was given in Section 5.3.3.

5.3.8 Hardness

Tablet hardness was performed by a hardness tester (Holland C50, U.K.). Three tablets from each formulation were selected.

5.3.9 Friability

This test was carried out by taking twenty tablets from each formulation and weighing them. These tablets were then placed into the friabilator drum (Erweka type, GmbH, Germany). The rotation speed was fixed at 25 rpm for 4 minutes. The tablets were weighed again after removing the dust and the percentage of the weight lost was calculated which should be not more than 1% for the batch to be accepted.

5.4 Results and discussion

5.4.1 Effect of compression force on tablets hardness

Figure 5.1 shows the effect of compression force on the hardness of the six formulations. The compression force that was applied is between 4-12 kN. In all cases increasing the compression force leads to an increase in the resulting tablets hardness. There are no obvious discontinuities in any of the the plots. For the maximum compression force of 12 kN, five of the formulations exhibited hardnesses of 15-21 kP, with one (Vivasol) only achieving 5 kP under the same conditions. It was previously reported that increasing the compression force results in increasing the hardness of ibuprofen ODTs that containing Vivasol, Polyplasdone XL and Kollidon [132].

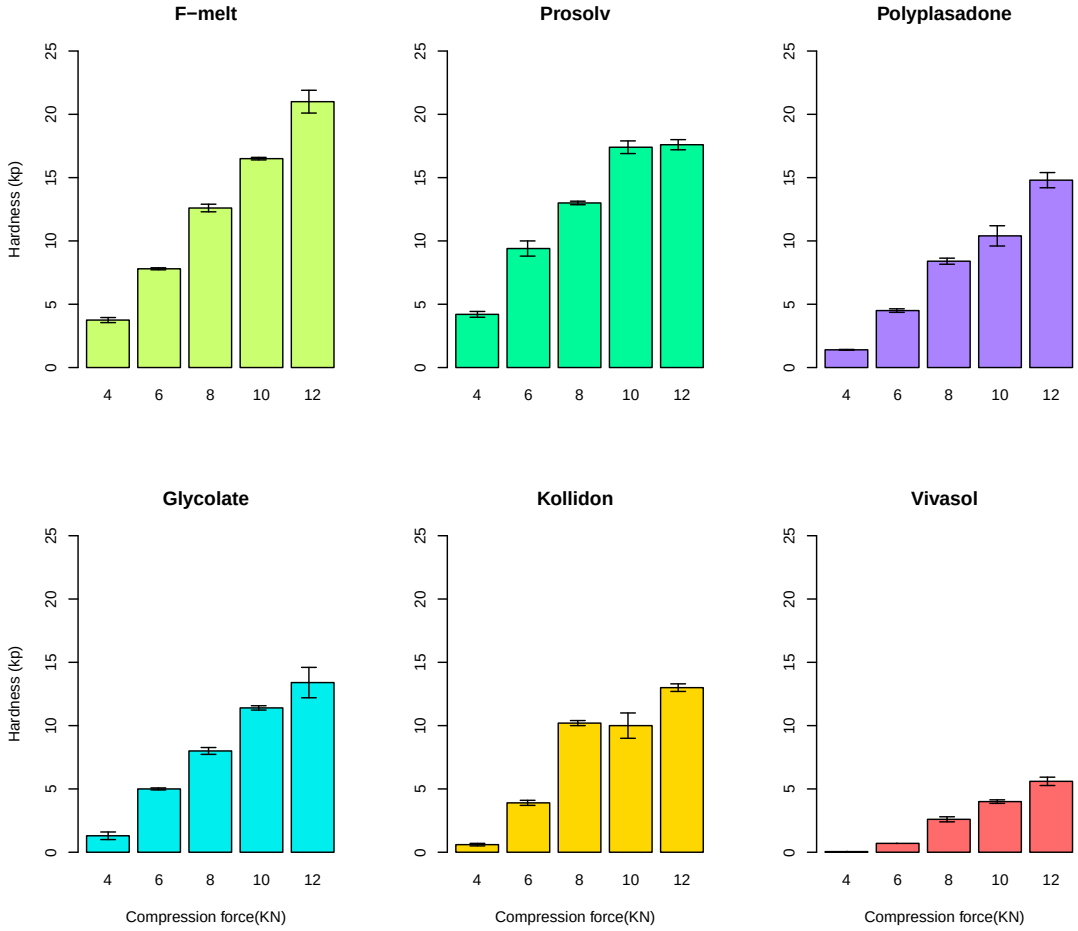

Figure 5.1: Schematic diagram of ODTs hardness at various compaction forces for all formulations.

5.4.2 Effect of compression force on the tablets friability

Figure 5.2 shows the effect of compression force on the tablets friability. All formulations at 4 kN compression force were friable and failed to pass the friability test. Increasing compression force to 6 kN only Polyplasdone XL and Vivasol were failed. At 8 and 10 kN all formulations passed the friability test except Vivasol. Finally at 12 kN all formulations passed the friability test in which the % of drug loss after the test should be less than 1%.

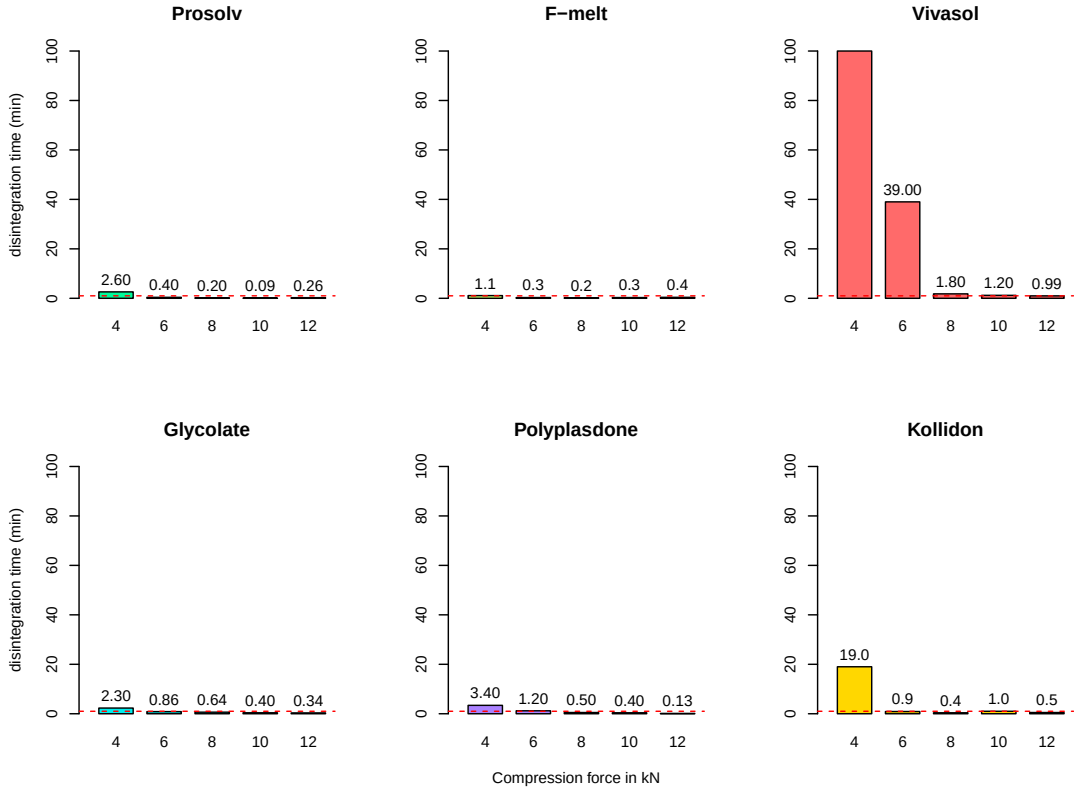

Figure 5.2: Schematic diagram of ODTs % friability at various compaction forces for all formulations. Red line represents the USP requirements for the tablets to accept the batch.

5.4.3 Effect of the compression force on the disintegration time

Figure 5.3 shows the effect of compression force on the disintegration time for all formulations. It is clearly seen that by increasing the compression force for Prosolve and Polyplasdone containing formulations results in an increase of the disintegration time. For Prosolve formulation the accepted disintegration time according to EP was until 6 kN compression force where it exhibits 3.39 minutes while for F-melt formulation the accepted disintegration time is until 8 kN compression force where it displays 1.35 minutes. It has been reported previously that increasing the compression force for ibuprofen ODTs formulated with F-melt as superdisintegrant results in increasing in the disintegration

time [133]. For Vivasol formulation increasing compression force resulted in no significant increase in the disintegration time and all compression forces applied leads to accepted disintegration time which is less than 3 minutes. For Glycolate, Polyplasdone and Kollidon formulations increasing the compression force minimally increases disintegration time which stayed below the EP stranded as it was between 15-50 seconds. This is comparable to the reported disintegration time for mefenamic acid ODTs (27 seconds) that were formulated with Polyplasdone that compressed at 4 kN and prepared by HME with Eudragit [299]. It was also comparable with felodipine ODTs prepared by spray drying method with HPMC by using Polyplasdone (28 seconds) [143]. The disintegration time of risperidone ODTs prepared by direct compression method by using spray drying method was reported to be 37 seconds [292]. Tablets in that study were formulated with Kollidon as superdisintegrant at minimum compression force nearly 2.4 kN [292]. From our results it can be concluded that F-melt and Prosolv containing tablets were the only formulations that affected by the compression force while other formulations were not.

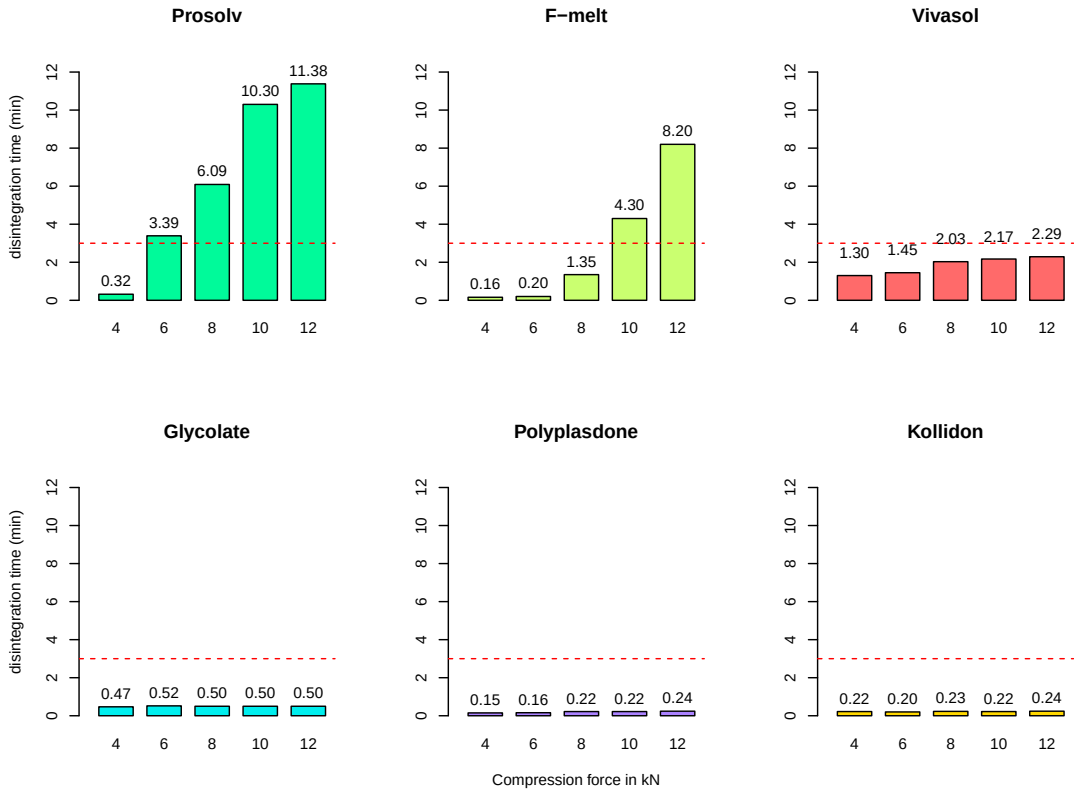

Figure 5.3: Schematic diagram of ODTs disintegration time at various compaction forces for all formulations. Red line represents the EP requirements for ODTs to be accepted.

5.4.4 Content uniformity

All formulations passed the content uniformity test in which no tablet above or below 85%-115% of the amount of felodipine that should be available.

5.4.5 Release from different formulations

Figure 5.4 shows the release results under sink conditions for all formulations containing felodipine-Soluplus physical mixture and co-cryomilled mixture. All co-cryomilled formulations shows higher release in comparison to the physical mixture after 10 minutes dissolution. Physical mixture formulations exhibited %

release between 31-64% which is lower than the USP threshold of 80%. However all co-cryomilled formulations exhibited % release between 76-94% which is around or higher than 80% as seen in Figure 5.5. The dissolution results from the our co-cryomilled formulations are comparable to previously reported work for ODTs felodipine containing Prosolv as superdisintegrant after 10 minutes dissolution in water [142] and comparable to felodipine release from ODTs prepared by solvent evaporation method with HPMC (1:1) by using Polyplasdone XL as superdisintegrant to get 80% release after 15 minutes dissolution [143].

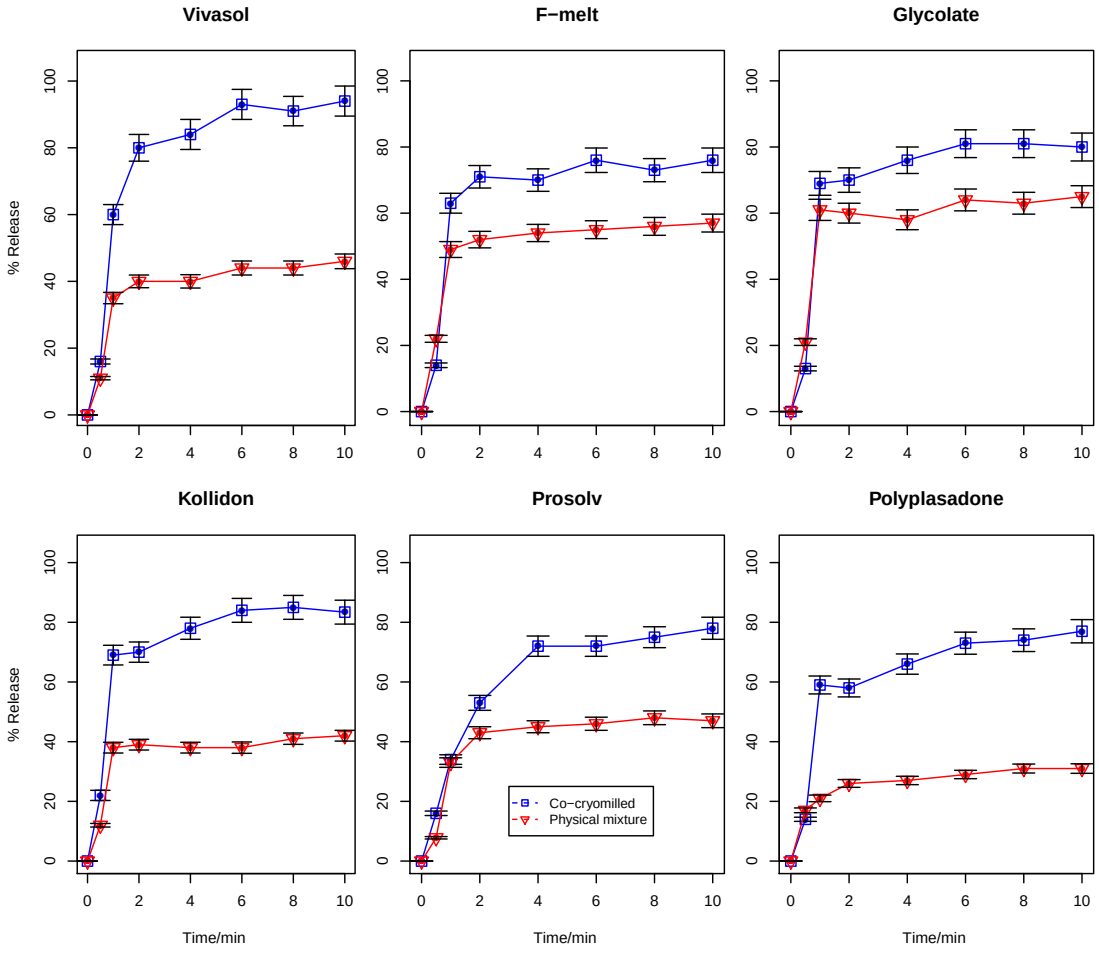

Figure 5.4: The release profile of felodipine form the physical mixtures and from co-cryomilled mixtures from different formulations by using different superdisintegrants (n=3).

To summarise all co-cryomilled ODTs formulations results, Figure 5.5 shows the

comparative study among the co-cryomilled mixtures which Vivasol containing formulation was the highest % release about 94% amongst the formulations. The formulation that contains F-melt shows the lowest % release which is about 76%.

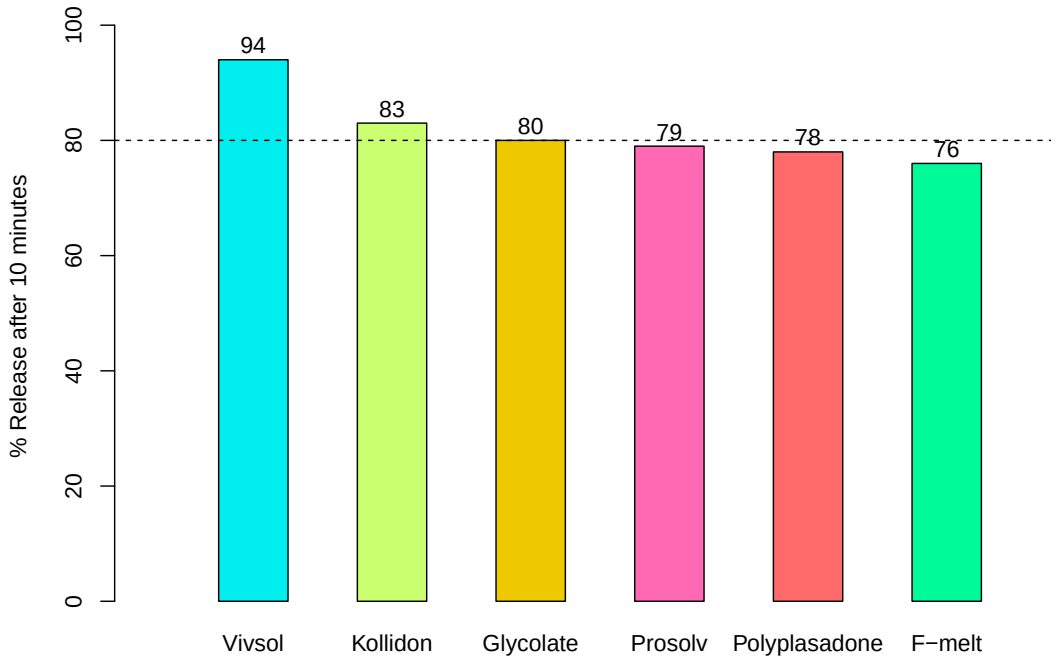

Figure 5.5: The cumulative release of felodipine form different formulations by using different superdisintegrants. Black line represents the USP accepted limit for the release from ODTs.

5.5 Conclusion

For the first time, ODTs can be made that satisfy the pharmacopoeia, for which cryomilling is an essential formulation step, at least for the six different formulations studied. The different in the release behaviour of felodipine from the physical mixture versus the co-cryomilled mixture is notably greater. The rapid onset of action due to the short disintegration time for felodipine ODTs via co-cryomilling can solve a geriatric or unresponsive patients problems to get

benefit from this dosage form in the emergency which could save their life.

The good friability, flowability (from good content uniformity) of the powder, disintegration and dissolution time according to USP lead us to put felodipine for further investigation such as *in vivo* test for future work to complete all the formulations requirements test for the ODTs. Other polymers that were used in our study in Chapter 3 for preparation of co-cryomilled dispersions can be formulated as ODTs in future to investigate their effect on the disintegration time and to evaluate felodipine release. In addition future work should involve the palatability of the formulation to increase the patient acceptance which is essential in this type of formulation.

Chapter 6

Conclusion and future prospects

6.1 Conclusion

Amorphous material from three different APIs (felodipine, paracetamol and aspirin) by co-cryomilling with HPMC was obtained. No degradation was observed from these three drugs by this method. There is no evidence for formation a H-bond between these drugs with HPMC and all drugs showed a poor miscibility with HPMC as the T_g showed no or slight increase with increasing HPMC concentrations. The % release of three selected drugs was either improved or not affected. All drugs formed amorphous solid dispersion but at different ratios. There was a variation in the amount of HPMC required for stabilisation of the solid dispersions formed. Felodipine was stable at 25% drug loading while both paracetamol and aspirin were stable only at 5% drug loading during the storage period.

Felodipine-Soluplus co-cryomilled mixture showed the best miscibility as it is the only mixture that displays only one T_g in all concentrations and the T_g value is comparable to that one estimated from Gordon-Taylor equation. It is stable under mild storage condition at 25 °C/0% RH but cannot withstand humid conditions for which it showed a clear sign of recrystallisation by XRPD. Other co-cryomilled mixture showed a partial miscibility with certain concentrations and their ranking criteria are mainly the hydrophobicity of the polymer and

the H-bond propensity(from CSD analysis) to be stable against the harshest conditions. Therefore felodipine-PMMA is the best regarding to the stability while felodipine-HPMC is the worst.

The release from all co-cryomilled mixture under sink conditions is high except for felodipine-PMMA mixture. All mixtures showed % release above 90% after 6 hours dissolution except felodipine-PMMA. By comparing the release in the first 15 minutes both felodipine-HPMC and felodipine-Soluplus give above 90% release within this time. Co-cryomilled felodipine-Soluplus mixtures showed no clear difference in the percentage release compared to one made by currently used HME procedure for production of amorphous solid dispersion. Felodipine-Soluplus co-cryomilled mixture was selected as the mixture to be added to the six different ODTs formulations that were designed to deliver fast onset of felodipine release. Six different types of superdisintegrant were used. The results from the official and non-official test was accepted and met the relevant pharmacopeial requirement.

The co-cryomilling approach for production of amorphous solid dispersion is attractive as neither heat nor solvent are used. Both particle size reduction and amorphous formation can solve the main problems in class II drugs which are either dissolution or solubility issue in which other techniques offer only one of these solutions. These two advantages enable the application of cryomilling for variable APIs.

6.2 Future Prospects

- The co-cryomilling approach can be potentially applied to other dosage forms including: nasal, transdermal, ocular etc. to investigate how widely applicable this approach is. Furthermore the effect of cryomilling on the permeability of the APIs should be studied with various route of drug administration because it might be the rate-limiting step.
- A realistic *in vivo* dissolution test can be applied for the manufactured

felodipine ODTs.

- A practically water insoluble drug felodipine could be formulated as fast acting dosage form using cryomilling. This technology can be applied for another essential medication during the emergency such as asthma, hypertension, angina etc. that might save a patients life.

References

[1] ME Aulton and K MG Taylor. *Aulton's pharmaceutics: the design and manufacture of medicines*. Elsevier Health Sciences, 2007.

[2] JM Butler and JB Dressman. The developability classification system: application of biopharmaceutics concepts to formulation development. *Journal of Pharmaceutical Sciences*, 99(12):4940–4954, 2010.

[3] T Feng, R Pinal, and MT Carvajal. Process induced disorder in crystalline materials: Differentiating defective crystals from the amorphous form of griseofulvin. *Journal of Pharmaceutical Sciences*, 97(8):3207–3221, 2008.

[4] N Wyttenbach and M Kuentz. Glass-forming ability of compounds in marketed amorphous drug products. *European Journal of Pharmaceutics and Biopharmaceutics*, 112:204–208, 2017.

[5] SRK Vaka, MM Bommana, D Desai, J Djordjevic, W Phuapradit, and N Shah. Excipients for amorphous solid dispersions. In *Amorphous Solid Dispersions*, pages 123–161. Springer, 2014.

[6] K J Edgar. Cellulose esters in drug delivery. *Cellulose*, 14(1):49–64, 2007.

[7] JT Schiele, R Quinzler, H Klimm, MG Pruszydlo, and WE Haefeli. Difficulties swallowing solid oral dosage forms in a general practice population: prevalence, causes, and relationship to dosage forms. *European Journal of Clinical Pharmacology*, 69(4):937–948, 2013.

[8] A Newman, G Knipp, and G Zografi. Assessing the performance of amorphous solid dispersions. *Journal of Pharmaceutical Sciences*, 101(4):1355–1377, 2012.

[9] GZ Zhang, D Law, EA Schmitt, and Y Qiu. Phase transformation considerations during process development and manufacture of solid oral dosage forms. *Advanced Drug Delivery Reviews*, 56(3):371–390, 2004.

[10] N J Babu and A Nangia. Solubility advantage of amorphous drugs and pharmaceutical cocrystals. *Crystal Growth & Design*, 11(7):2662–2679, 2011.

[11] S Stegemann, F Leveiller, D Franchi, H De Jong, and H Lindén. When poor solubility becomes an issue: from early stage to proof of concept. *European Journal of Pharmaceutical Sciences*, 31(5):249–261, 2007.

[12] GL Amidon, H Lennernäs, VP Shah, and JR Crison. A theoretical basis for a biopharmaceutic drug classification: the correlation of in vitro drug product dissolution and in vivo bioavailability. *Pharmaceutical Research*, 12(3):413–420, 1995.

[13] G Sandri, MC Bonferoni, F Ferrari, S Rossi, and CM Caramella. The role of particle size in drug release and absorption. In *Particulate Products*, pages 323–341. Springer, 2014.

[14] DP Elder, R Holm, and HL De Diego. Use of pharmaceutical salts and cocrystals to address the issue of poor solubility. *International Journal of Pharmaceutics*, 453(1): 88–100, 2013.

[15] T Taupitz, JB Dressman, CM Buchanan, and S Klein. Cyclodextrin-water soluble polymer ternary complexes enhance the solubility and dissolution behaviour of poorly soluble drugs. case example: itraconazole. *European Journal of Pharmaceutics and Biopharmaceutics*, 83(3):378–387, 2013.

[16] H Mu, R Holm, and A Müllertz. Lipid-based formulations for oral administration of poorly water-soluble drugs. *International Journal of Pharmaceutics*, 453(1):215–224, 2013.

[17] G Singh, S Sharma, and GD Gupta. Extensive diminution of particle size and amorphization of a crystalline drug attained by eminent technology of solid dispersion: a comparative study. *American Association of Pharmaceutical Scientists*, pages 1–15, 2016.

[18] AF Rumondor, SS Dhareshwar, and F Kesisoglou. Amorphous solid dispersions or prodrugs: complementary strategies to increase drug absorption. *Journal of Pharmaceutical Sciences*, 105(9):2498–2508, 2016.

[19] R Ho, SE Dilworth, DR Williams, and JY Heng. Role of surface chemistry and energetics in high shear wet granulation. *Industrial & Engineering Chemistry Research*, 50(16):9642–9649, 2011.

[20] A Krupa, M Descamps, J Willart, R Jachowicz, and F Danède. High energy ball milling and supercritical carbon dioxide impregnation as co-processing methods to improve dissolution of tadalafil. *European Journal of Pharmaceutical Sciences*, 95: 130–137, 2016.

[21] J Jinno, N Kamada, M Miyake, K Yamada, T Mukai, M Odomi, H Toguchi, GG Liversidge, K Higaki, and T Kimura. Effect of particle size reduction on dissolution and oral absorption of a poorly water-soluble drug, cilostazol, in beagle dogs. *Journal of Controlled Release*, 111(1):56–64, 2006.

[22] SM Wong, IW Kellaway, and S Murdan. Enhancement of the dissolution rate and oral absorption of a poorly water soluble drug by formation of surfactant-containing microparticles. *International Journal of Pharmaceutics*, 317(1):61–68, 2006.

[23] A TM Serajuddin. Salt formation to improve drug solubility. *Advanced Drug Delivery Reviews*, 59(7):603–616, 2007.

[24] SL Childs, GP Stahly, and A Park. The salt-cocrystal continuum: the influence of crystal structure on ionization state. *Molecular Pharmaceutics*, 4(3):323–338, 2007.

[25] H Gwak, J Choi, and H Choi. Enhanced bioavailability of piroxicam via salt formation with ethanolamines. *International Journal of Pharmaceutics*, 297(1):156–161, 2005.

[26] DJ Good and N Rodriguez-Hornedo. Solubility advantage of pharmaceutical cocrystals. *Crystal Growth and Design*, 9(5):2252–2264, 2009.

[27] M Jung, J Kim, M Kim, A Alhalaweh, W Cho, S Hwang, and SP Velaga. Bioavailability of indomethacin-saccharin cocrystals. *Journal of Pharmacy and Pharmacology*, 62(11):1560–1568, 2010.

[28] SL Childs, P Kandi, and SR Lingireddy. Formulation of a danazol cocrystal with controlled supersaturation plays an essential role in improving bioavailability. *Molecular Pharmaceutics*, 10(8):3112–3127, 2013.

[29] T Loftsson and ME Brewster. Pharmaceutical applications of cyclodextrins. 1. drug solubilization and stabilization. *Journal of Pharmaceutical Sciences*, 85(10): 1017–1025, 1996.

[30] ME Brewster and T Loftsson. Cyclodextrins as pharmaceutical solubilizers. *Advanced Drug Delivery Reviews*, 59(7):645–666, 2007.

[31] CW Pouton. Formulation of poorly water-soluble drugs for oral administration: physicochemical and physiological issues and the lipid formulation classification system. *European Journal of Pharmaceutical Sciences*, 29(3):278–287, 2006.

[32] CM O'driscoll and BT Griffin. Biopharmaceutical challenges associated with drugs with low aqueous solubility-the potential impact of lipid-based formulations. *Advanced Drug Delivery Reviews*, 60(6):617–624, 2008.

[33] B Testa. Prodrug research: futile or fertile? *Biochemical Pharmacology*, 68(11): 2097–2106, 2004.

[34] CE Müller. Prodrug approaches for enhancing the bioavailability of drugs with low solubility. *Chemistry & Biodiversity*, 6(11):2071–2083, 2009.

[35] BC Hancock and G Zografi. Characteristics and significance of the amorphous state in pharmaceutical systems. *Journal of Pharmaceutical Sciences*, 86(1):1–12, 1997.

[36] M Descamps and JF Willart. Perspectives on the amorphisation/milling relationship in pharmaceutical materials. *Advanced Drug Delivery Reviews*, 100:51–66, 2016.

[37] NS Trasi, SX Boerrigter, and SR Byrn. Investigation of the milling-induced thermal behavior of crystalline and amorphous griseofulvin. *Pharmaceutical Research*, 27 (7):1377–1389, 2010.

[38] Y Lin, RP Cogdill, and PLD Wildfong. Informatic calibration of a materials properties database for predictive assessment of mechanically activated disordering

potential for small molecule organic solids. *Journal of Pharmaceutical Sciences*, 98 (8):2696–2708, 2009.

[39] JF Willart and M Descamps. Solid state amorphization of pharmaceuticals. *Molecular Pharmaceutics*, 5(6):905–920, 2008.

[40] TN Drebushchak, AA Ogienko, and EV Boldyreva. 'hedvall effect'in cryogrinding of molecular crystals. a case study of a polymorphic transition in chlorpropamide. *Crystal Engineer Communication*, 13(13):4405–4410, 2011.

[41] KJ Crowley and G Zografi. Cryogenic grinding of indomethacin polymorphs and solvates: assessment of amorphous phase formation and amorphous phase physical stability. *Journal of Pharmaceutical Sciences*, 91(2):492–507, 2002.

[42] VV Boldyrev. Mechanochemistry and mechanical activation of solids. *Russian Chemical Reviews*, 75(3):177, 2006.

[43] M Descamps, JF Willart, E Dudognon, and V Caron. Transformation of pharmaceutical compounds upon milling and comilling: The role of tg. *Journal of Pharmaceutical Sciences*, 96(5):1398–1407, 2007.

[44] HJ Fecht. Defect-induced melting and solid-state amorphization. *Nature*, 356: 133–135, 1992.

[45] JF Willart, N Dujardin, E Dudognon, F Danède, and M Descamps. Amorphization of sugar hydrates upon milling. *Carbohydrate Research*, 345(11):1613–1616, 2010.

[46] GZ Zhang, C Gu, M T Zell, RT Burkhardt, EJ Munson, and DJW Grant. Crystallization and transitions of sulfamerazine polymorphs. *Journal of Pharmaceutical Sciences*, 91(4):1089–1100, 2002.

[47] Makoto O, Takahiro M, and Nobuyoshi K. Effect of environmental temperature on polymorphic solid-state transformation of indomethacin during grinding. *Chemical and Pharmaceutical Bulletin*, 34(4):1784–1793, 1986.

[48] S Qi, I Weuts, S De Cort, S Stokbroekx, R Leemans, M Reading, P Belton, and D Craig. An investigation into the crystallisation behaviour of an amorphous cryomilled pharmaceutical material above and below the glass transition temperature. *Journal of Pharmaceutical Sciences*, 99(1):196–208, 2010.

[49] AJ Megarry, J Booth, and J Burley. Amorphous trehalose dihydrate by cryogenic milling. *Carbohydrate Research*, 346(8):1061–1064, 2011.

[50] P Wildfong, BC Hancock, MD Moore, and KR Morris. Towards an understanding of the structurally based potential for mechanically activated disordering of small molecule organic crystals. *Journal of Pharmaceutical Sciences*, 95(12):2645–2656, 2006.

[51] J Ye and JM Schoenung. Technical cost modeling for the mechanical milling at cryogenic temperature (cryomilling). *Advanced Engineering Materials*, 6(8):656–664, 2004.

[52] IY Saleem and HDC Smyth. Micronization of a soft material: air-jet and micro-ball milling. *American Association of Pharmaceutical Scientists*, 11(4):1642–1649, 2010.

[53] Z Wojnarowska, K Grzybowska, K Adrjanowicz, K Kaminski, M Paluch, L Hawelek, R Wrzalik, M Dulski, W Sawicki, J Mazgalski, et al. Study of the amorphous glibenclamide drug: analysis of the molecular dynamics of quenched and cryomilled material. *Molecular Pharmaceutics*, 7(5):1692–1707, 2010.

[54] SP Chamarthy and R Pinal. The nature of crystal disorder in milled pharmaceutical materials. *Colloids and Surfaces A: Physicochemical and Engineering Aspects*, 331(1): 68–75, 2008.

[55] S Chattoraj, C Bhugra, C Telang, L Zhong, Z Wang, and C Sun. Origin of two modes of non-isothermal crystallization of glasses produced by milling. *Pharmaceutical Research*, 29(4):1020–1032, 2012.

[56] Y Hu, P Macfhionnghaile, V Caron, L Tajber, AM Healy, A Erxleben, and P McArdle. Formation, physical stability, and quantification of process-induced disorder in cryomilled samples of a model polymorphic drug. *Journal of Pharmaceutical Sciences*, 102(1):93–103, 2013.

[57] N Chieng, T Rades, and D Saville. Formation and physical stability of the amorphous phase of ranitidine hydrochloride polymorphs prepared by cryo-milling. *European Journal of Pharmaceutics and Biopharmaceutics*, 68(3):771–780, 2008.

[58] KA Graeser, CJ Strachan, JE Patterson, KC Gordon, and T Rades. Physicochemical properties and stability of two differently prepared amorphous forms of simvastatin. *Crystal Growth and Design*, 8(1):128–135, 2008.

[59] T Niwa, Y Nakanishi, and K Danjo. One-step preparation of pharmaceutical nanocrystals using ultra cryo-milling technique in liquid nitrogen. *European Journal of Pharmaceutical Sciences*, 41(1):78–85, 2010.

[60] V Martena, R Censi, E Hoti, L Malaj, and P Di Martino. Preparation of glibenclamide nanocrystals by a simple laboratory scale ultra cryo-milling. *Journal of Nanoparticle Research*, 15(6):1–10, 2013.

[61] T Davis, M Johnson, and SJL Billinge. Toward phase quantification at the nanoscale using the total scattering pair distribution function (tspdf) method: recrystallization of cryomilled sulfamerazine. *Crystal Growth & Design*, 13(10): 4239–4244, 2013.

[62] P Macfhionnghaile, Y Hu, K Gniado, S Curran, P Mcardle, and A Erxleben. Effects of ball-milling and cryomilling on sulfamerazine polymorphs: a quantitative study. *Journal of Pharmaceutical Sciences*, 103(6):1766–1778, 2014.

[63] P Karmwar, K Graeser, KC Gordon, CJ Strachan, and T Rades. Effect of different preparation methods on the dissolution behaviour of amorphous indomethacin. *European Journal of Pharmaceutics and Biopharmaceutics*, 80(2):459–464, 2012.

[64] T WY Lee, N A Boersen, HW Hui, SF Chow, KY Wan, and A HL Chow. Delivery of poorly soluble compounds by amorphous solid dispersions. *Current Pharmaceutical Design*, 20(3):303–324, 2014.

[65] A Newman and G Zografi. Critical considerations for the qualitative and quantitative determination of process-induced disorder in crystalline solids. *Journal of Pharmaceutical Sciences*, 103(9):2595–2604, 2014.

[66] JA Baird and LS Taylor. Evaluation of amorphous solid dispersion properties using thermal analysis techniques. *Advanced Drug Delivery Reviews*, 64(5):396–421, 2012.

[67] GA Ilevbare, H Liu, KJ Edgar, and LS Taylor. Understanding polymer properties important for crystal growth inhibition impact of chemically diverse polymers

on solution crystal growth of ritonavir. *Crystal Growth & Design*, 12(6):3133–3143, 2012.

[68] LA Wegiel, LJ Mauer, KJ Edgar, and LS Taylor. Crystallization of amorphous solid dispersions of resveratrol during preparation and storage-impact of different polymers. *Journal of Pharmaceutical Sciences*, 102(1):171–184, 2013.

[69] S Marano, SA Barker, BT Raimi-Abraham, S Missaghi, A Rajabi-Siahboomi, and D Craig. Development of micro-fibrous solid dispersions of poorly water-soluble drugs in sucrose using temperature-controlled centrifugal spinning. *European Journal of Pharmaceutics and Biopharmaceutics*, 103:84–94, 2016.

[70] G Van den Mooter. The use of amorphous solid dispersions: A formulation strategy to overcome poor solubility and dissolution rate. *Drug Discovery Today: Technologies*, 9(2):e79–e85, 2012.

[71] Y Tian, V Caron, DS Jones, AM Healy, and GP Andrews. Using flory-huggins phase diagrams as a pre-formulation tool for the production of amorphous solid dispersions: a comparison between hot-melt extrusion and spray drying. *Journal of Pharmacy and Pharmacology*, 66(2):256–274, 2014.

[72] K Löbmann, C Strachan, H Grohganz, T Rades, O Korhonen, and R Laitinen. Co-amorphous simvastatin and glipizide combinations show improved physical stability without evidence of intermolecular interactions. *European Journal of Pharmaceutics and Biopharmaceutics*, 81(1):159–169, 2012.

[73] N Chieng, J Aaltonen, D Saville, and T Rades. Physical characterization and stability of amorphous indomethacin and ranitidine hydrochloride binary systems prepared by mechanical activation. *European Journal of Pharmaceutics and Biopharmaceutics*, 71(1):47–54, 2009.

[74] R Hilfiker. *Polymorphism: in the pharmaceutical industry*. John Wiley & Sons, 2006.

[75] U Holzwarth and N Gibson. The scherrer equation versus the'debye-scherrer equation'. *Nature Nanotechnology*, 6(9):534–534, 2011.

[76] BC Hancock and G Zografi. The relationship between the glass transition temperature and the water content of amorphous pharmaceutical solids. *Pharmaceutical Research*, 11(4):471–477, 1994.

[77] G Ilevbare, P Marsac, and A Mitra. Performance and characterization of amorphous solid dispersions: an overview. In *Discovering and Developing Molecules with Optimal Drug-Like Properties*, pages 287–343. Springer, 2015.

[78] LA Wegiel, LJ Mauer, KJ Edgar, and LS Taylor. Mid-infrared spectroscopy as a polymer selection tool for formulating amorphous solid dispersions. *Journal of Pharmacy and Pharmacology*, 66(2):244–255, 2014.

[79] ME Lauer, M Siam, J Tardio, S Page, JH Kindt, and O Grassmann. Rapid assessment of homogeneity and stability of amorphous solid dispersions by atomic force microscopy-from bench to batch. *Pharmaceutical Research*, 30(8):2010–2022, 2013.

[80] AL Sarode, H Sandhu, N Shah, W Malick, and H Zia. Hot melt extrusion (hme) for amorphous solid dispersions: predictive tools for processing and impact of drug-polymer interactions on supersaturation. *European Journal of Pharmaceutical Sciences*, 48(3):371–384, 2013.

[81] RJ Chokshi, HK Sandhu, RM Iyer, NH Shah, AW Malick, and H Zia. Characterization of physico-mechanical properties of indomethacin and polymers to assess their suitability for hot-melt extrusion processs as a means to manufacture solid dispersion/solution. *Journal of Pharmaceutical Sciences*, 94(11):2463–2474, 2005.

[82] S Qi, A Gryczke, P Belton, and DQM Craig. Characterisation of solid dispersions of paracetamol and eudragit® e prepared by hot-melt extrusion using thermal, microthermal and spectroscopic analysis. *International Journal of Pharmaceutics*, 354(1):158–167, 2008.

[83] H Patil, RV Tiwari, and MA Repka. Hot-melt extrusion: from theory to application in pharmaceutical formulation. *American Association of Pharmaceutical Scientists*, 17 (1):20–42, 2016.

[84] J Baronsky-Probst, C-V Möltgen, W Kessler, and RW Kessler. Process design and control of a twin screw hot melt extrusion for continuous pharmaceutical tamper-resistant tablet production. *European Journal of Pharmaceutical Sciences*, 87: 14–21, 2016.

[85] RS Dhumal, AL Kelly, P York, PD Coates, and A Paradkar. Cocrystalization and simultaneous agglomeration using hot melt extrusion. *Pharmaceutical Research*, 27 (12):2725–2733, 2010.

[86] G Verreck, K Six, G Van den Mooter, L Baert, J Peeters, and ME Brewster. Characterization of solid dispersions of itraconazole and hydroxypropylmethylcellulose prepared by melt extrusion-part i. *International Journal of Pharmaceutics*, 251(1): 165–174, 2003.

[87] A Paudel, ZA Worku, J Meeus, S Guns, and G Van den Mooter. Manufacturing of solid dispersions of poorly water soluble drugs by spray drying: formulation and process considerations. *International Journal of Pharmaceutics*, 453(1):253–284, 2013.

[88] A Paudel and G Van den Mooter. Influence of solvent composition on the miscibility and physical stability of naproxen/PVP k 25 solid dispersions prepared by cosolvent spray-drying. *Pharmaceutical Research*, 29(1):251–270, 2012.

[89] T Vasconcelos, B Sarmento, and P Costa. Solid dispersions as strategy to improve oral bioavailability of poor water soluble drugs. *Drug Discovery Today*, 12(23): 1068–1075, 2007.

[90] G Van den Mooter, M Wuyts, N Blaton, R Busson, P Grobet, P Augustijns, and R Kinget. Physical stabilisation of amorphous ketoconazole in solid dispersions with polyvinylpyrrolidone k25. *European Journal of Pharmaceutical Sciences*, 12(3): 261–269, 2001.

[91] S Janssens and G Van den Mooter. Review: physical chemistry of solid dispersions. *Journal of Pharmacy and Pharmacology*, 61(12):1571–1586, 2009.

[92] JT Carstensen, F Attarchi, and X Hou. Decomposition of aspirin in the solid state in the presence of limited amounts of moisture. *Journal of Pharmaceutical Sciences*, 74(7):741–745, 1985.

[93] M Allesø, N Chieng, S Rehder, J Rantanen, T Rades, and J Aaltonen. Enhanced dissolution rate and synchronized release of drugs in binary systems through formulation: Amorphous naproxen–cimetidine mixtures prepared by mechanical activation. *Journal of Controlled Release*, 136(1):45–53, 2009.

[94] K Löbmann, H Grohganz, R Laitinen, C Strachan, and T Rades. Amino acids as co-amorphous stabilizers for poorly water soluble drugs–part 1: Preparation, stability and dissolution enhancement. *European Journal of Pharmaceutics and Biopharmaceutics*, 85(3):873–881, 2013.

[95] A Mahieu, J Willart, E Dudognon, F Danede, and M Descamps. A new protocol to determine the solubility of drugs into polymer matrixes. *Molecular Pharmaceutics*, 10(2):560–566, 2013.

[96] P Mura, M Cirri, MT Faucci, JM Ginès-Dorado, and GP Bettinetti. Investigation of the effects of grinding and co-grinding on physicochemical properties of glisentide. *Journal of Pharmaceutical and Biomedical Analysis*, 30(2):227–237, 2002.

[97] MK Gupta, A Vanwert, and Robin H Bogner. Formation of physically stable amorphous drugs by milling with neusilin. *Journal of Pharmaceutical Sciences*, 92 (3):536–551, 2003.

[98] E Dudognon, JF Willart, V Caron, F Capet, T Larsson, and M Descamps. Formation of budesonide/α-lactose glass solutions by ball-milling. *Solid State Communications*, 138(2):68–71, 2006.

[99] R Lim, W Ng, and R Tan. Dissolution enhancement of indomethacin via amorphization using co-milling and supercritical co-precipitation processing. *Powder Technology*, 240:79–87, 2013.

[100] JE Patterson, MB James, AH Forster, RW Lancaster, JM Butler, and T Rades. Preparation of glass solutions of three poorly water soluble drugs by spray drying, melt extrusion and ball milling. *International Journal of Pharmaceutics*, 336(1):22–34, 2007.

[101] V Caron, JF Willart, F Danede, and M Descamps. The implication of the glass transition in the formation of trehalose/mannitol molecular alloys by ball milling. *Solid State Communications*, 144(7):288–292, 2007.

[102] YE Sun, J Tao, G Zhang, and L Yu. Solubilities of crystalline drugs in polymers: an improved analytical method and comparison of solubilities of indomethacin and nifedipine in PVP, PVP/VA, and PVAc. *Journal of Pharmaceutical Sciences*, 99 (9):4023–4031, 2010.

[103] J Tao, Y Sun, G Zhang, and L Yu. Solubility of small-molecule crystals in polymers: D-mannitol in PVP, indomethacin in PVP/VA, and nifedipine in PVP/VA. *Pharmaceutical Research*, 26(4):855–864, 2009.

[104] Y Gao, J Lim, Y Han, L Wang, MS Chong, S Teoh, and C Xu. Cryomilling for the fabrication of doxorubicin-containing silica-nanoparticle/polycaprolactone nanocomposite films. *Nanoscale*, 8(5):2568–2574, 2016.

[105] S Sugimoto, T Niwa, Y Nakanishi, and K Danjo. Novel ultra-cryo milling and co-grinding technique in liquid nitrogen to produce dissolution-enhanced nanoparticles for poorly water-soluble drugs. *Chemical and Pharmaceutical Bulletin*, 60(3): 325–333, 2012.

[106] TP Shakhtshneider, F Danède, F Capet, JF Willart, M Descamps, SA Myz, EV Boldyreva, and VV Boldyrev. Grinding of drugs with pharmaceutical excipients at cryogenic temperatures. *Journal of Thermal Analysis and Calorimetry*, 89 (3):699–707, 2007.

[107] T Shakhtshneider, F Danède, F Capet, J Willart, Marc Descamps, l Paccou, EV Surov, E Boldyreva, and V Boldyrev. Grinding of drugs with pharmaceutical excipients at cryogenic temperatures. *Journal of Thermal Analysis and Calorimetry*, 89(3):703–715, 2007.

[108] F Qian, J Huang, and M Hussain. Drug–polymer solubility and miscibility: stability consideration and practical challenges in amorphous solid dispersion development. *Journal of Pharmaceutical Sciences*, 99(7):2941–2947, 2010.

[109] Y He and C Ho. Amorphous solid dispersions: utilization and challenges in drug discovery and development. *Journal of Pharmaceutical Sciences*, 104(10):3237–3258, 2015.

[110] H Konno and LS Taylor. Influence of different polymers on the crystallization tendency of molecularly dispersed amorphous felodipine. *Journal of Pharmaceutical Sciences*, 95(12):2692–2705, 2006.

[111] RJ Chokshi, NH Shah, HK Sandhu, AW Malick, and H Zia. Stabilization of low glass transition temperature indomethacin formulations: Impact of polymer-type and its concentration. *Journal of Pharmaceutical Sciences*, 97(6):2286–2298, 2008.

[112] AF Rumondor, H Konno, PJ Marsac, and LS Taylor. Analysis of the moisture sorption behavior of amorphous drug–polymer blends. *Journal of Applied Polymer Science*, 117(2):1055–1063, 2010.

[113] AF Rumondor, I Ivanisevic, S Bates, DE Alonzo, and LS Taylor. Evaluation of drug-polymer miscibility in amorphous solid dispersion systems. *Pharmaceutical Research*, 26(11):2523–2534, 2009.

[114] PJ Marsac, H Konno, and LS Taylor. A comparison of the physical stability of amorphous felodipine and nifedipine systems. *Pharmaceutical Research*, 23(10): 2306–2316, 2006.

[115] H Konno, T Handa, DE Alonzo, and LS Taylor. Effect of polymer type on the dissolution profile of amorphous solid dispersions containing felodipine. *European Journal of Pharmaceutics and biopharmaceutics*, 70(2):493–499, 2008.

[116] V Caron, L Tajber, OI Corrigan, and AM Healy. A comparison of spray drying and milling in the production of amorphous dispersions of sulfathiazole/polyvinylpyrrolidone and sulfadimidine/polyvinylpyrrolidone. *Molecular Pharmaceutics*, 8(2):532–542, 2011.

[117] Y Tian, J Booth, E Meehan, DS Jones, S Li, and GP Andrews. Construction of drug–polymer thermodynamic phase diagrams using flory–huggins interaction theory: identifying the relevance of temperature and drug weight fraction to phase separation within solid dispersions. *Molecular Pharmaceutics*, 10(1):236–248, 2012.

[118] PJ Marsac, SL Shamblin, and LS Taylor. Theoretical and practical approaches for prediction of drug–polymer miscibility and solubility. *Pharmaceutical Research*, 23 (10):2417–2426, 2006.

[119] SB Murdande, MJ Pikal, RM Shanker, and RH Bogner. Solubility advantage of amorphous pharmaceuticals: Ii. application of quantitative thermodynamic relationships for prediction of solubility enhancement in structurally diverse insoluble pharmaceuticals. *Pharmaceutical Research*, 27(12):2704–2714, 2010.

[120] J Gupta, C Nunes, S Vyas, and S Jonnalagadda. Prediction of solubility parameters and miscibility of pharmaceutical compounds by molecular dynamics simulations. *The Journal of Physical Chemistry B*, 115(9):2014–2023, 2011.

[121] A Rumondor, LA Stanford, and LS Taylor. Effects of polymer type and storage relative humidity on the kinetics of felodipine crystallization from amorphous solid dispersions. *Pharmaceutical research*, 26(12):2599–2606, 2009.

[122] E Karavas, G Ktistis, A Xenakis, and E Georgarakis. Miscibility behavior and formation mechanism of stabilized felodipine-polyvinylpyrrolidone amorphous solid dispersions. *Drug Development and Industrial Pharmacy*, 31(6):473–489, 2005.

[123] PJ Marsac, H Konno, A Rumondor, and LS Taylor. Recrystallization of nifedipine and felodipine from amorphous molecular level solid dispersions containing poly (vinylpyrrolidone) and sorbed water. *Pharmaceutical Research*, 25(3):647–656, 2008.

[124] GA Ilevbare, H Liu, KJ Edgar, and LS Taylor. Effect of binary additive combinations on solution crystal growth of the poorly water-soluble drug, ritonavir. *Crystal Growth & Design*, 12(12):6050–6060, 2012.

[125] GA Ilevbare, H Liu, KJ Edgar, and LS Taylor. Impact of polymers on crystal growth rate of structurally diverse compounds from aqueous solution. *Molecular Pharmaceutics*, 10(6):2381–2393, 2013.

[126] C Goddeeris, T Willems, K Houthoofd, JA Martens, and G Van den Mooter. Dissolution enhancement of the anti-hiv drug uc 781 by formulation in a ternary solid dispersion with tpgs 1000 and eudragit e100. *European Journal of Pharmaceutics and Biopharmaceutics*, 70(3):861–868, 2008.

[127] C Goddeeris, T Willems, and G Van den Mooter. Formulation of fast disintegrating tablets of ternary solid dispersions consisting of tpgs 1000 and hpmc 2910 or pvpva 64 to improve the dissolution of the anti-hiv drug uc 781. *European Journal of Pharmaceutical Sciences*, 34(4):293–302, 2008.

[128] S Janssens, S Denivelle, P Rombaut, and G Van den Mooter. Influence of polyethylene glycol chain length on compatibility and release characteristics of ternary solid dispersions of itraconazole in polyethylene glycol/hydroxypropylmethylcellulose 2910 e5 blends. *European Journal of Pharmaceutical Sciences*, 35(3):203–210, 2008.

[129] S Janssens, HN de Armas, W D Autry, A Van Schepdael, and G Van den Mooter. Characterization of ternary solid dispersions of itraconazole in polyethylene

glycol 6000/polyvidone-vinylacetate 64 blends. *European Journal of Pharmaceutics and Biopharmaceutics*, 69(3):1114–1120, 2008.

[130] J Kraemer, J Gajendran, A Guillot, J Schichtel, and A Tuereli. Dissolution testing of orally disintegrating tablets. *Journal of Pharmacy and Pharmacology*, 64(7):911–918, 2012.

[131] JE Aguilar-Díaz, E García-Montoya, J Suñe-Negre, P Pérez-Lozano, M Miñarro, and José R Ticó. Predicting orally disintegrating tablets formulations of ibuprophen tablets: an application of the new sedem-odt expert system. *European Journal of Pharmaceutics and Biopharmaceutics*, 80(3):638–648, 2012.

[132] A Gryczke, S Schminke, M Maniruzzaman, J Beck, and D Douroumis. Development and evaluation of orally disintegrating tablets (odts) containing ibuprofen granules prepared by hot melt extrusion. *Colloids and surfaces B: biointerfaces*, 86(2): 275–284, 2011.

[133] W Brniak, R Jachowicz, A Krupa, T Skorka, and K Niwinski. Evaluation of co-processed excipients used for direct compression of orally disintegrating tablets (odt) using novel disintegration apparatus. *Pharmaceutical Development and Technology*, 18(2):464–474, 2013.

[134] S Stegemann, M Gosch, and J Breitkreutz. Swallowing dysfunction and dysphagia is an unrecognized challenge for oral drug therapy. *International Journal of Pharmaceutics*, 430(1):197–206, 2012.

[135] HK Ibrahim and DA El-Setouhy. Valsartan orodispersible tablets: formulation, in vitro/in vivo characterization. *American Association of Pharmaceutical Scientists*, 11 (1):189–196, 2010.

[136] F Lai, E Pini, G Angioni, ML Manca, J Perricci, C Sinico, and AM Fadda. Nanocrystals as tool to improve piroxicam dissolution rate in novel orally disintegrating tablets. *European Journal of Pharmaceutics and Biopharmaceutics*, 79(3):552–558, 2011.

[137] DD Douroumis, A Gryczke, and S Schminke. Development and evaluation of cetirizine hcl taste-masked oral disintegrating tablets. *AAPS PharmSciTech*, 12(1): 141–151, 2011.

[138] S Bandari, RK Mittapalli, and R Gannu. Orodispersible tablets: An overview. *Asian Journal of Pharmaceutics (AJP): Free full text articles from Asian J Pharm*, 2(1), 2014.

[139] James R Waller and Derek G Waller. Drugs for systemic hypertension and angina. *Medicine*, 42(9):538–543, 2014.

[140] T Risler, R Bohm, D Wetzchewald, H-P Nast, H-H Koch, G Stein, and CM Erley. A comparison of the antihypertensive efficacy and safety of felodipine iv and nifedipine iv in patients with hypertensive crisis or emergency not responding to oral nifedipine. *European Journal of Clinical Pharmacology*, 54(4):295–298, 1998.

[141] HE Sluiter, FM Huysmans, TA Thien, and R Koene. Haemodynamic effects of intravenous felodipine in normotensive and hypertensive subjects. *Drugs*, 29(2): 144–153, 1985.

[142] EB Basalious, W El-Sebaie, and O El-Gazayerly. Rapidly absorbed orodispersible tablet containing molecularly dispersed felodipine for management of hypertensive crisis: development, optimization and in vitro/in vivo studies. *Pharmaceutical Development and Technology*, 18(2):407–416, 2013.

[143] N Tung, M Hung, X Vo, T Nguyen, et al. Formulation optimization of orally disintegrating tablets containing solid dispersion of felodipine and hydroxypropyl methylcellulose using face-centered central composite design. *Journal of Pharmaceutical Investigation*, 44(2):111–118, 2014.

[144] KV Kande, DJ Kotak, MS Degani, D Kirsanov, A Legin, and PV Devarajan. Microwave-assisted development of orally disintegrating tablets by direct compression. *American Association of Pharmaceutical Scientists*, pages 1–12, 2016.

[145] M Slavkova and J Breitkreutz. Orodispersible drug formulations for children and elderly. *European Journal of Pharmaceutical Sciences*, 75:2–9, 2015.

[146] Z Yang, K Nollenberger, J Albers, and S Qi. Molecular implications of drug–polymer solubility in understanding the destabilization of solid dispersions by milling. *Molecular Pharmaceutics*, 11(7):2453–2465, 2014.

[147] S Gurunath, SP Kumar, NK Basavaraj, and PA Patil. Amorphous solid dispersion method for improving oral bioavailability of poorly water-soluble drugs. *Journal of Pharmacy Research*, 6(4):476–480, 2013.

[148] H Konno and LS Taylor. Ability of different polymers to inhibit the crystallization of amorphous felodipine in the presence of moisture. *Pharmaceutical Research*, 25 (4):969–978, 2008.

[149] NS Trasi and LS Taylor. Effect of polymers on nucleation and crystal growth of amorphous acetaminophen. *Crystal Engineer Communication*, 14(16):5188–5197, 2012.

[150] NS Trasi, KA Oucherif, JD Litster, and LS Taylor. Evaluating the influence of polymers on nucleation and growth in supersaturated solutions of acetaminophen. *Crystal Engineer Communication*, 17(6):1242–1248, 2015.

[151] S Qi and D Craig. Recent developments in micro-and nanofabrication techniques for the preparation of amorphous pharmaceutical dosage forms. *Advanced Drug Delivery Reviews*, 100:67–84, 2016.

[152] JA Marks, LA Wegiel, LS Taylor, and KJ Edgar. Pairwise polymer blends for oral drug delivery. *Journal of Pharmaceutical Sciences*, 103(9):2871–2883, 2014.

[153] NS Trasi and SR Byrn. Mechanically induced amorphization of drugs: A study of the thermal behavior of cryomilled compounds. *American Association of Pharmaceutical Scientists*, 13(3):772–784, 2012.

[154] A Otte and MT Carvajal. Assessment of milling-induced disorder of two pharmaceutical compounds. *Journal of Pharmaceutical Sciences*, 100(5):1793–1804, 2011.

[155] E Kaminska, K Adrjanowicz, K Kaminski, P Wlodarczyk, L Hawelek, K Kolodziejczyk, M Tarnacka, D Zakowiecki, I Kaczmarczyk-Sedlak, J Pilch, et al. A new way of stabilization of furosemide upon cryogenic grinding by using acylated saccharides matrices. the role of hydrogen bonds in decomposition mechanism. *Molecular Pharmaceutics*, 10(5):1824–1835, 2013.

[156] AJ Megarry, J Booth, and J Burley. Sucrose/glucose molecular alloys by cryomilling. *Journal of Pharmaceutical Sciences*, 103(7):2098–2106, 2014.

[157] A Żarów, B Zhou, X Wang, R Pinal, and Z Iqbal. Spectroscopic and x-ray diffraction study of structural disorder in cryomilled and amorphous griseofulvin. *Applied Spectroscopy*, 65(2):135–143, 2011.

[158] J Willart, L Carpentier, F Danède, and M Descamps. Solid-state vitrification of crystalline griseofulvin by mechanical milling. *Journal of Pharmaceutical Sciences*, 101(4):1570–1577, 2012.

[159] S Desprez and M Descamps. Transformations of glassy indomethacin induced by ball-milling. *Journal of Non-crystalline Solids*, 352(42):4480–4485, 2006.

[160] A De Gusseme, C Neves, JF Willart, A Rameau, and M Descamps. Ordering and disordering of molecular solids upon mechanical milling: The case of fananserine. *Journal of Pharmaceutical Sciences*, 97(11):5000–5012, 2008.

[161] M Descamps, A Aumelas, S Desprez, and JF Willart. The amorphous state of pharmaceuticals obtained or transformed by milling: Sub-tg features and rejuvenation. *Journal of Non-Crystalline Solids*, 407:72–80, 2015.

[162] W Jones and MD Eddleston. Introductory lecture: Mechanochemistry, a versatile synthesis strategy for new materials. *Faraday Discussions*, 170:9–34, 2014.

[163] JP Bøtker, P Karmwar, CJ Strachan, C Cornett, F Tian, Z Zujovic, J Rantanen, and T Rades. Assessment of crystalline disorder in cryo-milled samples of indomethacin using atomic pair-wise distribution functions. *International Journal of Pharmaceutics*, 417(1):112–119, 2011.

[164] E Kim, M Chun, J Jang, I Lee, K Lee, and H Choi. Preparation of a solid dispersion of felodipine using a solvent wetting method. *European Journal of Pharmaceutics and Biopharmaceutics*, 64(2):200–205, 2006.

[165] Y Song, L Wang, P Yang, RM Wenslow, B Tan, H Zhang, and Z Deng. Physicochemical characterization of felodipine-kollidon va64 amorphous solid dispersions prepared by hot-melt extrusion. *Journal of Pharmaceutical Sciences*, 102(6): 1915–1923, 2013.

[166] S Yoo, SL Krill, Z Wang, and C Telang. Miscibility/stability considerations in binary solid dispersion systems composed of functional excipients towards the

design of multi-component amorphous systems. *Journal of Pharmaceutical Sciences*, 98(12):4711–4723, 2009.

[167] T Miyazaki, S Yoshioka, Y Aso, and S Kojima. Ability of polyvinylpyrrolidone and polyacrylic acid to inhibit the crystallization of amorphous acetaminophen. *Journal of Pharmaceutical Sciences*, 93(11):2710–2717, 2004.

[168] TN Pham, SA Watson, AJ Edwards, M Chavda, JS Clawson, M Strohmeier, and FG Vogt. Analysis of amorphous solid dispersions using 2d solid-state nmr and 1h t 1 relaxation measurements. *Molecular Pharmaceutics*, 7(5):1667–1691, 2010.

[169] M Yang, P Wang, C Huang, M S Ku, H Liu, and C Gogos. Solid dispersion of acetaminophen and poly (ethylene oxide) prepared by hot-melt mixing. *International Journal of Pharmaceutics*, 395(1):53–61, 2010.

[170] MF Nascimento, LA Souza, EB Ferreira, and ED Zanotto. Can glass stability parameters infer glass forming ability? *Journal of Non-Crystalline Solids*, 351(40): 3296–3308, 2005.

[171] A Alhalaweh, A Alzghoul, W Kaialy, D Mahlin, and CS BergstroÌĹm. Computational predictions of glass-forming ability and crystallization tendency of drug molecules. *Molecular Pharmaceutics*, 11(9):3123–3132, 2014.

[172] SA Raina, G Zhang, DE Alonzo, J Wu, D Zhu, ND Catron, Y Gao, and LS Taylor. Enhancements and limits in drug membrane transport using supersaturated solutions of poorly water soluble drugs. *Journal of Pharmaceutical Sciences*, 103(9): 2736–2748, 2014.

[173] R Ca Heading, J Nimmo, LF Prescott, and P Tothill. The dependence of paracetamol absorption on the rate of gastric emptying. *British Journal of Pharmacology*, 47 (2):415–421, 1973.

[174] L Kalantzi, C Reppas, JB Dressman, GL Amidon, HE Junginger, KK Midha, VP Shah, SA Stavchansky, and Dirk M Barends. Biowaiver monographs for immediate release solid oral dosage forms: Acetaminophen (paracetamol). *Journal of Pharmaceutical Sciences*, 95(1):4–14, 2006.

[175] PJ Goddard, BA Hills, and LM Lichtenberger. Does aspirin damage canine gastric mucosa by reducing its surface hydrophobicity? *American Journal of Physiology-Gastrointestinal and Liver Physiology*, 252(3):G421–G430, 1987.

[176] Y Tang and J Singh. Controlled delivery of aspirin: effect of aspirin on polymer degradation and in vitro release from plga based phase sensitive systems. *International Journal of Pharmaceutics*, 357(1):119–125, 2008.

[177] K Bica, C Rijksen, M Nieuwenhuyzen, and RD Rogers. In search of pure liquid salt forms of aspirin: ionic liquid approaches with acetylsalicylic acid and salicylic acid. *Physical Chemistry Chemical Physics*, 12(8):2011–2017, 2010.

[178] Ch B Aakeröy. Crystal engineering: strategies and architectures. *Acta Crystallographica Section B: Structural Science*, 53(4):569–586, 1997.

[179] F Zordan, L Brammer, and P Sherwood. Supramolecular chemistry of halogens: Complementary features of inorganic (m- x) and organic (c- x âĂŸ) halogens applied to m- xâŁŹâŁŹâŁŹ x âĂŸ- c halogen bond formation. *Journal of the American Chemical Society*, 127(16):5979–5989, 2005.

[180] P Metrangolo, H Neukirch, T Pilati, and G Resnati. Halogen bonding based recognition processes: a world parallel to hydrogen bonding. *Accounts of Chemical Research*, 38(5):386–395, 2005.

[181] S Datta and DW Grant. Crystal structures of drugs: advances in determination, prediction and engineering. *Nature Reviews Drug Discovery*, 3(1):42–57, 2004.

[182] W Klooster, T Koetzle, P Siegbahn, T Richardson, and R Crabtree. Study of the n- hâŁŹâŁŹâŁŹ h- b dihydrogen bond including the crystal structure of bh3nh3 by neutron diffraction. *Journal of the American Chemical Society*, 121(27):6337–6343, 1999.

[183] K Nakamoto, M Margoshes, and RE Rundle. Stretching frequencies as a function of distances in hydrogen bonds. *Journal of the American Chemical Society*, 77(24): 6480–6486, 1955.

[184] XC Tang, MJ Pikal, and LS Taylor. A spectroscopic investigation of hydrogen bond patterns in crystalline and amorphous phases in dihydropyridine calcium channel blockers. *Pharmaceutical Research*, 19(4):477–483, 2002.

[185] MC Etter. Encoding and decoding hydrogen-bond patterns of organic compounds. *Accounts of Chemical Research*, 23(4):120–126, 1990.

[186] B Van Eerdenbrugh and LS Taylor. An ab initio polymer selection methodology to prevent crystallization in amorphous solid dispersions by application of crystal engineering principles. *Crystal Engineer Communication*, 13(20):6171–6178, 2011.

[187] P Scherrer. Bestimmung der inneren struktur und der größe von kolloidteilchen mittels röntgenstrahlen. In *Kolloidchemie E Lehrbuch*, pages 387–409. Springer, 1912.

[188] RT Nassu and L Guaraldo Gonçalves. Determination of melting point of vegetable oils and fats by differential scanning calorimetry (dsc) technique. *Grasas y Aceites*, 50(1):16–21, 1999.

[189] JL Zhang, WH Wu, HW Zhou, XZ Guo, and YN Huang. Obtaining the glass transition temperature by measuring the crack healing process of glassformers. *Applied Physics Letters*, 92(13):131906, 2008.

[190] Q Lu and G Zografi. Phase behavior of binary and ternary amorphous mixtures containing indomethacin, citric acid, and pvp. *Pharmaceutical Research*, 15(8): 1202–1206, 1998.

[191] S Bates, G Zografi, D Engers, K Morris, K Crowley, and A Newman. Analysis of amorphous and nanocrystalline solids from their x-ray diffraction patterns. *Pharmaceutical Research*, 23(10):2333–2349, 2006.

[192] AL Patterson. The scherrer formula for x-ray particle size determination. *Physical Review*, 56(10):978, 1939.

[193] A Zen, J Pflaum, S Hirschmann, W Zhuang, F Jaiser, U Asawapirom, JP Rabe, U Scherf, and D Neher. Effect of molecular weight and annealing of poly (3-hexylthiophene) s on the performance of organic field-effect transistors. *Advanced Functional Materials*, 14(8):757–764, 2004.

[194] Andrew M. *Cryomilling of Molecular Alloy*. PhD thesis, University of Nottingham, may 2012.

[195] BS Luisi, Al Medek, Z Liu, P Mudunuri, and B Moulton. Milling-induced disorder of pharmaceuticals: One-phase or two-phase system? *Journal of Pharmaceutical Sciences*, 101(4):1475–1485, 2012.

[196] RN Panda, MF Hsieh, RJ Chung, and TS Chin. Ftir, xrd, sem and solid state nmr investigations of carbonate-containing hydroxyapatite nano-particles synthesized by hydroxide-gel technique. *Journal of Physics and Chemistry of Solids*, 64(2):193–199, 2003.

[197] I Fix and K-J Steffens. Quantifying low amorphous or crystalline amounts of alpha-lactose-monohydrate using x-ray powder diffraction, near-infrared spectroscopy, and differential scanning calorimetry. *Drug development and industrial pharmacy*, 30 (5):513–523, 2004.

[198] E Karavas, M Georgarakis, A Docoslis, and D Bikiaris. Combining sem, tem, and micro-raman techniques to differentiate between the amorphous molecular level dispersions and nanodispersions of a poorly water-soluble drug within a polymer matrix. *International Journal of Pharmaceutics*, 340(1):76–83, 2007.

[199] P Di Martino, P Conflant, M Drache, J-P Huvenne, and A-M Guyot-Hermann. Preparation and physical characterization of forms ii and iii of paracetamol. *Journal of Thermal Analysis*, 48(3):447–458, 1997.

[200] A Meena, T Parikh, S Singh Gupta, and AT Serajuddin. Investigation of thermal and viscoelastic properties of polymers relevant to hot melt extrusion, ii: Cellulosic polymers. *Journal of Excipients and Food Chemicals*, 5(1):46–55, 2014.

[201] K Six, H Berghmans, C Leuner, J Dressman, K Van Werde, J Mullens, L Benoist, M Thimon, L Meublat, G Verreck, et al. Characterization of solid dispersions of itraconazole and hydroxypropylmethylcellulose prepared by melt extrusion, part ii. *Pharmaceutical Research*, 20(7):1047–1054, 2003.

[202] GP Andrews, OA AbuDiak, and DS Jones. Physicochemical characterization of hot melt extruded bicalutamide–polyvinylpyrrolidone solid dispersions. *Journal of Pharmaceutical Sciences*, 99(3):1322–1335, 2010.

[203] AM Kaushal, AK Chakraborti, and AK Bansal. Ftir studies on differential intermolecular association in crystalline and amorphous states of structurally related non-steroidal anti-inflammatory drugs. *Molecular Pharmaceutics*, 5(6):937–945, 2008.

[204] Z Yang, K Nollenberger, Je Albers, J Moffat, D Craig, and S Qi. The effect of processing on the surface physical stability of amorphous solid dispersions. *European Journal of Pharmaceutics and Biopharmaceutics*, 88(3):897–908, 2014.

[205] J Willart, M Durand, L Briggner, A Marx, F Danède, and M Descamps. Solid-state amorphization of linaprazan by mechanical milling and evidence of polymorphism. *Journal of Pharmaceutical Sciences*, 102(7):2214–2220, 2013.

[206] R Fossheim. Crystal structure of the dihydropyridine calcium antagonist felodipine. dihydropyridine binding prerequisites assessed from crystallographic data. *Journal of Medicinal Chemistry*, 29(2):305–307, 1986.

[207] L Martínez, M Videa, G A López-Silva, A Carlos, J Cruz-Angeles, and N González. Stabilization of amorphous paracetamol based systems using traditional and novel strategies. *International Journal of Pharmaceutics*, 477(1):294–305, 2014.

[208] H Wen, KR Morris, and K Park. Hydrogen bonding interactions between adsorbed polymer molecules and crystal surface of acetaminophen. *Journal of Colloid and Interface Science*, 290(2):325–335, 2005.

[209] D Yu, C Branford-White, K White, X Li, and L Zhu. Dissolution improvement of electrospun nanofiber-based solid dispersions for acetaminophen. *American Association of Pharmaceutical Scientists*, 11(2):809–817, 2010.

[210] Agam R Sheth, Joseph W Lubach, Eric J Munson, Francis X Muller, and David JW Grant. Mechanochromism of piroxicam accompanied by intermolecular proton transfer probed by spectroscopic methods and solid-phase changes. *Journal of the American Chemical Society*, 127(18):6641–6651, 2005.

[211] R Lefort, V Caron, J Willart, and M Descamps. Mutarotational kinetics and glass transition of lactose. *Solid State Communications*, 140(7):329–334, 2006.

[212] M Vasanthavada, W Tong, Y Joshi, and M Kislalioglu. Phase behavior of amorphous molecular dispersions ii: Role of hydrogen bonding in solid solubility and phase separation kinetics. *Pharmaceutical Research*, 22(3):440–448, 2005.

[213] A Scholz, B Abrahamsson, SM Diebold, E Kostewicz, BI Polentarutti, A Ungell, and JB Dressman. Influence of hydrodynamics and particle size on the absorption of felodipine in labradors. *Pharmaceutical Research*, 19(1):42–46, 2002.

[214] A Noyes and WR Whitney. The rate of solution of solid substances in their own solutions. *Journal of the American Chemical Society*, 19(12):930–934, 1897.

[215] E Karavas, G Ktistis, A Xenakis, and E Georgarakis. Effect of hydrogen bonding interactions on the release mechanism of felodipine from nanodispersions with polyvinylpyrrolidone. *European Journal of Pharmaceutics and Biopharmaceutics*, 63 (2):103–114, 2006.

[216] BA Johnson, J Kreuter, and G Zografi. Effects of surfactants and polymers on advancing and receding contact angles. *Colloids and Surfaces*, 17(4):325–342, 1986.

[217] C Leuner and J Dressman. Improving drug solubility for oral delivery using solid dispersions. *European Journal of Pharmaceutics and Biopharmaceutics*, 50(1):47–60, 2000.

[218] CR Wilke and Pin Chang. Correlation of diffusion coefficients in dilute solutions. *American Institute of Chemical Engineers*, 1(2):264–270, 1955.

[219] R Villalobos, P Hernández-Muñoz, and A Chiralt. Effect of surfactants on water sorption and barrier properties of hydroxypropyl methylcellulose films. *Food Hydrocolloids*, 20(4):502–509, 2006.

[220] VJ Sovilj and LB Petrović. Influence of hydroxypropylmethyl cellulose–sodium dodecylsulfate interaction on the solution conductivity and viscosity and emulsion stability. *Carbohydrate Polymers*, 64(1):41–49, 2006.

[221] S Nilsson. Interactions between water-soluble cellulose derivatives and surfactants. 1. the hpmc/sds/water system. *Macromolecules*, 28(23):7837–7844, 1995.

[222] J Albers, K Matthée, K Knop, and P Kleinebudde. Evaluation of predictive models for stable solid solution formation. *Journal of Pharmaceutical Sciences*, 100(2):667–680, 2011.

[223] MK Beyer and H Clausen-Schaumann. Mechanochemistry: the mechanical activation of covalent bonds. *Chemical Reviews*, 105(8):2921–2948, 2005.

[224] A Newman, D Engers, S Bates, I Ivanisevic, RC Kelly, and G Zografi. Characterization of amorphous api: Polymer mixtures using x-ray powder diffraction. *Journal of Pharmaceutical Sciences*, 97(11):4840–4856, 2008.

[225] MM Knopp, NE Olesen, Y Huang, R Holm, and T Rades. Statistical analysis of a method to predict drug–polymer miscibility. *Journal of Pharmaceutical Sciences*, 105 (1):362–367, 2016.

[226] RA Shmeis, Z Wang, and SL Krill. A mechanistic investigation of an amorphous pharmaceutical and its solid dispersions, part i: A comparative analysis by thermally stimulated depolarization current and differential scanning calorimetry. *Pharmaceutical Research*, 21(11):2025–2030, 2004.

[227] H Grohganz, PA Priemel, K Löbmann, LH Nielsen, R Laitinen, A Mullertz, G Van den Mooter, and T Rades. Refining stability and dissolution rate of amorphous drug formulations. *Expert Opinion on Drug Delivery*, 11(6):977–989, 2014.

[228] M Gordon and JS Taylor. Ideal copolymers and the second-order transitions of synthetic rubbers. i. non-crystalline copolymers. *Journal of Applied Chemistry*, 2(9): 493–500, 1952.

[229] SL Shamblin, LS Taylor, and G Zografi. Mixing behavior of colyophilized binary systems. *Journal of Pharmaceutical Sciences*, 87(6):694–701, 1998.

[230] F Weuts, Iand Van Dycke, J Voorspoels, S De Cort, S Stokbroekx, R Leemans, ME Brewster, D Xu, B Segmuller, YA Turner, et al. Physicochemical properties of the amorphous drug, cast films, and spray dried powders to predict formulation probability of success for solid dispersions: etravirine. *Journal of Pharmaceutical Sciences*, 100(1):260–274, 2011.

[231] MM Knopp, L Tajber, Y Tian, NE Olesen, DS Jones, A Kozyra, K LoÌĹbmann, K Paluch, CM Brennan, R Holm, et al. Comparative study of different methods for the prediction of drug–polymer solubility. *Molecular Pharmaceutics*, 12(9): 3408–3419, 2015.

[232] T Tadros. Flory-huggins interaction parameter. *Encyclopedia of Colloid and Interface Science*, pages 523–524, 2013.

[233] Y Huang and W Dai. Fundamental aspects of solid dispersion technology for poorly soluble drugs. *Acta Pharmaceutica Sinica B*, 4(1):18–25, 2014.

[234] K Pajula, M Taskinen, V Lehto, J Ketolainen, and O Korhonen. Predicting the formation and stability of amorphous small molecule binary mixtures from com-

putationally determined flory- huggins interaction parameter and phase diagram. *Molecular Pharmaceutics*, 7(3):795–804, 2010.

[235] R Laitinen, E Suihko, K Toukola, M Björkqvist, J Riikonen, VP Lehto, K Järvinen, and J Ketolainen. Intraorally fast-dissolving particles of a poorly soluble drug: preparation and in vitro characterization. *European Journal of Pharmaceutics and Biopharmaceutics*, 71(2):271–281, 2009.

[236] Y Zhao, P Inbar, HP Chokshi, A Malick, and D Choi. Prediction of the thermal phase diagram of amorphous solid dispersions by flory–huggins theory. *Journal of Pharmaceutical Sciences*, 100(8):3196–3207, 2011.

[237] S Janssens, A De Zeure, A Paudel, J Van Humbeeck, P Rombaut, and G Van den Mooter. Influence of preparation methods on solid state supersaturation of amorphous solid dispersions: a case study with itraconazole and eudragit e100. *Pharmaceutical Research*, 27(5):775–785, 2010.

[238] M Knopp, NE Olesen, P Holm, P Langguth, R Holm, and T Rades. Influence of polymer molecular weight on drug–polymer solubility: a comparison between experimentally determined solubility in pvp and prediction derived from solubility in monomer. *Journal of Pharmaceutical Sciences*, 104(9):2905–2912, 2015.

[239] M Maniruzzaman, MT Islam, HG Moradiya, SA Halsey, IJ Slipper, BZ Chowdhry, MJ Snowden, and D Douroumis. Prediction of polymorphic transformations of paracetamol in solid dispersions. *Journal of Pharmaceutical Sciences*, 103(6): 1819–1828, 2014.

[240] MM Knopp, NErik Olesen, P Holm, K LÖBmann, R Holm, P Langguth, and T Rades. Evaluation of drug–polymer solubility curves through formal statistical analysis: Comparison of preparation techniques. *Journal of Pharmaceutical Sciences*, 104(1):44–51, 2015.

[241] M Vasanthavada, W Tong, Y Joshi, and M Kislalioglu. Phase behavior of amorphous molecular dispersions i: Determination of the degree and mechanism of solid solubility. *Pharmaceutical Research*, 21(9):1598–1606, 2004.

[242] C Ahlneck and G Zografi. The molecular basis of moisture effects on the physical and chemical stability of drugs in the solid state. *International Journal of Pharmaceutics*, 62(2):87–95, 1990.

[243] Z Yang, K Nollenberger, J Albers, D Craig, and S Qi. Microstructure of an immiscible polymer blend and its stabilization effect on amorphous solid dispersions. *Molecular Pharmaceutics*, 10(7):2767–2780, 2013.

[244] GA Ilevbare, H Liu, KJ Edgar, and LS Taylor. Inhibition of solution crystal growth of ritonavir by cellulose polymers–factors influencing polymer effectiveness. *Crystal Engineer Communication*, 14(20):6503–6514, 2012.

[245] S Okonogi and S Puttipipatkhachorn. Dissolution improvement of high drug-loaded solid dispersion. *American Association of Pharmaceutical Scientists*, 7(2): E148–E153, 2006.

[246] T Vasconcelos, S Marques, J das Neves, and B Sarmento. Amorphous solid dispersions: Rational selection of a manufacturing process. *Advanced Drug Delivery Reviews*, 100:85–101, 2016.

[247] PJ Marsac, T Li, and LS Taylor. Estimation of drug–polymer miscibility and solubility in amorphous solid dispersions using experimentally determined interaction parameters. *Pharmaceutical Research*, 26(1):139–151, 2009.

[248] Z Chen, Z Liu, and F Qian. Crystallization of bifonazole and acetaminophen within the matrix of semicrystalline, peo–ppo–peo triblock copolymers. *Molecular Pharmaceutics*, 12(2):590–599, 2015.

[249] F Meng, A Trivino, D Prasad, and H Chauhan. Investigation and correlation of drug polymer miscibility and molecular interactions by various approaches for the preparation of amorphous solid dispersions. *European Journal of Pharmaceutical Sciences*, 71:12–24, 2015.

[250] F Meng, V Dave, and H Chauhan. Qualitative and quantitative methods to determine miscibility in amorphous drug–polymer systems. *European Journal of Pharmaceutical Sciences*, 77:106–111, 2015.

[251] S Qi, JG Moffat, and Z Yang. Early stage phase separation in pharmaceutical solid dispersion thin films under high humidity: improved spatial understanding using probe-based thermal and spectroscopic nanocharacterization methods. *Molecular Pharmaceutics*, 10(3):918–930, 2013.

[252] AM Agrawal, S Dudhedia, and E Zimny. Hot melt extrusion: development of an amorphous solid dispersion for an insoluble drug from mini-scale to clinical scale. *American Association of Pharmaceutical Scientists*, 17(1):133–147, 2016.

[253] DO Corrigan, AM Healy, and OI Corrigan. The effect of spray drying solutions of bendroflumethiazide/polyethylene glycol on the physicochemical properties of the resultant materials. *International Journal of Pharmaceutics*, 262(1):125–137, 2003.

[254] V Caron, Y Hu, L Tajber, A Erxleben, OI Corrigan, P McArdle, and AM Healy. Amorphous solid dispersions of sulfonamide/soluplus® and sulfonamide/pvp prepared by ball milling. *American Association of Pharmaceutical Scientists*, 14(1): 464–474, 2013.

[255] CR Groom and FH Allen. The cambridge structural database in retrospect and prospect. *Angewandte Chemie International Edition*, 53(3):662–671, 2014.

[256] J Liu, Y Xiao, and C Allen. Polymer–drug compatibility: a guide to the development of delivery systems for the anticancer agent, ellipticine. *Journal of Pharmaceutical Sciences*, 93(1):132–143, 2004.

[257] B Van E, L Froyen, J Van Humbeeck, JA Martens, P Augustijns, and G Van den Mooter. Drying of crystalline drug nanosuspensions-the importance of surface hydrophobicity on dissolution behavior upon redispersion. *European Journal of Pharmaceutical Sciences*, 35(1):127–135, 2008.

[258] AF Rumondor and LS Taylor. Effect of polymer hygroscopicity on the phase behavior of amorphous solid dispersions in the presence of moisture. *Molecular Pharmaceutics*, 7(2):477–490, 2010.

[259] S Ozaki, I Kushida, T Yamashita, T Hasebe, O Shirai, and K Kano. Inhibition of crystal nucleation and growth by water-soluble polymers and its impact on the supersaturation profiles of amorphous drugs. *Journal of Pharmaceutical Sciences*, 102(7):2273–2281, 2013.

[260] S Verma and VS Rudraraju. A systematic approach to design and prepare solid dispersions of poorly water-soluble drug. *American Association of Pharmaceutical Scientists*, 15(3):641–657, 2014.

[261] N Shah, H Sandhu, W Phuapradit, R Pinal, R Iyer, A Albano, A Chatterji, S Anand, D Choi, K Tang, et al. Development of novel microprecipitated bulk powder (mbp) technology for manufacturing stable amorphous formulations of poorly soluble drugs. *International Journal of Pharmaceutics*, 438(1):53–60, 2012.

[262] J Li, J Zhao, L Tao, J Wang, V Waknis, D Pan, M Hubert, K Raghavan, and J Patel. The effect of polymeric excipients on the physical properties and performance of amorphous dispersions: part i, free volume and glass transition. *Pharmaceutical Research*, 32(2):500–515, 2015.

[263] ZK Nagy, A Balogh, B Vajna, A Farkas, and G Patyi. Comparison of electrospun and extruded soluplus®-based solid dosage forms of improved dissolution.

[264] R Hoogenboom, C Becer, C Guerrero-Sanchez, S Hoeppener, and US Schubert. Solubility and thermoresponsiveness of pmma in alcohol-water solvent mixtures. *Australian Journal of Chemistry*, 63(8):1173–1178, 2010.

[265] M Deka and A Kumar. Enhanced electrical and electrochemical properties of pmma–clay nanocomposite gel polymer electrolytes. *Electrochimica Acta*, 55(5): 1836–1842, 2010.

[266] A Siciliano, A Seves, T De Marco, S Cimmino, E Martuscelli, and C Silvestre. Miscibility and thermal and crystallization behaviors of poly (d-(-)-3-hydroxybutyrate)/atactic poly (methyl methacrylate) blends. *Macromolecules*, 28 (24):8065–8072, 1995.

[267] H Shintani and H Tanaka. Universal link between the boson peak and transverse phonons in glass. *Nature Materials*, 7(11):870–877, 2008.

[268] T Grigera, V Martin-Mayor, G Parisi, and P Verrocchio. Phonon interpretation of the "boson peak" in supercooled liquids. *Nature*, 422(6929):289–292, 2003.

[269] BC Hancock, SL Shamblin, and G Zografi. Molecular mobility of amorphous pharmaceutical solids below their glass transition temperatures. *Pharmaceutical Research*, 12(6):799–806, 1995.

[270] D Hörter and J Dressman. Influence of physicochemical properties on dissolution of drugs in the gastrointestinal tract. *Advanced Drug Delivery Reviews*, 25(1):3–14, 1997.

[271] Shahla Jamzad and Reza Fassihi. Role of surfactant and ph on dissolution properties of fenofibrate and glipizideâĂŤa technical note. *American Association of Pharmaceutical Scientists*, 7(2):E17–E22, 2006.

[272] A Serajuddin. Solid dispersion of poorly water-soluble drugs: Early promises, subsequent problems, and recent breakthroughs. *Journal of Pharmaceutical Sciences*, 88(10):1058–1066, 1999.

[273] H De Waard, W Hinrichs, M Visser, C Bologna, and E Frijlink. Unexpected differences in dissolution behavior of tablets prepared from solid dispersions with a surfactant physically mixed or incorporated. *International Journal of Pharmaceutics*, 349(1):66–73, 2008.

[274] N Fotaki, CM Long, K Tang, and H Chokshi. Dissolution of amorphous solid dispersions: theory and practice. In *Amorphous Solid Dispersions*, pages 487–514. Springer, 2014.

[275] BC Hancock and M Parks. What is the true solubility advantage for amorphous pharmaceuticals? *Pharmaceutical Research*, 17(4):397–404, 2000.

[276] J Brouwers, ME Brewster, and P Augustijns. Supersaturating drug delivery systems: The answer to solubility-limited oral bioavailability? *Journal of Pharmaceutical Sciences*, 98(8):2549–2572, 2009.

[277] J Hecq, M Deleers, D Fanara, H Vranckx, and K Amighi. Preparation and characterization of nanocrystals for solubility and dissolution rate enhancement of nifedipine. *International Journal of Pharmaceutics*, 299(1):167–177, 2005.

[278] M Vogt, K Kunath, and JB Dressman. Dissolution enhancement of fenofibrate by micronization, cogrinding and spray-drying: comparison with commercial preparations. *European Journal of Pharmaceutics and Biopharmaceutics*, 68(2):283–288, 2008.

[279] D Craig. The mechanisms of drug release from solid dispersions in water-soluble polymers. *International Journal of Pharmaceutics*, 231(2):131–144, 2002.

[280] E Karavas, E Georgarakis, MP Sigalas, K Avgoustakis, and D Bikiaris. Investigation of the release mechanism of a sparingly water-soluble drug from solid dispersions in hydrophilic carriers based on physical state of drug, particle size

distribution and drug–polymer interactions. *European Journal of Pharmaceutics and Biopharmaceutics*, 66(3):334–347, 2007.

[281] T Watanabe, S Hasegawa, N Wakiyama, A Kusai, and M Senna. Comparison between polyvinylpyrrolidone and silica nanoparticles as carriers for indomethacin in a solid state dispersion. *International Journal of Pharmaceutics*, 250(1):283–286, 2003.

[282] T Yamada, N Saito, T Imai, and M Otagiri. Effect of grinding with hydroxypropyl cellulose on the dissolution and particle size of a poorly water-soluble drug. *Chemical and Pharmaceutical Bulletin*, 47(9):1311–1313, 1999.

[283] P Dunselman, B Edgar, and A Scaf. Pharmacokinetics of felodipine after intravenous and chronic oral administration in patients with congestive heart failure. *British Journal of Clinical Pharmacology*, 28(1):45–52, 1989.

[284] T Ohara, S Kitamura, T Kitagawa, and K Terada. Dissolution mechanism of poorly water-soluble drug from extended release solid dispersion system with ethylcellulose and hydroxypropylmethylcellulose. *International Journal of Pharmaceutics*, 302 (1):95–102, 2005.

[285] RN Shamma and M Basha. Soluplus®: A novel polymeric solubilizer for optimization of carvedilol solid dispersions: Formulation design and effect of method of preparation. *Powder Technology*, 237:406–414, 2013.

[286] A Homayouni, F Sadeghi, J Varshosaz, HA Garekani, and A Nokhodchi. Promising dissolution enhancement effect of Soluplus on crystallized celecoxib obtained through antisolvent precipitation and high pressure homogenization techniques. *Colloids and Surfaces B: Biointerfaces*, 122:591–600, 2014.

[287] K Punčochová, AV Ewing, M Gajdošová, N Sarvašová, SG Kazarian, J Beránek, and F Štěpánek. Identifying the mechanisms of drug release from amorphous solid dispersions using MRI and ATR-FTIR spectroscopic imaging. *International Journal of Pharmaceutics*, 483(1):256–267, 2015.

[288] B Ljung. Vascular selectivity of felodipine. *Drugs*, 29(2):46–58, 1985.

[289] MJ Eisenberg, A Brox, and AN Bestawros. Calcium channel blockers: an update. *The American Journal of Medicine*, 116(1):35–43, 2004.

[290] S Sahney. A review of calcium channel antagonists in the treatment of pediatric hypertension. *Pediatric Drugs*, 8(6):357–373, 2006.

[291] PA Todd and D Faulds. Felodipine. *Drugs*, 44(2):251–277, 1992.

[292] Z Rahman, AS Zidan, and MA Khan. Risperidone solid dispersion for orally disintegrating tablet: its formulation design and non-destructive methods of evaluation. *International Journal of Pharmaceutics*, 400(1):49–58, 2010.

[293] RA Shoukri, IS Ahmed, and RN Shamma. In vitro and in vivo evaluation of nimesulide lyophilized orally disintegrating tablets. *European Journal of Pharmaceutics and Biopharmaceutics*, 73(1):162–171, 2009.

[294] M Manyikana, YE Choonara, LK Tomar, C Tyagi, P Kumar, LC du Toit, and V Pillay. A review of formulation techniques that impact the disintegration and mechanical properties of oradispersible drug delivery technologies. *Pharmaceutical Development and Technology*, 21(3):354–366, 2016.

[295] G Abdelbary, P Prinderre, C Eouani, J Joachim, JP Reynier, and PH Piccerelle. The preparation of orally disintegrating tablets using a hydrophilic waxy binder. *International Journal of Pharmaceutics*, 278(2):423–433, 2004.

[296] Wolfgang A Ritschel and Annette Bauer-Brandl. *Die Tablette: Handbuch der Entwicklung, Herstellung und Qualitätssicherung*. ECV-Editio-Cantor-Verlag, 2002.

[297] A Agrawal, M Dudhedia, W Deng, K Sd, L Zhong, E Povilaitis, and E Zimny. Development of tablet formulation of amorphous solid dispersions prepared by hot melt extrusion using quality by design approach. *American Association of Pharmaceutical Scientists*, 17(1):214–232, 2016.

[298] F Jijun, X Lishuang, W Xiaoli, Z Shu, T Xiaoguang, Z Xingna, H Haibing, and T Xing. Nimodipine (nm) tablets with high dissolution containing nm solid dispersions prepared by hot-melt extrusion. *Drug development and industrial pharmacy*, 37(8):934–944, 2011.

[299] SM Alshehri, J Park, BB Alsulays, RV Tiwari, B Almutairy, AS Alshetaili, J Morott, S Shah, V Kulkarni, S Majumdar, et al. Mefenamic acid taste-masked oral disintegrating tablets with enhanced solubility via molecular interaction produced by

hot melt extrusion technology. *Journal of Drug Delivery Science and Technology*, 27: 18–27, 2015.

[300] GM El Maghraby and RN Elsergany. Fast disintegrating tablets of nisoldipine for intra-oral administration. *Pharmaceutical Development and Technology*, 19(6): 641–650, 2014.

[301] H Wen and K Park. *Oral controlled release formulation design and drug delivery: Theory to practice*. John Wiley & Sons, 2011.

[302] JP Remington, DB Troy, and P Beringer. *Remington: The science and practice of pharmacy*, volume 1. Lippincott Williams & Wilkins, 2006.

Appendix

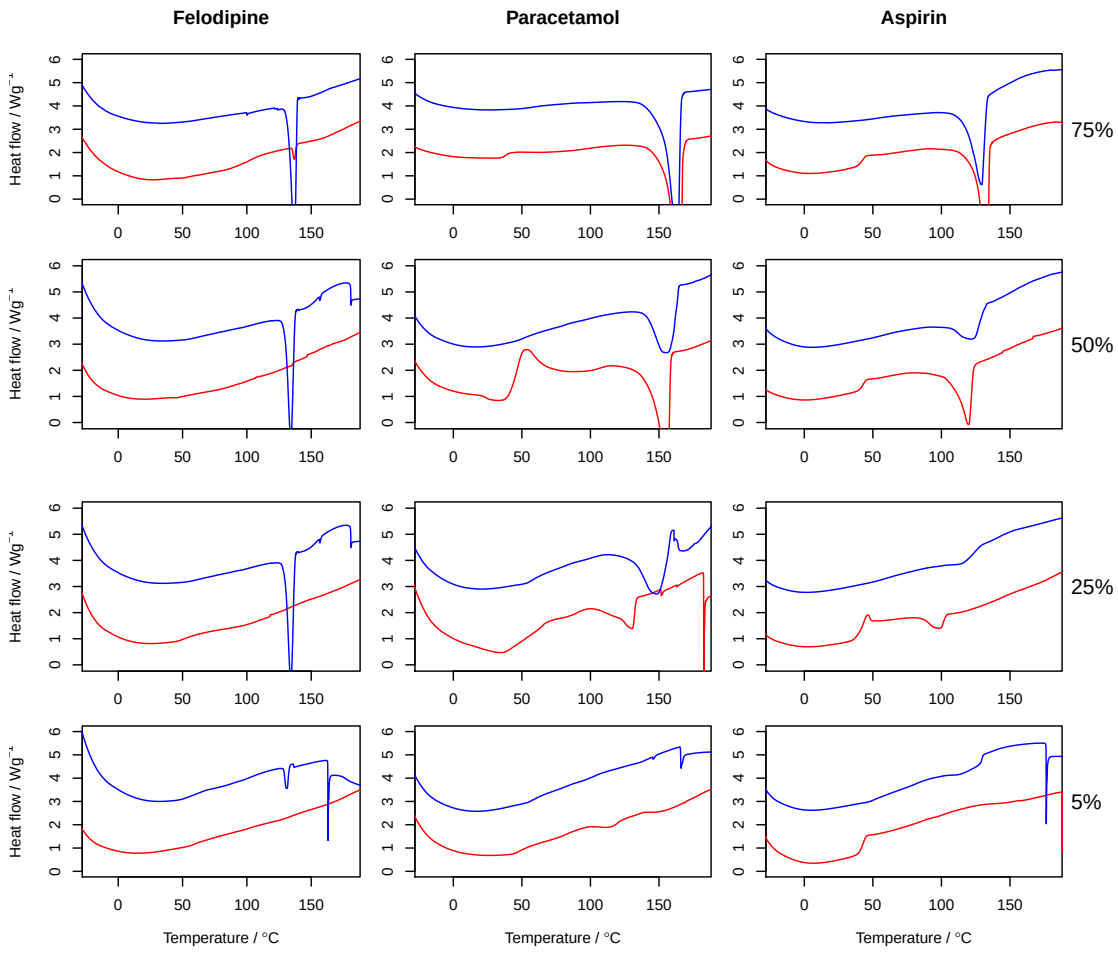

Figure 1: The thermogram of 75, 50, 25 and 5 % drug loading cryomilled separately (red color), cryomilled together (blue color) of felodipine, paracetamol and aspirin. Offsets applied for presentational purpose.